CURRENT AND CHARGE MEASUREMENTS ON SCALE MODEL EC-130 AIRCRAFT

Valdis V. Liepa

The Radiation Laboratory
Department of Electrical and Computer Engineering
University of Michigan
Ann Arbor, Michigan 48109

September 1978

ABSTRACT

Measured data are presented for the surface currents and charges induced on scale model EC-130 aircraft when illuminated by a plane electromagnetic wave in a simulated free space environment. The measurements were made on 1/144 and 1/72 scale models over the frequency range 225 to 4400 MHz, simulating 1.5 to 51.1 MHz full scale. The data are for 6 test points and 6 excitations chosen to compliment the full-scale HPD/VPD ground and the VPD fly-by tests made at Kirtland Air Force Base.

PREFACE

It is a pleasure to acknowledge the assistance of Messrs. J. Tedesco, D. Brown and F. Lenning of the Radiation Laboratory in performing the measurements, data processing and data preparation. The assistance of Dr. E. O'Donnell of SAI and Mr. W. Prather of AFWL is also appreciated.

TABLE OF CONTENTS

SECTION I

INTRODUCTION

The data presented here were obtained for Science Applications, Inc. (SAI) to be used in determining the surface response extrapolation function [1] for the EC-130 aircraft. The test points and excitation conditions in the scale model measurements were therefore chosen in conformity with those of the full scale measurements made in the Horizontally Polarized Dipole (HPD) and Vertically Polarized Dipole (VPD) simulators at Kirtland AFB, but measurements were also made for excitation conditions similar to those of the VPD flight exposure tests performed at Kirtland [2].

Surface current and charge data are presented at 6 locations or test points on the aircraft for 6 different excitation conditions. The measured quantities are the axial current component J_a, the circumferential current component J_c, and the normal electric field component E_n. One hundred and eight measurement situations were therefore possible, but since some of these correspond to null field situations or to low excitation levels in the case of the VPD flight exposure simulation, the number of actual measurements was only 54. The resulting data are shown in the form of amplitude and phase plots as a function of the full scale frequency, and have also been furnished to SAI in digital form on computer cards.

---

1. Carl E. Baum, "Extrapolation Techniques for Interpreting the Results of Tests in EMP Simulators in Terms of EMP Criteria," AFWL Sensor and Simulation Notes, Note 222, 1977.
2. R.W. Sutton and D.R. Stribling, "TEMPAT I/AFWL Add-On Test Requirements," Science Applications, Inc., Report No. SAI-78-638-WA, 1977.

SECTION II

MODELS, MEASUREMENTS AND DATA

2.1 MODELS

Two scale models of the C-130 were acquired, the first coming in the form of a plastic kit (MPC, No. 20552) 1/72 in scale, and the other being a solid plastic model (Precise Model Co., Elyrio, OH) 1/144 in scale. Figure 1 is a photograph of the models as C-130's. Note that the smaller model in the background has stretched strings that were eventually replaced by metallic wires to simulate the HF antenna.

To convert the models into their EC-130 counterparts, VLF antenna drogues were added at the bottom of the fuselage and tail and wires were added to represent the HF antenna. The wires were 0.02 mm diameter beryllium copper, and pieces of plastic and nylon string were used for the insulators. For mounting the HF wire we followed the specifications given in [2]. However, after conferring with SAI personnel, it was determined that the HF 3 wire attachement at the fuselage should be at STA:F480T instead of F320. The models were prepared accordingly and Figure 2 shows the location of the HF wires. The HF 1, 2 and 3 wires were shorted at the fuselage but open-circuited at the vertical stabilizer. The so-called "dogleg" HF 4 and 5 wires were left open-circuit at both the vertical and horizontal stabilizers, and Figure 3 is a photograph of the installed wires on the models.

Inspection of a C-130 commercial aircraft showed that the weather radar in the nose extends almost to the tip of the radome, suggesting that

for the purposes of this study the nose can be treated as metallic. The radome portions of our models were therefore left in place and metallized like the rest of the surface. However, after about 50 percent of our measurements had been completed, we were informed that on the EC-130, the instrumentation under the radome extends only inches beyond the bulkhead. It would therefore have been more realistic to have left the radome off, but because of the advanced state of our program, we continued with the metallized radome through the rest of the measurements.

After construction and modification as indicated above, the models were given at least three coats of silver paint to make them conducting. The lengths and wingspans were then measured to determine the actual scale factors. Because neither model was an exact replica of the EC-130, the scale factors deduced from the fuselage and wingspan differed slightly, as indicated in Table 1. The actual factor used in converting a measured result to the full scale frequency was that appropriate to the location of the test point and the excitation.

2.2 MEASUREMENTS

The measurements were made in the Radiation Laboratory's anechoic chamber, a facility specially designed, constructed and instrumented for surface field measurements. A block diagram of the facility is shown in Figure 4. The measurement procedures were similar to those used in previous programs [3, 4, 5], apart from changes resulting from the continued upgrading of the facility and the measurement techniques. In particular, for this program a new broadband transmitting antenna was installed which reduced the lower end of the frequency range from 450 to 225 MHz, thereby providing coverage in the three overlapping frequency ranges 225-1100, 950-2200 and 2000-4400 MHz.

The currents and charges on the models were measured using miniature sensors 2-3 mm in dimension constructed from 0.05 cm diameter semirigid coax. Most of the current data were obtained using a surface mounted half-loop probe (SP) whose signal lead was taken from the model at a place remote from the test point and chosen to produce least interaction with the model. A few current measurements were made using an external or

---

3. Valdis V. Liepa, "Sweep Frequency Surface Field Measurements," University of Michigan Radiation Laboratory Report No. 013378-1-F; AFWL-TR-75-217; Sensor and Simulation Notes, Note 210; 1975.

4. Valdis V. Liepa, "Surface Field Measurements on Scale Model EC-135 Aircraft," University of Michigan Radiation Laboratory Report No. 014182-1-F; AFWL-TR-77-101; Interaction Application Memos, Memo 15; 1978.

5. Valdis V. Liepa, "Surface Field Measurements on Scale Model E-4 Aircraft," University of Michigan Radiation Laboratory Report No. 014182-2-F; AFWL-TR-77-111; 1978.

free space probe (FSP), but these were confined to situations where the interaction of the model and the probe lead is negligible, e.g. the measurement of J_c at STA:F345T for top illumination with E parallel to the wings, the case when only the antisymmetric modes are excited which do not couple to the probe lead. For the charge measurements only surface mounted probes were available, and with these the mounting procedures were the same as for the surface mounted current probes. Figure 5 shows the typical taping required for installing a surface mounted probe.

Figure 6 illustrates how the use of more than one scale model can increase the range of full scale frequencies for which data can be obtained. With the measured frequency range 225-4400 MHz (approximately a 20:1 bandwidth), a 1/144 scale model will provide coverage from 1.56 to 30.6 MHZ, and a 1/72 model covers 3.1 to 61.1 MHz, yielding the overall coverage 1.56 to 61.1 MHz, corresponding to a 40.1 bandwidth.

2.3 DATA

For each measurement situation the data obtained from the two models over the three frequency ranges results in six data files for the transfer function. At the request of SAI, the three bands of data for each model were combined into a single data set in which the sampling was uniform in frequency. These sampled data were obtained by linear interpolation between adjacent measured values, and in regions where two bands overlap, a single curve was produced by application of a linearly increasing weighting to one data set relative to the other. In the final format, the data measured using the 1/144 scale model are presented at increments of 0.065 MHz in frequency, and the data for the 1/72 model at 0.13 MHz increments.

Figure 7 shows the directions of excitation used and the convention adopted in specifying the circumferential and axial components, J_c and J_a respectively, of the surface current. Because the wings and stabilizers of the EC-130 are all essentially perpendicular to fuselage axis, the components J_a on the wings and stabilizers was in all cases measured perpendicular to the axis. The component J_c is perpendicular to J_a. The data presented are all normalized relative to the incident field: J/H_o and E_n/E_o for the current and charge amplitudes respectively. The phase reference is that of the incident field at the station where the measurement was made, based on the $e^{i\omega t}$ time convention.

Tables 2 and 3 summarize the situations for which data have been obtained, and give the Figure numbers where the data for each case can be

found. Each Figure number is followed by a letter L (large model, scale 1/72) or S (small model, scale 1/144) specifying the model used in the measurements. The presence of other numbers indicate that the measurement was repeated, usually for a different HF wire configuration (open or short-circuited condition) or made with a different probe.

Table 4 details the conditions under which the measurements were made. In measurements with the actual aircraft, it had been observed that a high energy pulse produced arcing across the insulators of the HF wire antennas, thereby shorting them. Our initial instructions were to short the HF 1, 2 and 3 antennas at the vertical stabilizer, as well as the "dogleg" antennas, HF 4 and 5, at the horizontal and vertical stabilizers, and data sets 1 through 18 were all obtained under these short-circuited conditions. For sets 19 through 66, however, the conditions were changed: the insulators shown in Figure 2 were now left open-circuited except in the case of top illumination with E parallel to the fuselage for which the HF 1, 2 and 3 antennas were shorted at the vertical stabilizer.

In addition to the above intentional change in the condition of the HF wire antennas during the course of the program, there may have been an unintentional change. When most of the 54 measurements had been completed, it was discovered that the short-circuit condition of the HF 1, 2 and 3 wires at the top of the (forward) fuselage was questionable on the 1/144 scale model. Cracks were observed in the silver paint bonding the wires to the model, and when the contact resistance

was measured with an ohm meter, the reading varied from zero (short circuit) to infinity (open circuit). The wires were then checked on the 1/72 scale model, but these were still shorted to the fuselage, as required. To see what effect the questionable short could have on the data, some of the measurements were repeated with the wires reattached and checked for a proper short circuit. These repeat measurements, plus others made under different conditions, are contained in sets 55 through 66: see Table 4 for details of the measurement configuration.

Plots of the measured current and charge data are given on the following pages. In addition, the data has been furnished to SAI in digital form on punched cards. The format is

Line	1	FILENAME (4A4)
	2	Comments (18A4)
	3	Comments (18A4)
	4	TITLE used in plotting (18A4)
	5	FMIN, FMAX, AMPMIN, AMPMAX, PHASEMIN, PHASEMAX, NN (4F8.3, 2F8.2, I5)
	6	F(1) AMP(1) PHASE(1) F(2) AMP(2) PHASE(2) F(3) AMP(3) PHASE(3) (3(2F8.3, F8.2)
↑ data ↓		
		..... F(NN) AMP(NN) PHASE(NN)

where NN is the number of data points in the set. Table 5 is an example of a typical data file.

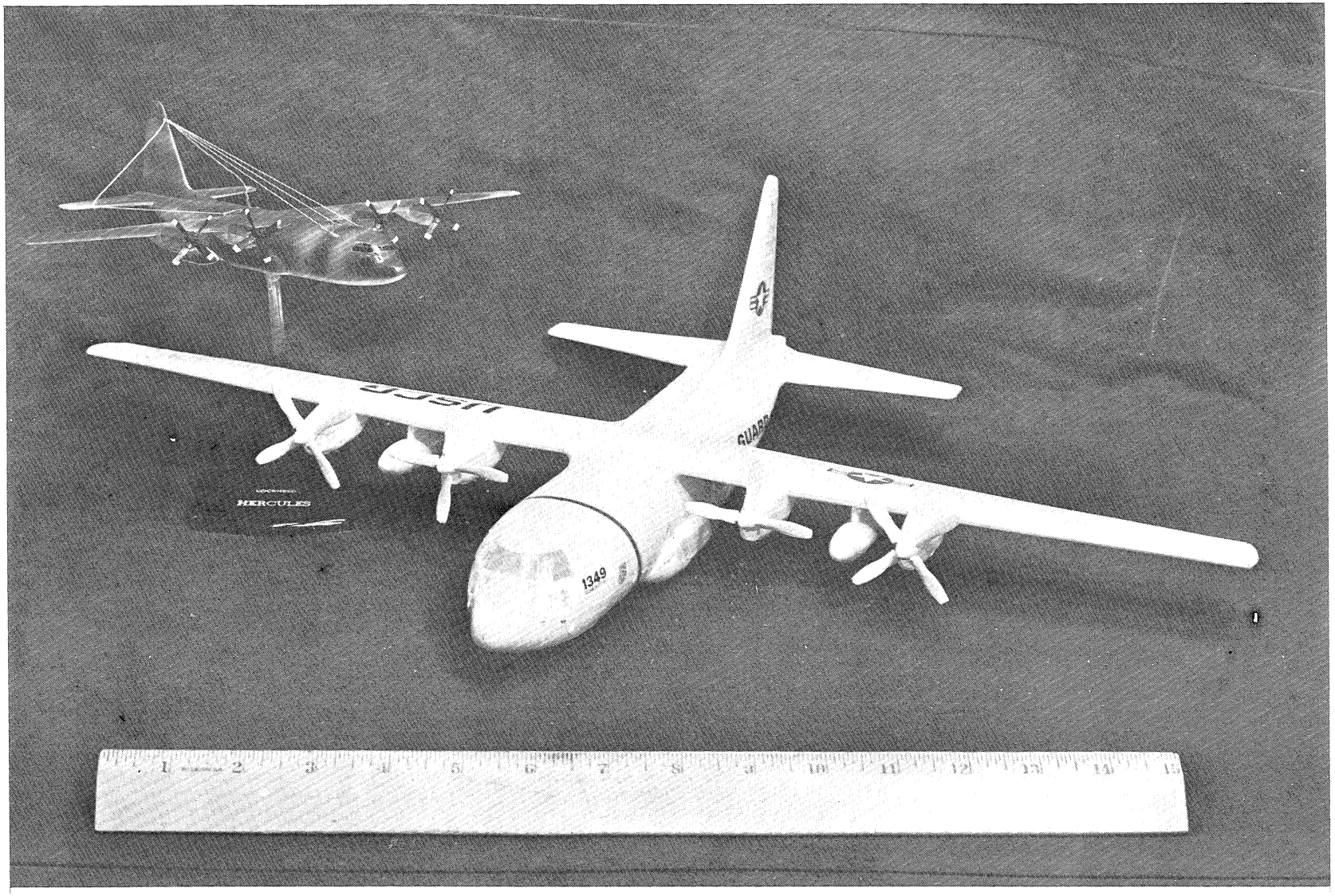

Figure 1. C-130 models similar to these were modified into EC-130 versions used in measurements.

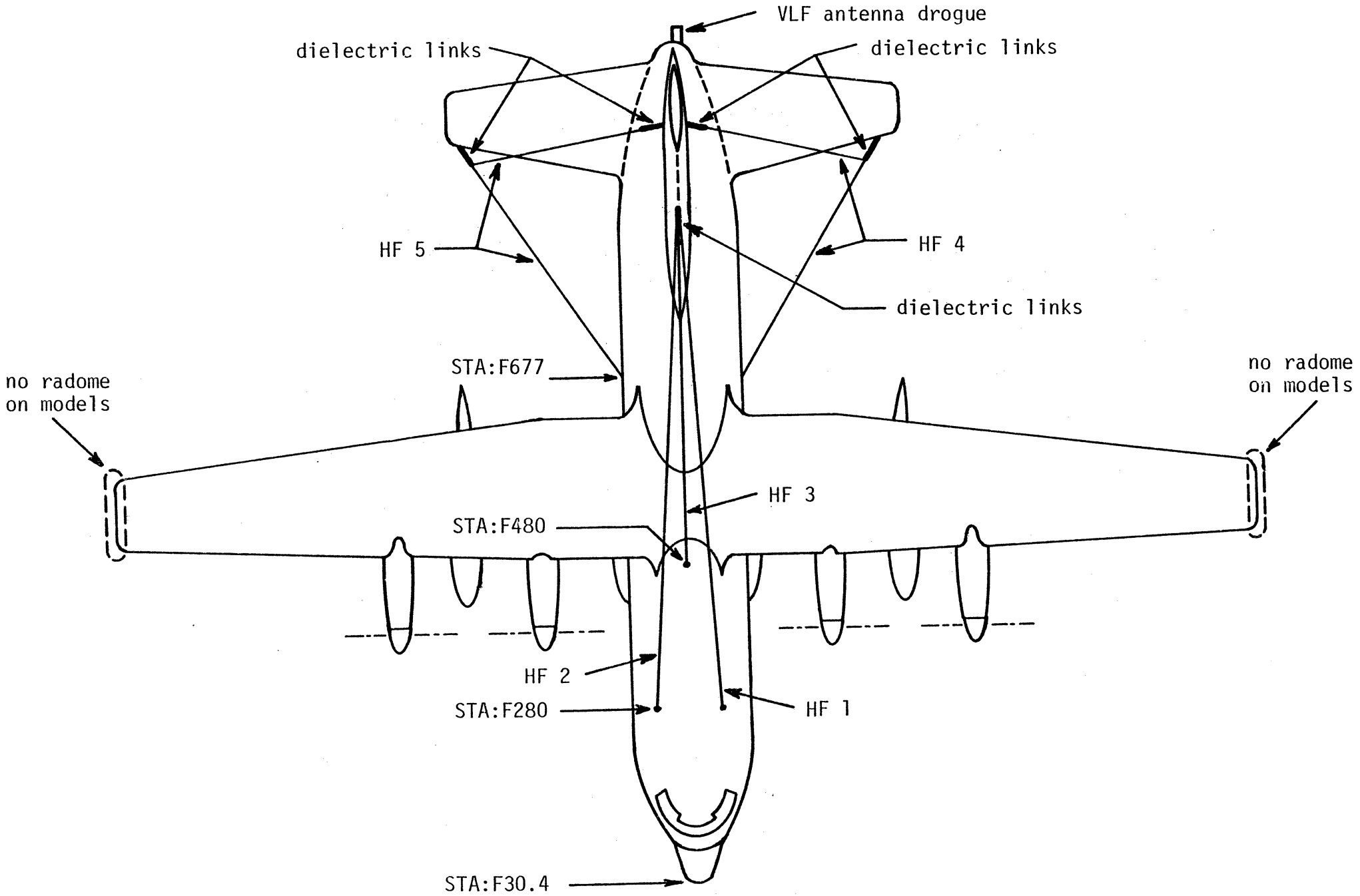

Figure 2. Implementation of HF antennas on scale models.

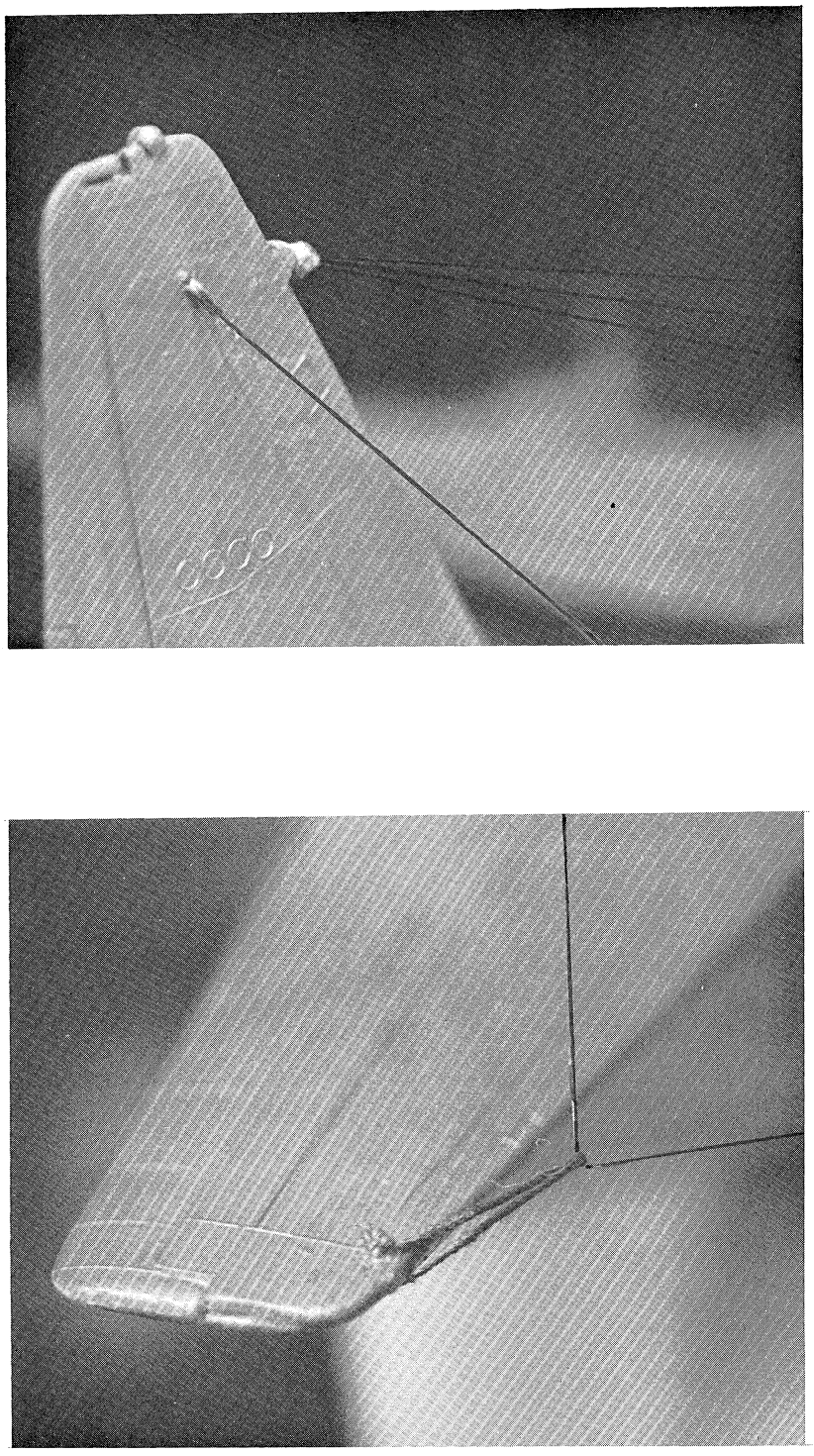

Figure 3. Attachment of the HF wires at the stabilizers. The upper photo shows the insulated attachment at the vertical stabilizer. The HF 1, 2 and 3 wires are embedded in plastic and isolated from each other, while the "dogleg" wires are isolated with strings at the vertical and horizontal (see lower photo) stabilizers. The photographs have been re-touched to emphasize the wires.

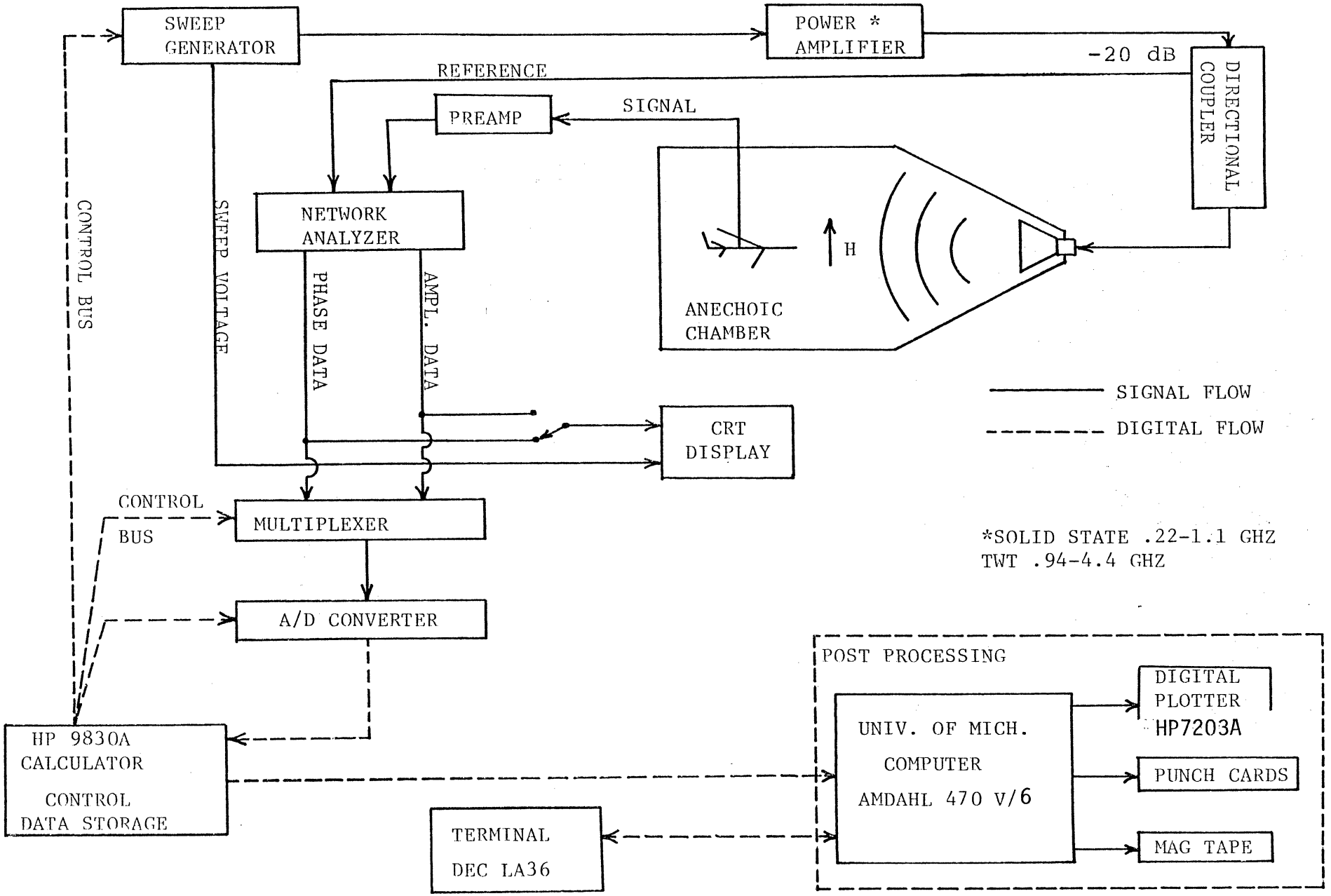

Figure 4. Block diagram of the measurement facility.

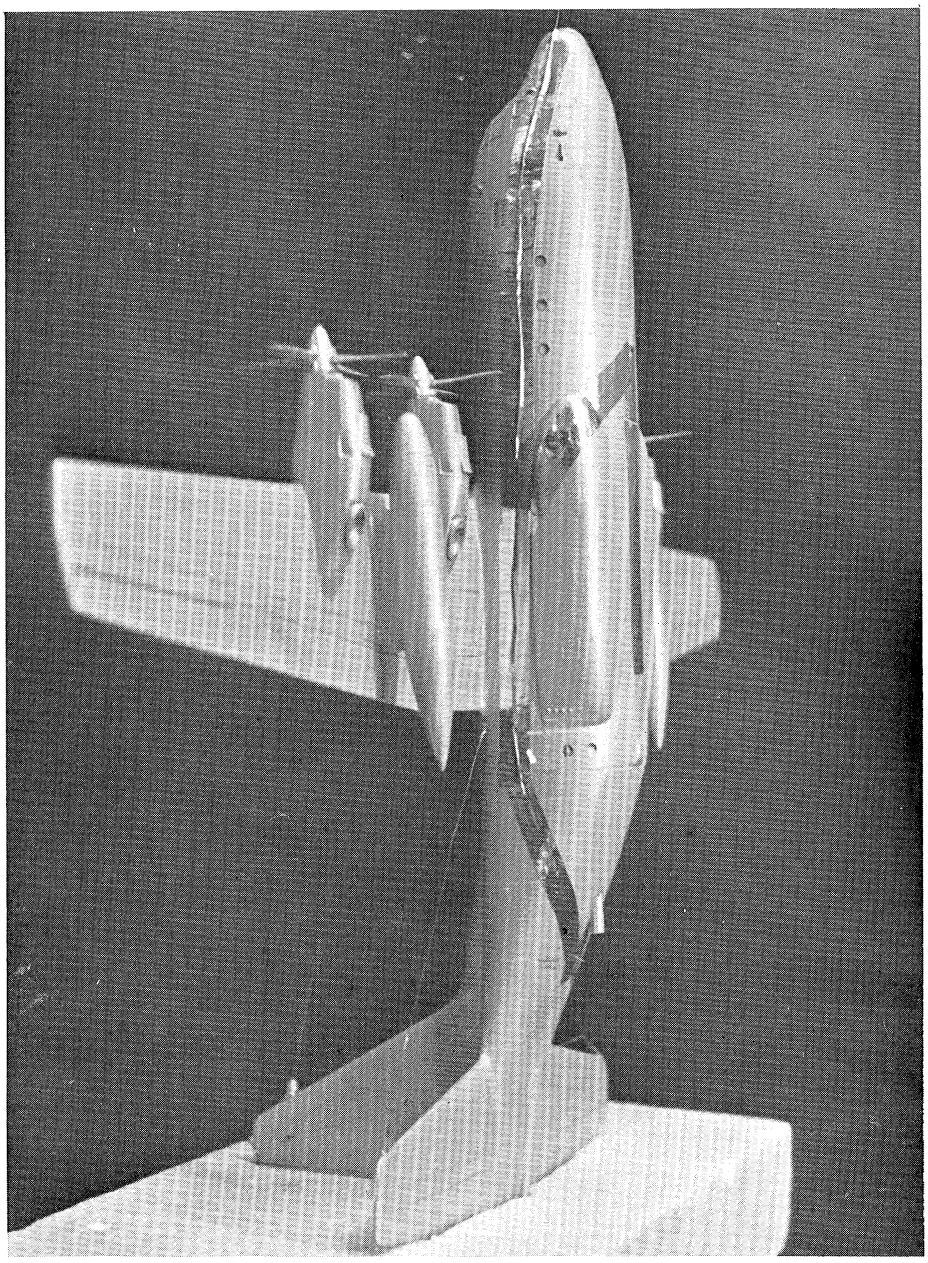

Figure 5. 1/72 scale model with a probe mounted to measure the charge at STA:F870B, top illumination, with E parallel to the wings. The probe lead is taped along the fuselage and leaves the model at the nose. For top illumination with E parallel to the fuselage, the lead would be taped along a wing and leave the model at the wing tip.

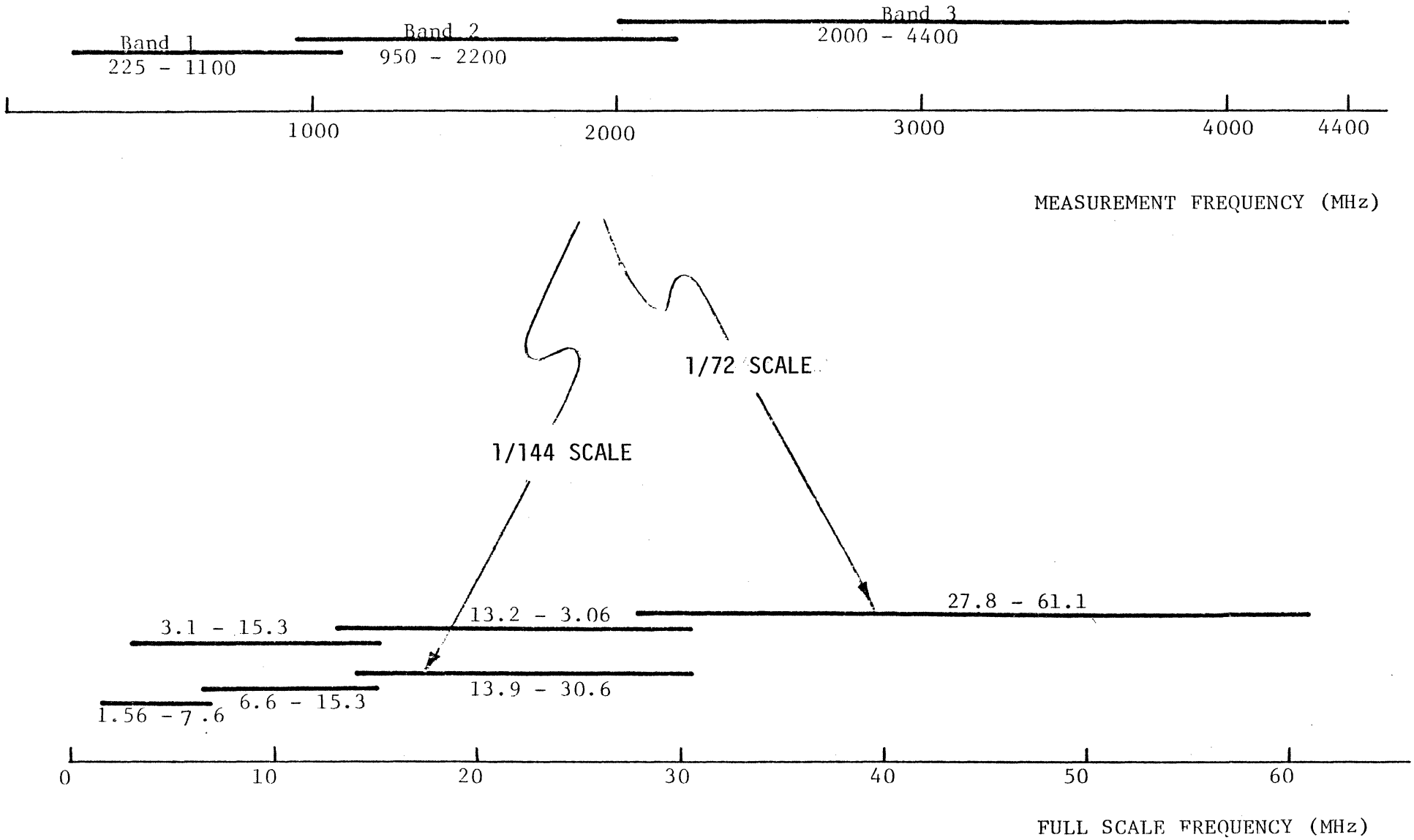

Figure 6. EC-130 measurement frequency coverage.

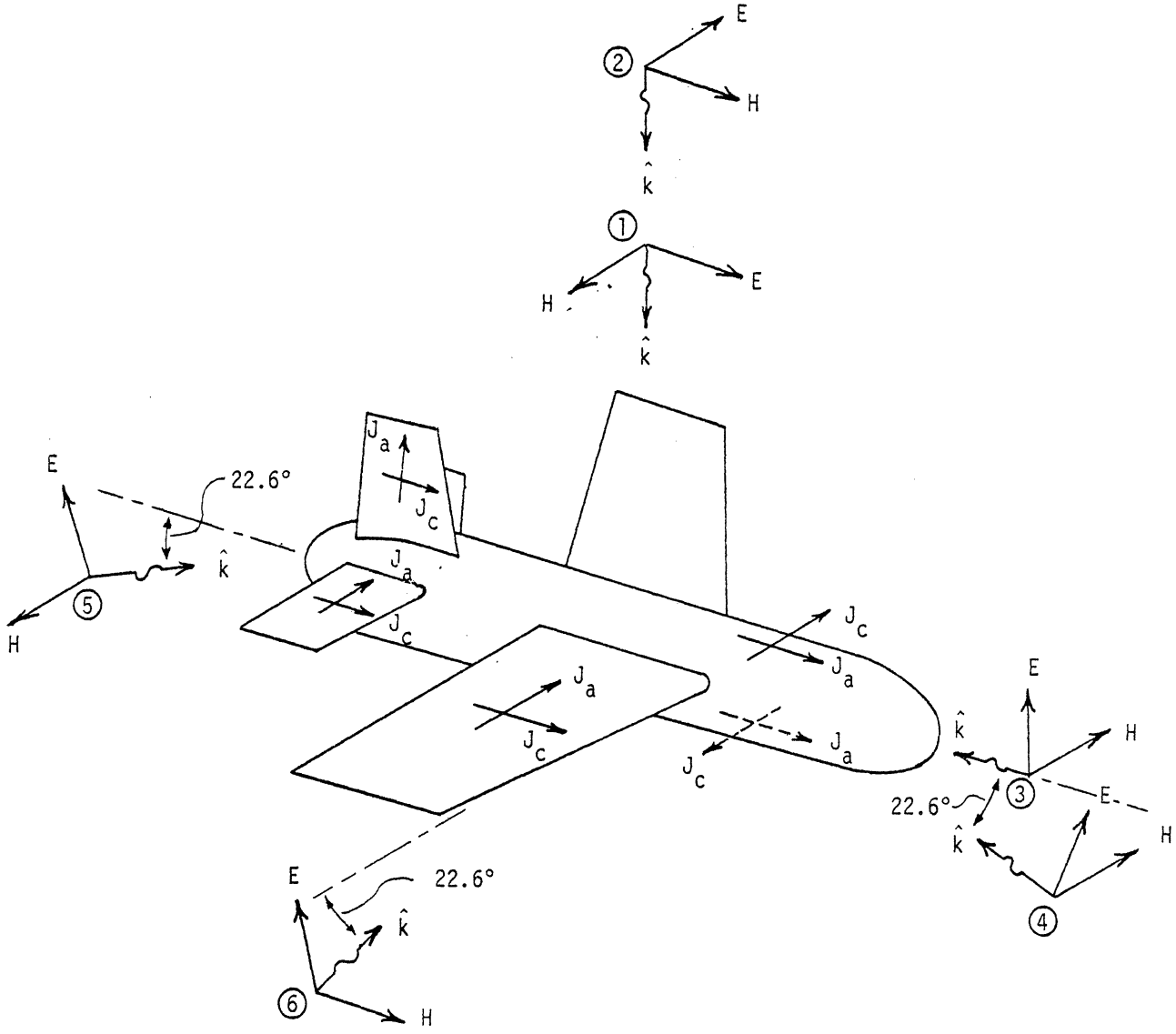

Figure 7. Convention for illumination and the measured current components.

TABLE 1: MODEL SCALE FACTORS

Model	Fuselage Length* (cm)	Wingspan (cm)	Fuselage scale	Wingspan scale
1/72	42.70	55.68	1/71.15	1/72.58
1/144	20.81 (20.41)**	28.54	1/146.00 (1/148.79)**	1/141.62

Full scale length with drogue: 30.38 m

Full scale wingspan without wing tip radomes: 40.41 m

*Including the drogue

**The length of the 1/144 scale model originally measured was slightly in error, leading to the use of the incorrect scale factors shown in parentheses in the conversion of the model frequencies to the full scale ones. The data affected are those for the 1/144 model in orientations 1, 3, 4 and 5, and can be corrected by multiplying the frequency by a factor 1.019.

TABLE 2: VPD/HPD MODE DATA

TEST POINT	STATION NO.	LOCATIONS	EXCITATION 1 E// Fus.			EXCITATION 2 E// Wings			EXCITATION 3 Nose - On		
			J_a	J_c	E_n	J_a	J_c	E_n	J_a	J_c	E_n
101	F345T	Fwd Fus. Top	01L,S 55L,S 61L,S		02L,S		03L,S 56L,S		04L,S 57L,S		07L,S
103	F345B	Fwd Fus. Bottom	10L,S 60L 63L,S		11L,S		12L,S		13L,S 64L,S		16L,S
121	HS158T	Mid Horiz. Stab. (R)	33L,S		39L,S 62S	34L,S		40L,S	35L,S		41L,S
123	VS140	Mid Vert. Stab. (R)	44L,S		49L,S				45L,S		50L,S
140	W90T	Mid Wing Top (R)				29L,S		31L,S			
141	F870B	Rear Fus. Bottom	19L,S		24L,S		23L,S		20L,S		25L,S

More than one entry per box indicates repeated measurements.

TABLE 3: FLY-BY MODE DATA

TEST POINT	STATION NO.	LOCATIONS	EXCITATION 4 E// Fus.			EXCITATION 5 E// Wings			EXCITATION 6 Nose - On		
			J_a	J_c	E_n	J_a	J_c	E_n	J_a	J_c	E_n
101	F345T	Fwd Fus. Top	05L,S 58L,S		08L,S	06L,S 59L,S		09L,S			
103	F345B	Fwd Fus. Bottom	14L,S 65L,S		17L,S	15L,S 66L,S		18L,S			
121	HS158T	Mid Horiz. Stab. (R)	36L,S		42L,S	37L,S		43L,S	38L,S		
123	VS140	Mid Vert. Stab. (R)	46L,S		51L,S	47L,S		52L,S	48L,S		53L,S
140	W90T	Mid Wing Top (R)							30L,S		32L,S
141	F870B	Rear Fus. Bottom	21L,S		26L,S	22L,S		27L,S	54L,S		28L,S

More than one entry per box indicates repeated measurements.

TABLE 4: CONDITION OF HF ANTENNAS WHEN MEASUREMENTS WERE MADE

DATA SET	PROBE USED	HF 1, 2, 3 at Fwd Fus.	HF 1, 2, 3 at Vert. Stab.	HF 4, 5 at Vert. & Horz. Stab.
1-18	SP(J, Q)	Questionable Short Circuit on the 1/144 Model	Shorted	Shorted
19	FSP(J)		Shorted	Open
20-23	FSP(J)		Open	Open
24	SP(Q)		Shorted	Open
25-28	SP(Q)		Open	Open
29-30	FSP(J)		Open	Open
31-32	SP(J)		Open	Open
33	SP(J)		Shorted	Open
34	FSP(J)		Open	Open
35-37	SP(J)		Open	Open
38	FSP(J)		Open	Open
39	SP(Q)		Shorted	Open
40-43	SP(Q)		Open	Open
44	SP(J)		Shorted	Open
45-47	SP(J)		Open	Open
48	FSP(J)		Open	Open
49	SP(Q)		Shorted	Open
50-54	SP(J, Q)		Open	Open
55-59	FSP(J)		Open	Open
60L	FSP(J)		Open	Open
61	FSP(J)	Shorted	Shorted	Open
62S	SP(Q)	Shorted	Shorted	Open
63	FSP(J)	Shorted	Shorted	Open
64-66	FSP(J)	Shorted	Open	Open

SP(J, Q) = Surface Probe (Current, Charge)

FSP(J) = Free Space Probe (Current)

TABLE 5: LISTING OF A TYPICAL DATA FILE

```
      1     TOOS
      2     EC-130,144,1,Q,Q10,B,8/28/78,DB
      3     SCALE FACTOR=148.15
      4     TACAMO SAMPLE DATA
      5        1.505  29.604   0.042   7.019 -178.23  179.80  282
      6        1.505   2.151  133.05   1.605   1.678  149.38   1.705   0.491  169.11
      7        1.805   2.169  112.88   1.905   2.189  150.93   2.005   2.609  138.11
      8        2.105   2.657  144.53   2.205   3.104  110.71   2.305   4.362  125.74
      9        2.405   4.206   97.25   2.505   4.604   84.12   2.605   5.402   72.88
     10        2.705   4.940   46.08   2.805   4.337   36.27   2.905   4.358   27.68
     11        3.005   3.864    9.02   3.105   3.461   -3.15   3.205   3.163  -12.23
     12        3.305   2.593  -19.80   3.405   2.206  -35.10   3.505   1.391  -34.17
     13        3.605   1.160  -31.60   3.705   0.932   -2.29   3.805   1.295   -4.08
     14        3.905   1.428    3.54   4.005   1.624   -8.34   4.105   1.555  -10.69
     15        4.205   1.764  -12.60   4.305   1.877  -13.90   4.405   1.957  -13.89
     16        4.505   2.273  -21.45   4.605   2.473  -25.30   4.705   2.322  -33.25
     17        4.805   2.729  -24.29   4.905   3.231  -28.81   5.005   3.924  -34.89
     18        5.105   4.907  -40.22   5.205   6.180  -61.02   5.305   6.335  -76.17
     19        5.405   6.761  -89.02   5.505   7.013 -106.74   5.605   7.019 -123.04
     20        5.705   6.605 -140.21   5.805   5.885 -154.75   5.905   5.345 -163.82
     21        6.005   4.117 -170.71   6.105   4.972 -175.38   6.205   4.396  166.98
     22        6.305   3.574  163.21   6.405   3.550  155.76   6.505   3.258  144.59
     23        6.605   2.955  136.37   6.705   2.729  124.13   6.805   2.430  119.75
     24        6.905   2.130  110.43   7.005   1.997   98.92   7.105   1.680   91.92
     25        7.205   1.438   81.60   7.305   1.239   78.01   7.405   1.052   69.02
               .
               .
               .
               .
     80       23.704   0.184   21.39  23.804   0.166   16.16  23.904   0.162   15.92
     81       24.004   0.165   17.58  24.104   0.170   17.18  24.204   0.173   14.28
     82       24.304   0.180   11.25  24.404   0.193    9.45  24.504   0.201    1.74
     83       24.604   0.194   -3.13  24.704   0.205   -6.88  24.804   0.209  -13.12
     84       24.904   0.203  -19.09  25.004   0.197  -21.02  25.104   0.197  -18.57
     85       25.204   0.205  -16.03  25.304   0.229  -21.06  25.404   0.229  -26.79
     86       25.504   0.239  -32.63  25.604   0.240  -37.91  25.704   0.235  -42.30
     87       25.804   0.233  -46.91  25.904   0.236  -51.13  26.004   0.239  -53.12
     88       26.104   0.250  -58.73  26.204   0.245  -66.59  26.304   0.236  -67.12
     89       26.404   0.248  -67.67  26.504   0.268  -72.86  26.604   0.275  -79.12
     90       26.704   0.268  -83.53  26.804   0.267  -85.86  26.904   0.277  -88.33
     91       27.004   0.279  -89.92  27.104   0.290  -94.09  27.204   0.298  -97.65
     92       27.304   0.308 -101.04  27.404   0.309 -104.89  27.504   0.304 -108.04
     93       27.604   0.304 -109.08  27.704   0.308 -109.87  27.804   0.319 -114.12
     94       27.904   0.313 -117.06  28.004   0.320 -116.84  28.104   0.325 -118.95
     95       28.204   0.336 -120.14  28.304   0.356 -123.21  28.404   0.371 -129.21
     96       28.504   0.366 -134.42  28.604   0.351 -135.53  28.704   0.365 -138.02
     97       28.804   0.383 -138.93  28.904   0.383 -141.28  29.004   0.399 -145.17
     98       29.104   0.414 -149.32  29.204   0.414 -153.52  29.304   0.409 -157.73
     99       29.404   0.398 -161.20  29.504   0.394 -160.84  29.604   0.431 -164.47
END OF FILE
```

- - D A T A - -

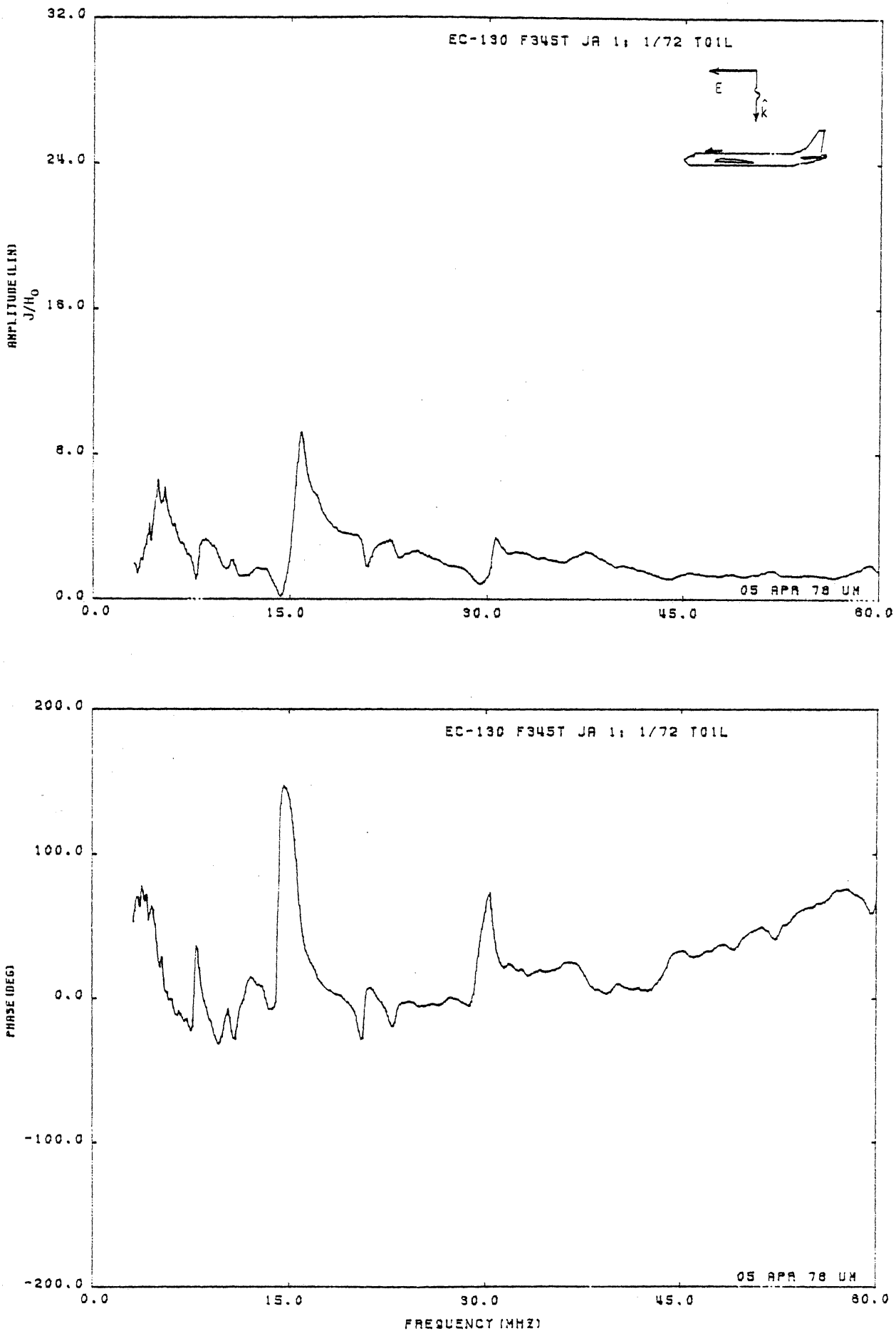

Figure 01L. Axial Current at STA:F345T, Excitation 1, 1/72 Model.

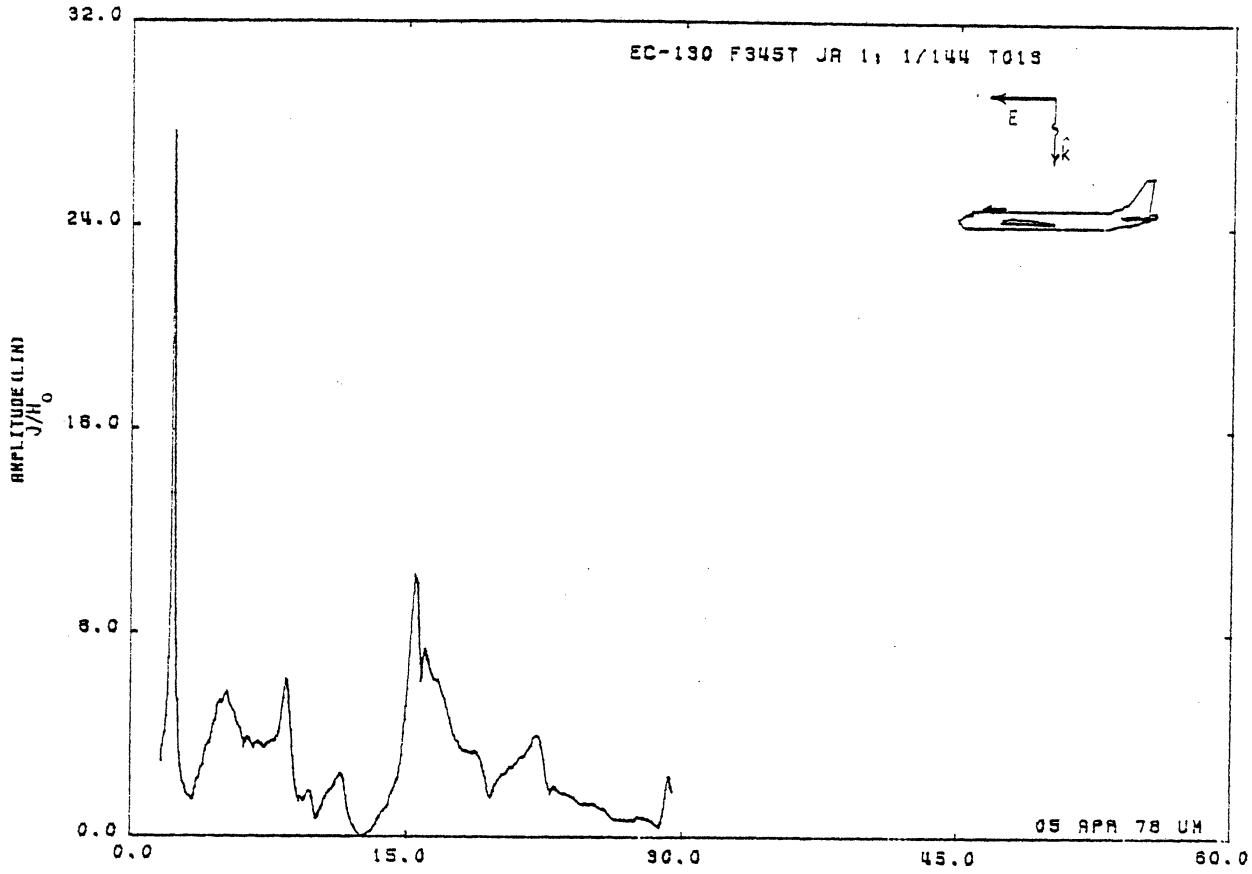

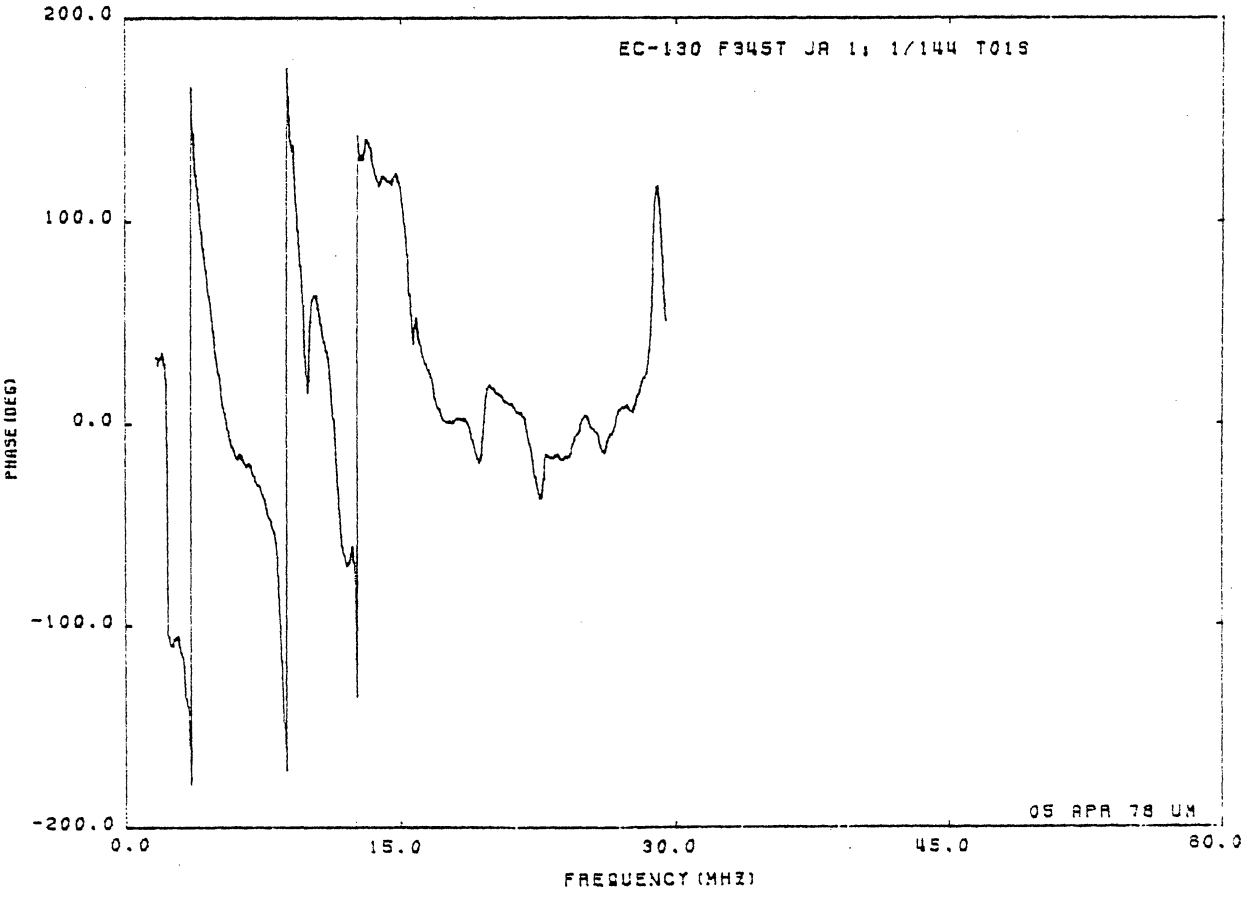

Figure 01S. Axial Current at STA:F345T, Excitation 1, 1/144 Model.

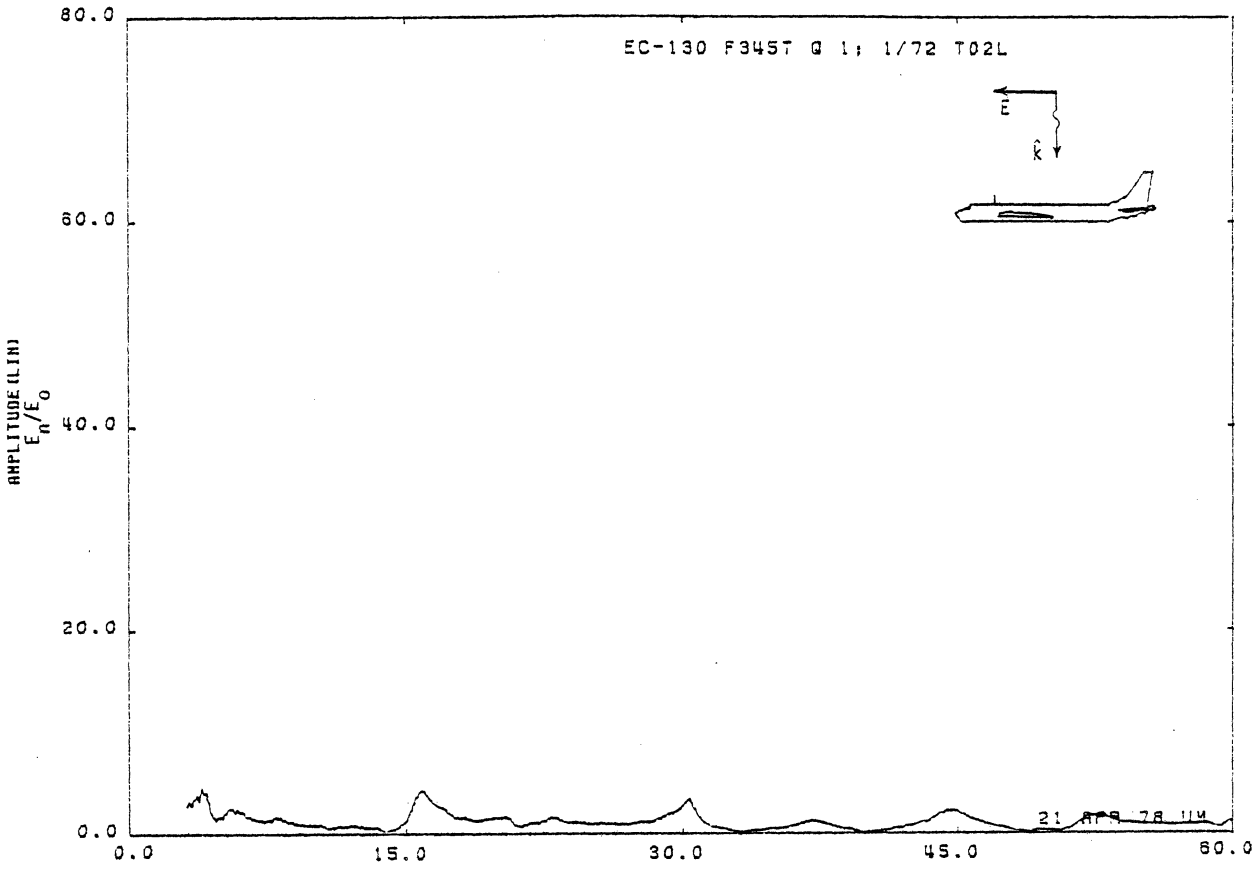

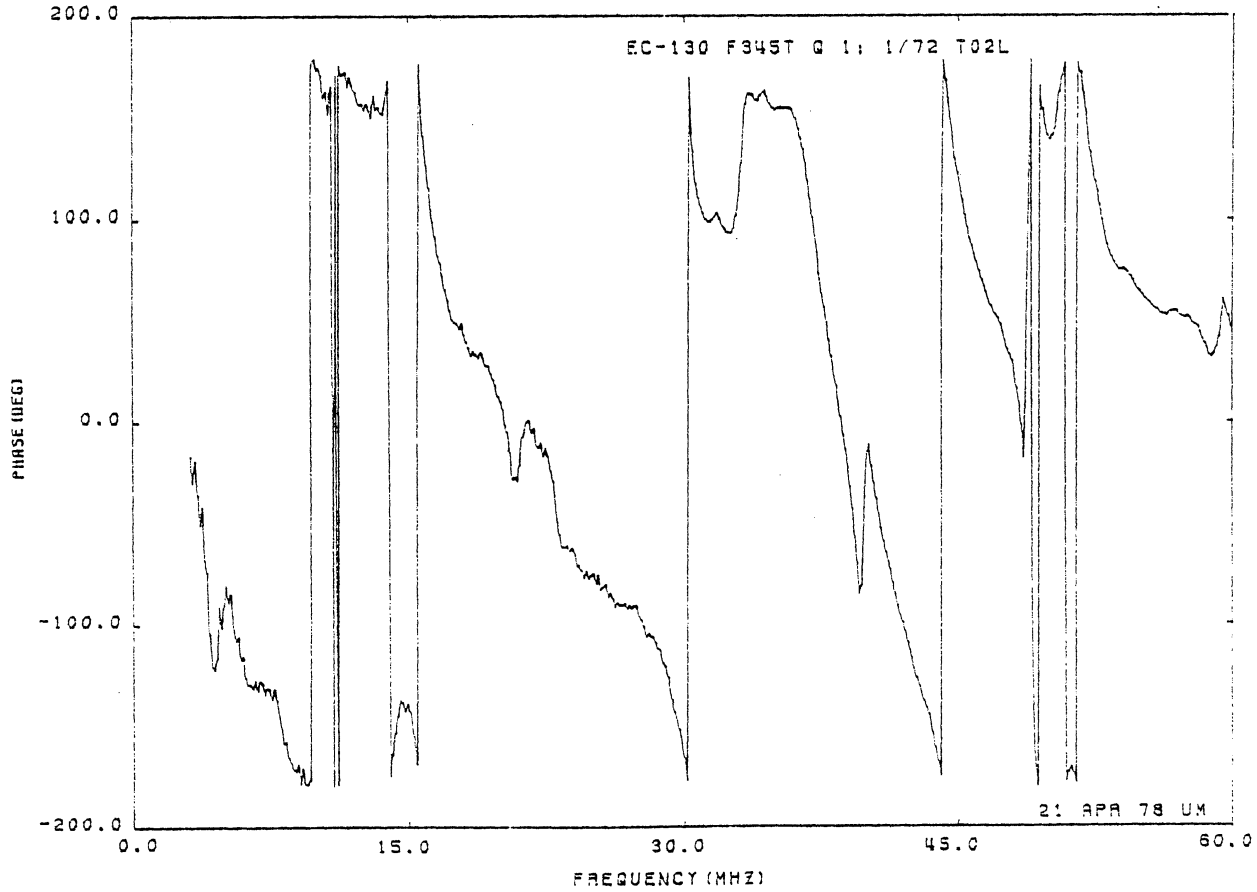

Figure 02L. Charge at STA:F345T, Excitation 1, 1/72 Model.

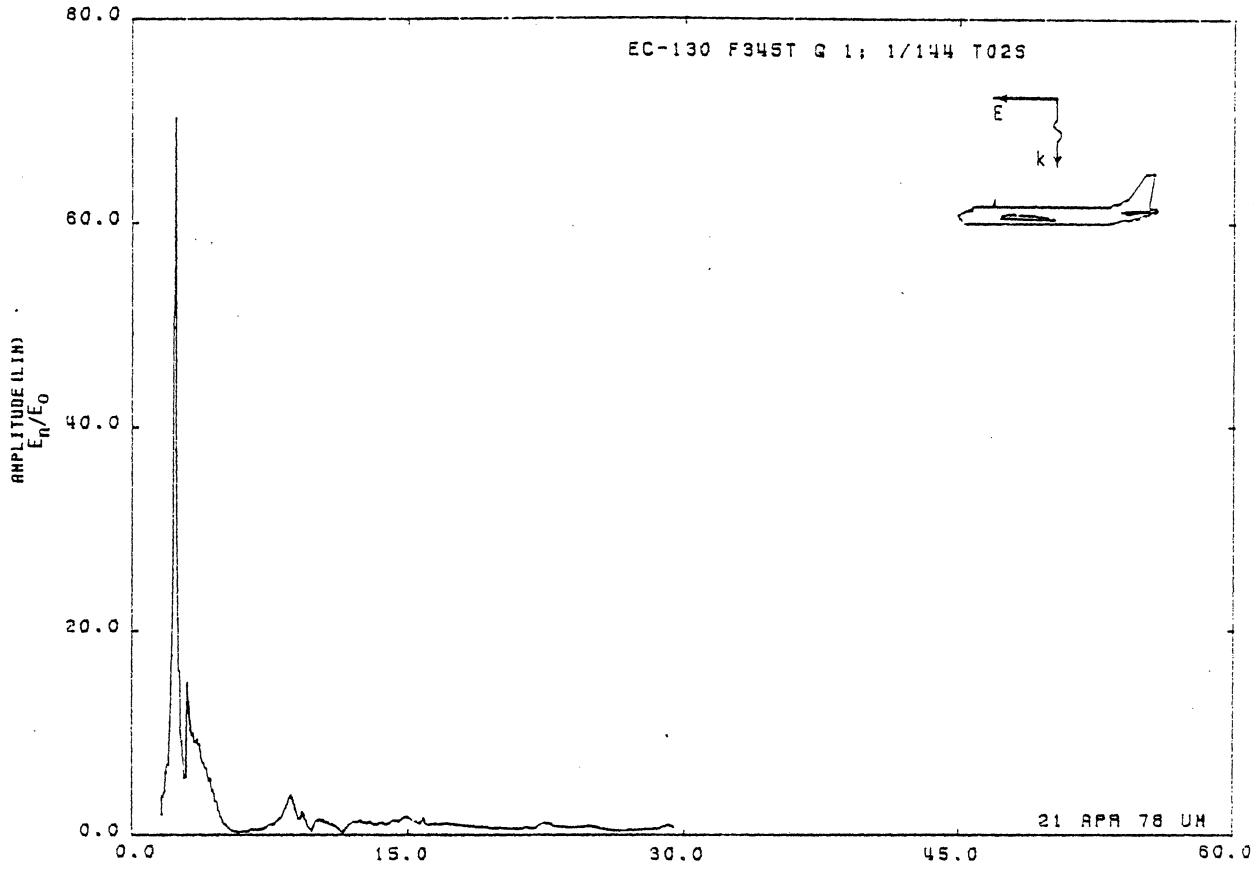

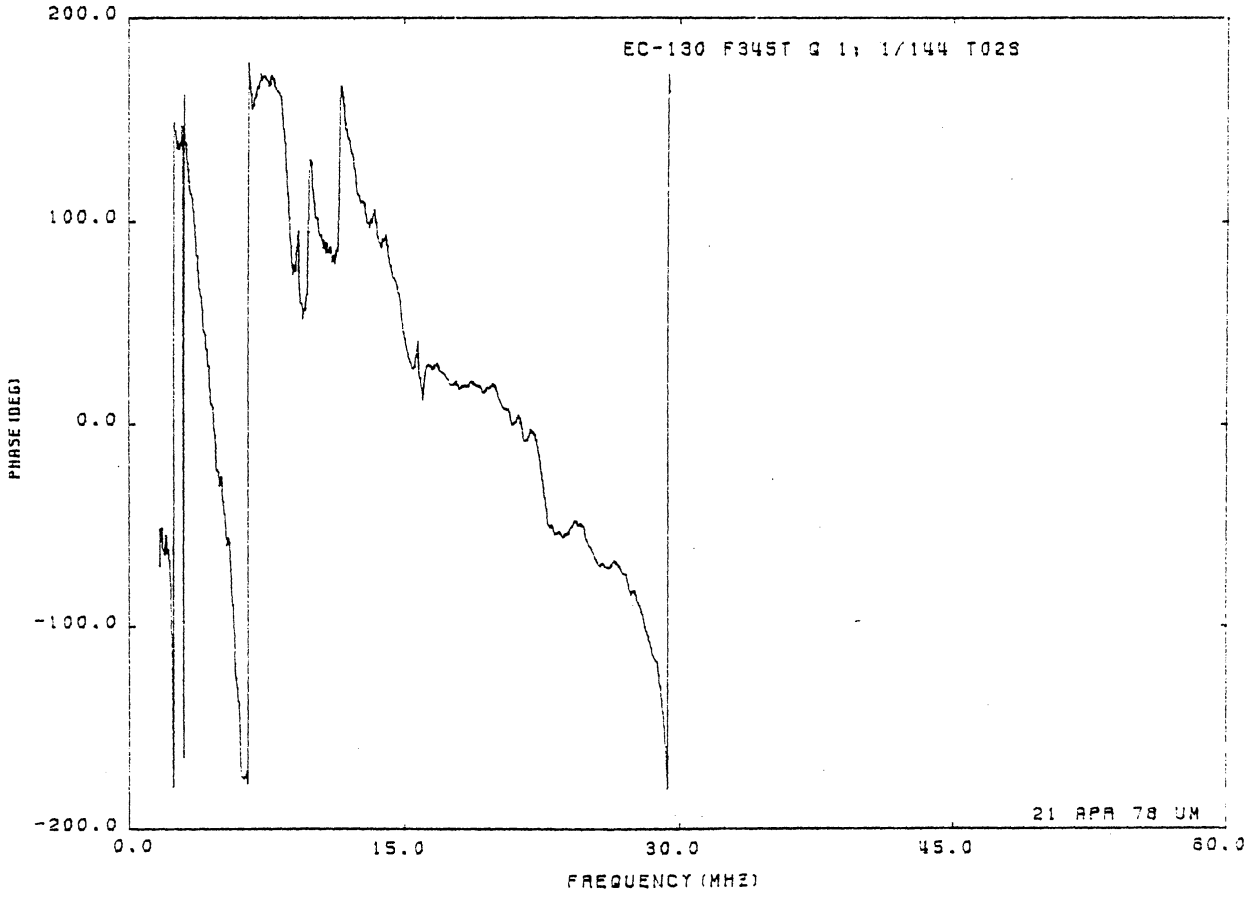

Figure 02S. Charge at STA:F345T, Excitation 1, 1/144 Model.

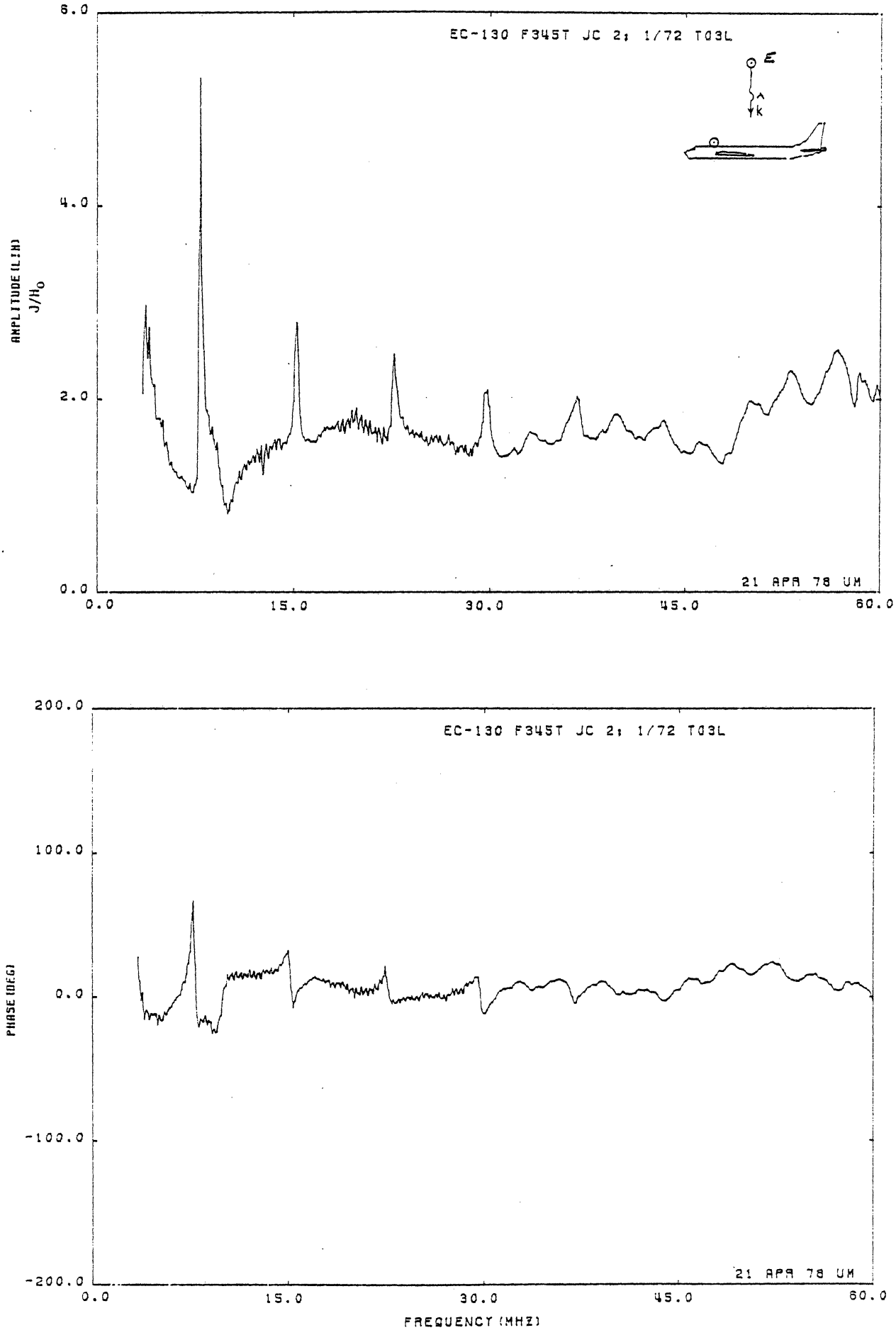

Figure 03L. Circumferential Current at STA:F345T, Excitation 2, 1/72 Model

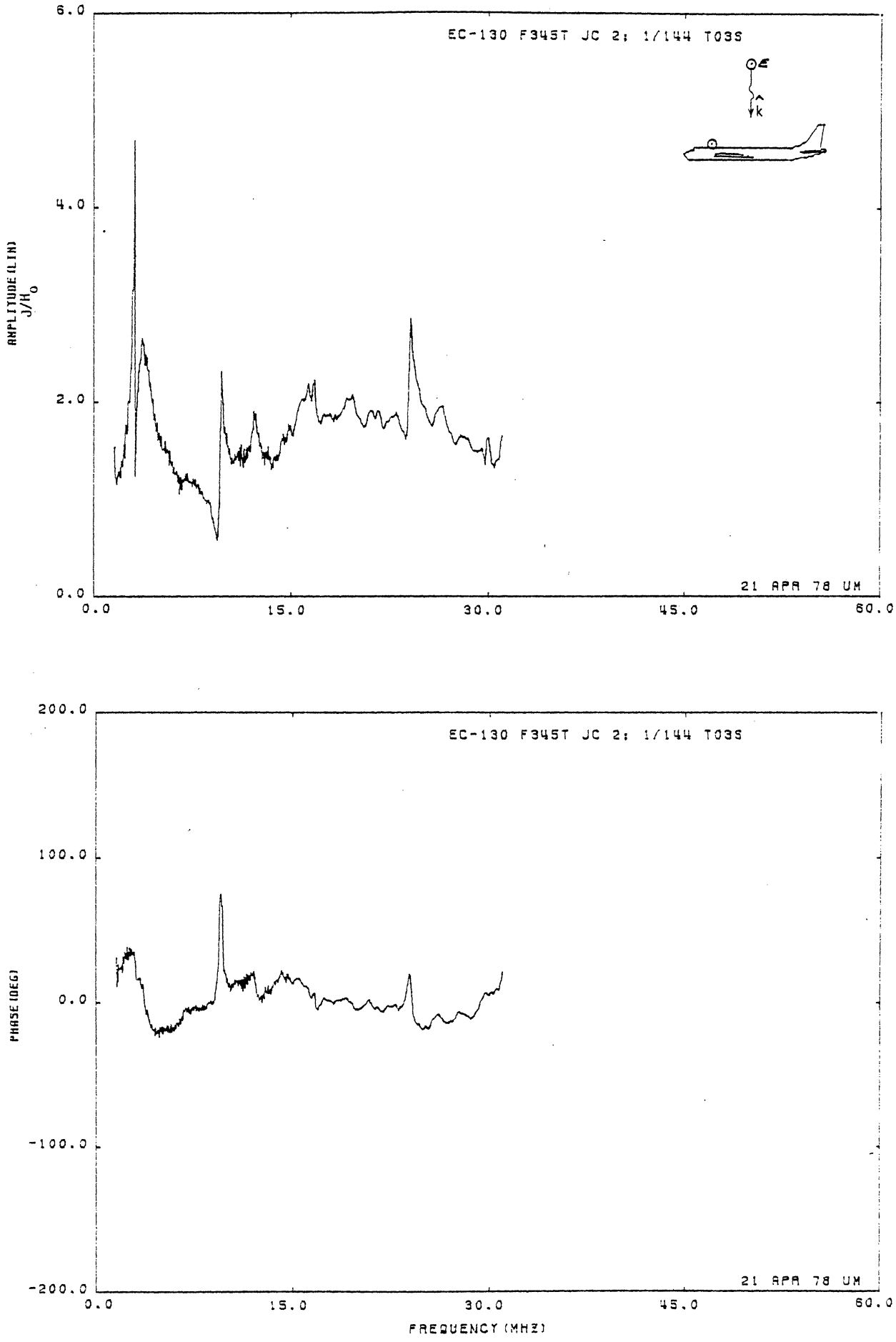

Figure 03S. Circumferential Current at STA:F345T, Excitation 2, 1/144 Model.

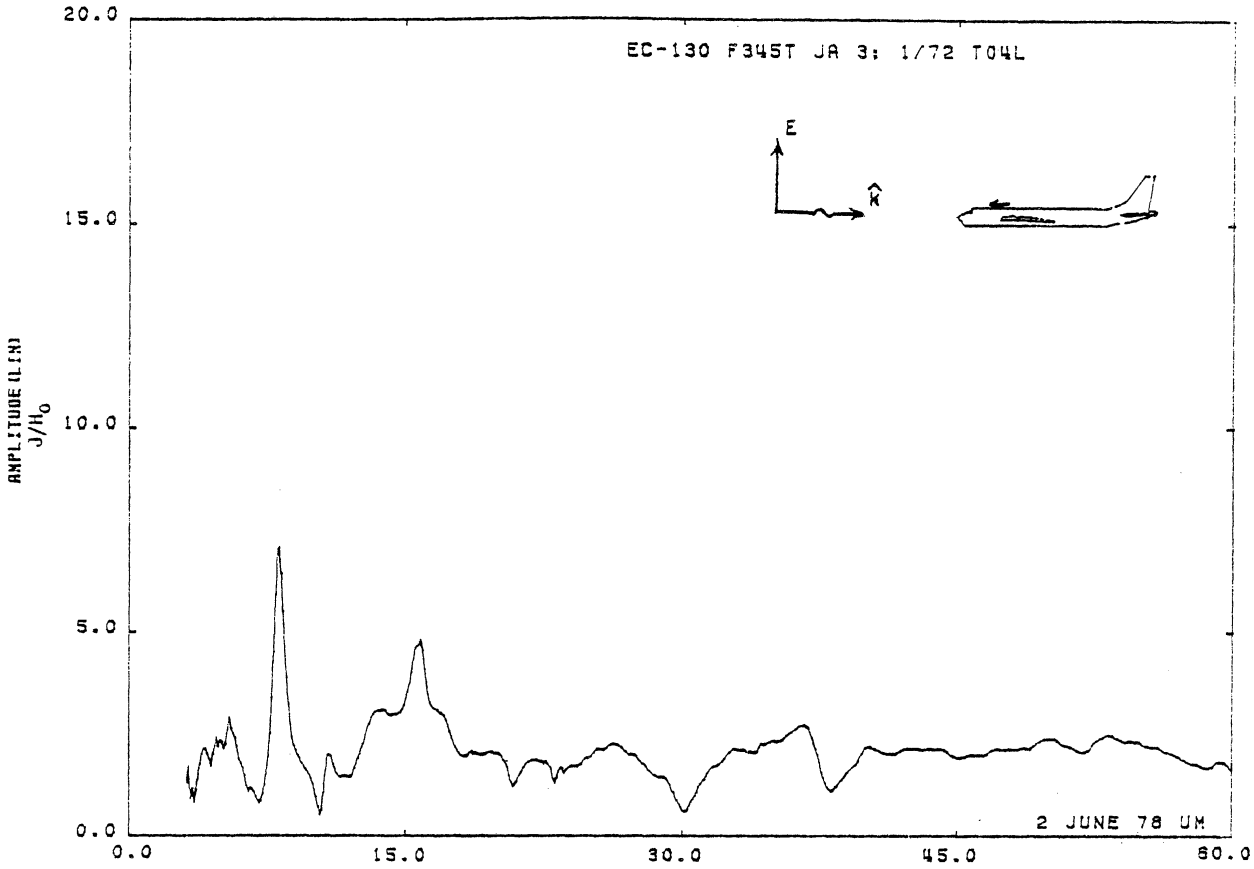

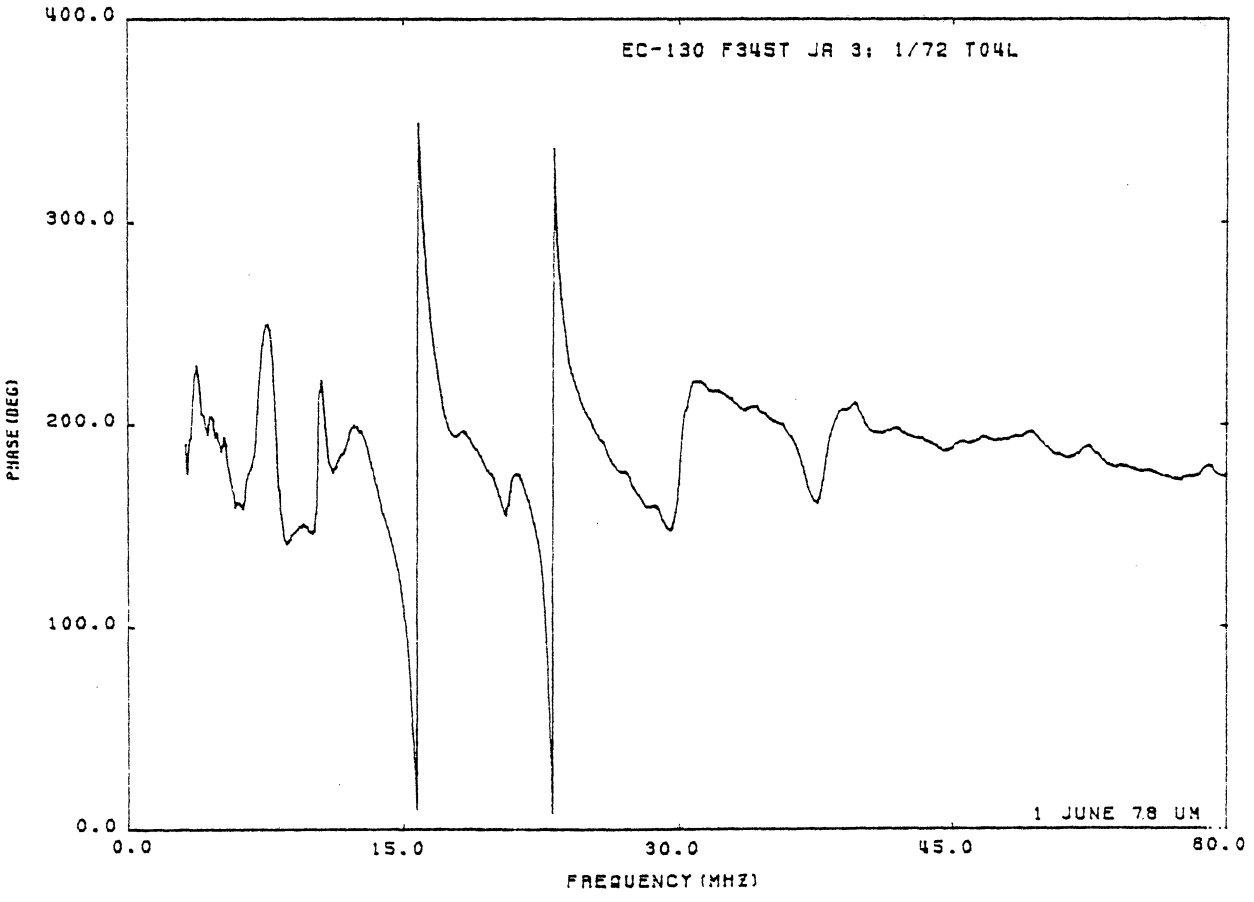

Figure 04L. Axial Current at STA:F345T, Excitation 3, 1/72 Model.

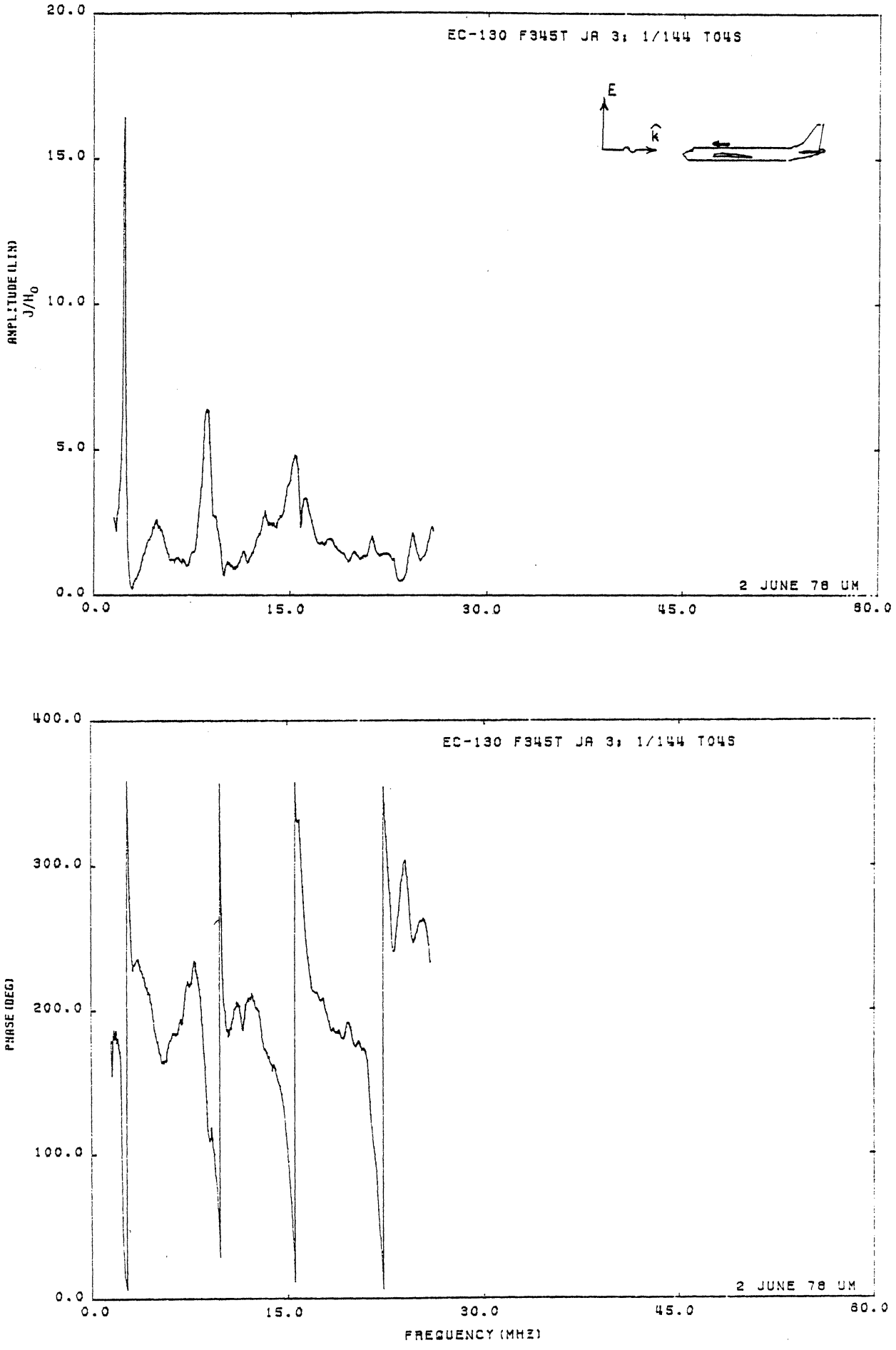

Figure 04S. Axial Current at STA:F345T, Excitation 3, 1/144 Model.

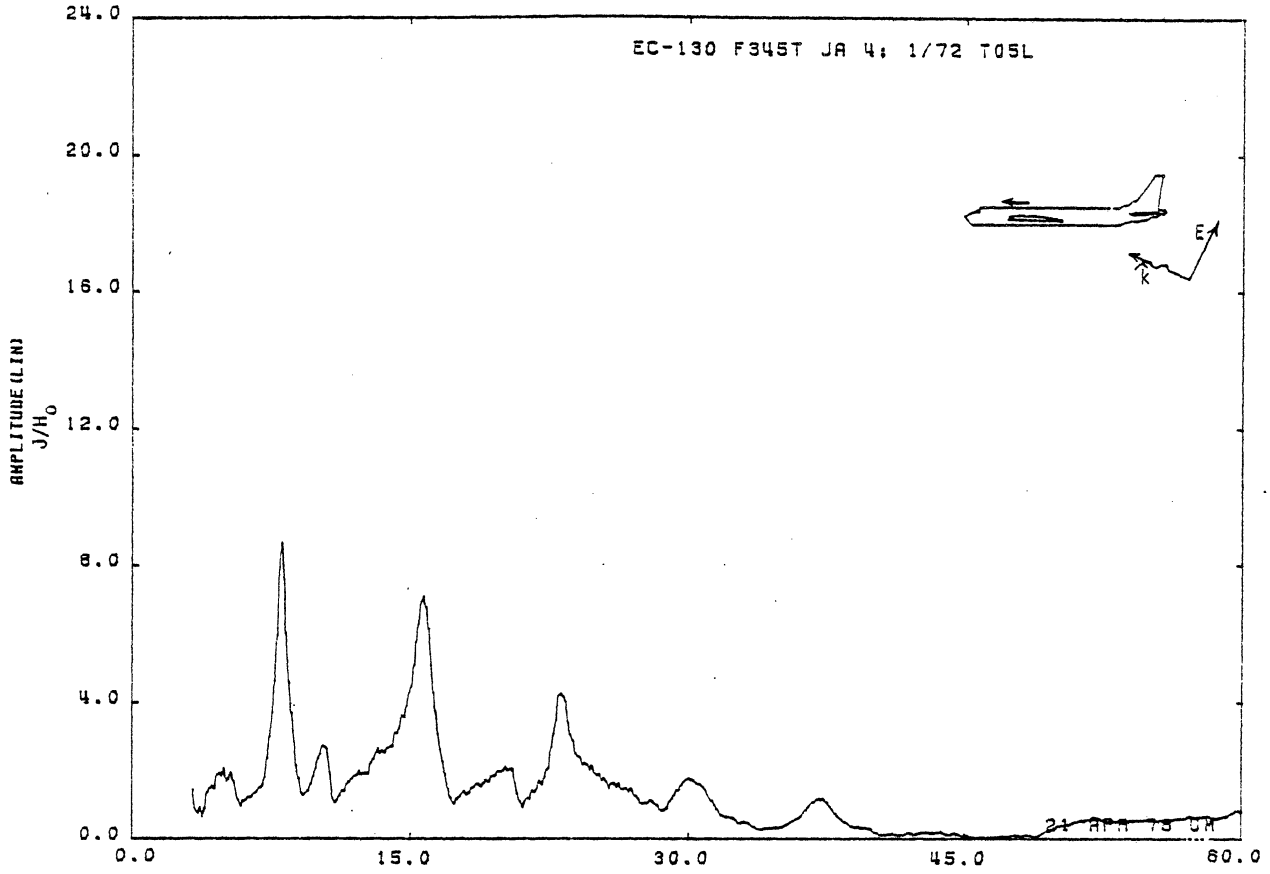

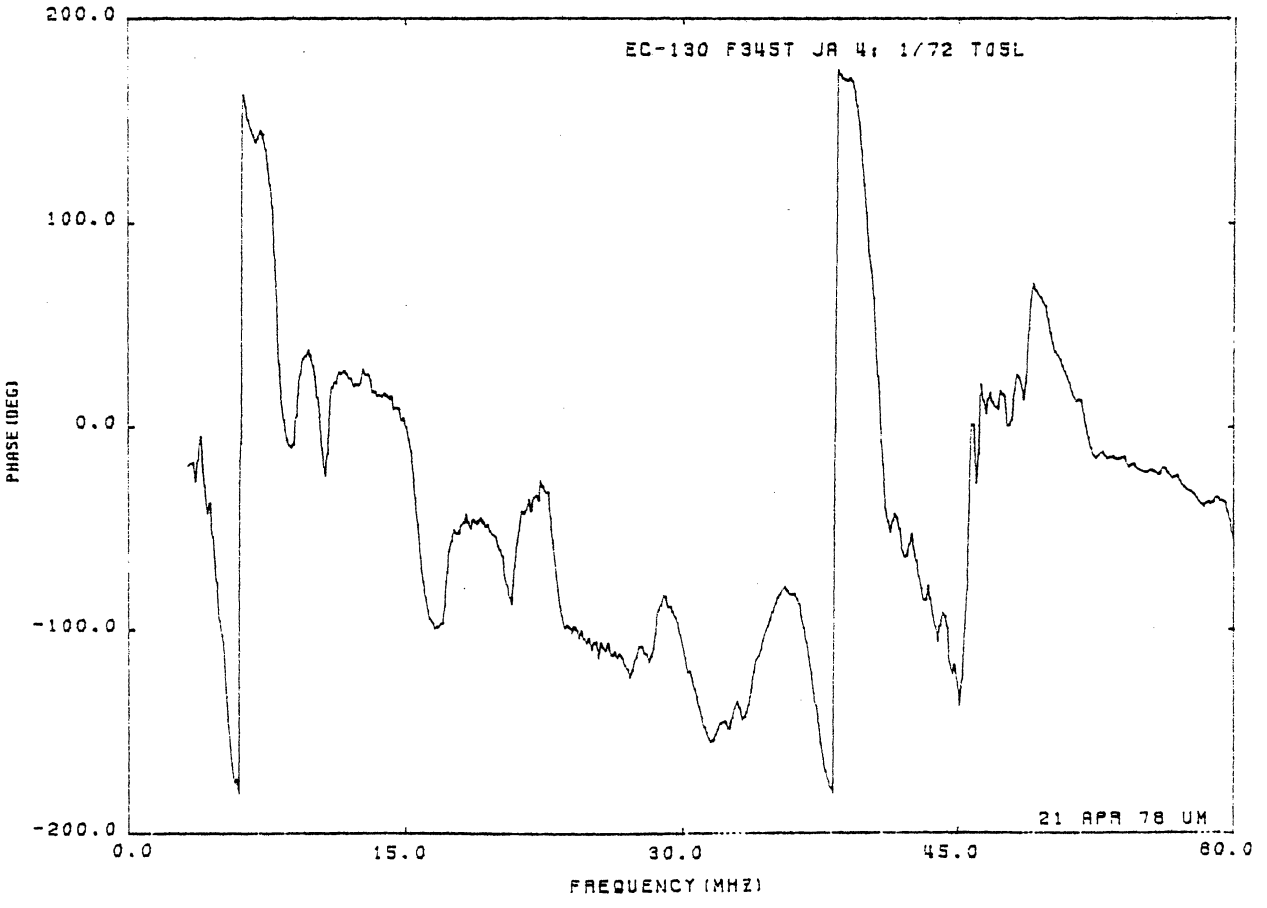

Figure 05L. Axial Current at STA:F345T, Excitation 4, 1/72 Model.

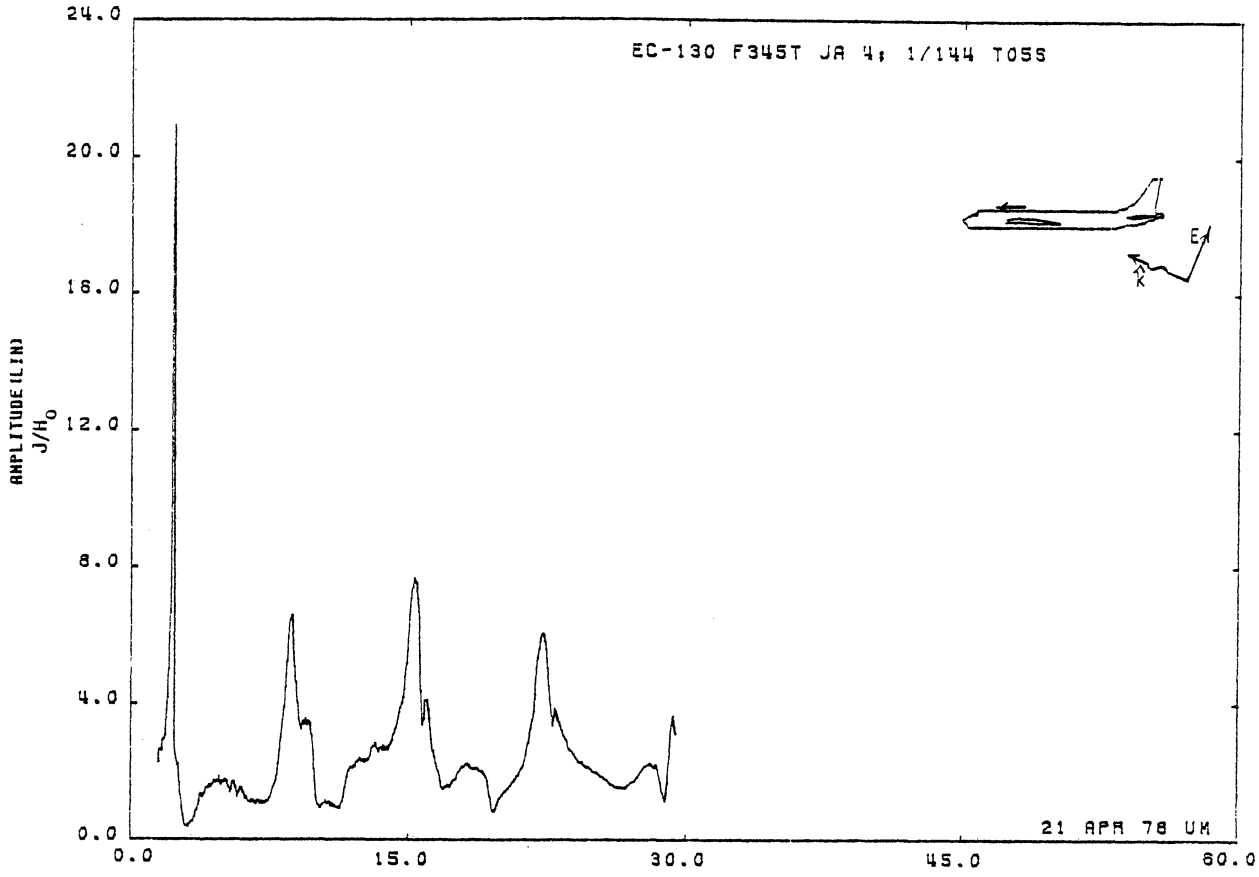

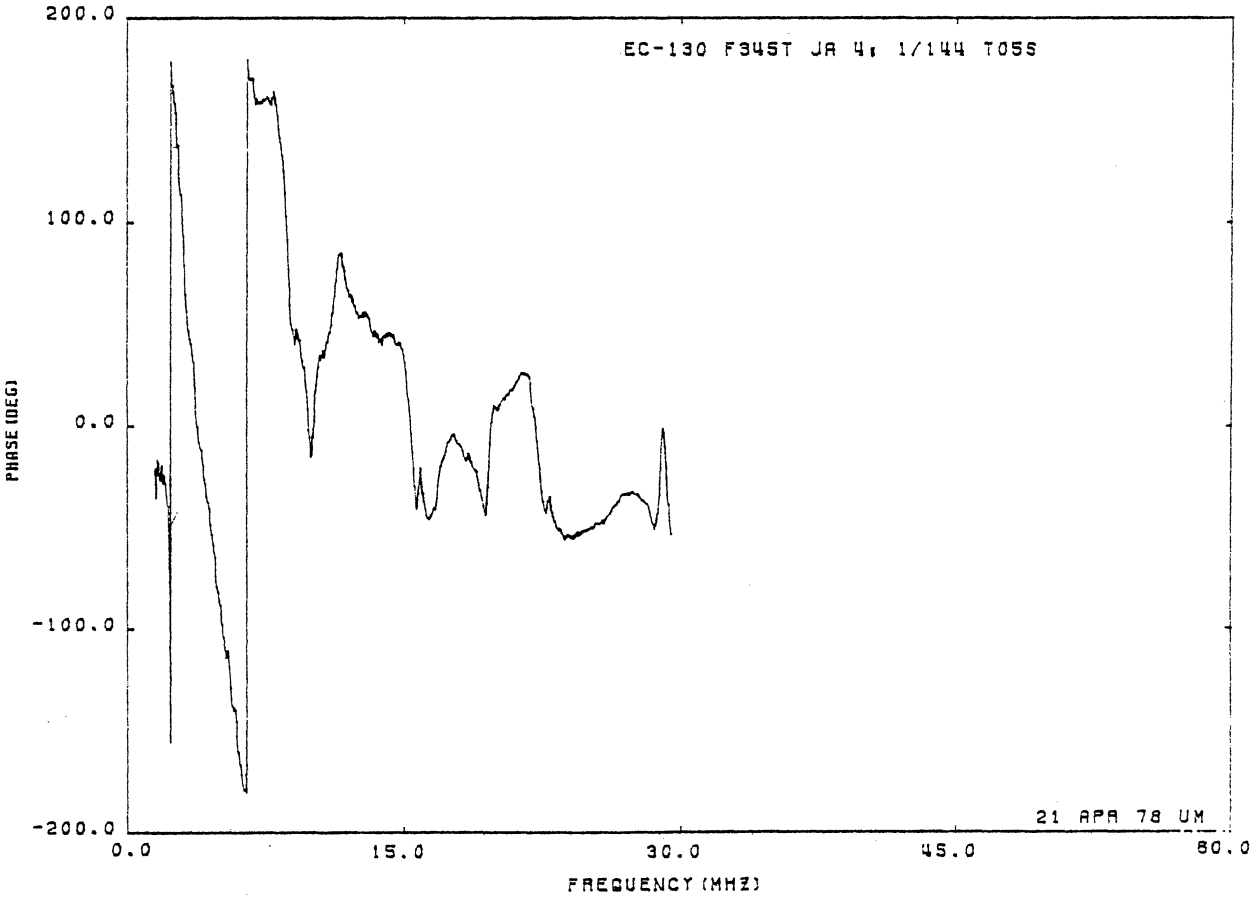

Figure 05S. Axial Current at STA:F345T, Excitation 4, 1/144 Model.

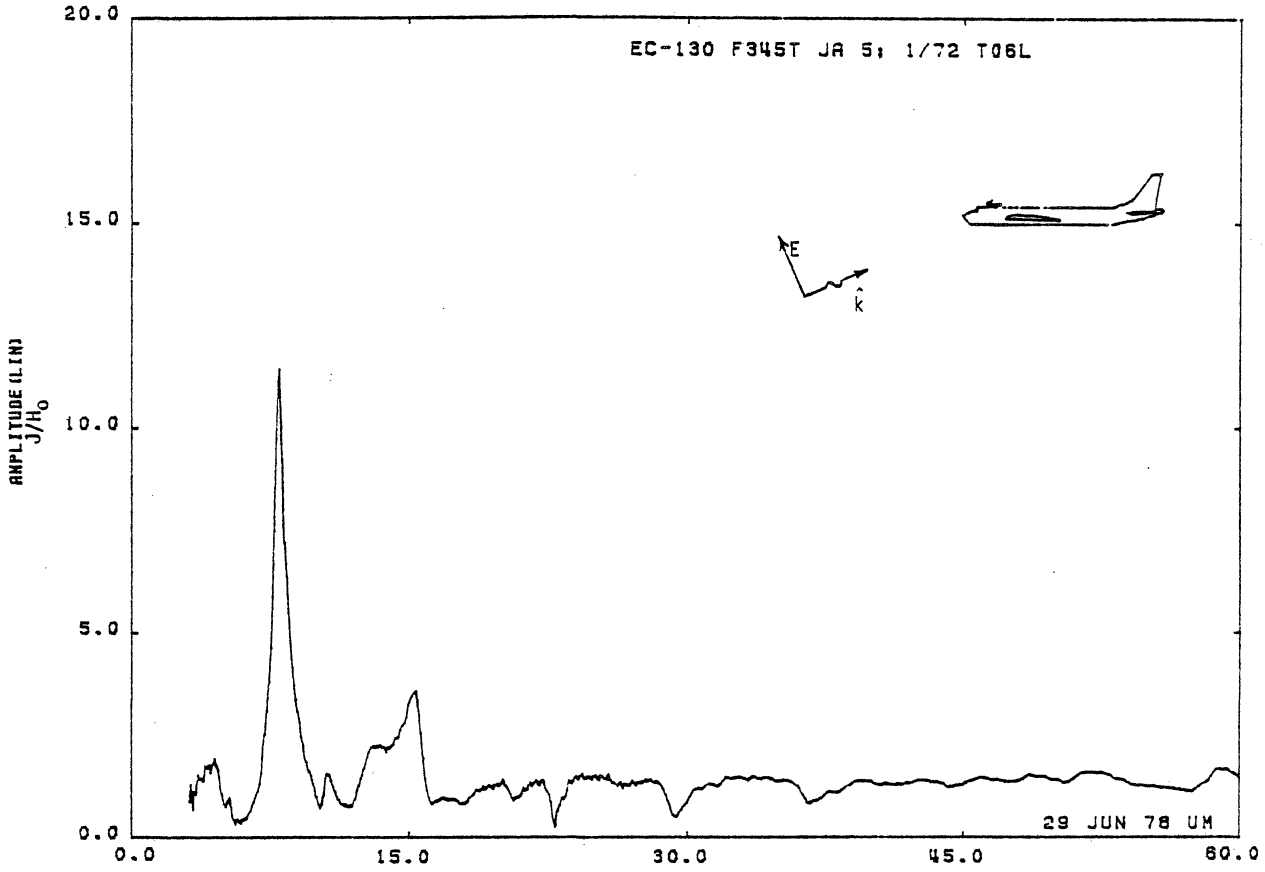

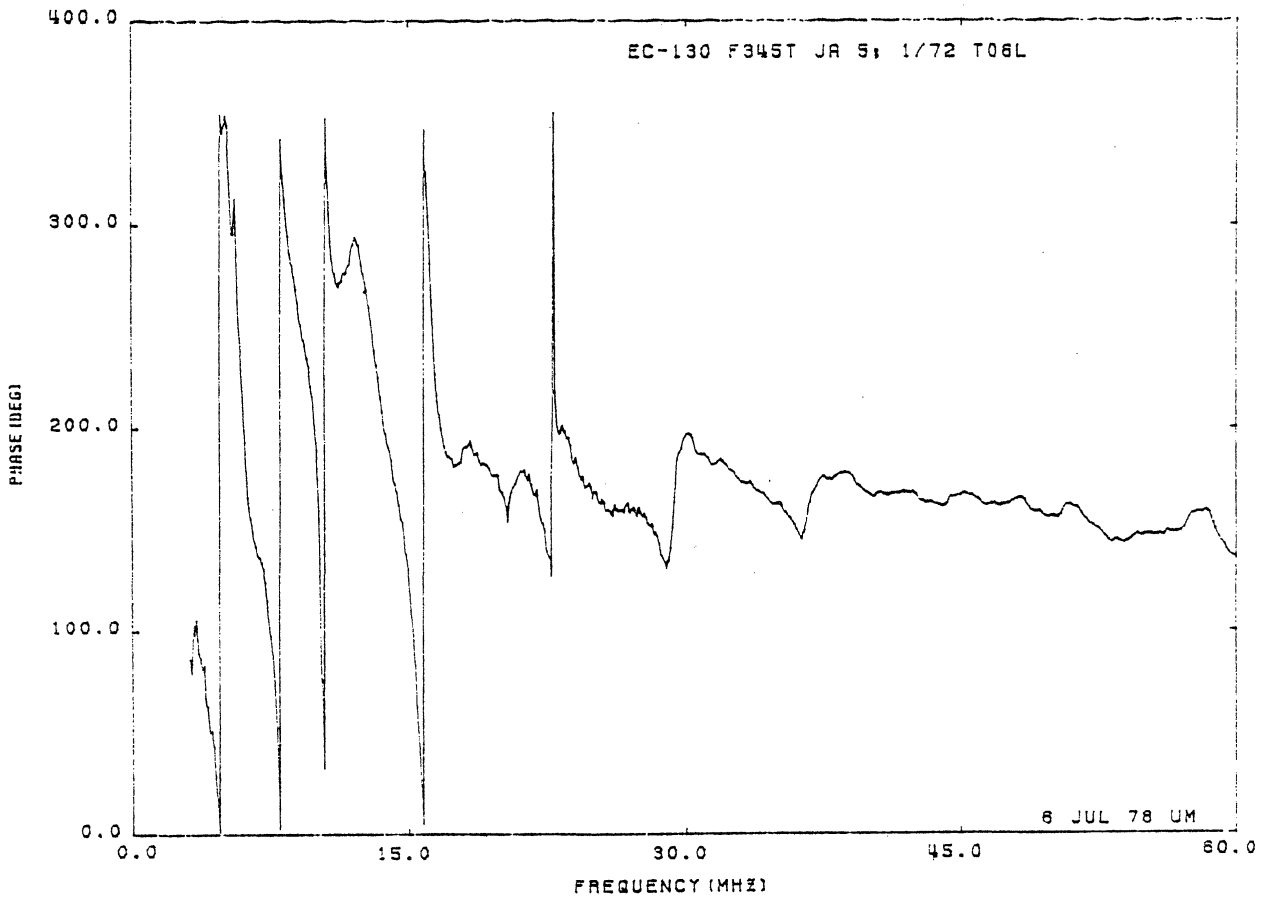

Figure 06L. Axial Current at STA:F345T, Excitation 5, 1/72 Model.

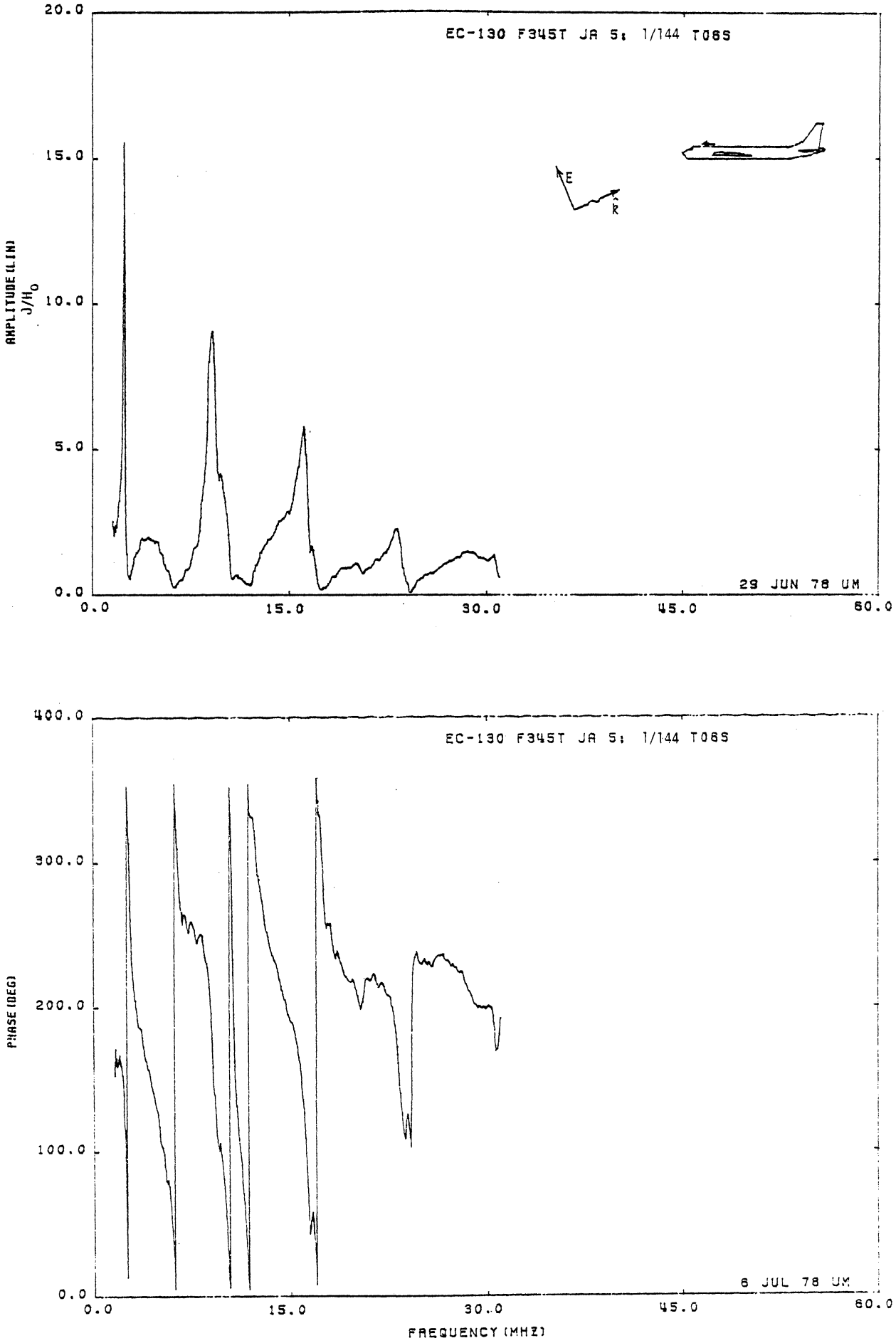

Figure 06S. Axial Current at STA:F345T, Excitation 5, 1/144 Model.

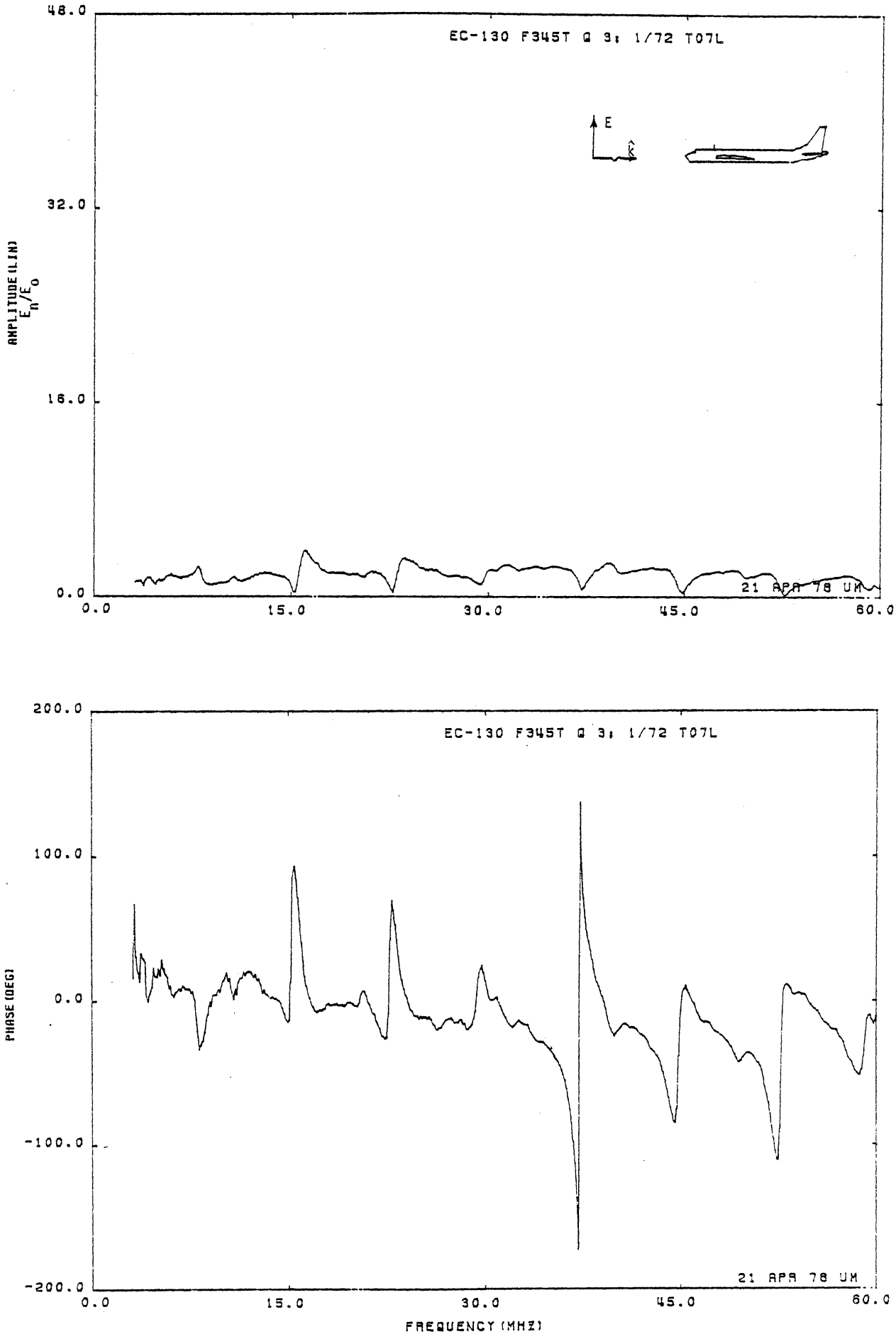

Figure 07L. Charge at STA:F345T, Excitation 3, 1/72 Model.

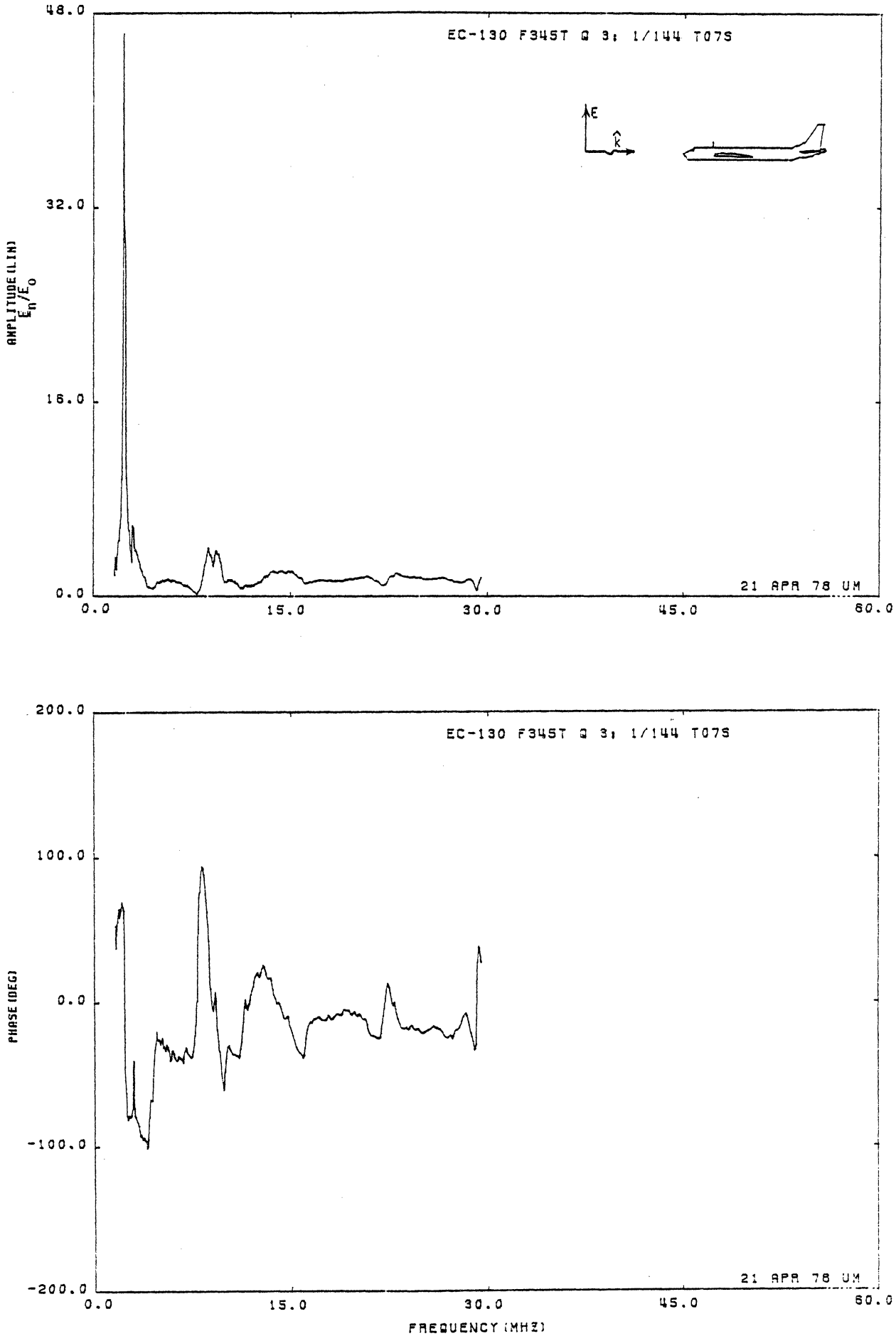

Figure 07S. Charge at STA:F345T, Excitation 3, 1/144 Model.

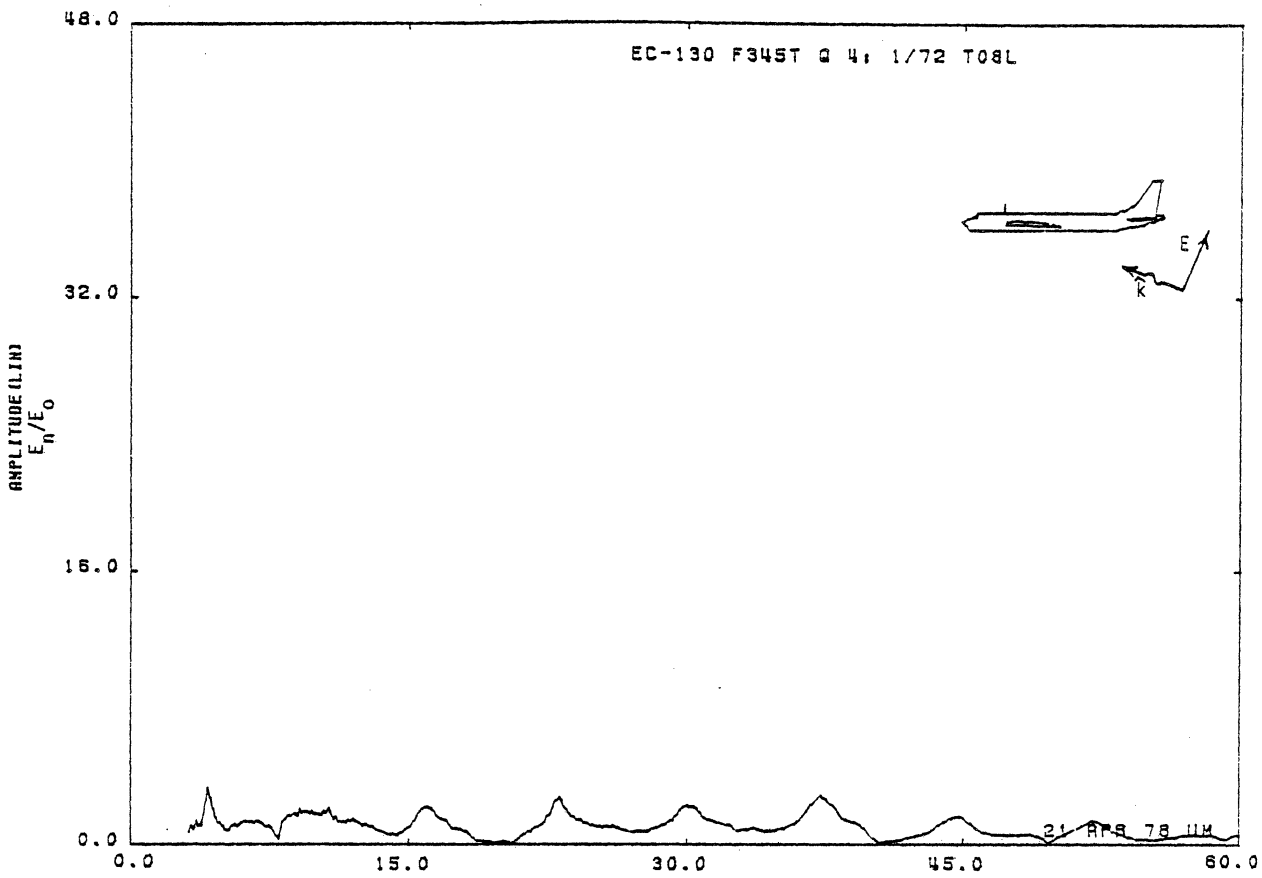

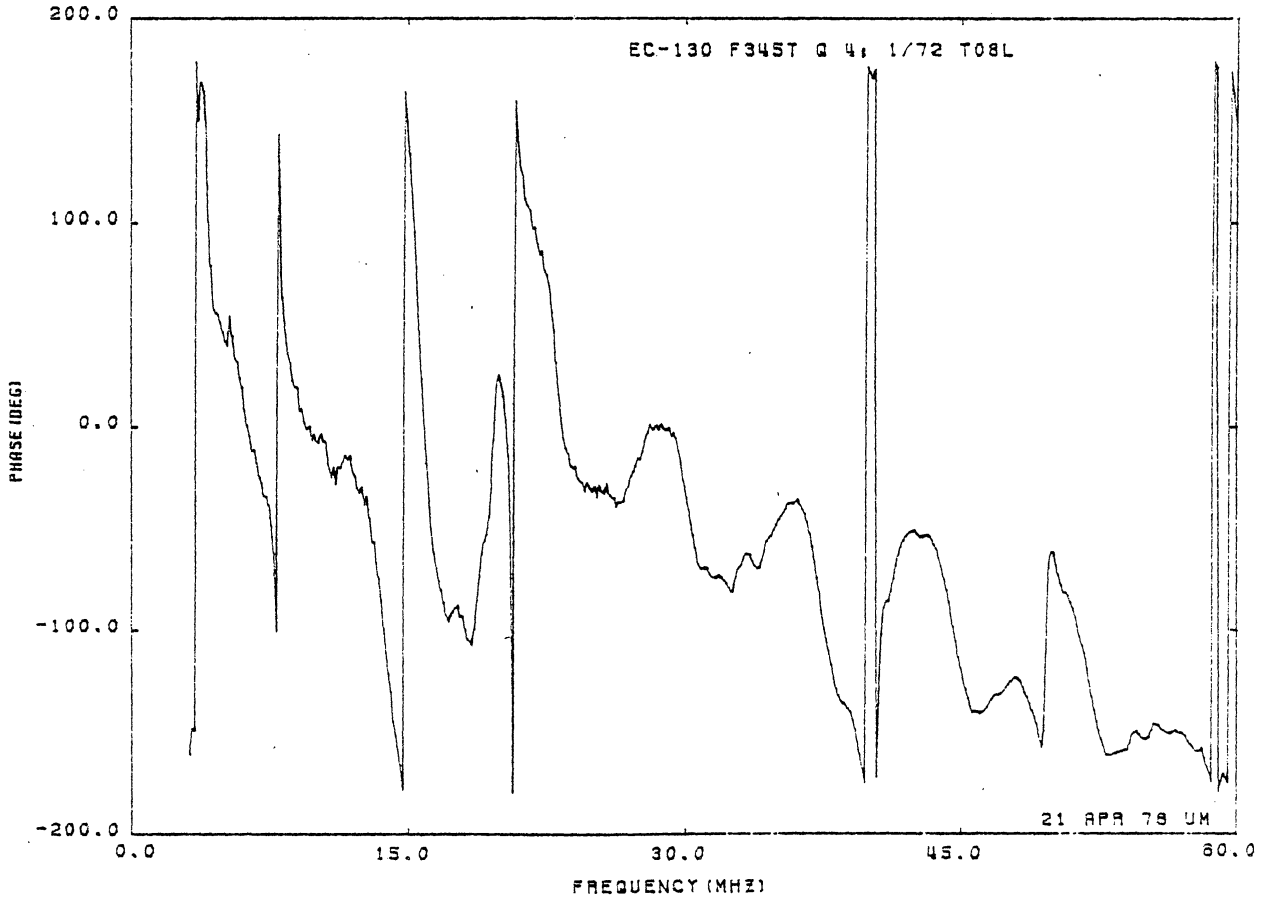

Figure 08L. Charge at STA:F345T, Excitation 4, 1/72 Model.

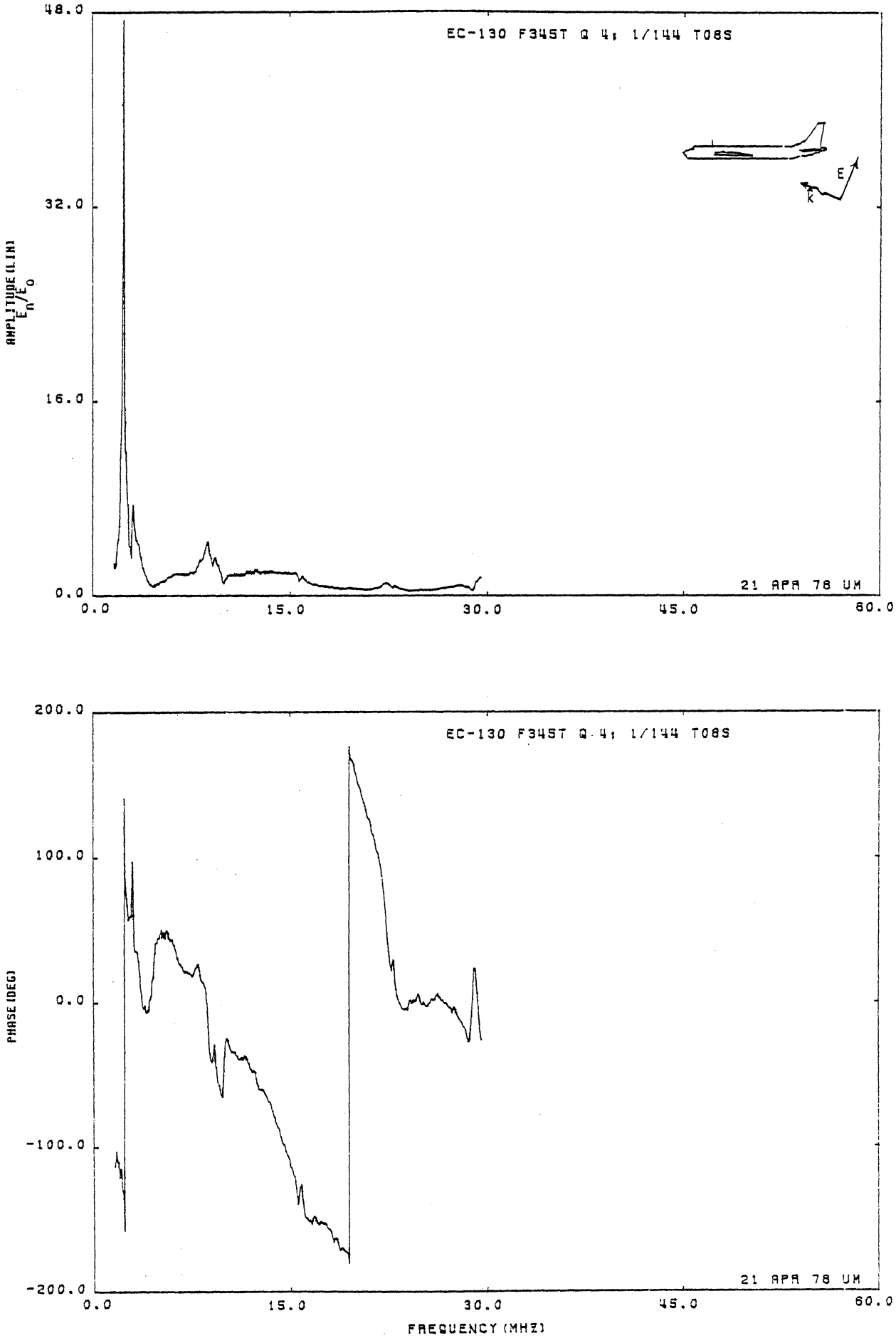

Figure 08S. Charge at STA:F345T, Excitation 4, 1/144 Model.

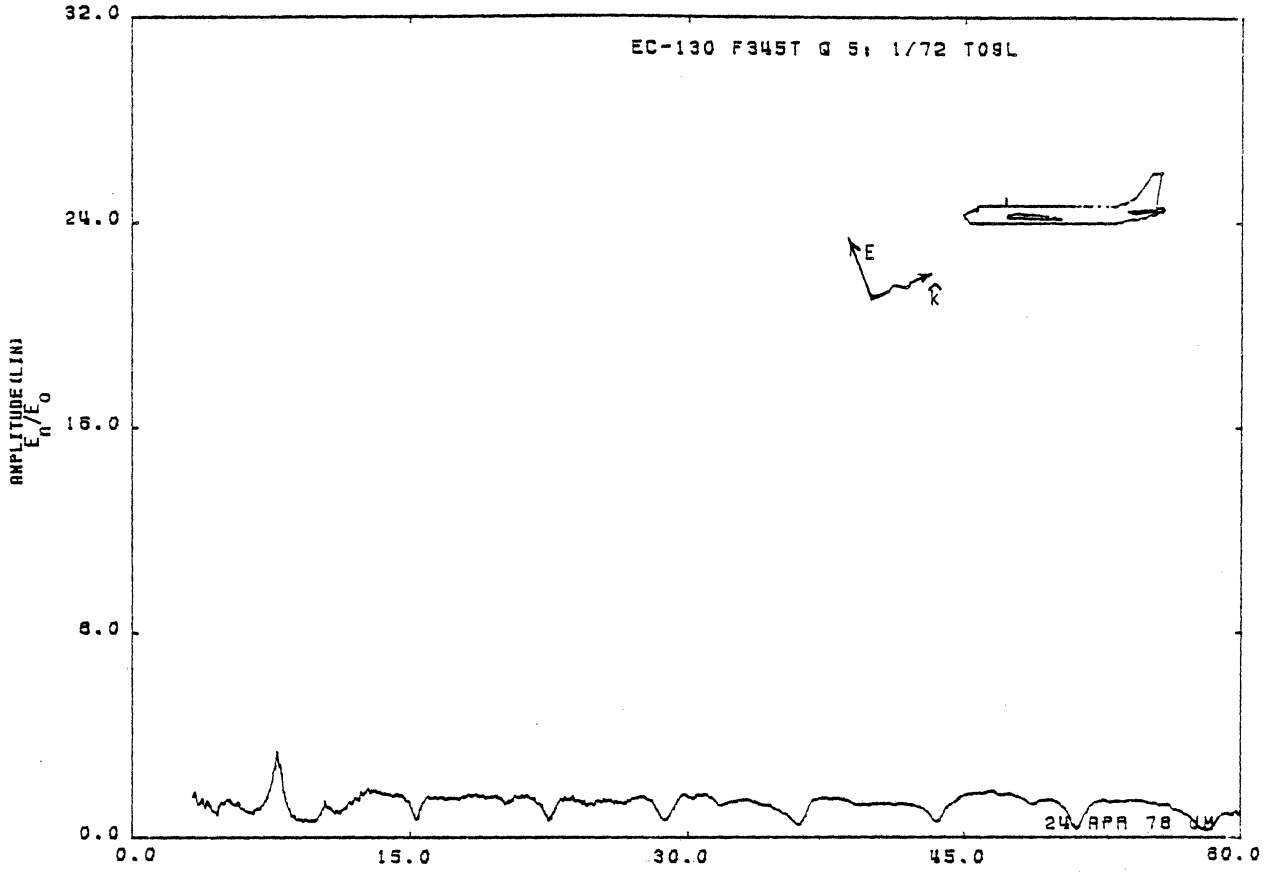

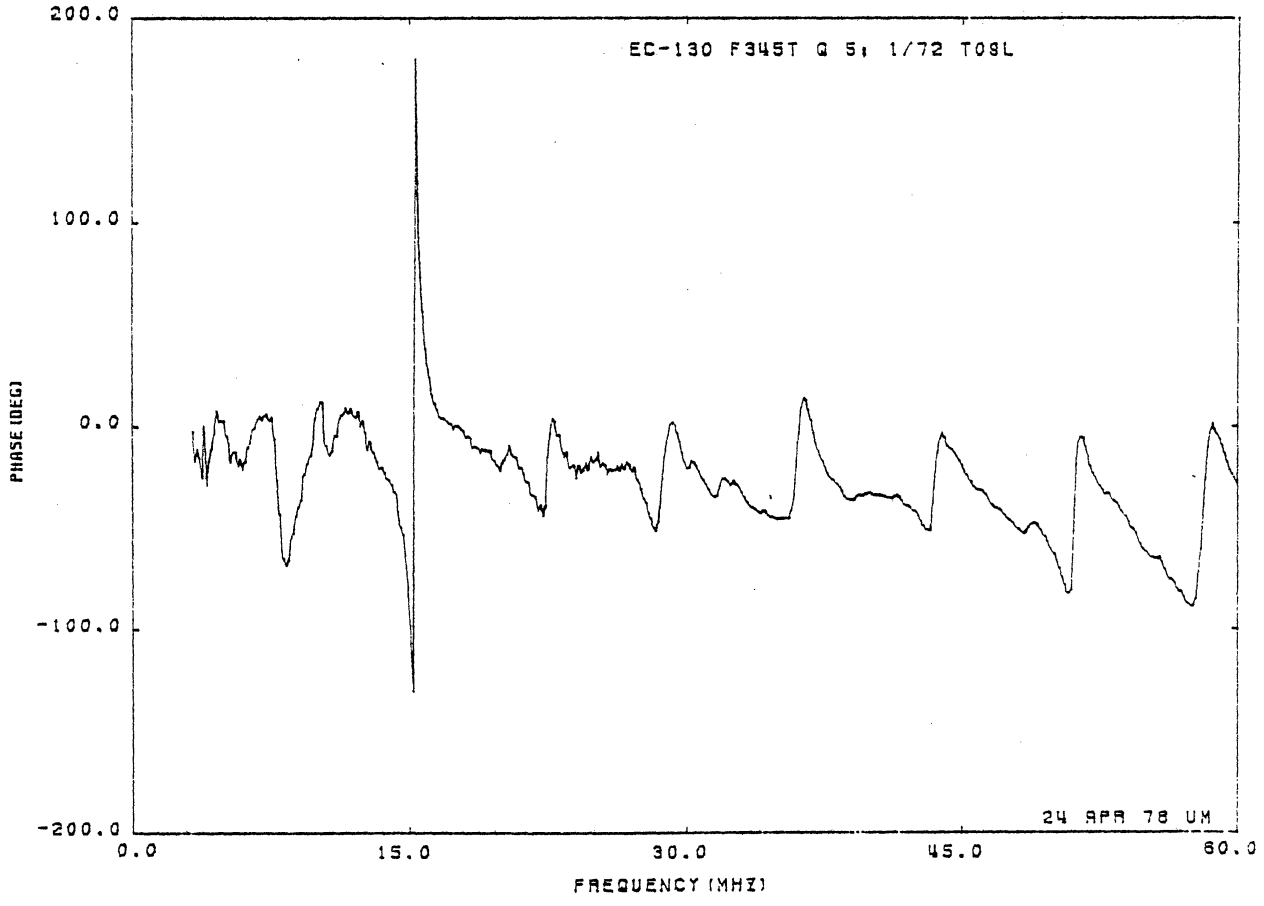

Figure 09L. Charge at STA:F345T, Excitation 5, 1/72 Model.

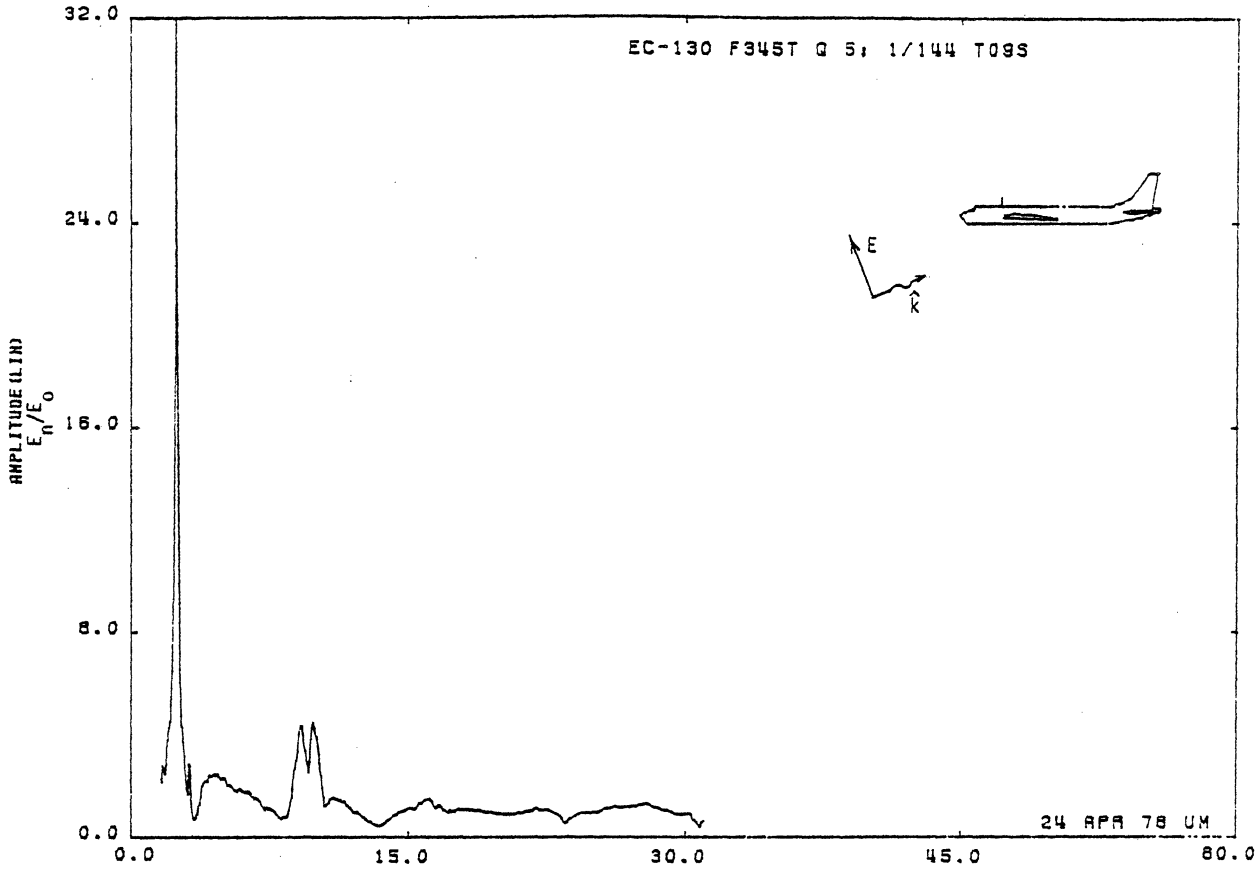

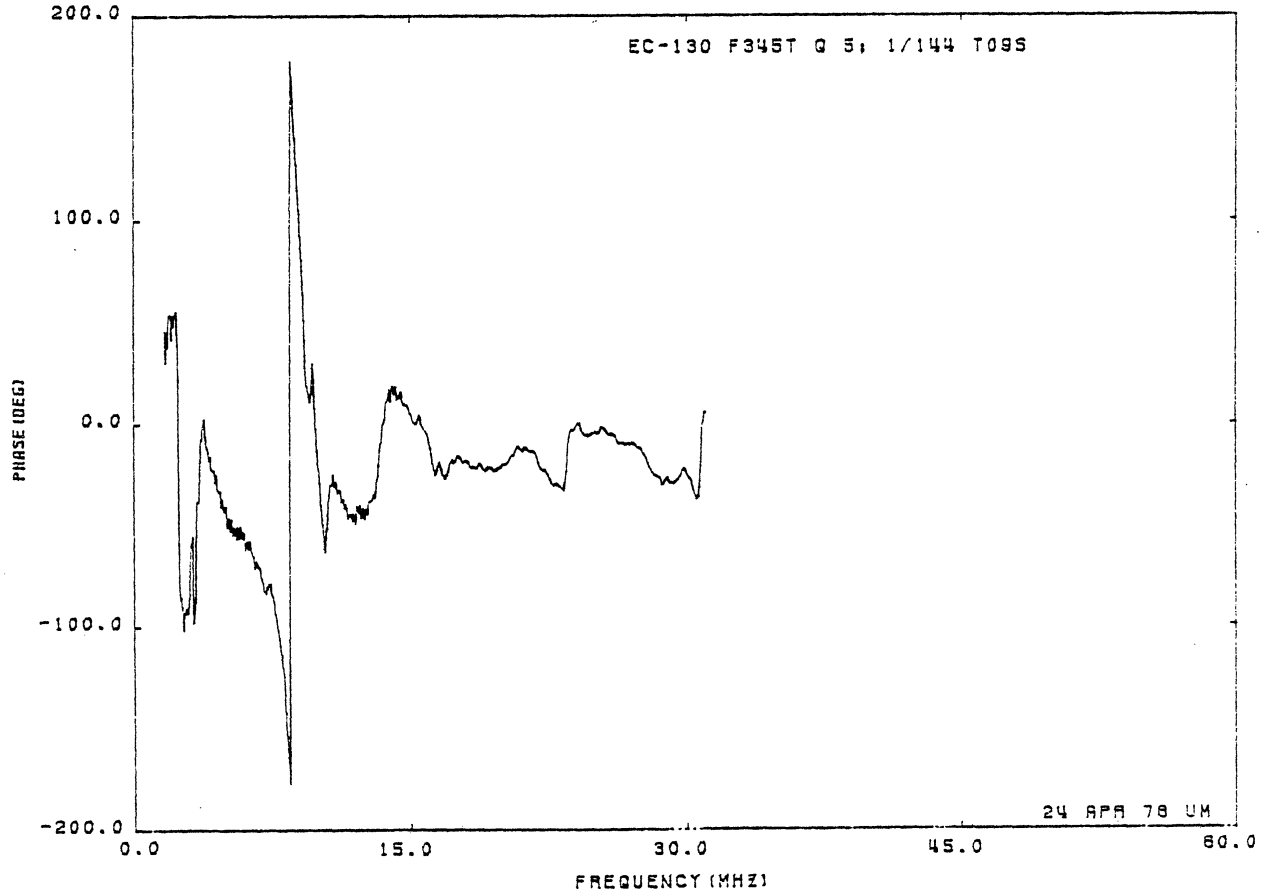

Figure 09S. Charge at STA:F345T, Excitation 5, 1/144 Model.

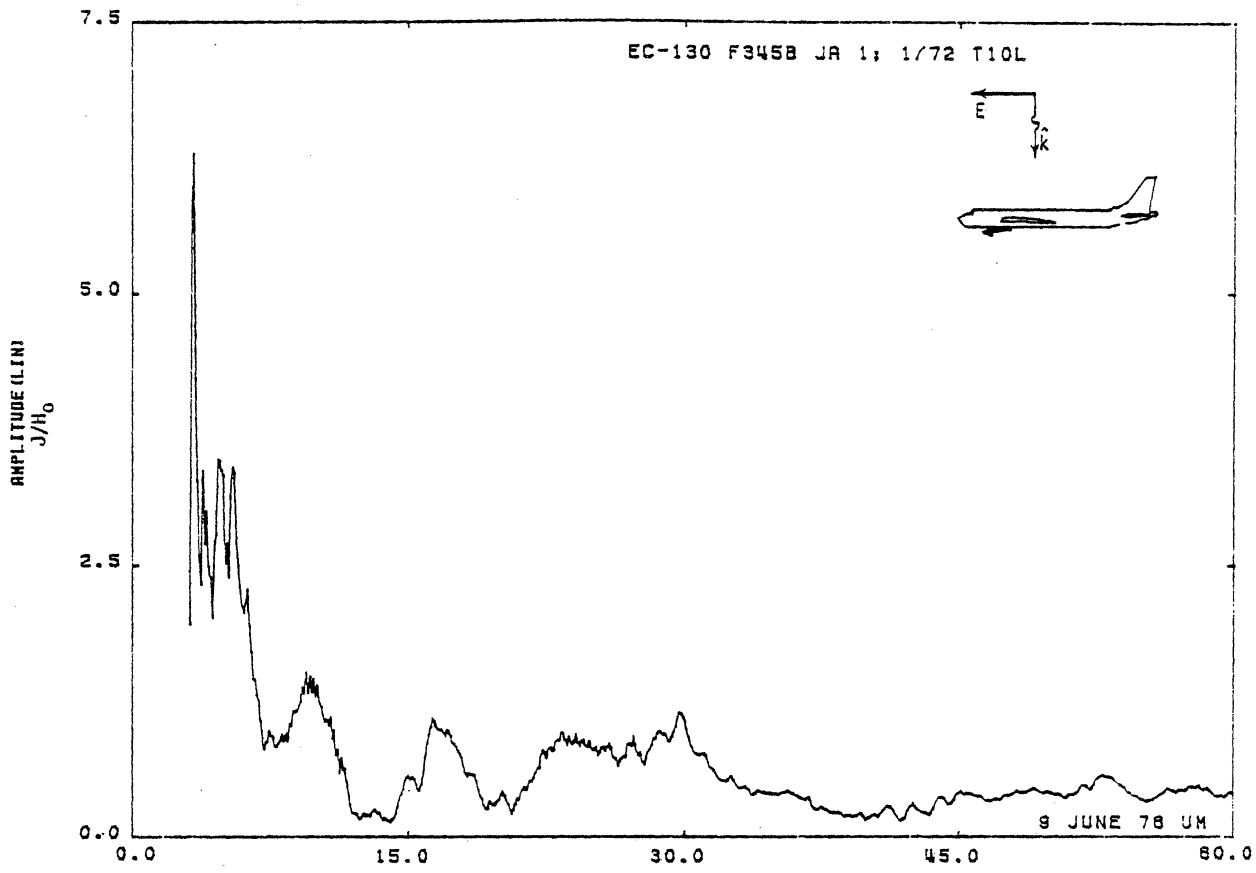

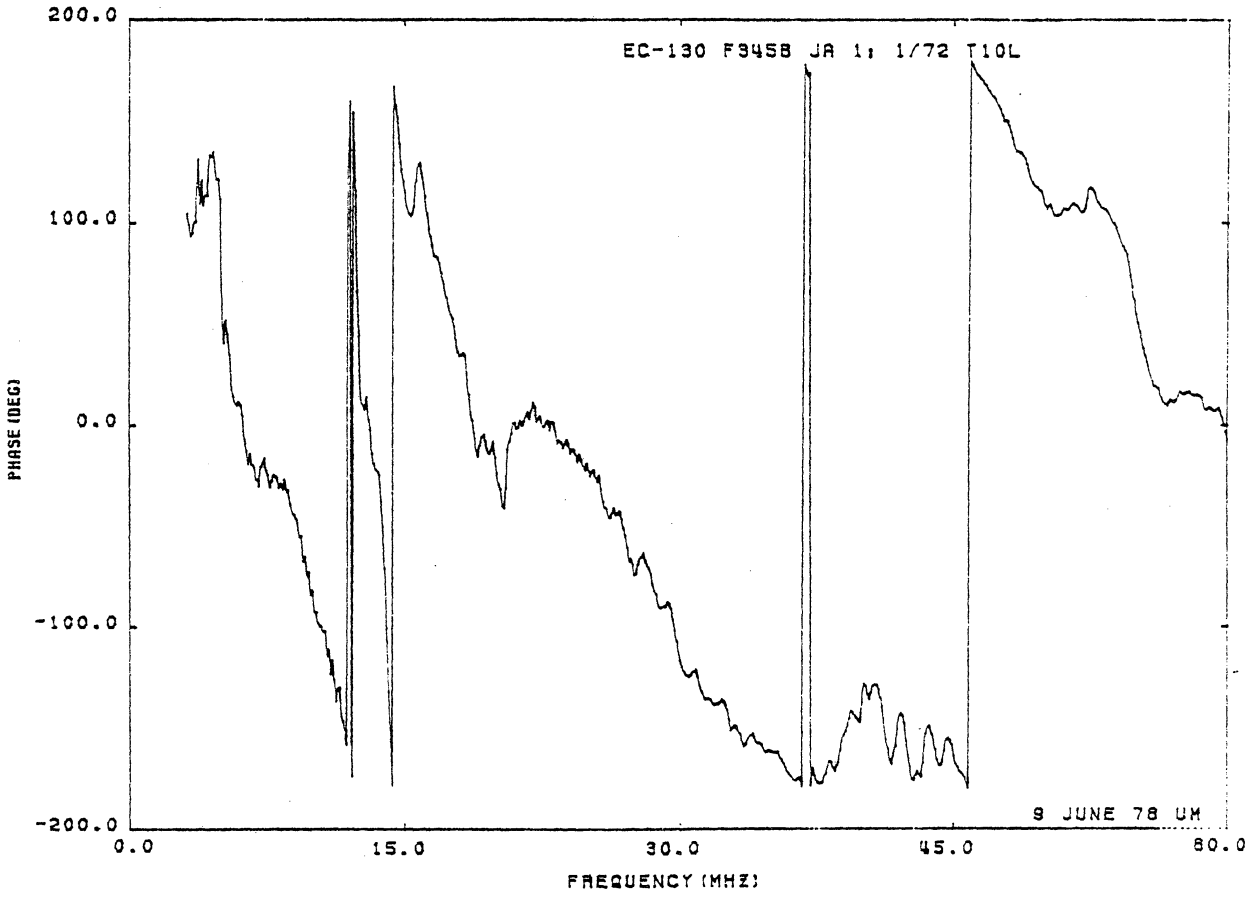

Figure 10L. Axial Current at STA:F345B, Excitation 1, 1/72 Model.

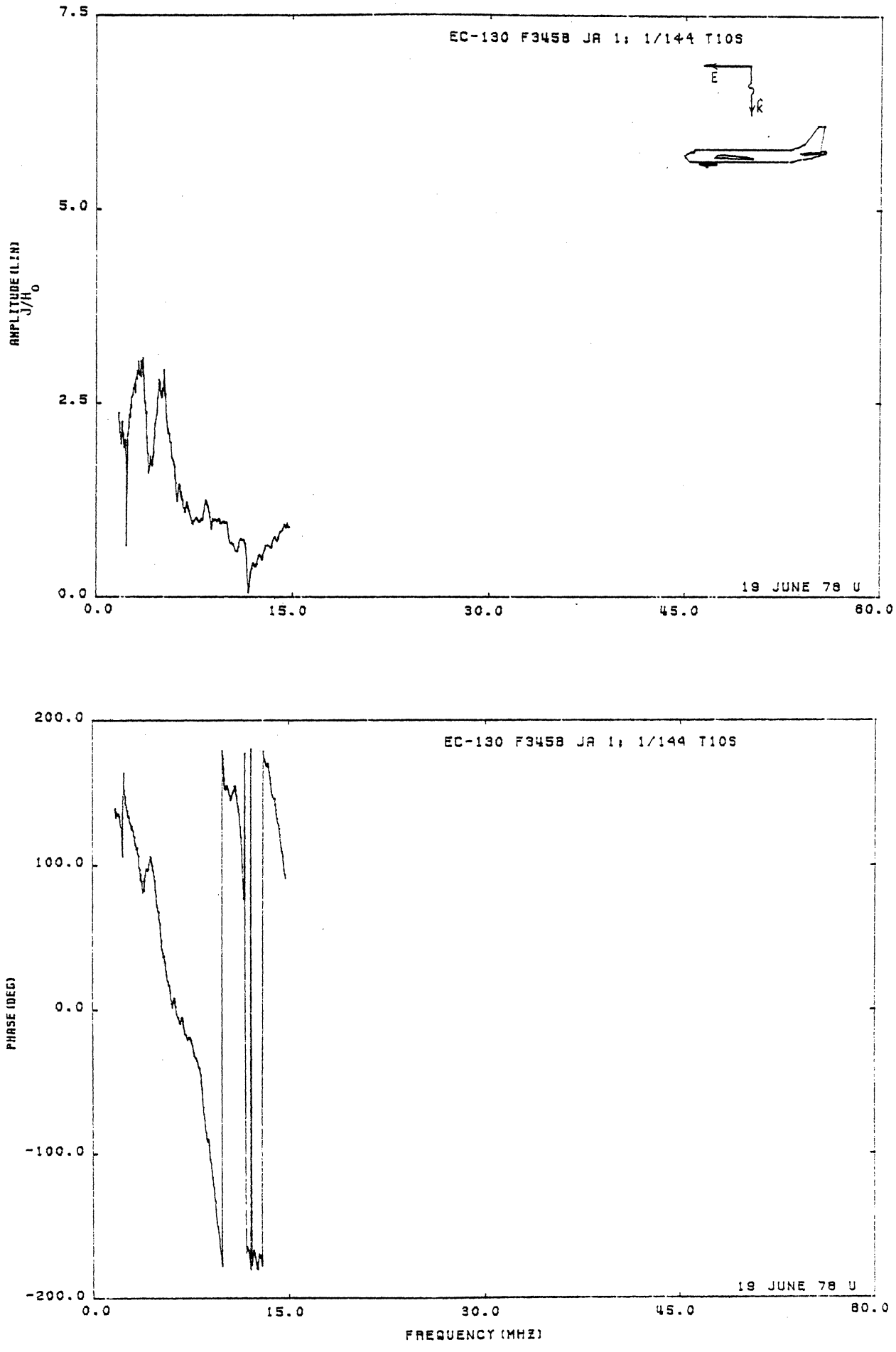

Figure 10S. Axial Current at STA:F345B, Excitation 1, 1/72 Model.

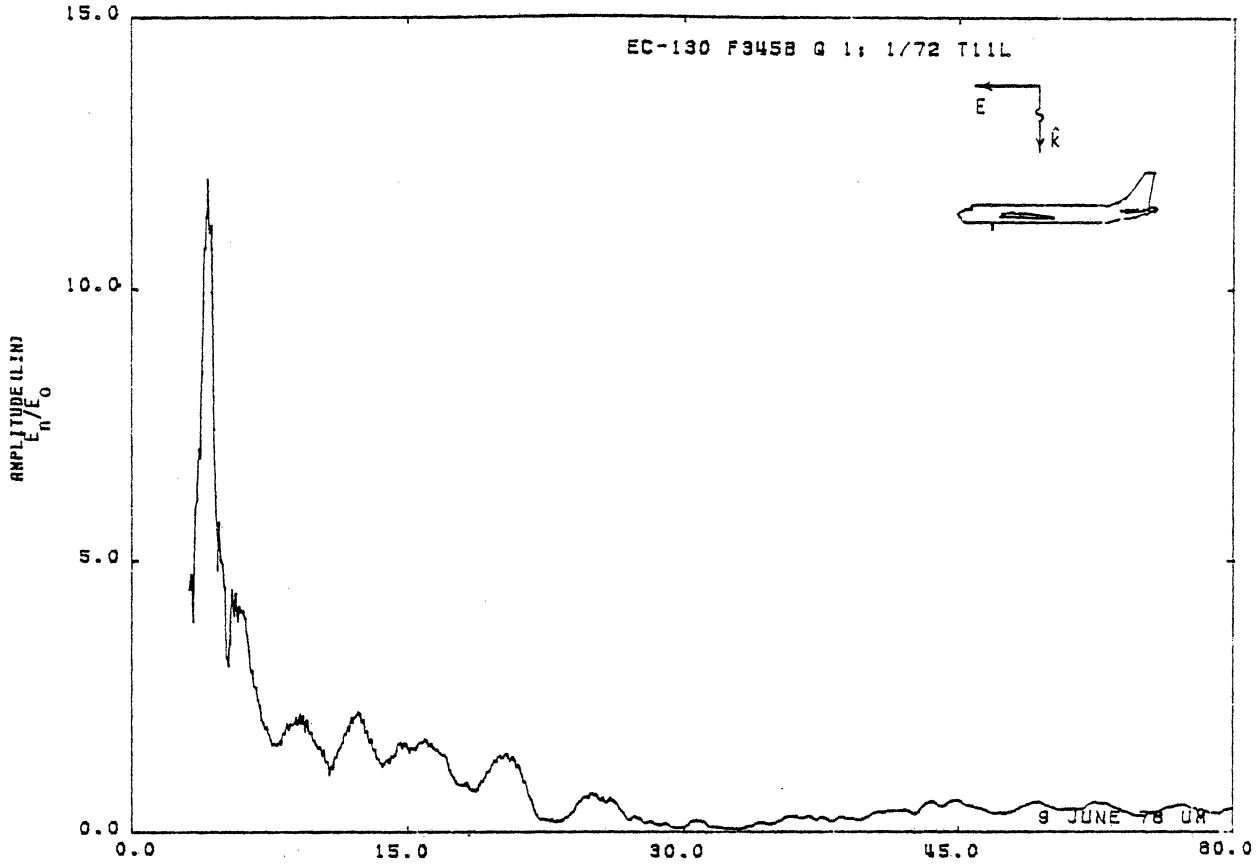

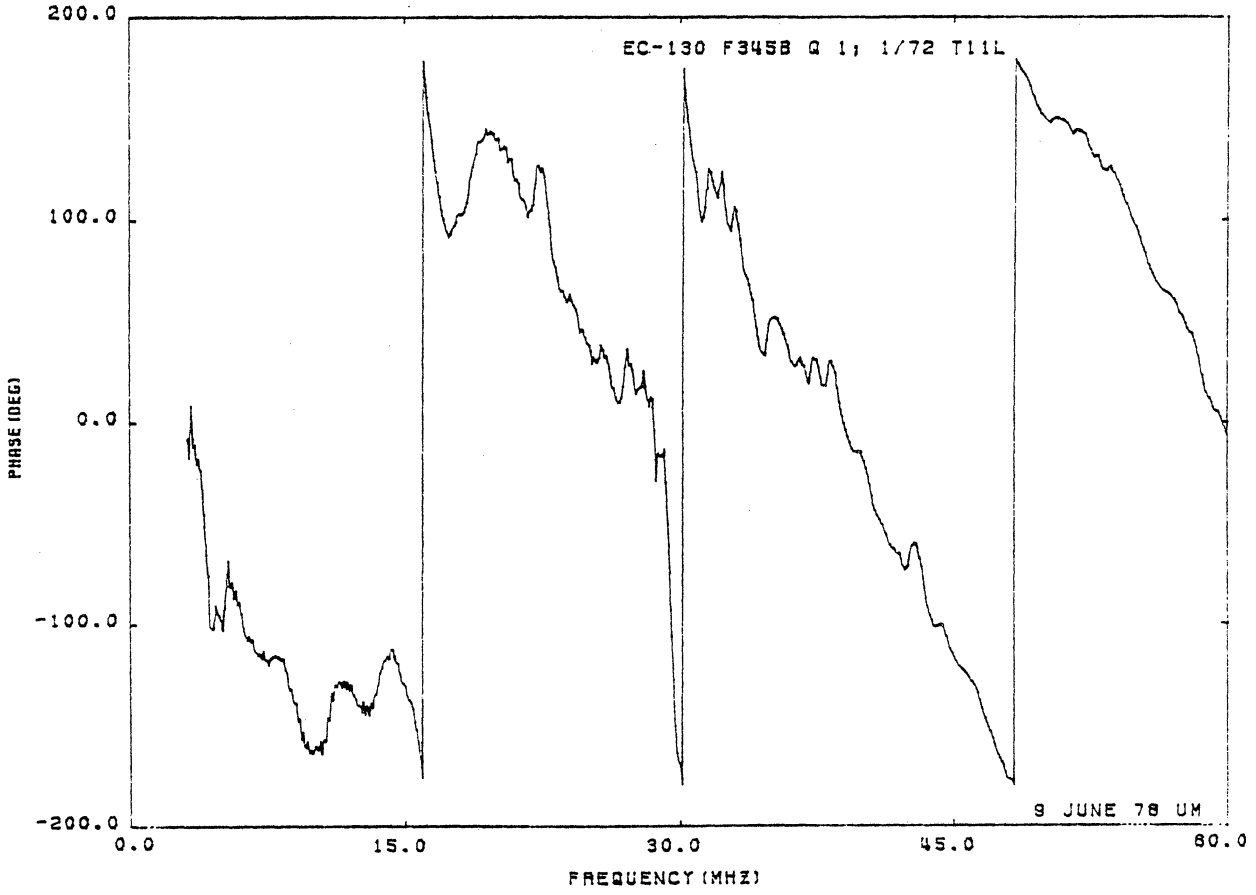

Figure 11L. Charge at STA:F345B, Excitation 1, 1/72 Model.

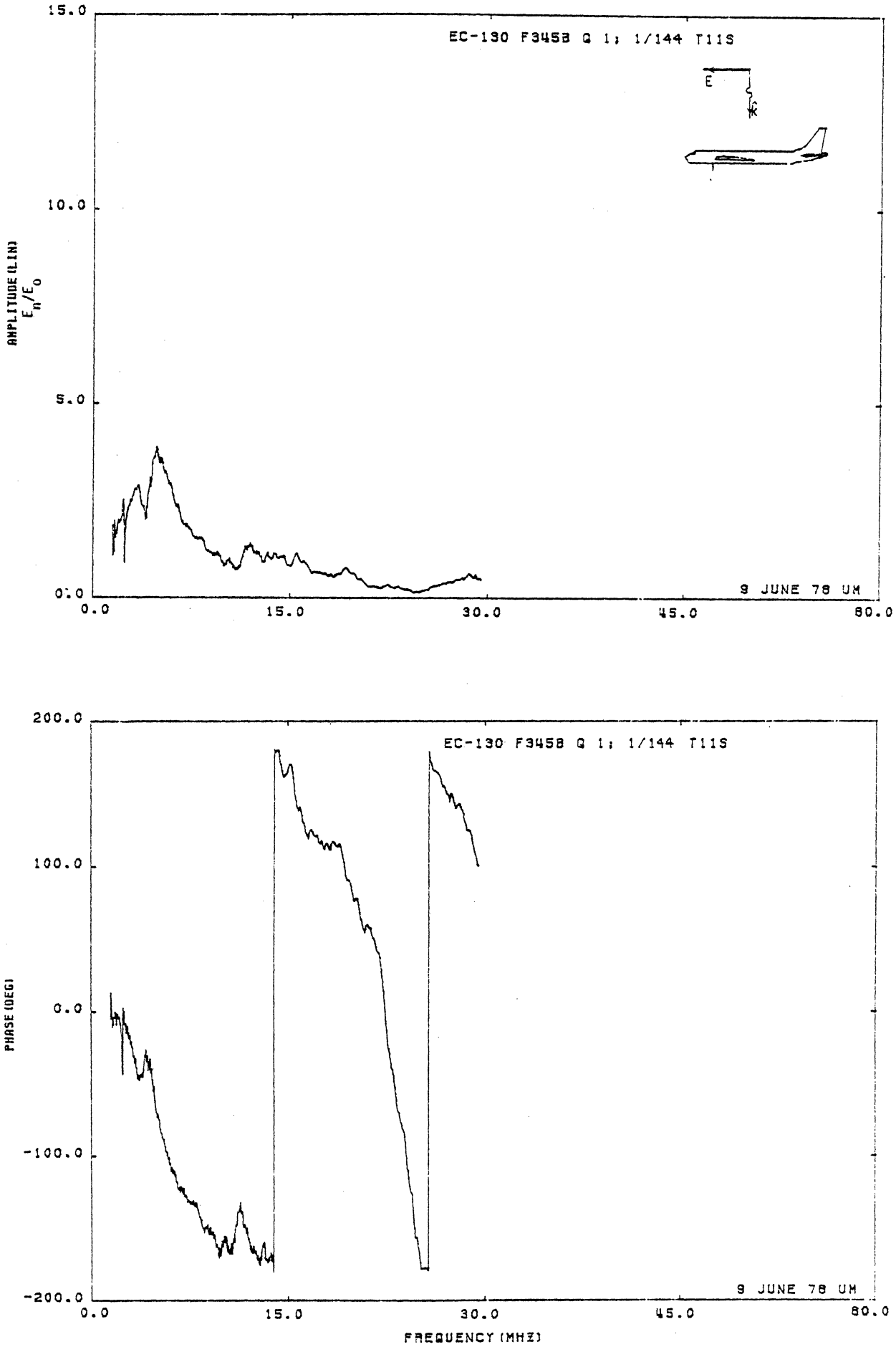

Figure 11S. Charge at STA:F345B, Excitation 1, 1/144 Model.

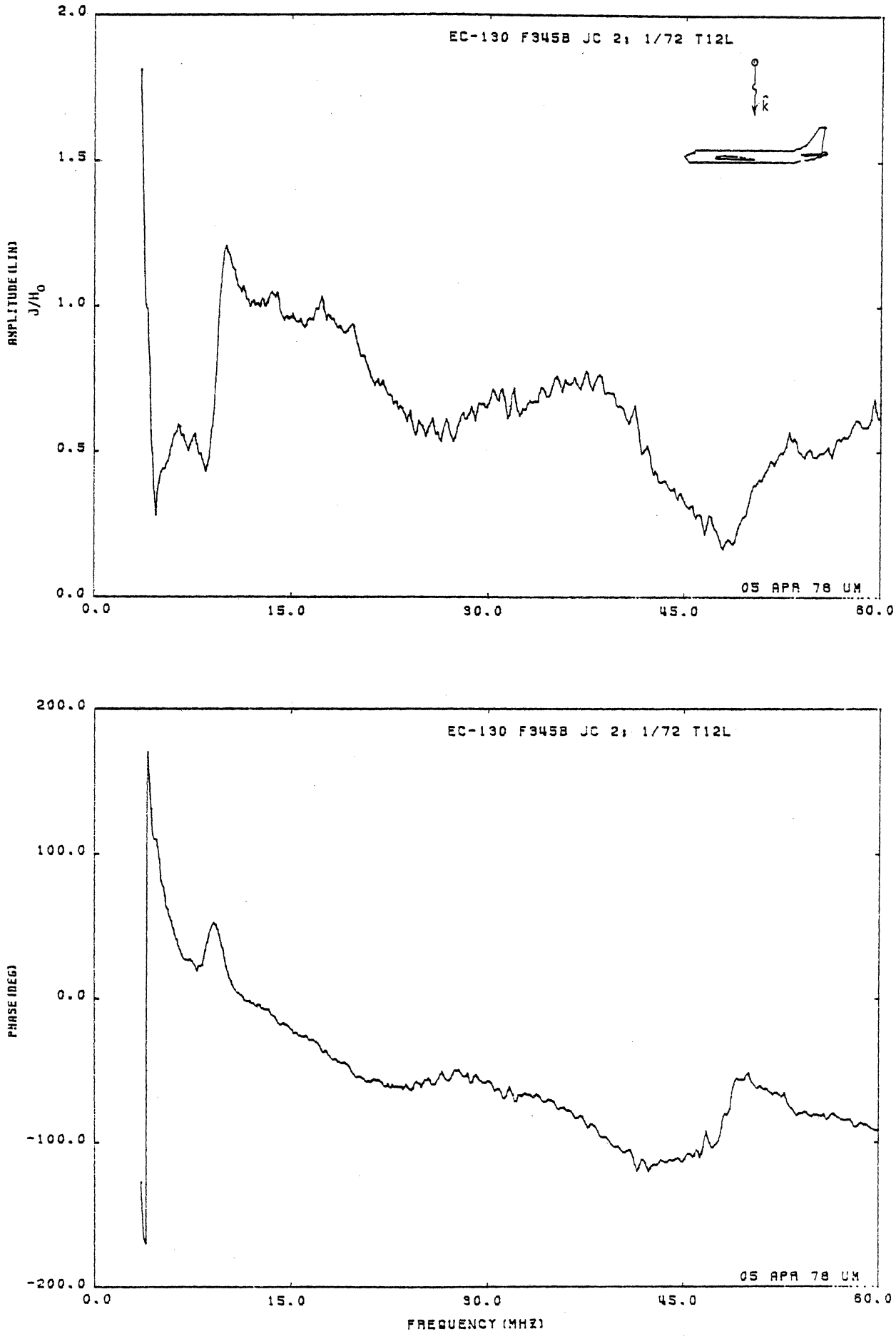

Figure 12L. Circumferential Current at STA:F345B, Excitation 2, 1/72 Model.

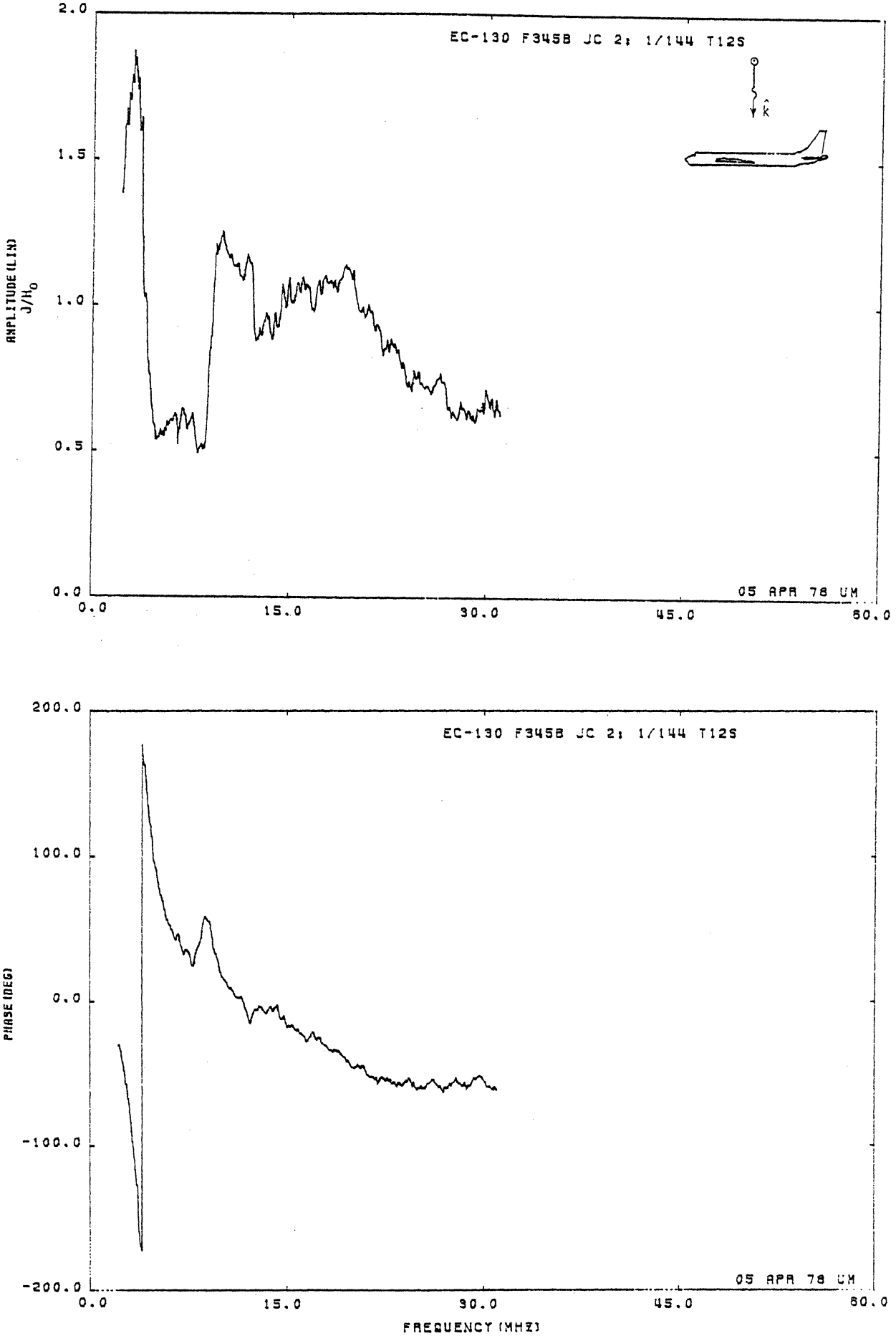

Figure 12S. Circumferential Current at STA:F345B, Excitation 2, 1/144 Model.

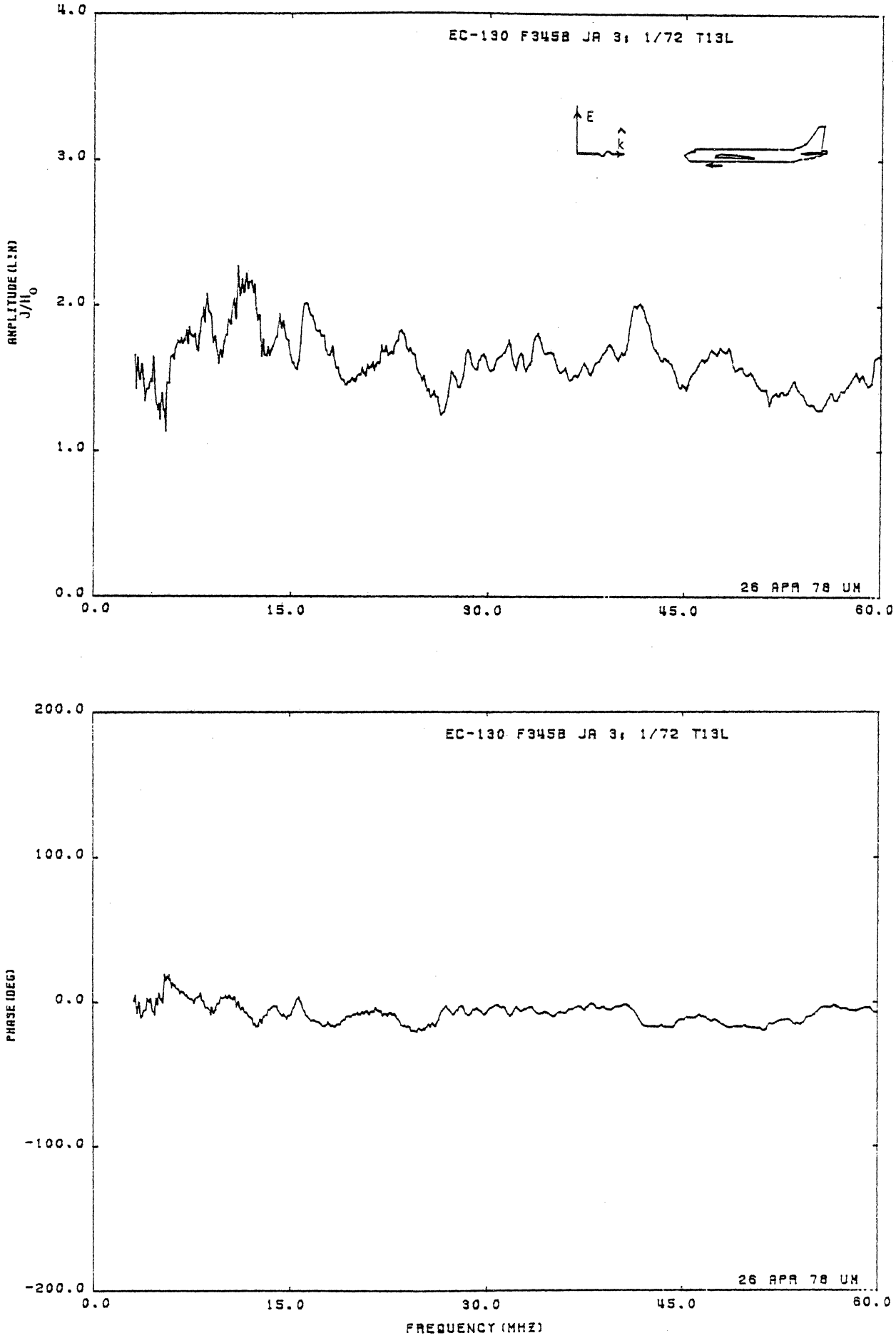

Figure 13L. Axial Current at STA:F345B, Excitation 3, 1/72 Model.

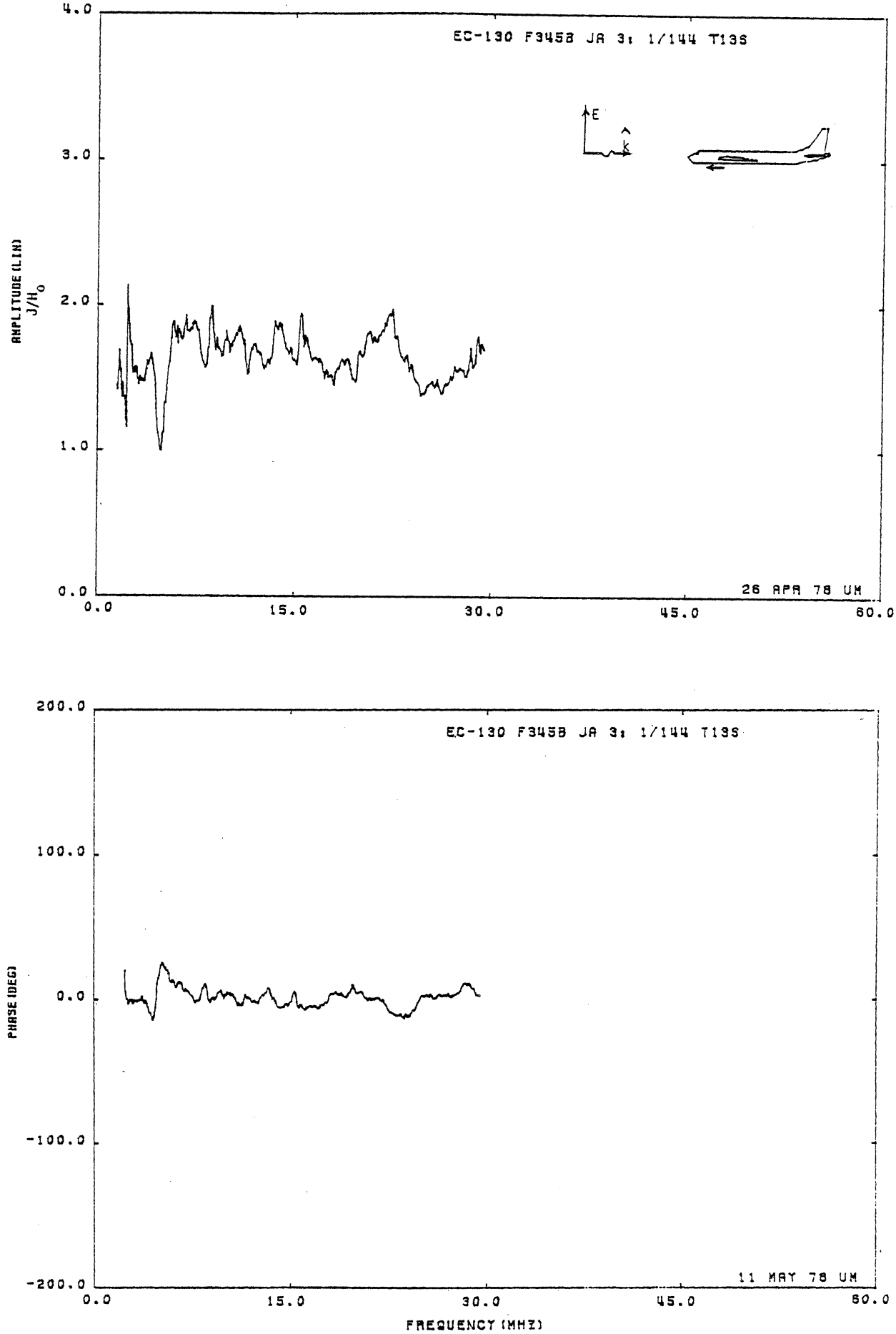

Figure 13S. Axial Current at STA:F345B, Excitation 3, 1/144 Model.

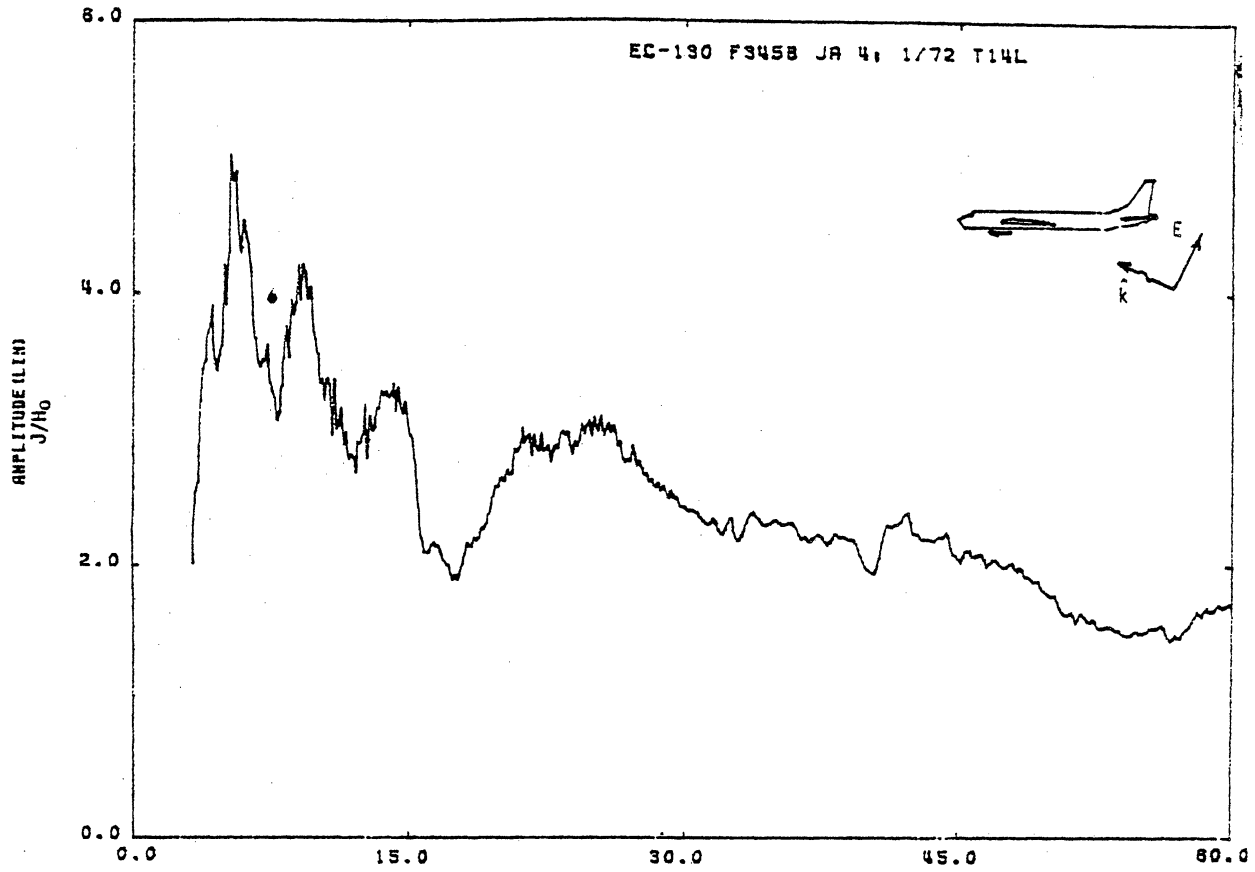

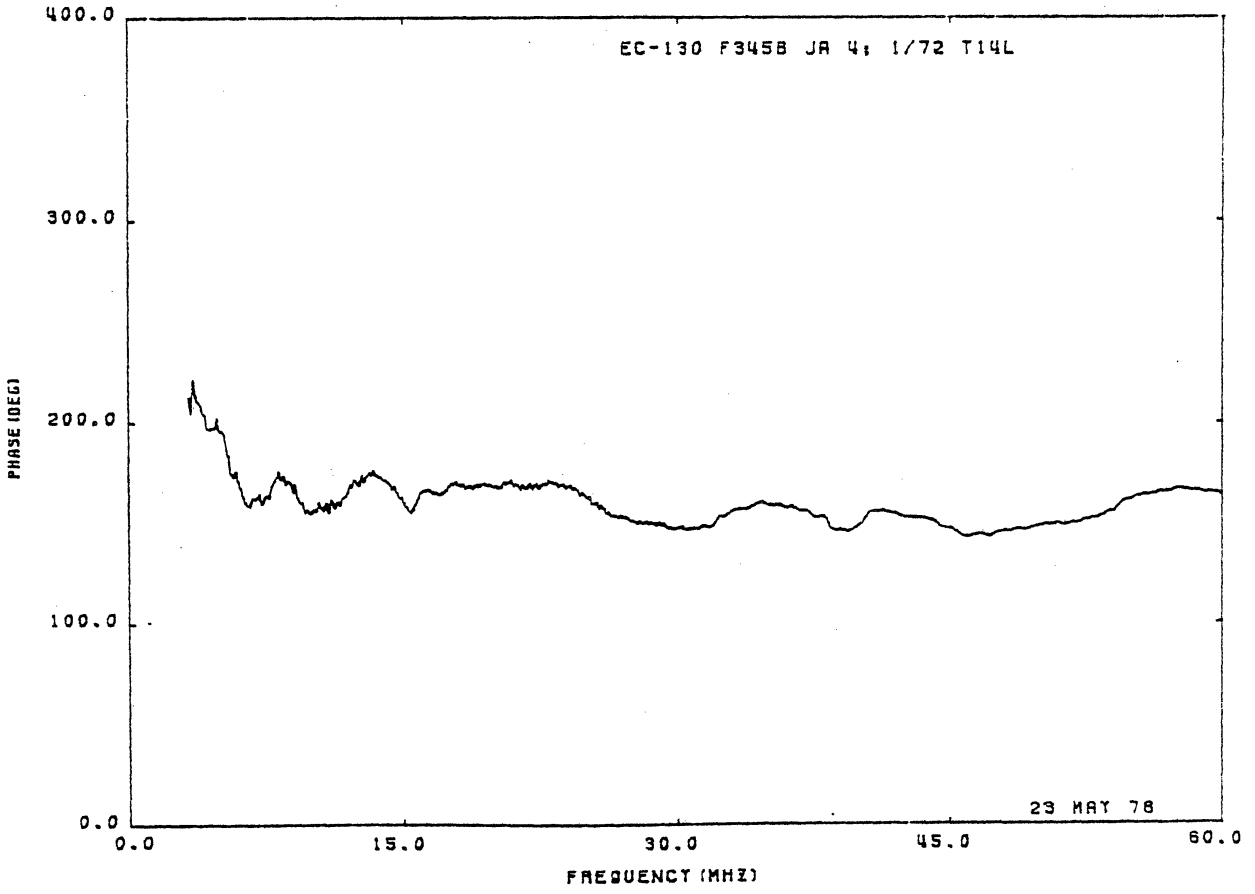

Figure 14L. Axial Current at STA:F345B, Excitation 4, 1/72 Model.

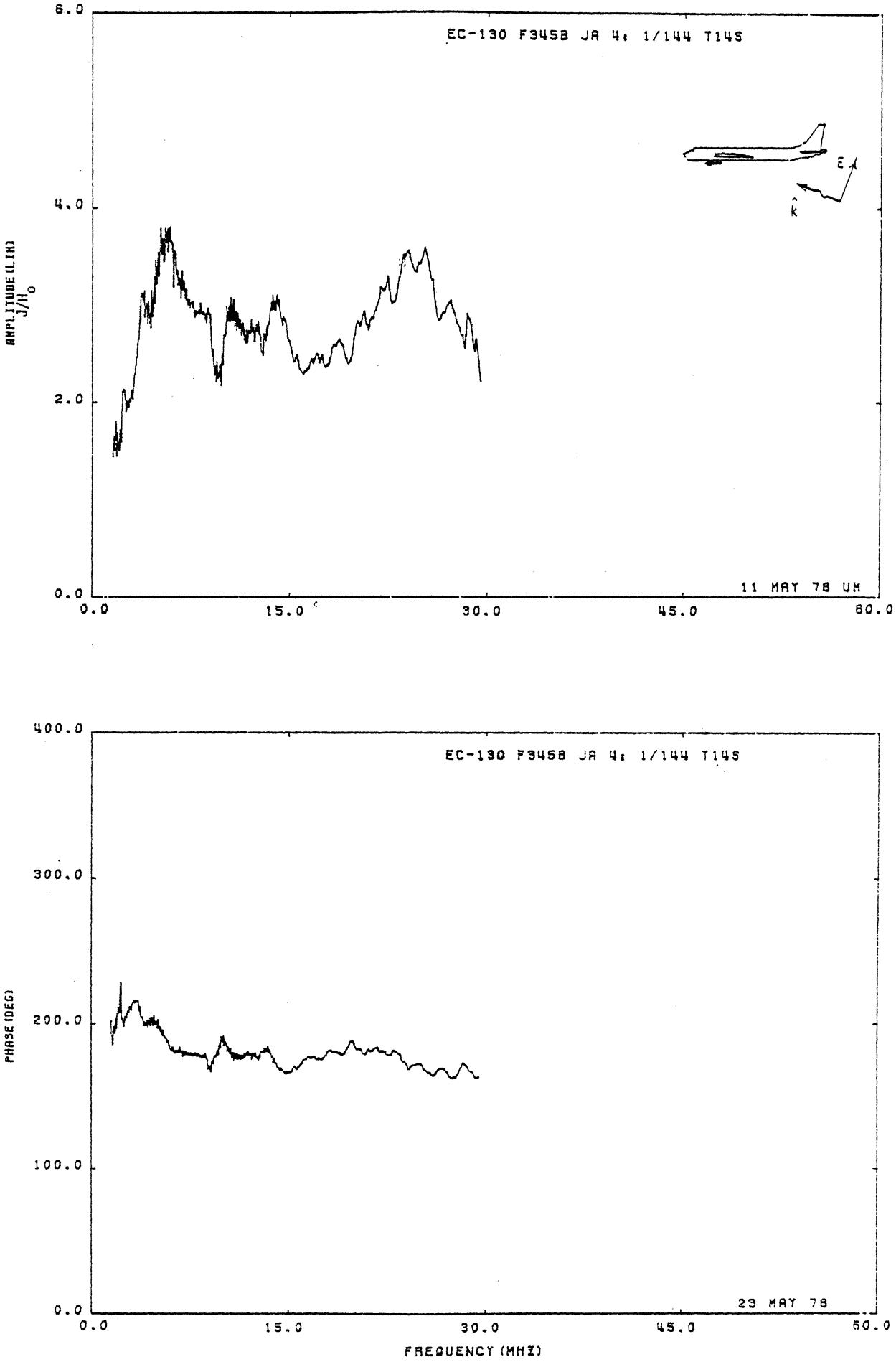

Figure 14S. Axial Current at STA:F345B, Excitation 4, 1/144 Model.

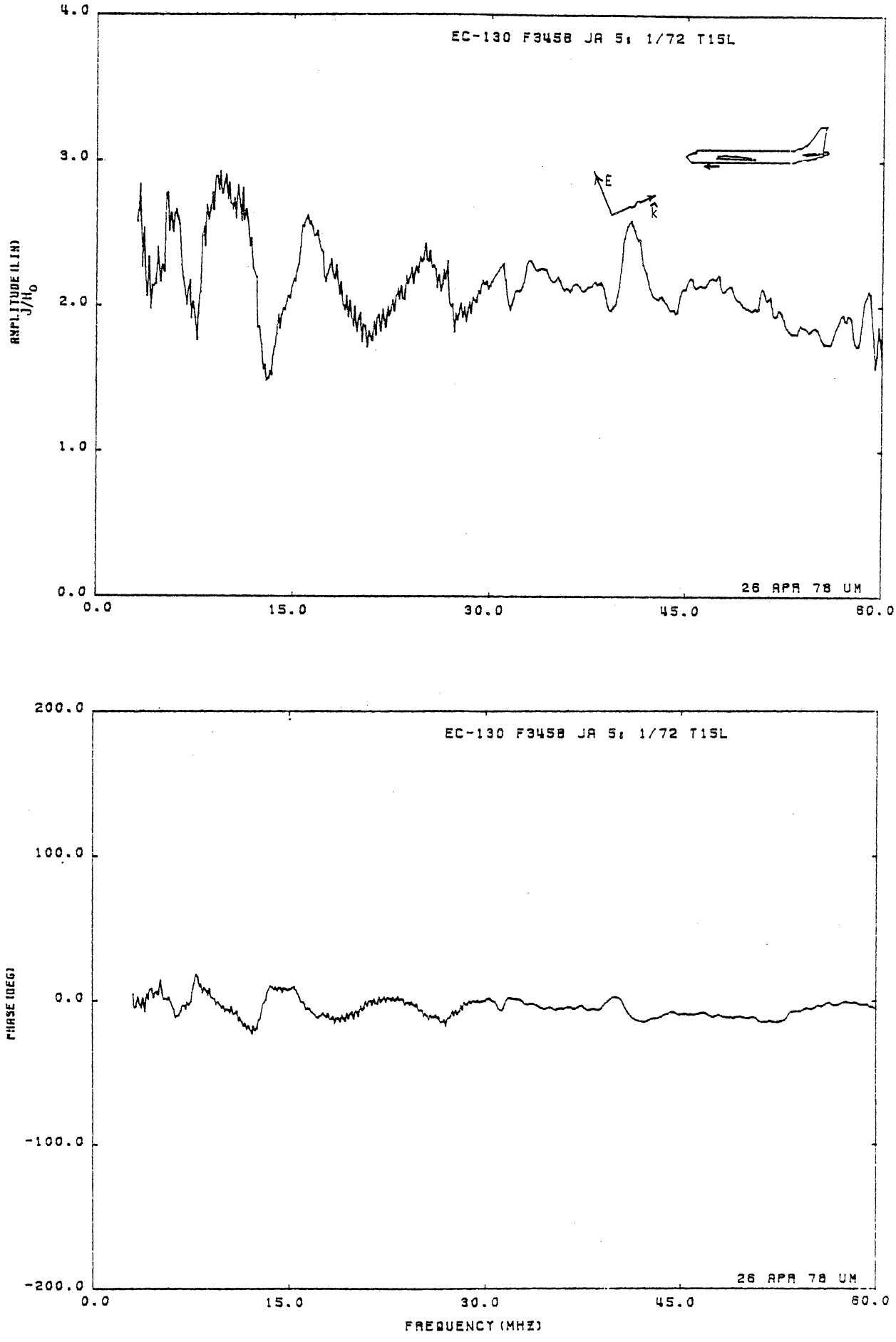

Figure 15L. Axial Current at STA:F345B, Excitation 5, 1/72 Model.

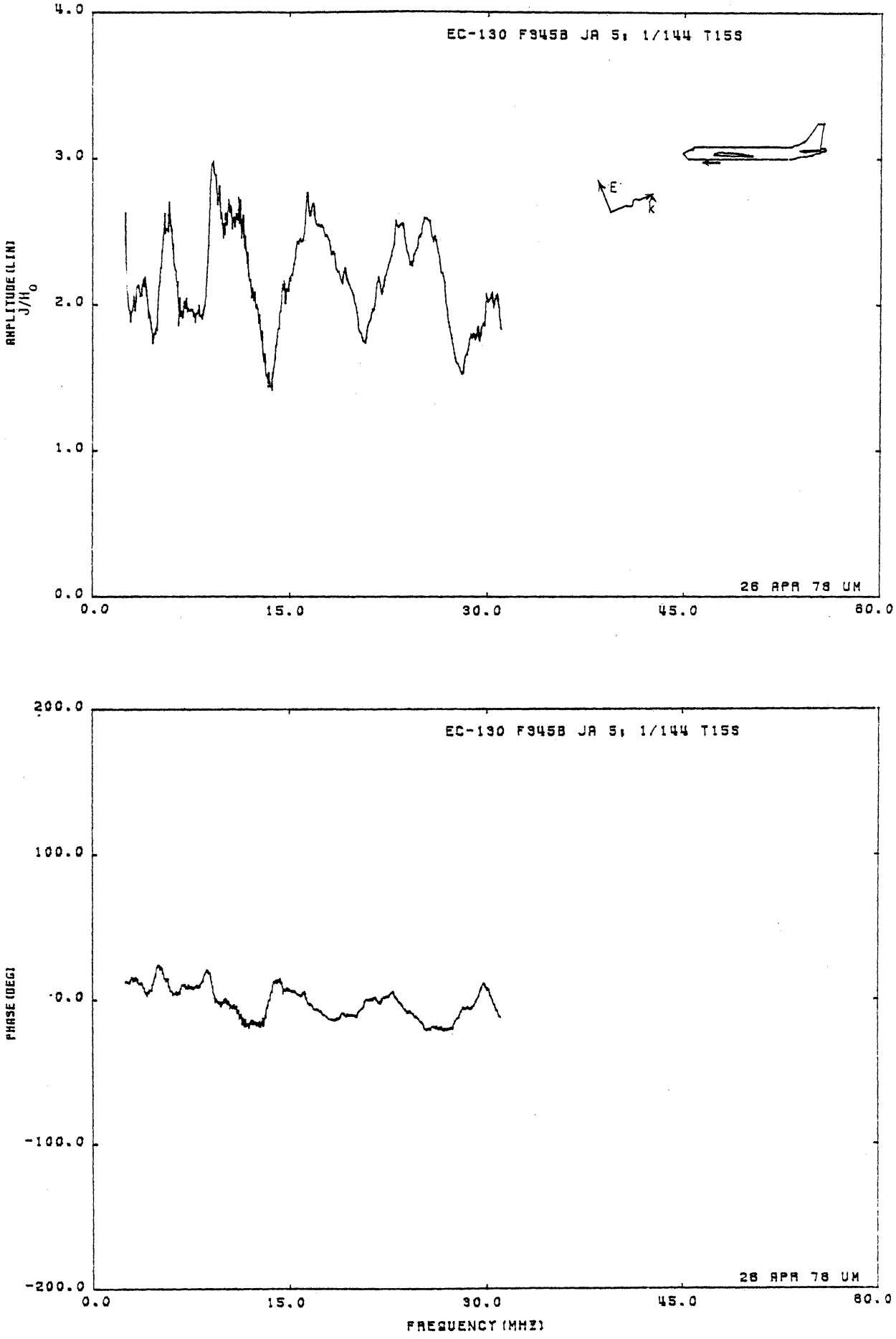

Figure 15S. Axial Current at STA:F345B, Excitation 5, 1/144 Model.

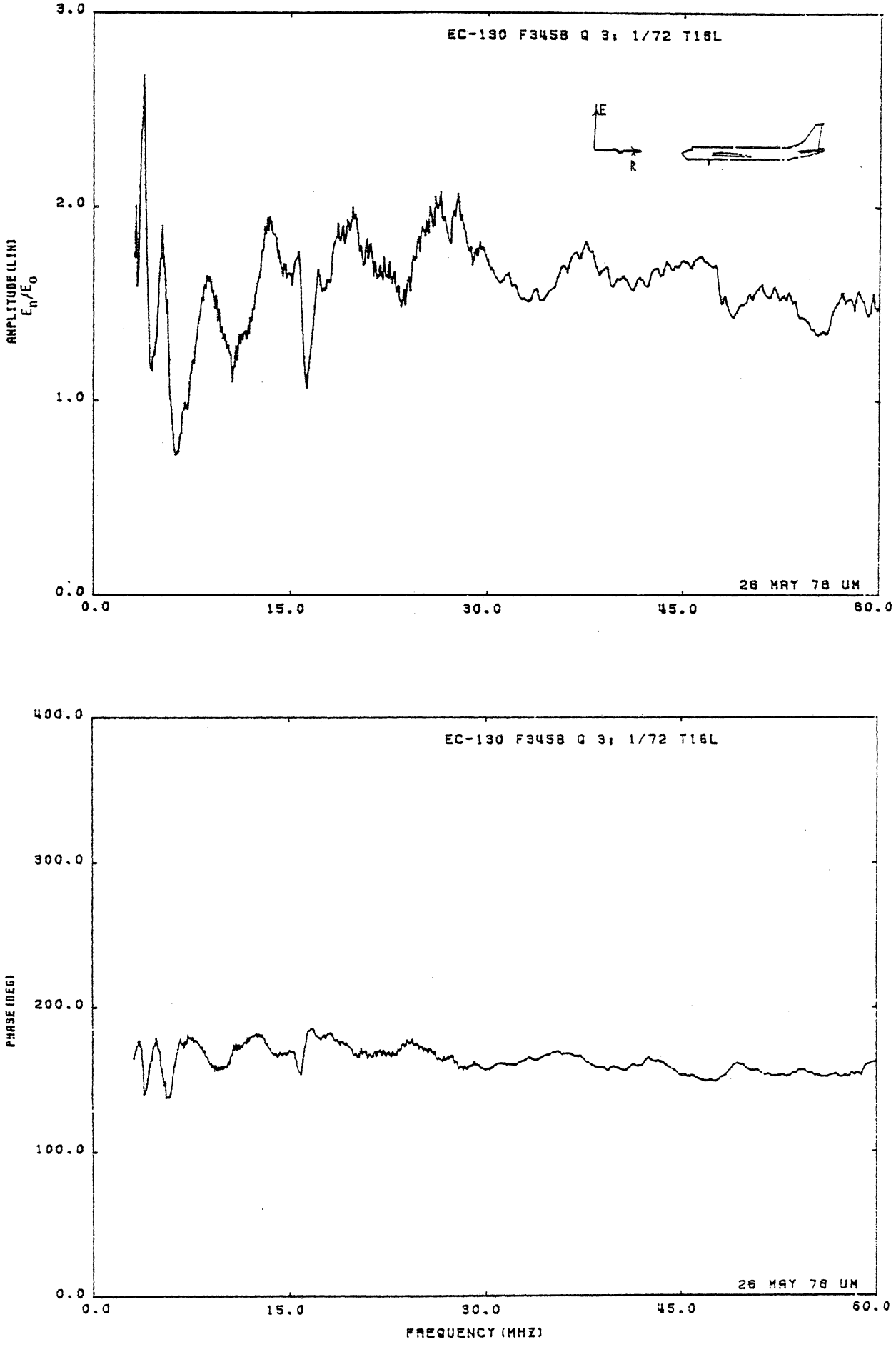

Figure 16L. Charge at STA:F345B, Excitation 3, 1/72 Model.

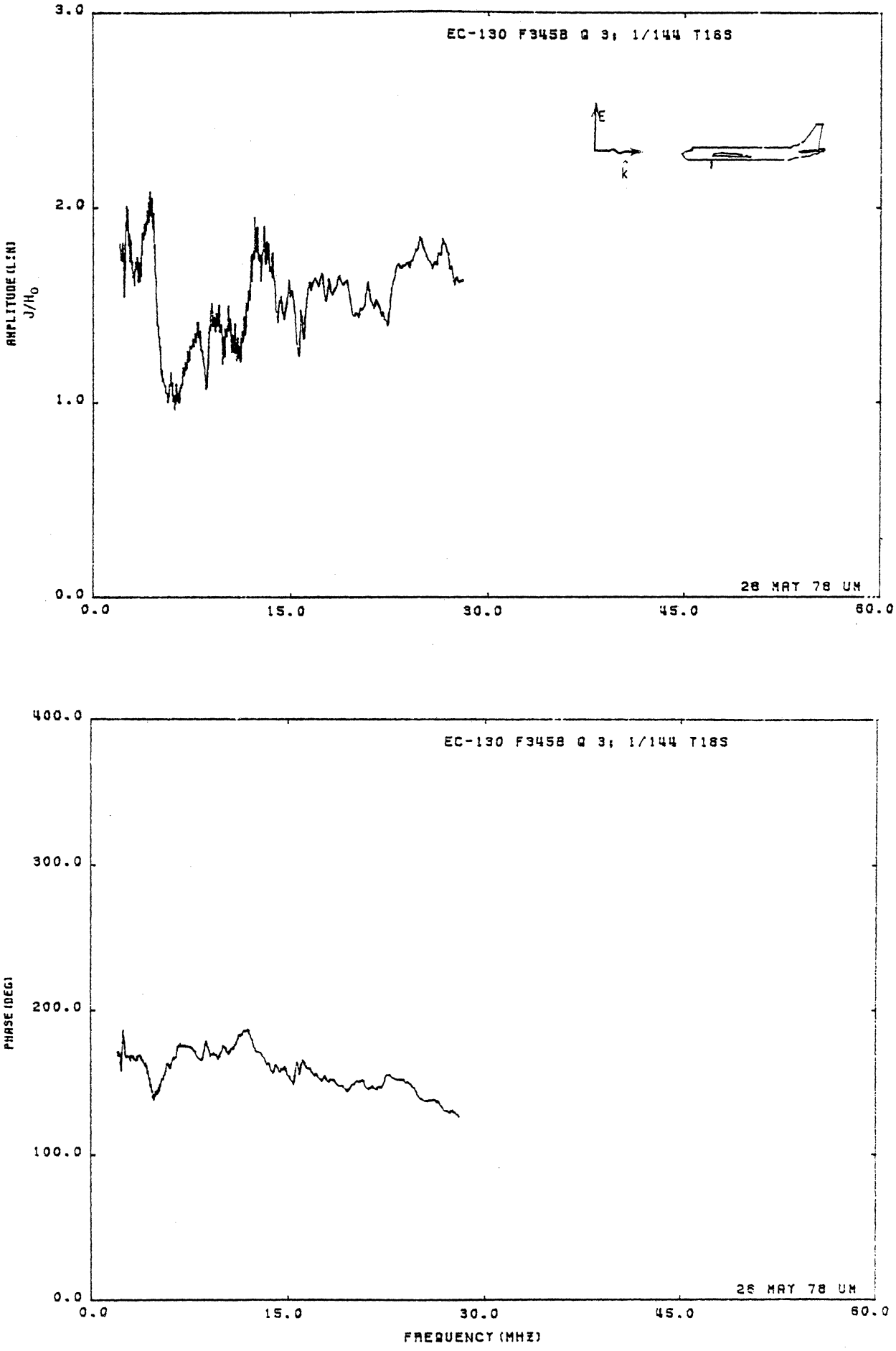

Figure 16S. Charge at STA:F345B, Excitation 3, 1/144 Model.

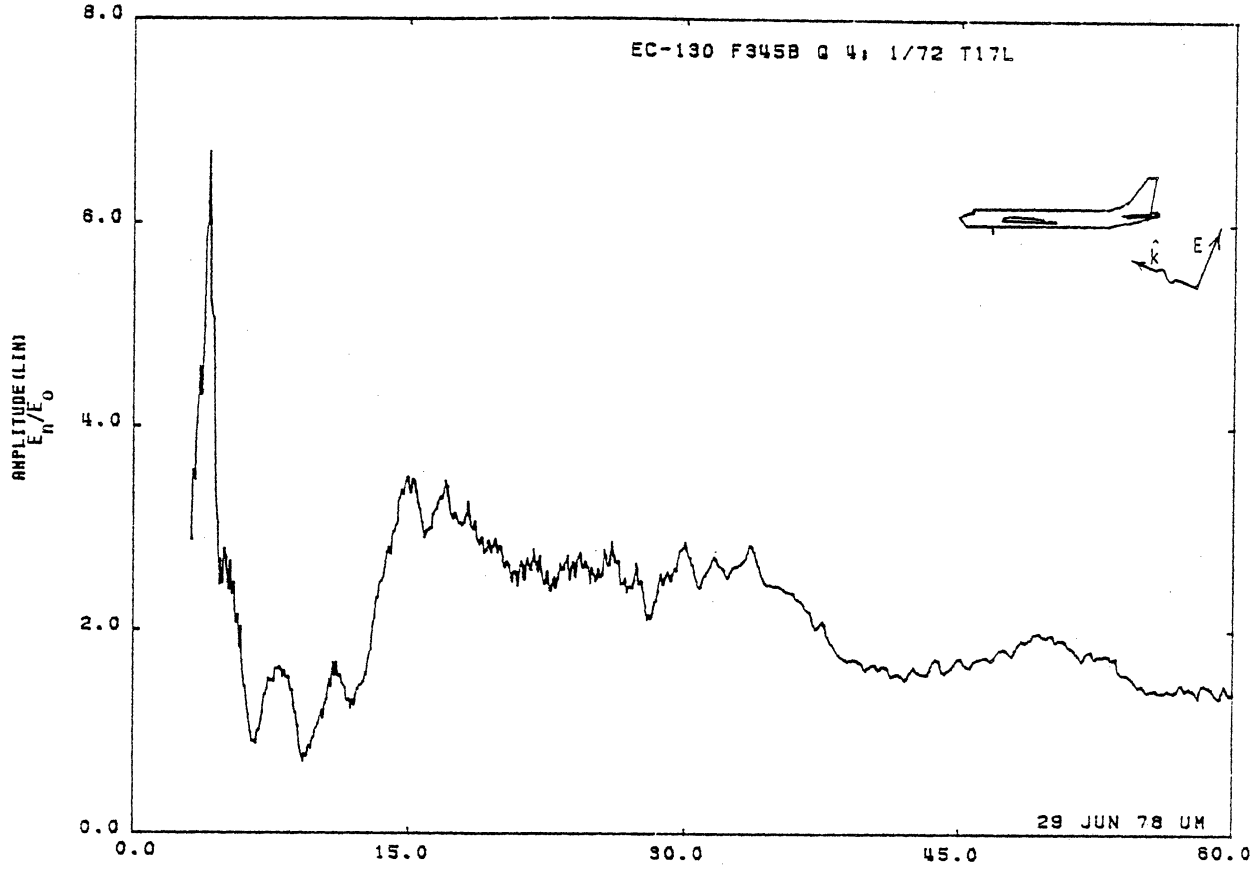

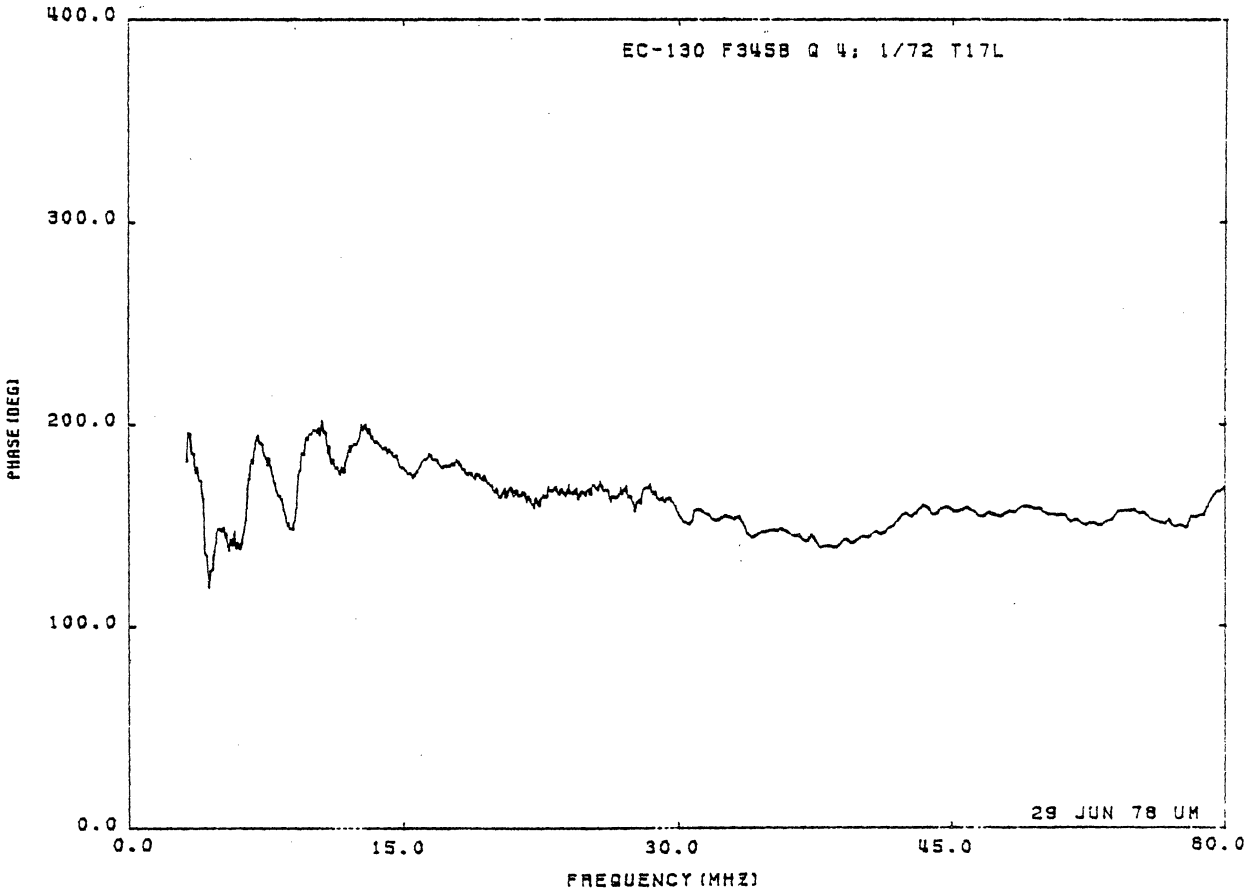

Figure 17L. Charge at STA:F345B, Excitation 4, 1/72 Model.

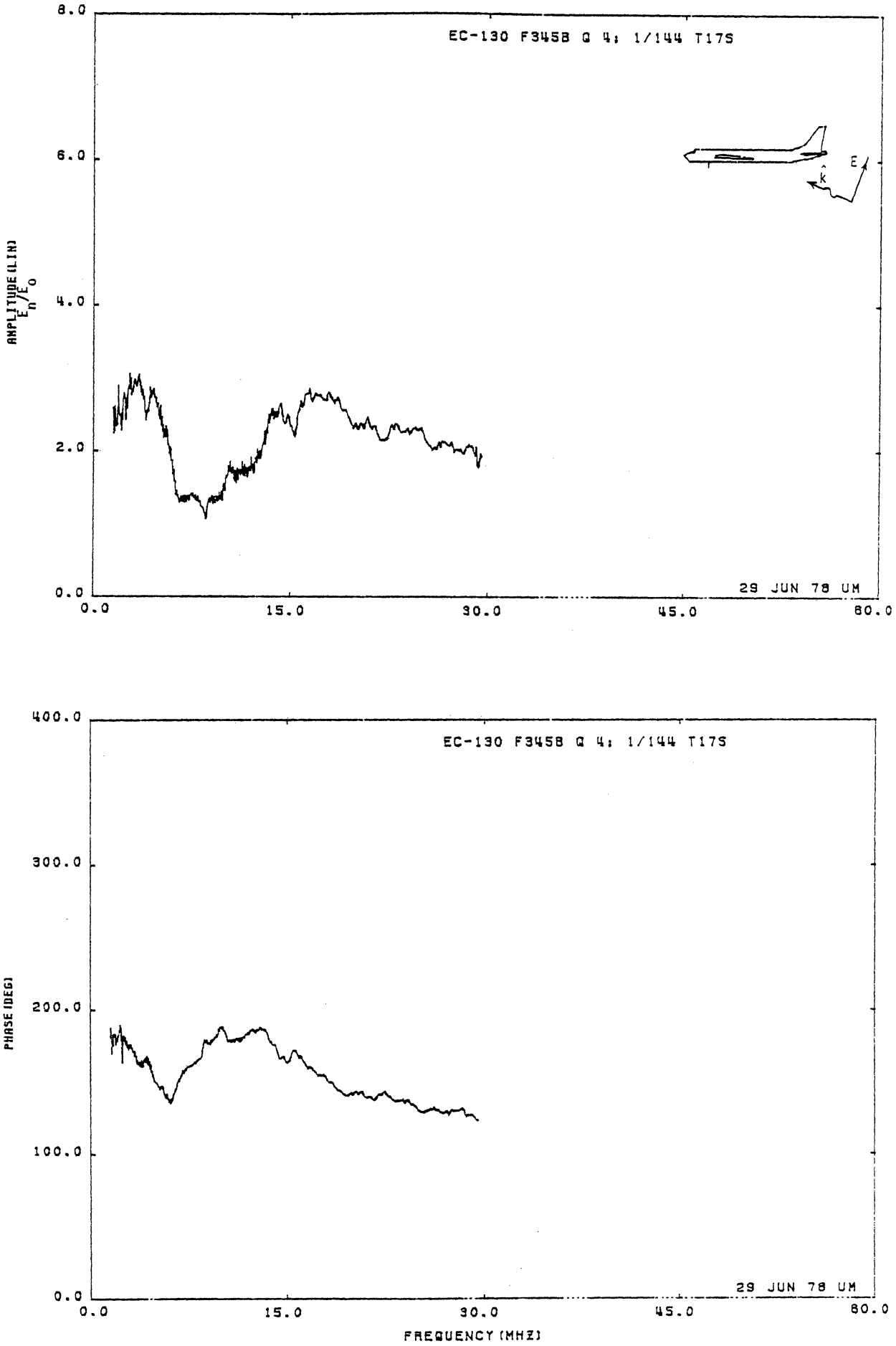

Figure 17S. Charge at STA:F345B, Excitation 4, 1/144 Model.

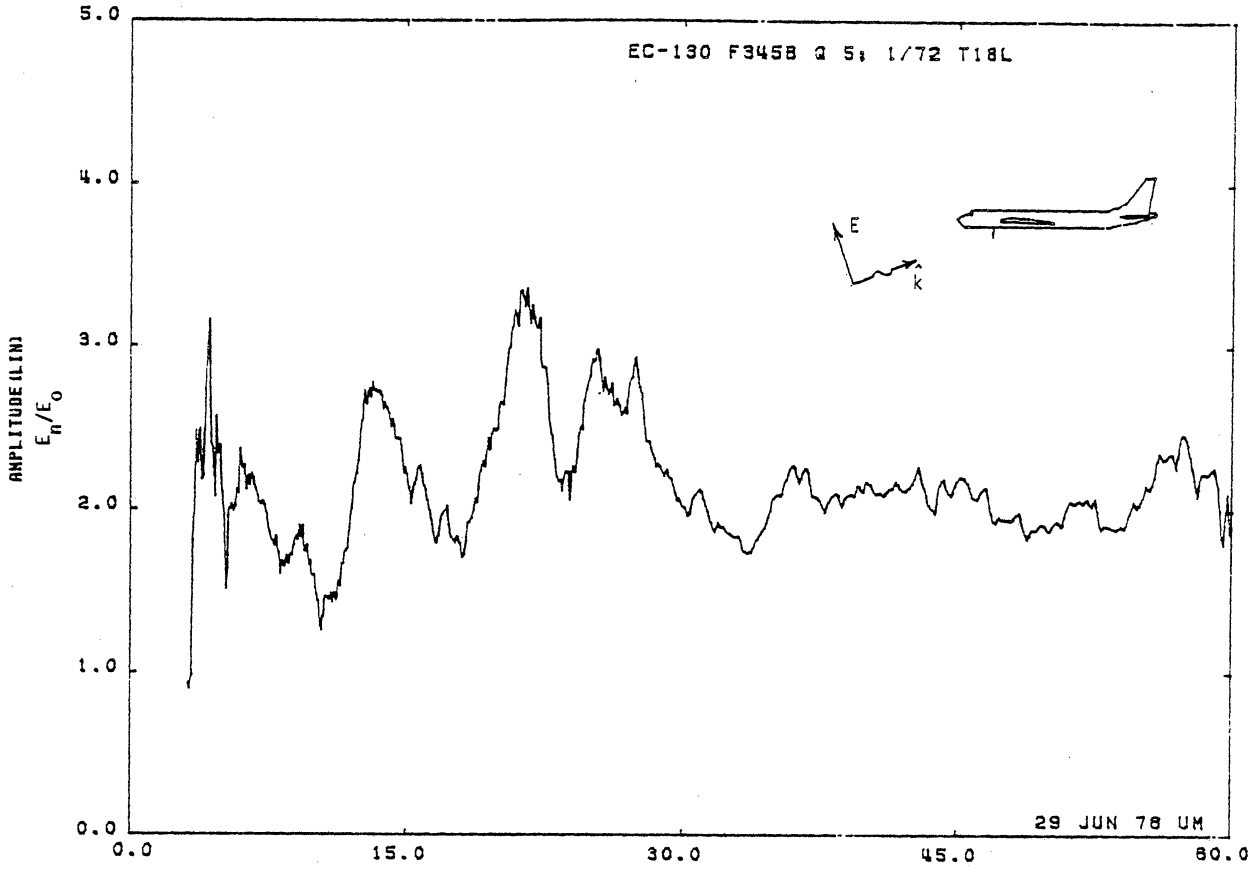

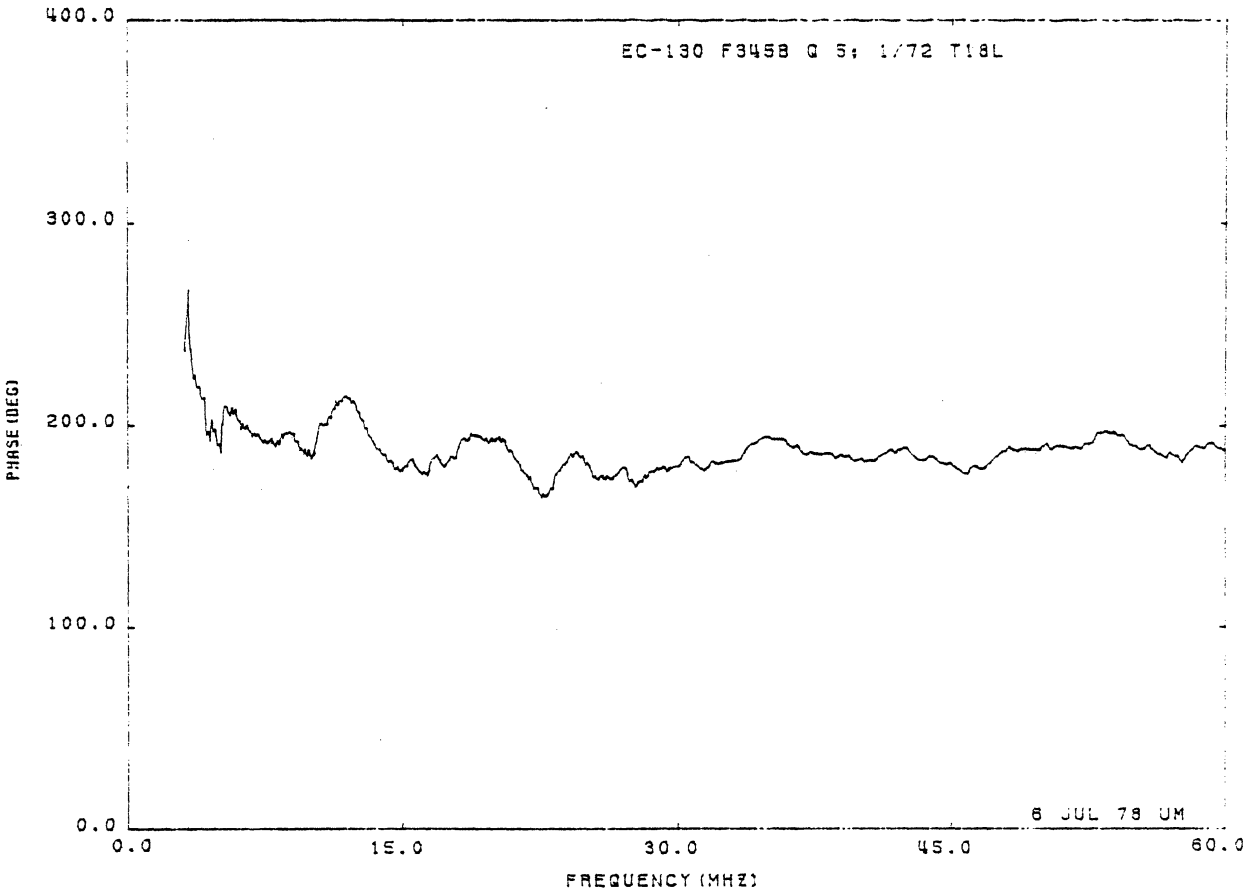

Figure 18L. Charge at STA:F345B, Excitation 5, 1/72 Model.

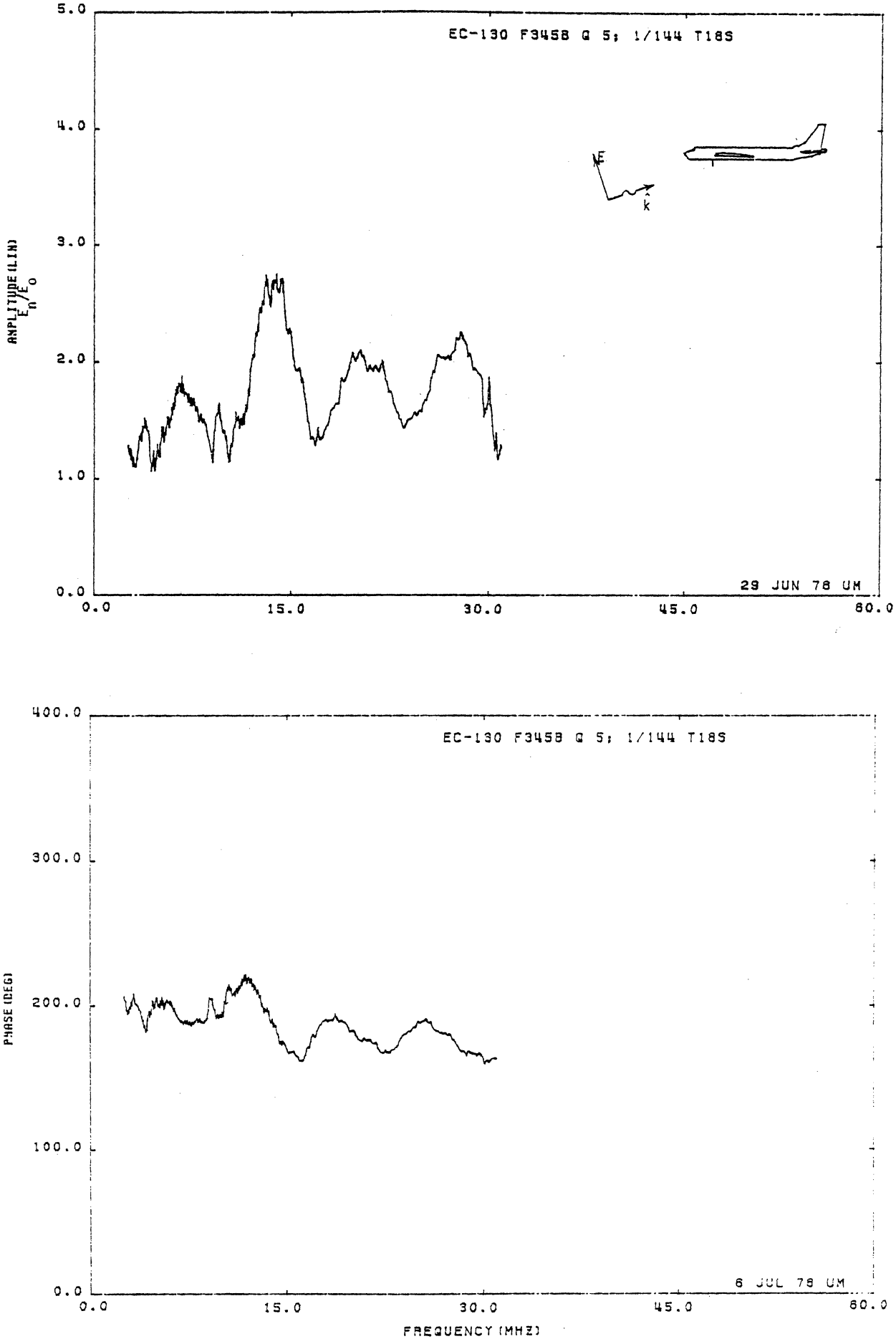

Figure 18S. Charge at STA:F345B, Excitation 5, 1/144 Model.

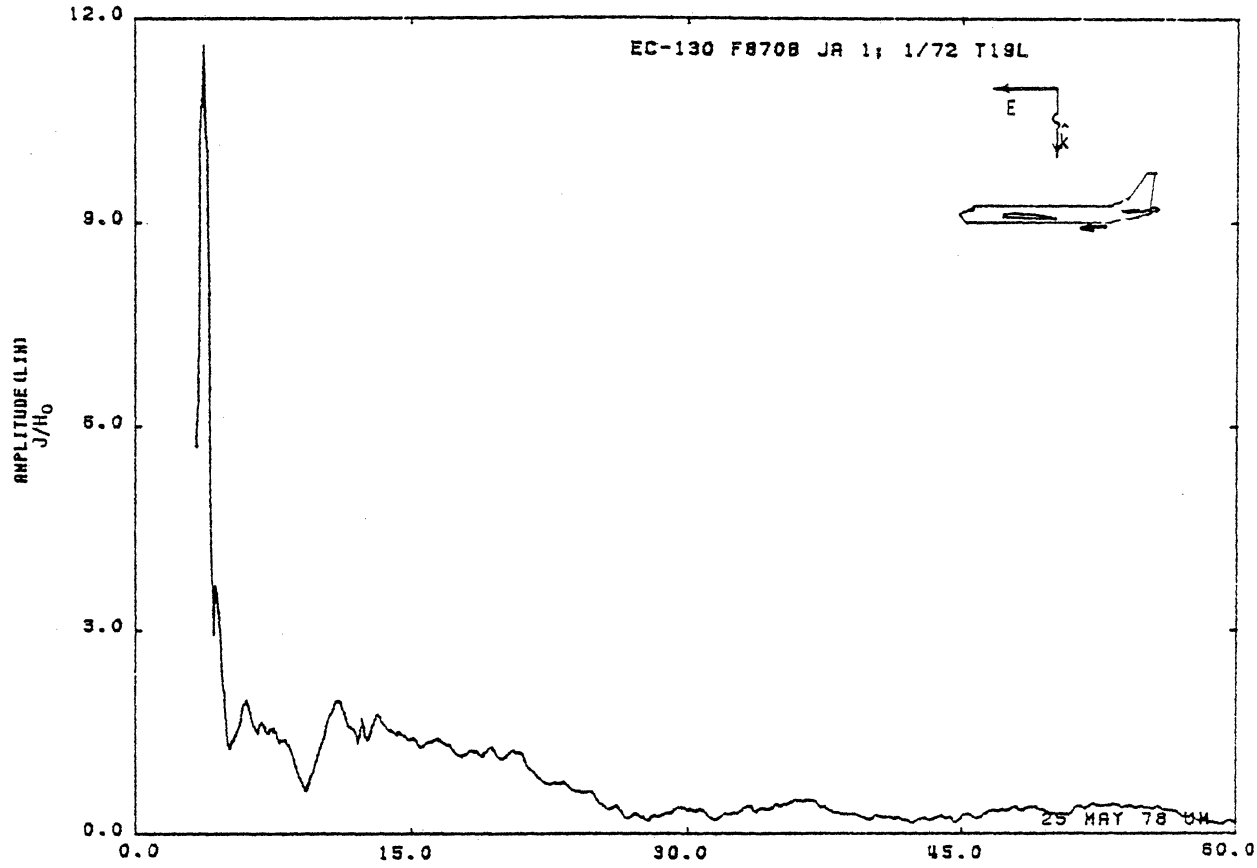

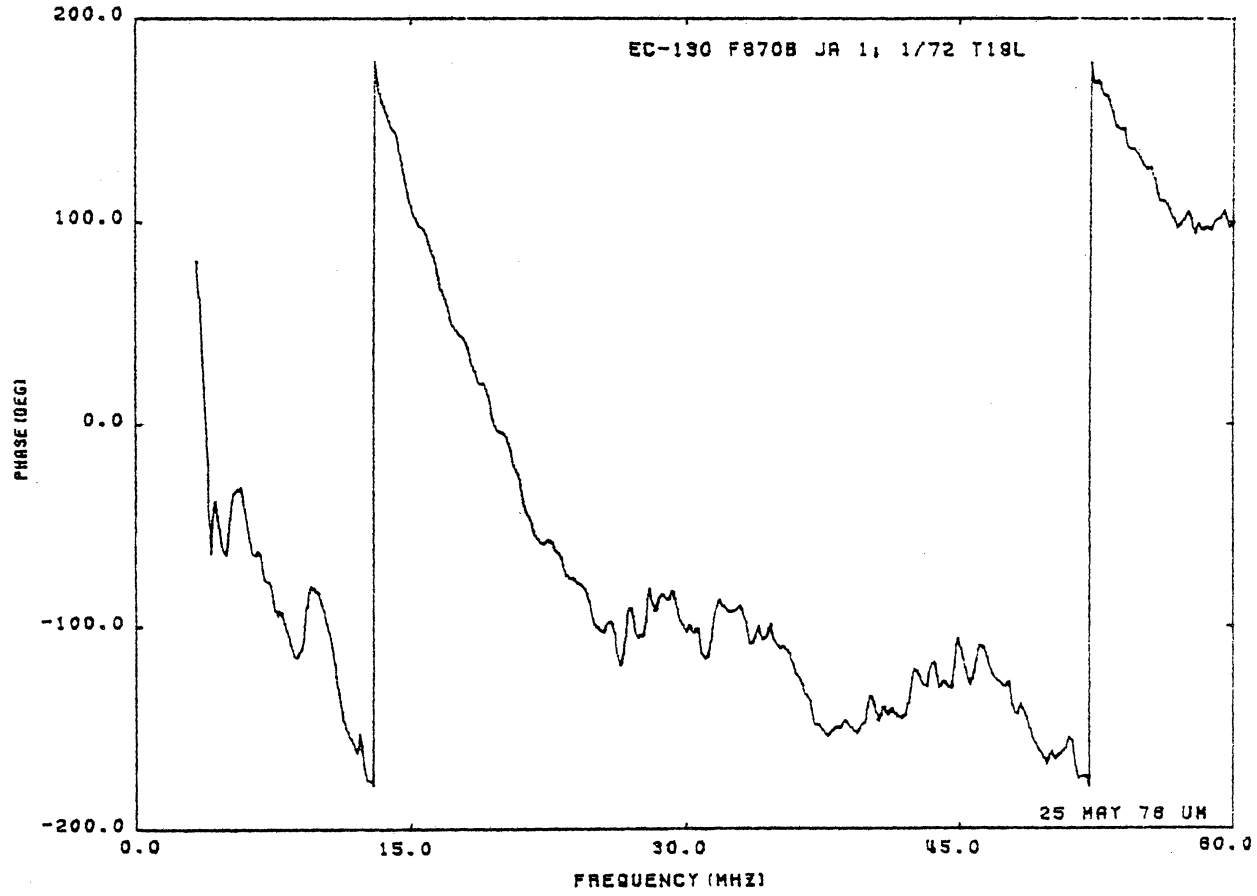

Figure 19L. Axial Current at STA:F870B, Excitation 1, 1/72 Model.

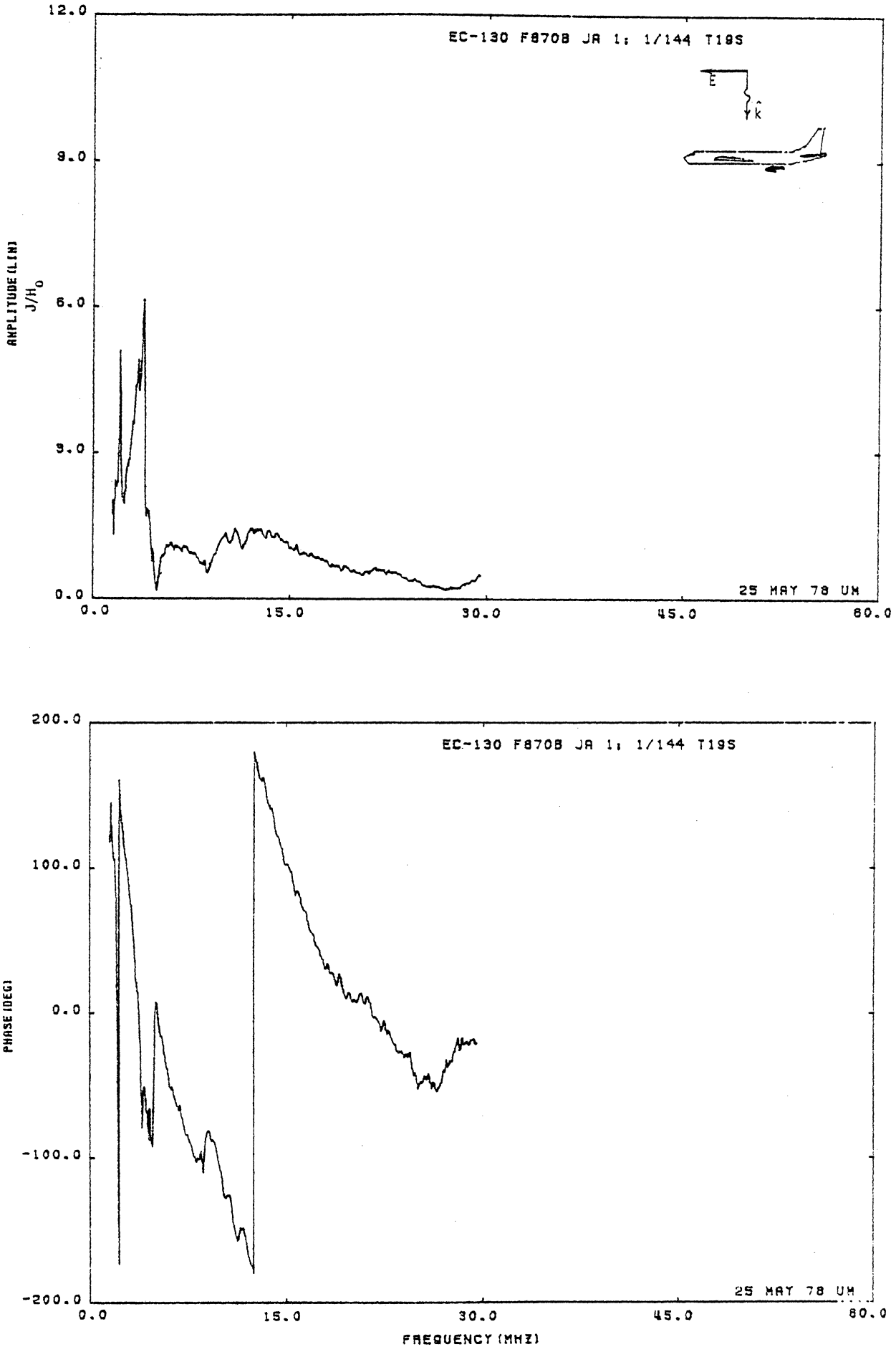

Figure 19S. Axial Current at STA:F870B, Excitation 1, 1/144 Model.

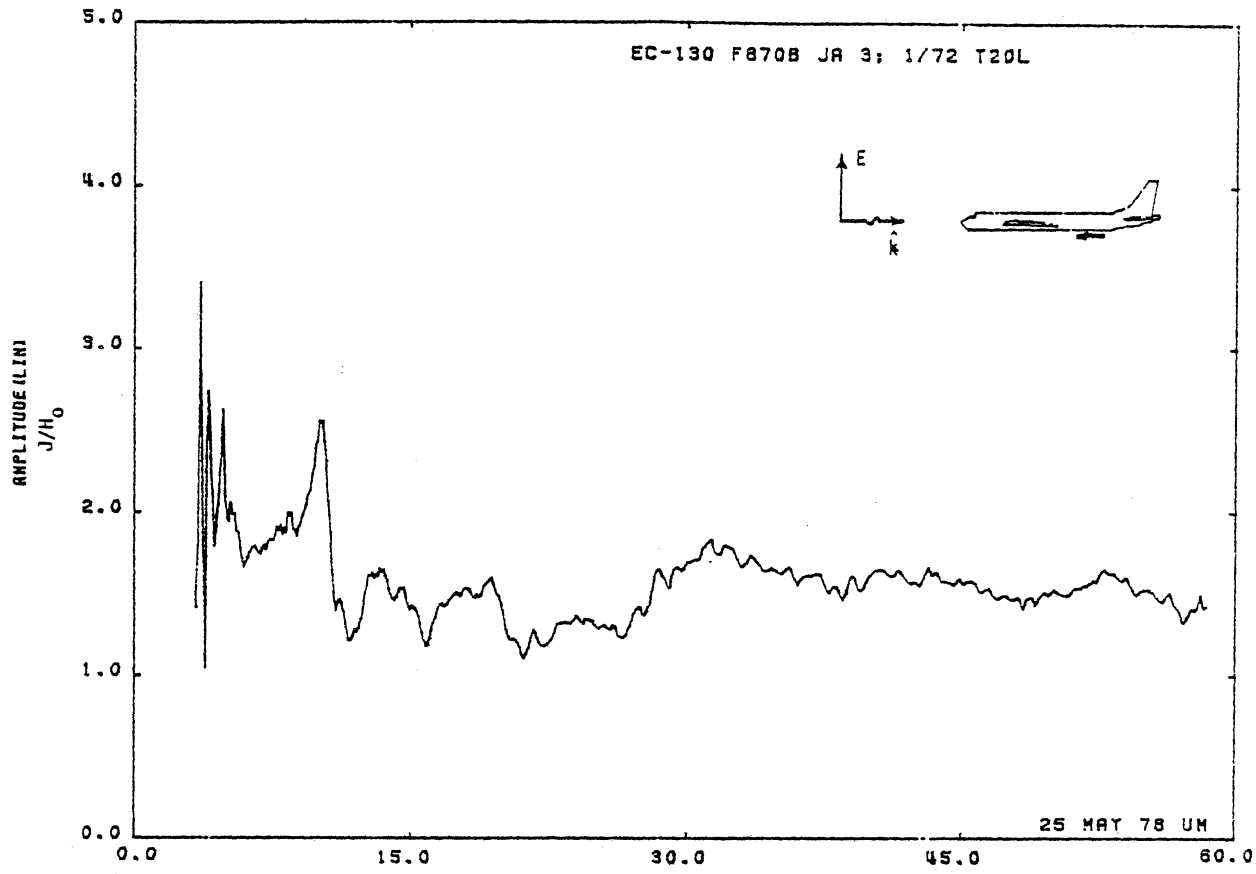

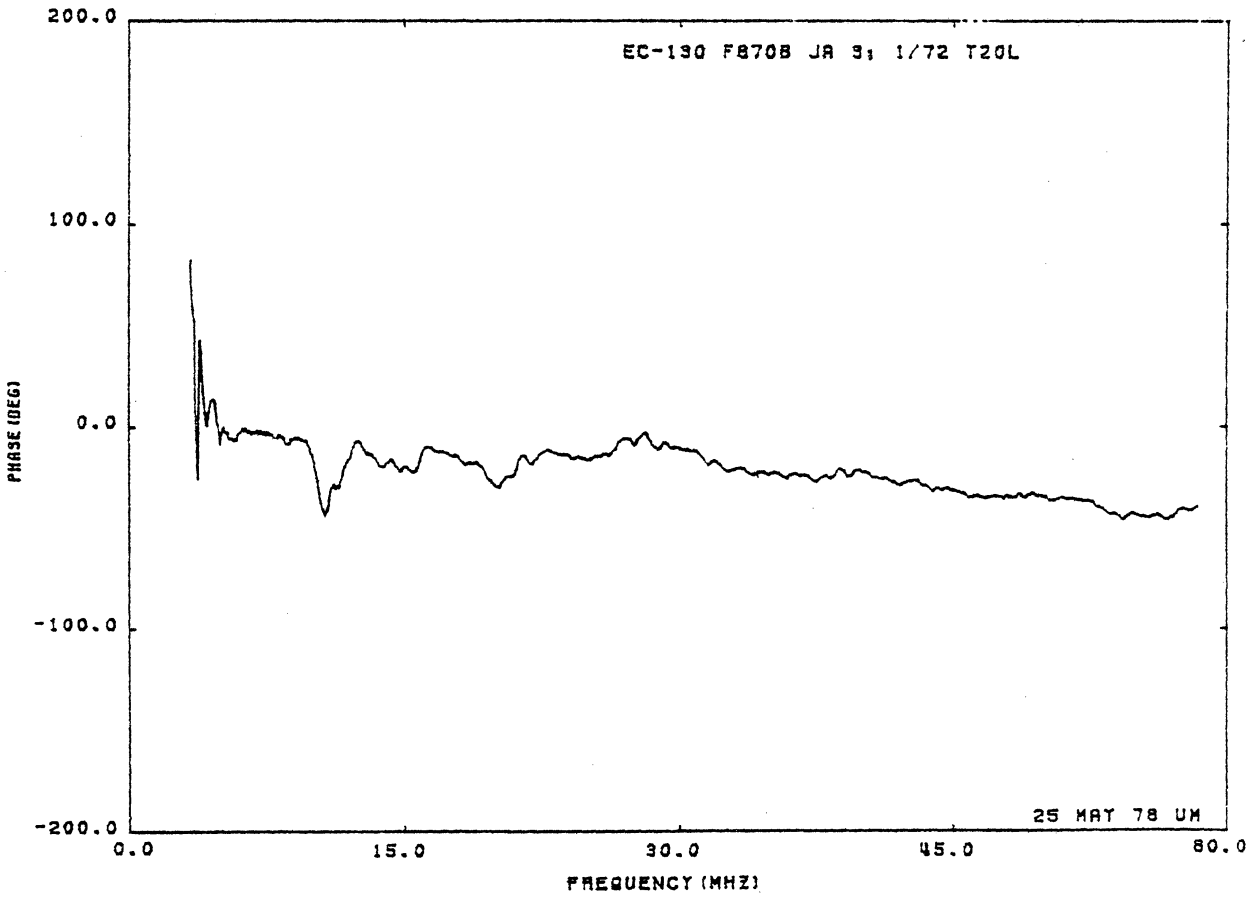

Figure 20L. Axial Current at STA:F870B, Excitation 3, 1/72 Model.

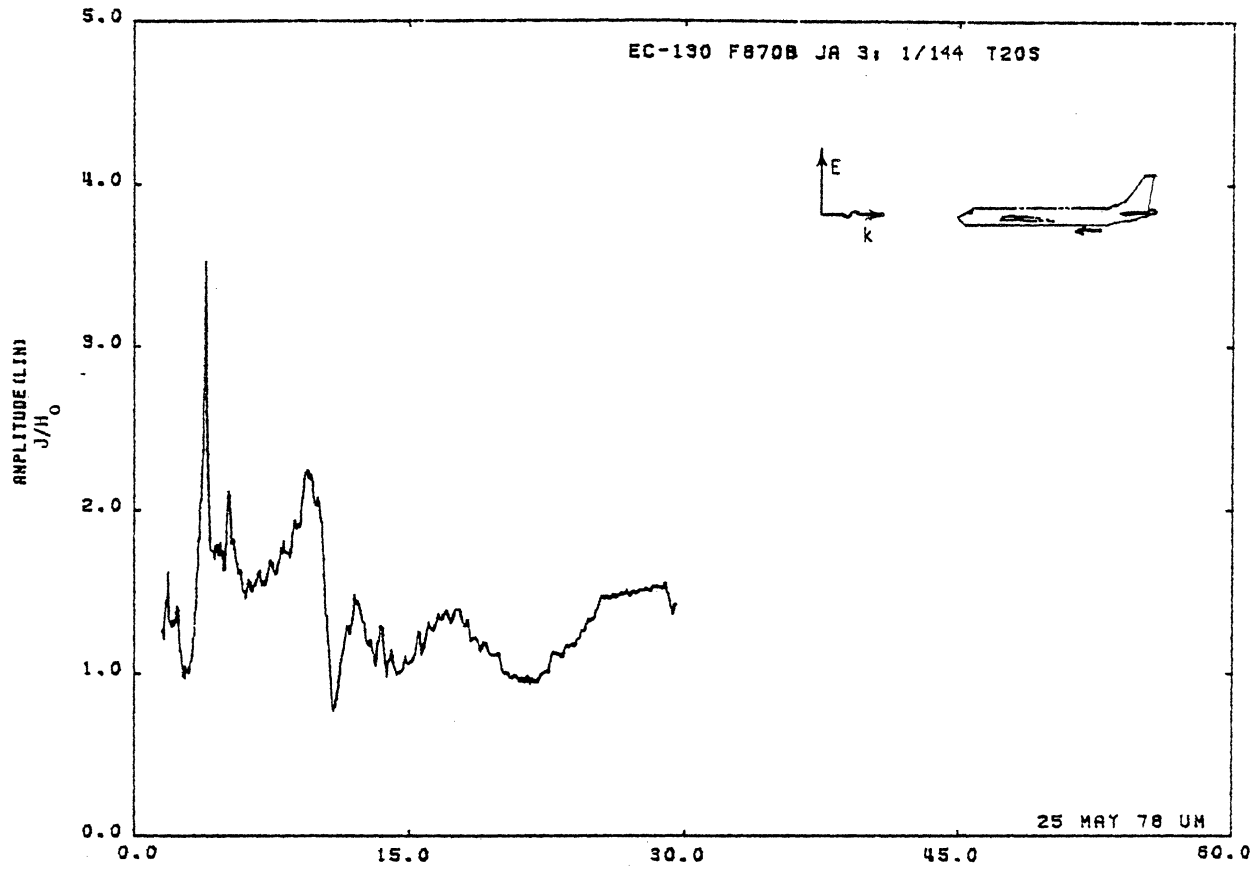

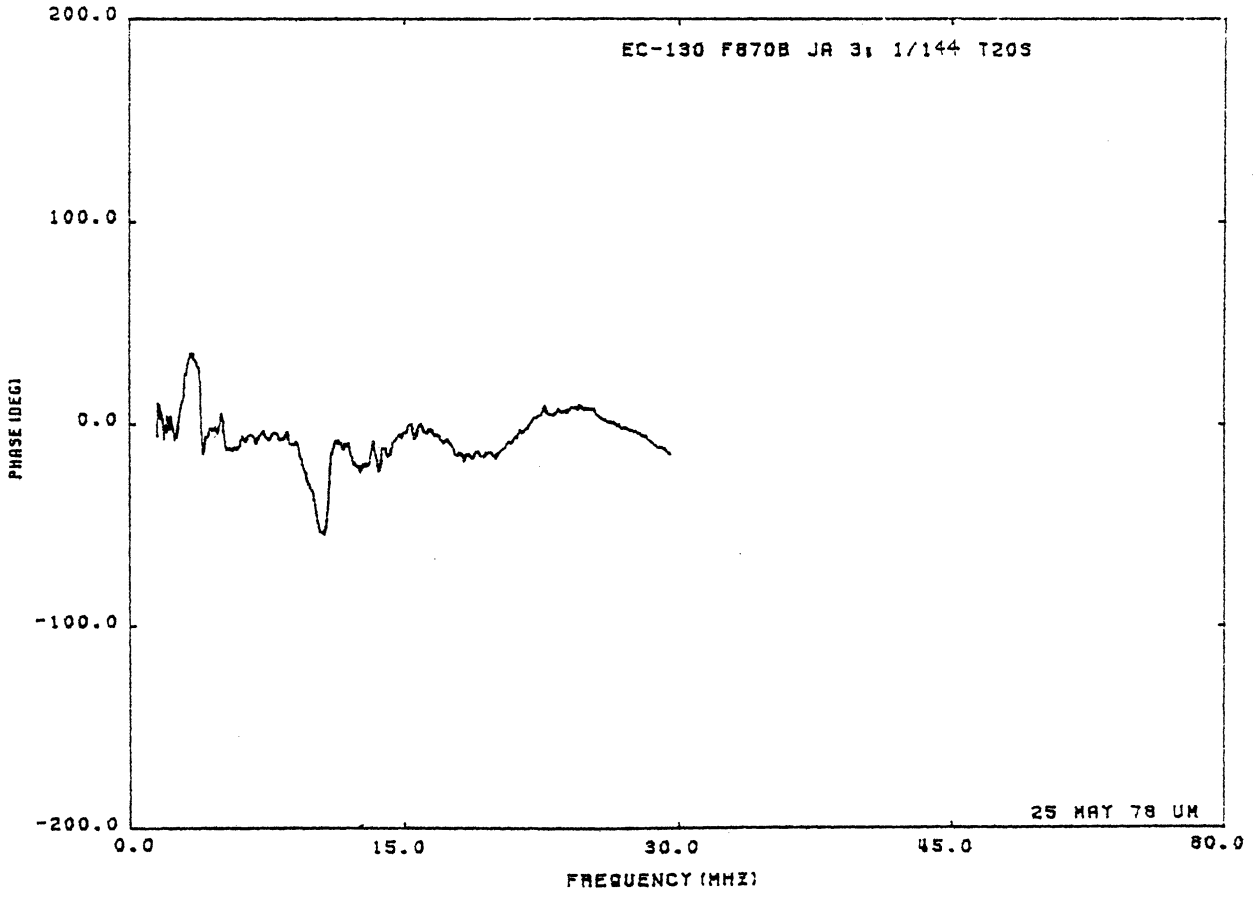

Figure 20S. Axial Current at STA:F870B, Excitation 3, 1/144 Model.

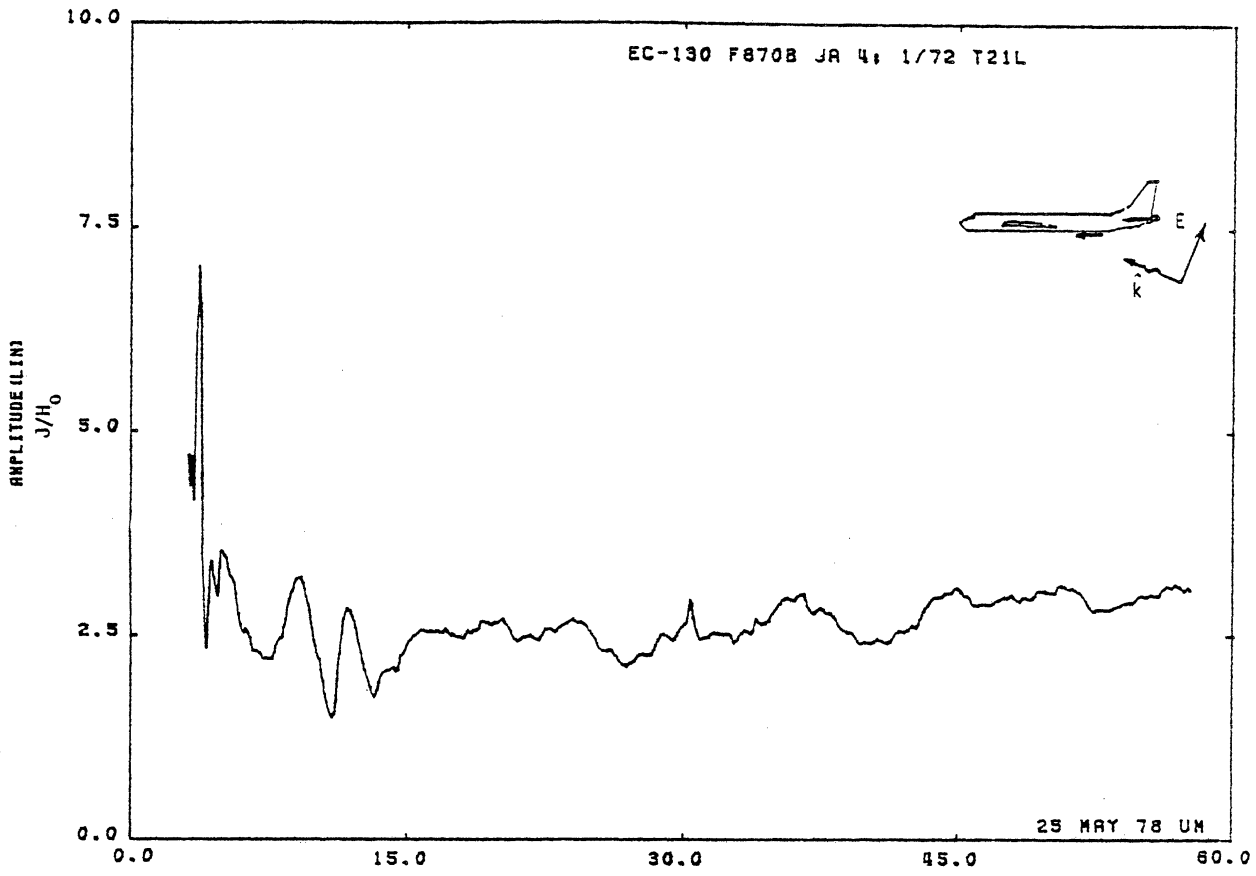

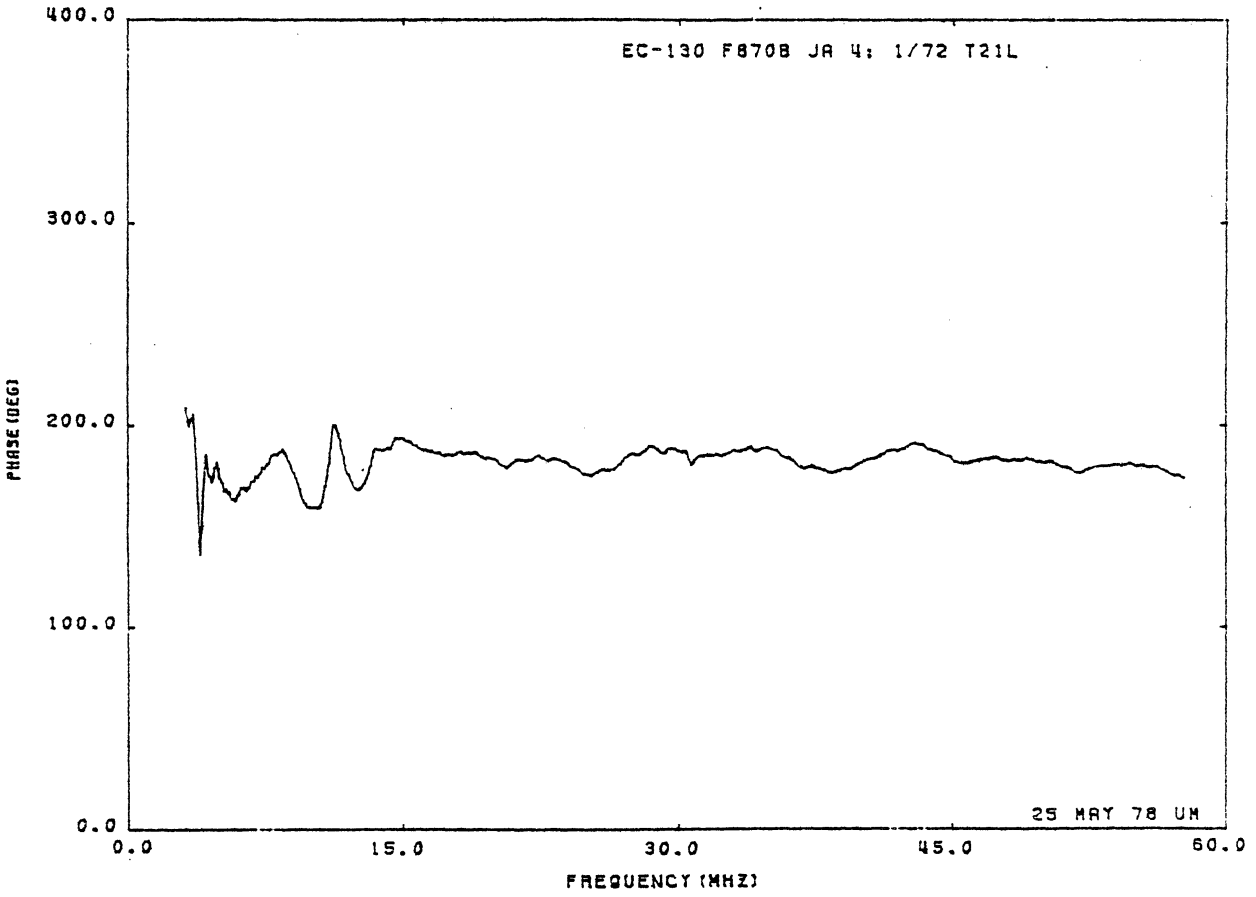

Figure 21L. Axial Current at STA:F870B, Excitation 4, 1/72 Model.

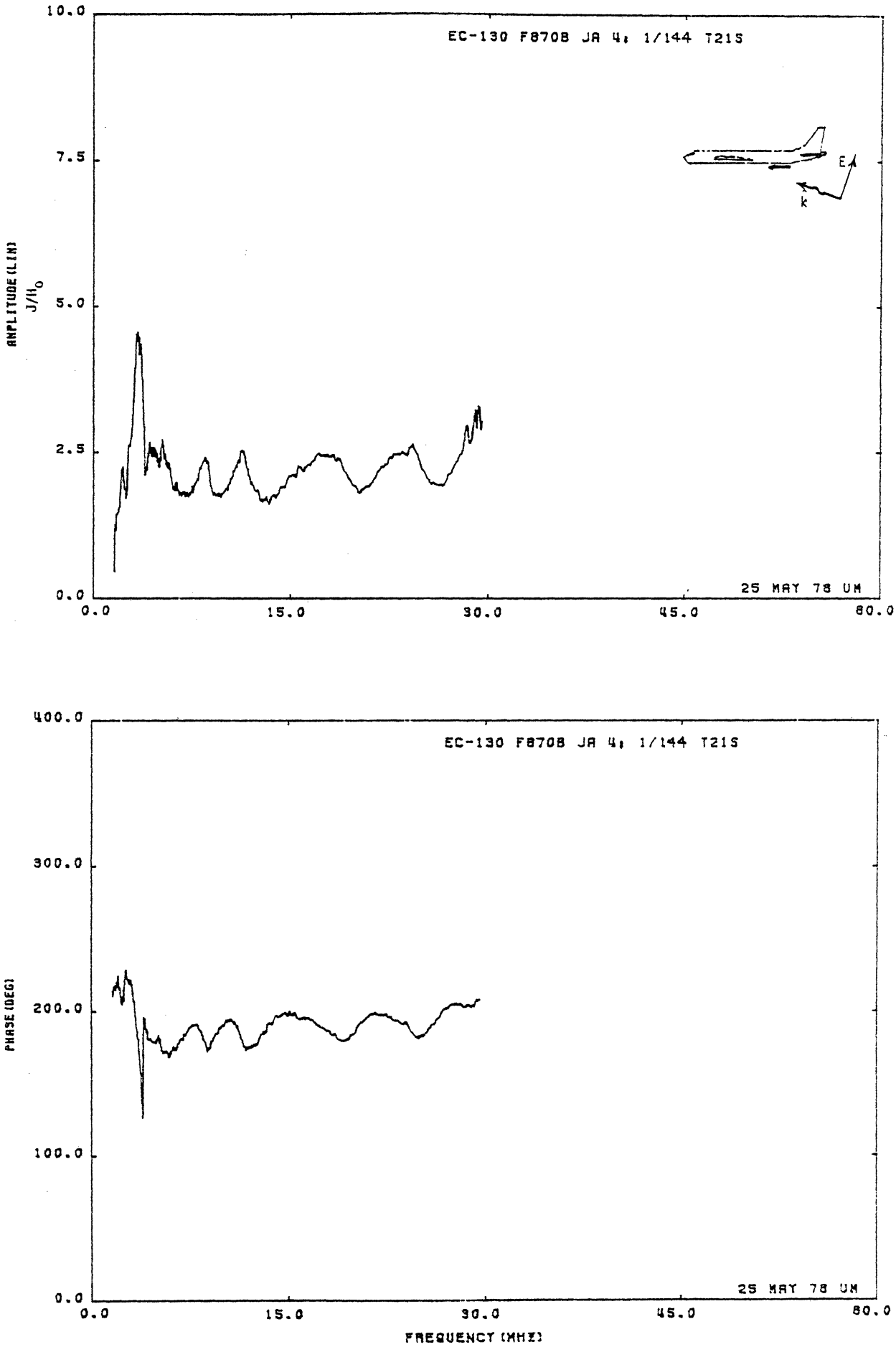

Figure 21S. Axial Current at STA:F870B, Excitation 4, 1/144 Model.

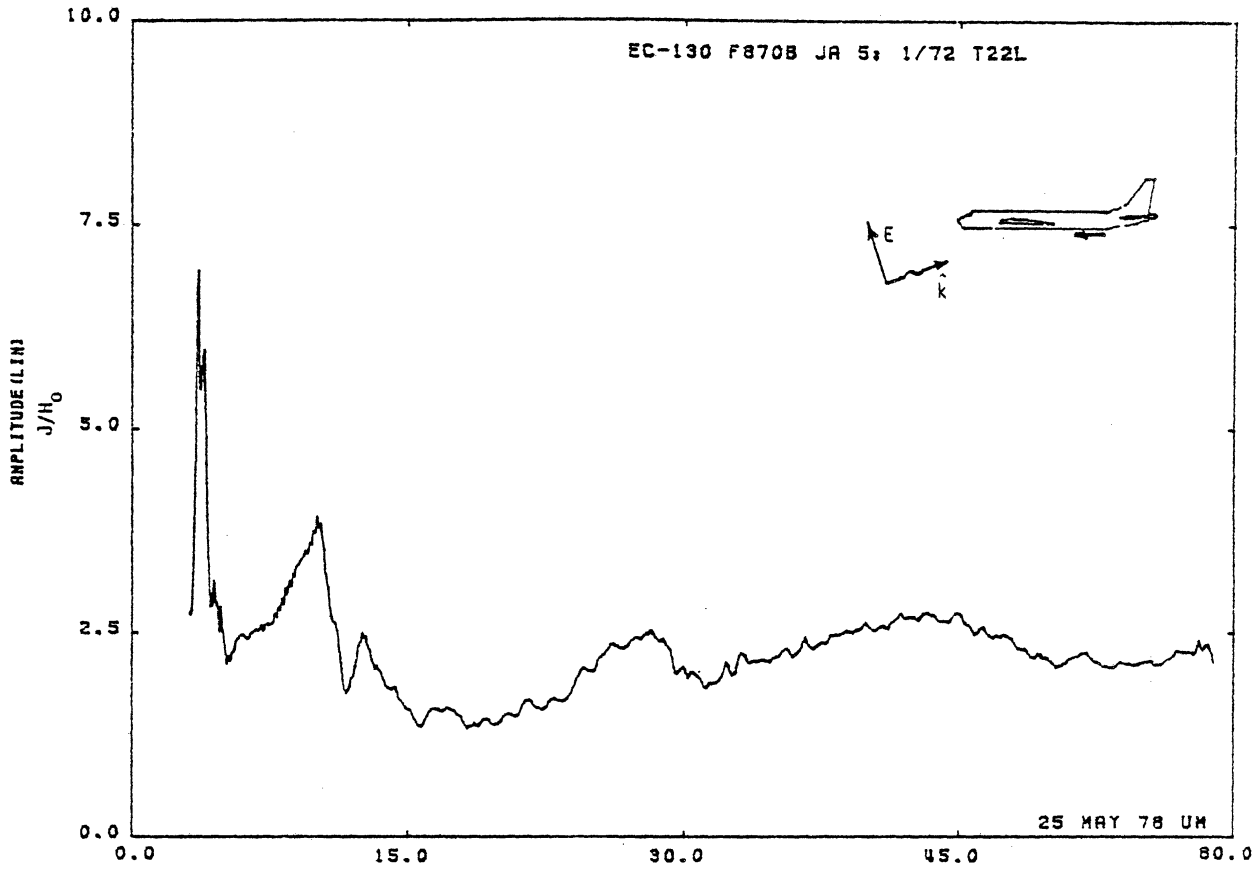

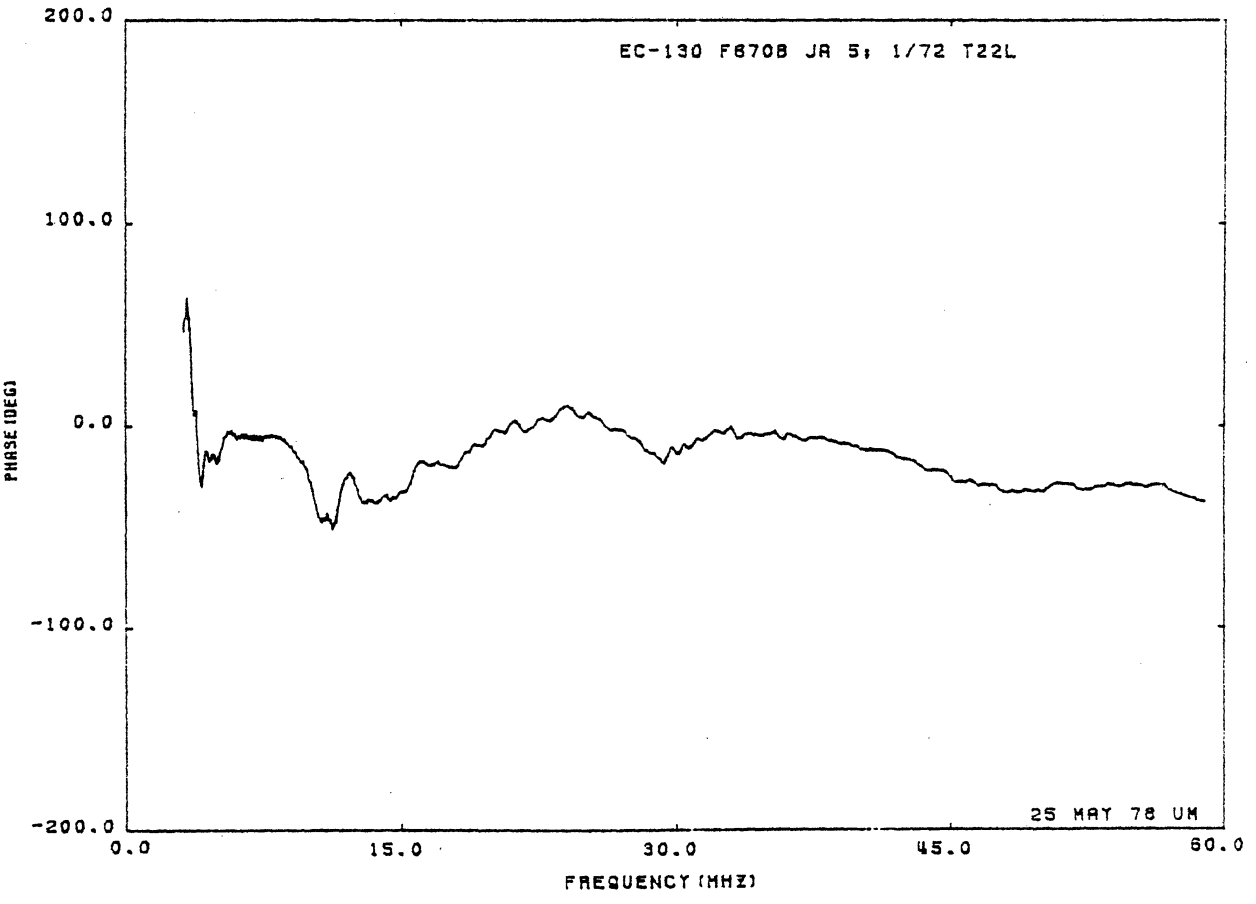

Figure 22L. Axial Current at STA:F870B, Excitation 5, 1/72 Model.

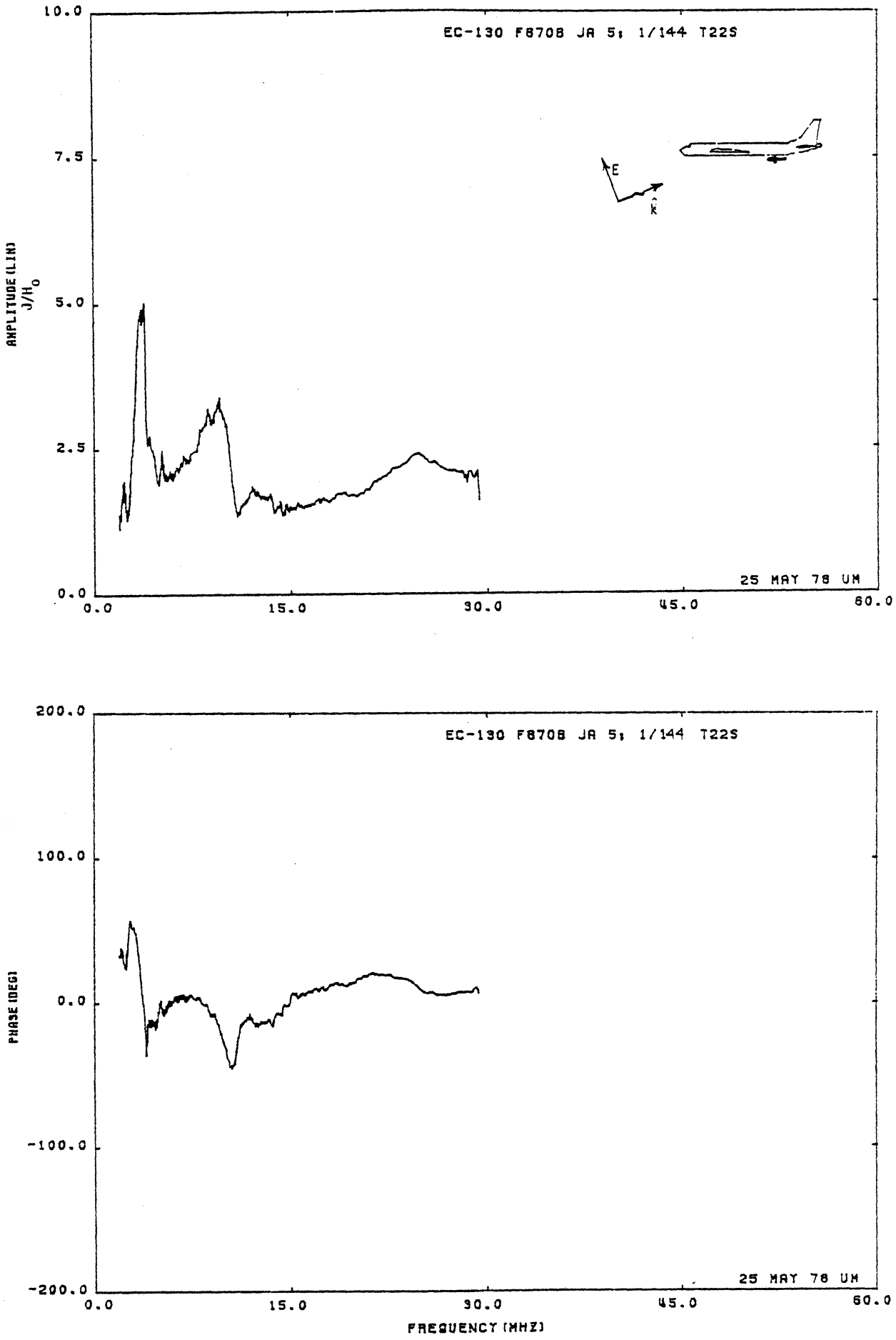

Figure 22S. Axial Current at STA:F870B, Excitation 5, 1/144 Model.

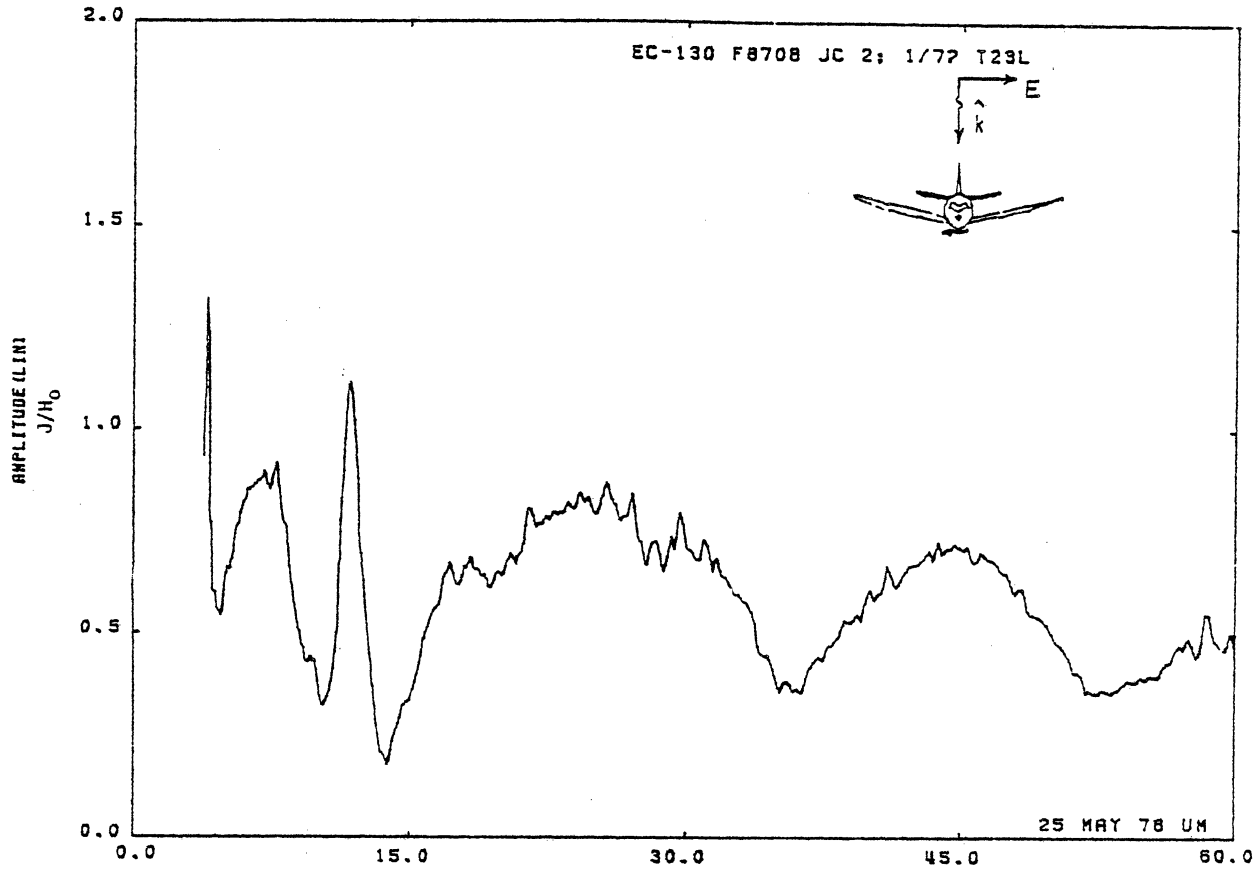

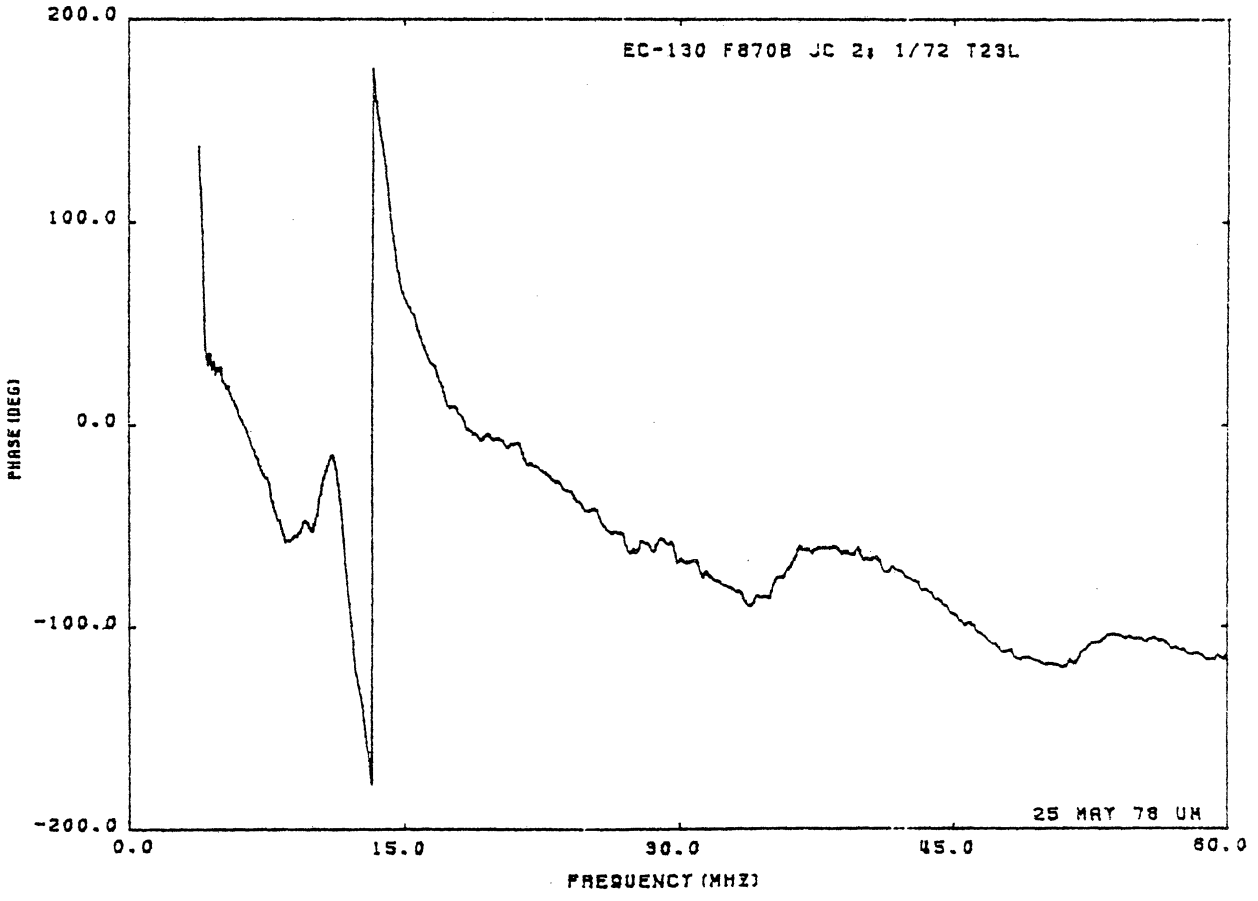

Figure 23L. Circumferential Current at STA:F870B, Excitation 2, 1/72 Model.

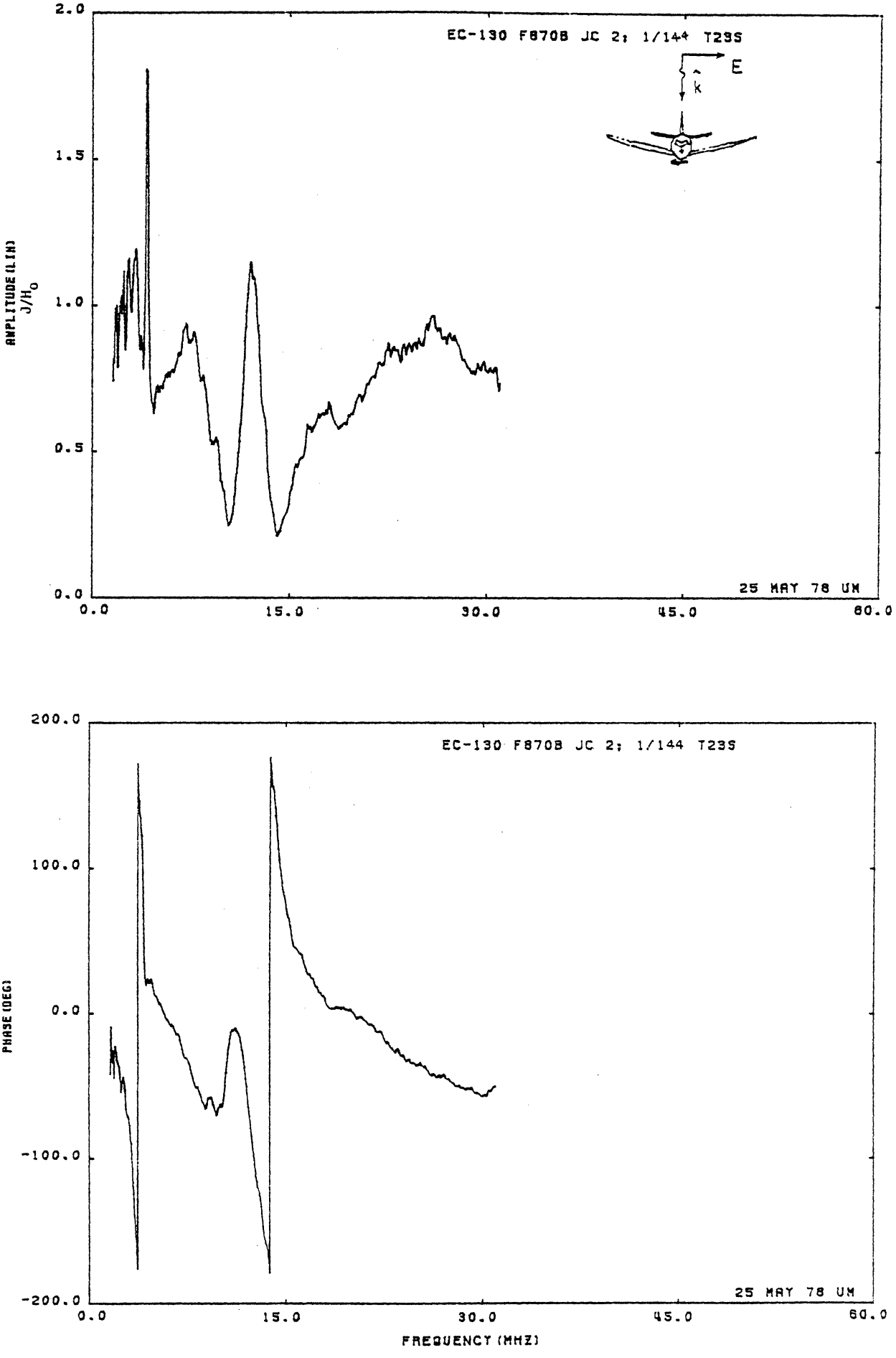

Figure 23S. Circumferential Current at STA:F870B, Excitation 2, 1/144 Model.

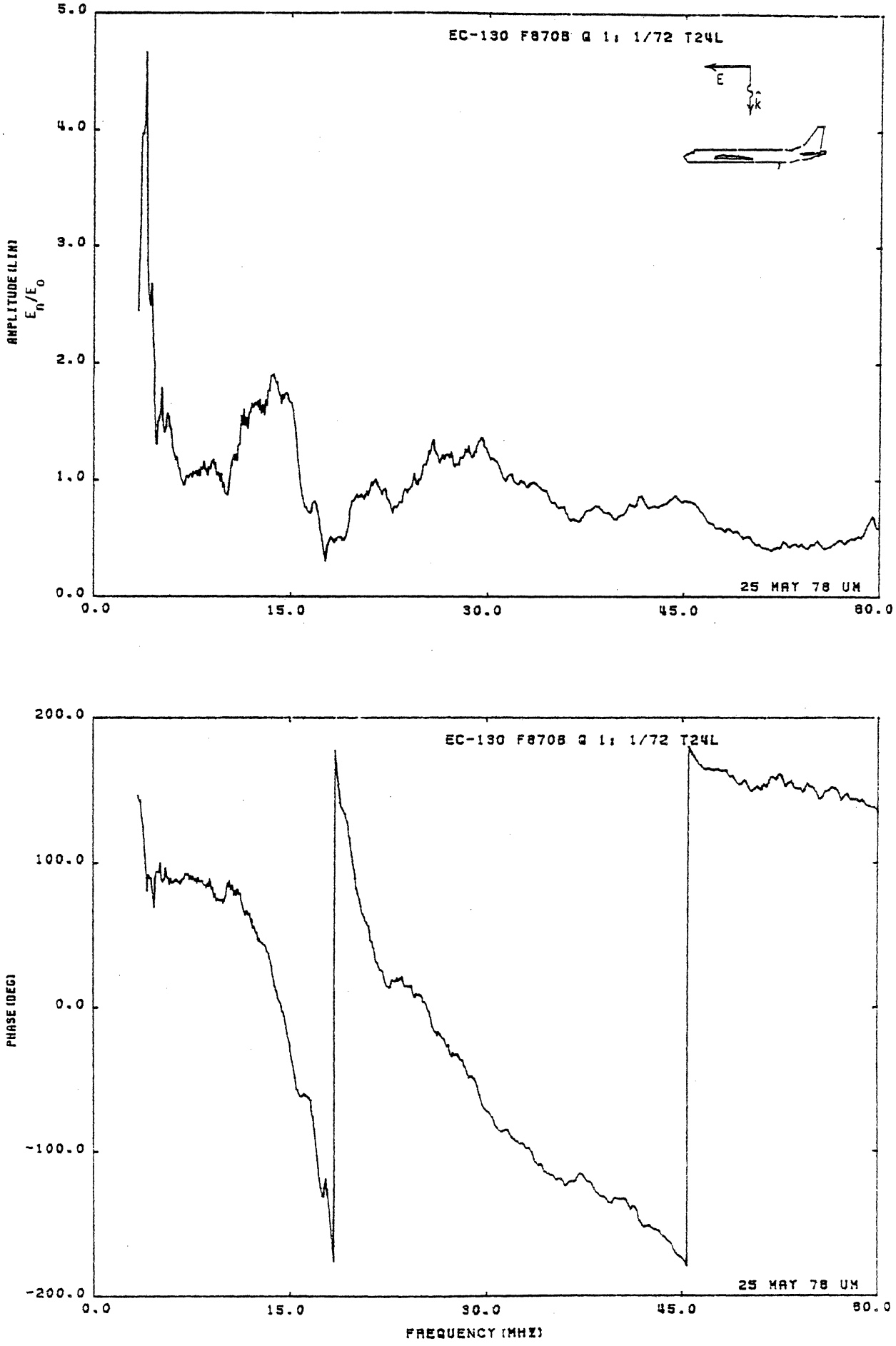

Figure 24L. Charge at STA:F870B, Excitation 1, 1/72 Model.

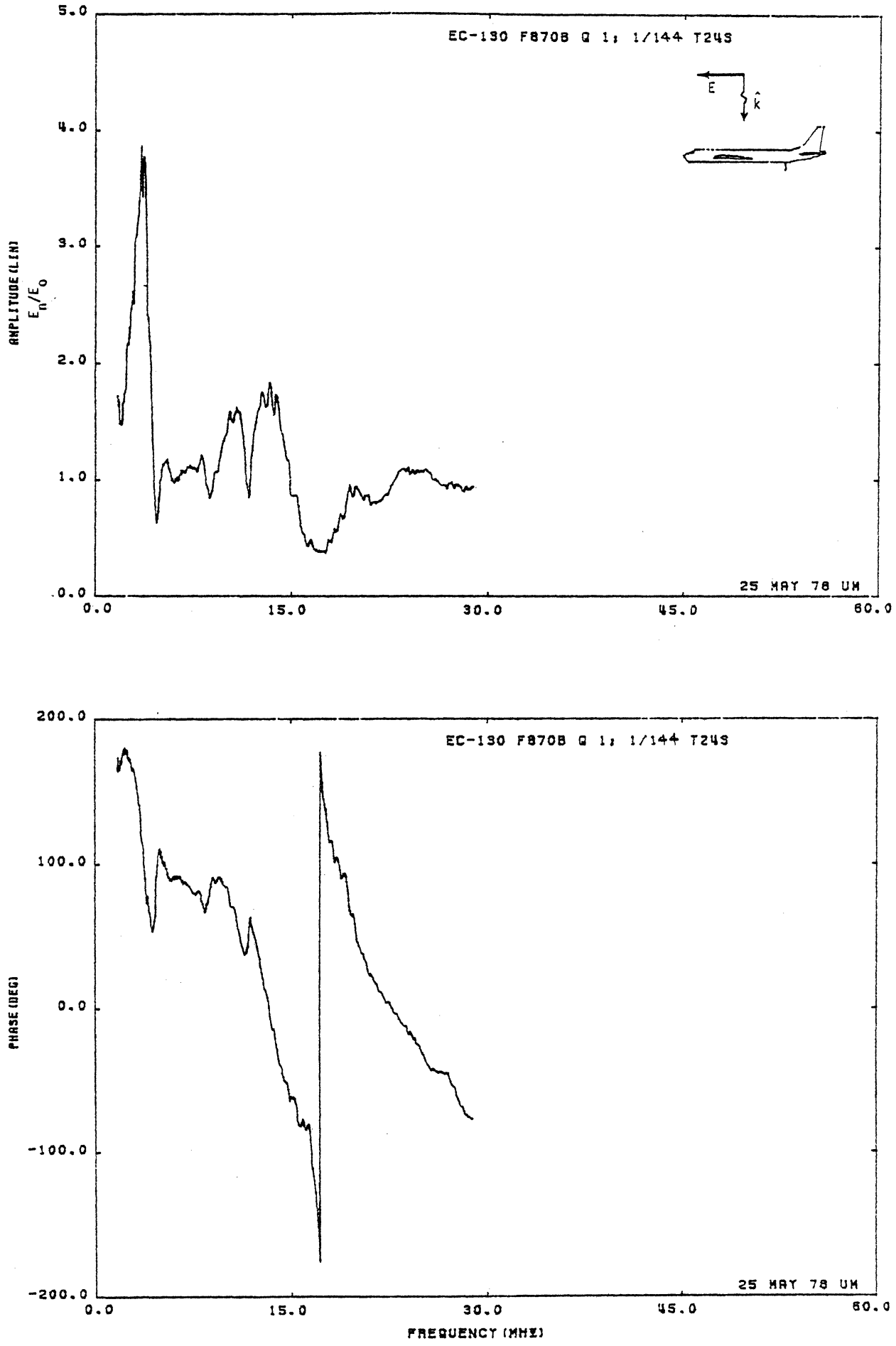

Figure 24S. Charge at STA:F870B, Excitation 1, 1/144 Model.

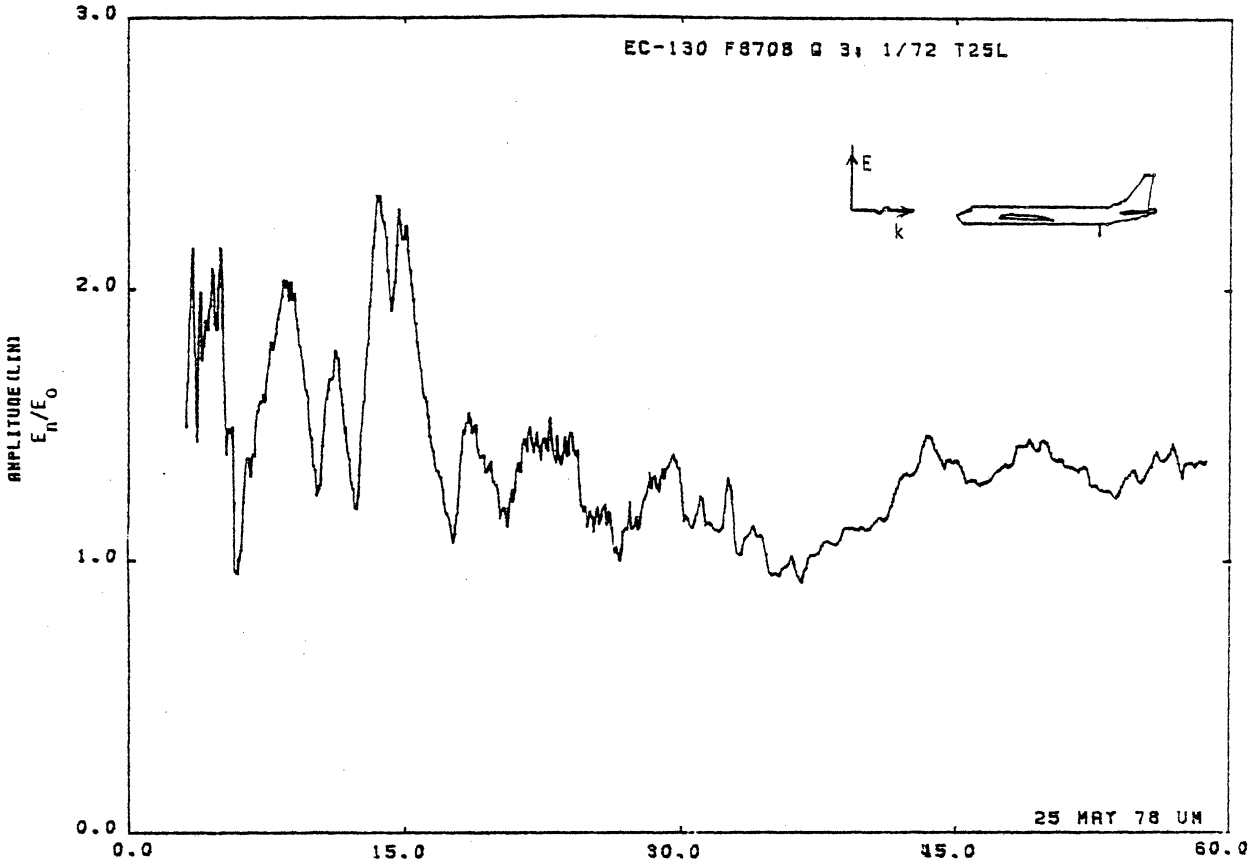

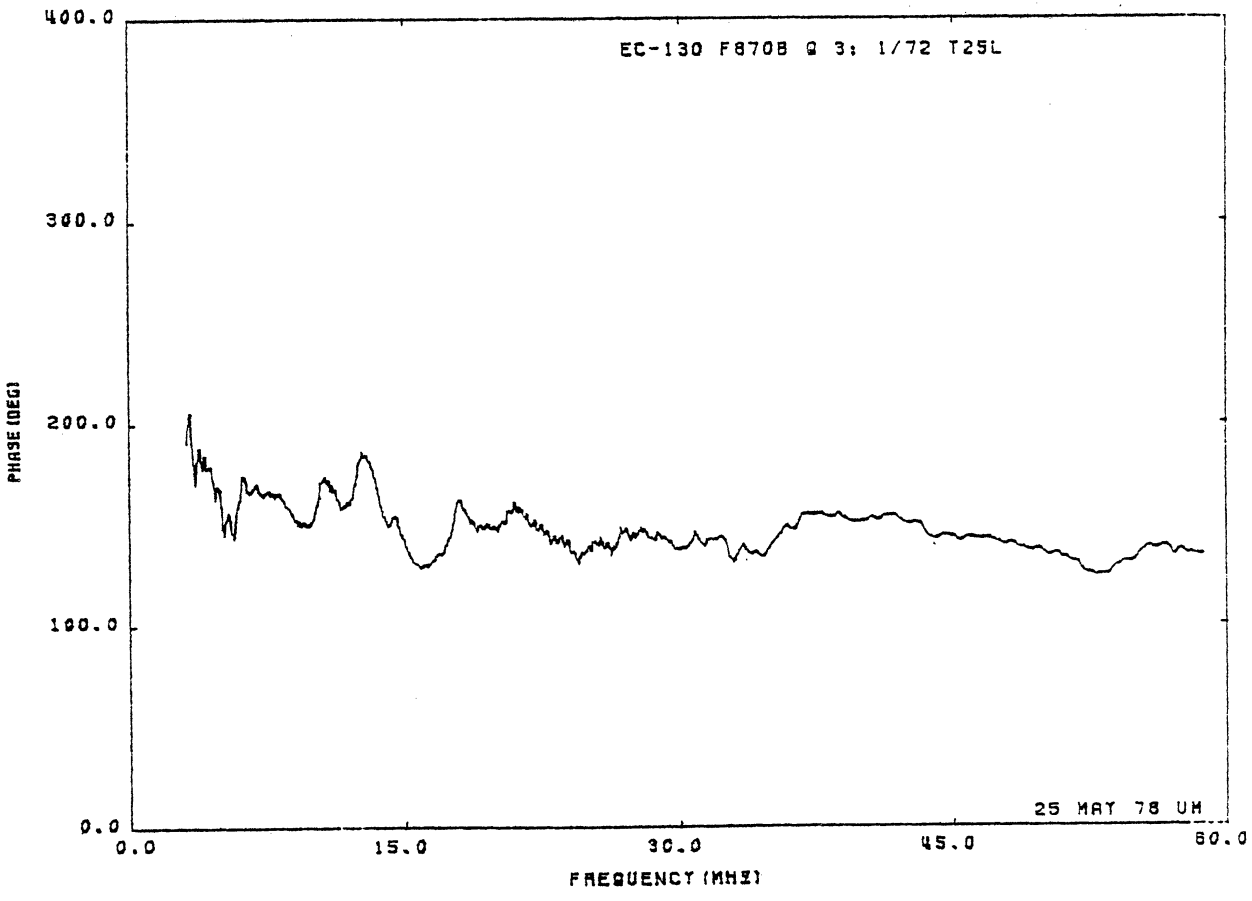

Figure 25L. Charge at STA:F870B, Excitation 3, 1/72 Model.

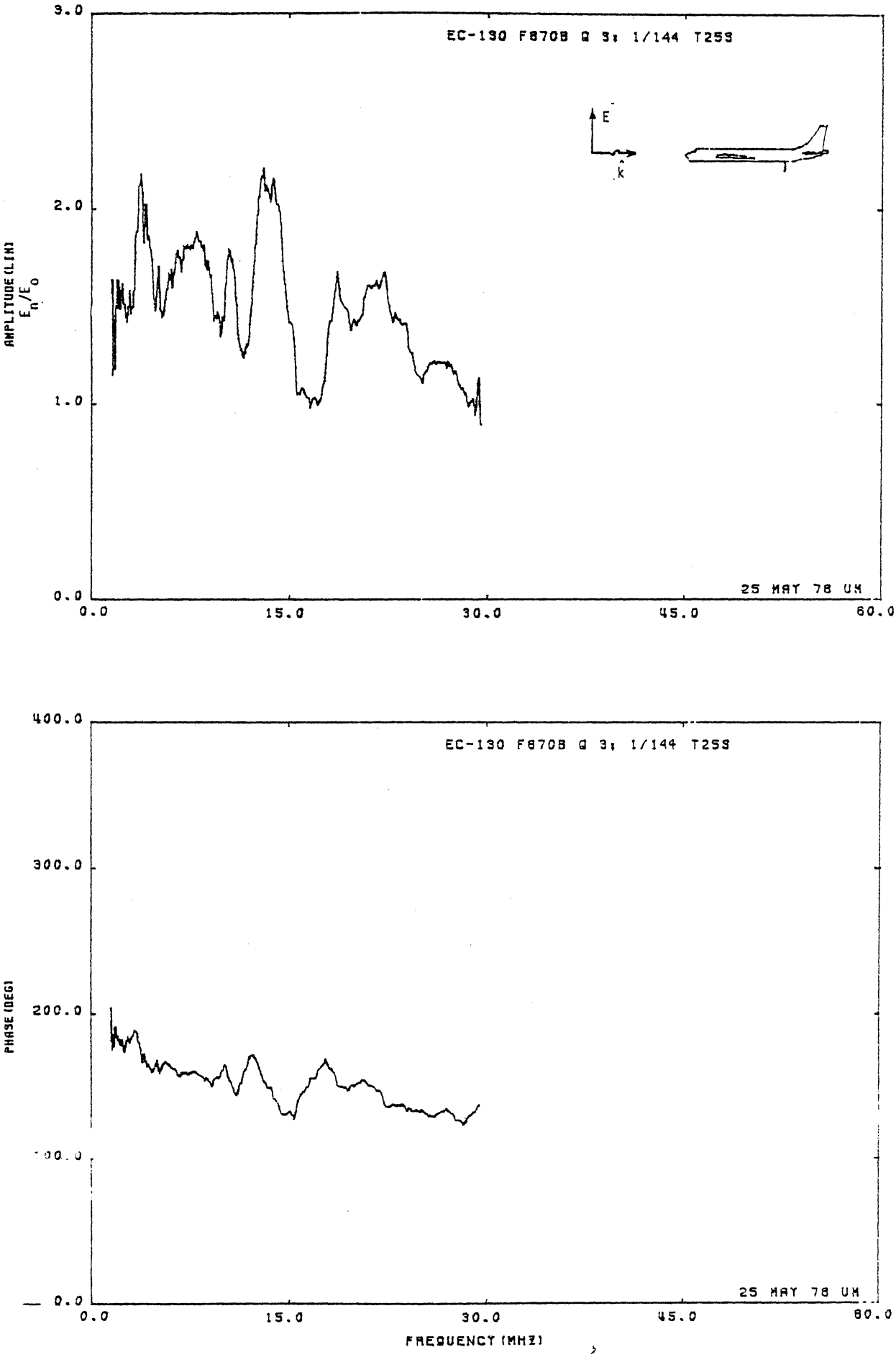

Figure 25S. Charge at STA:F870B, Excitation 3, 1/144 Model.

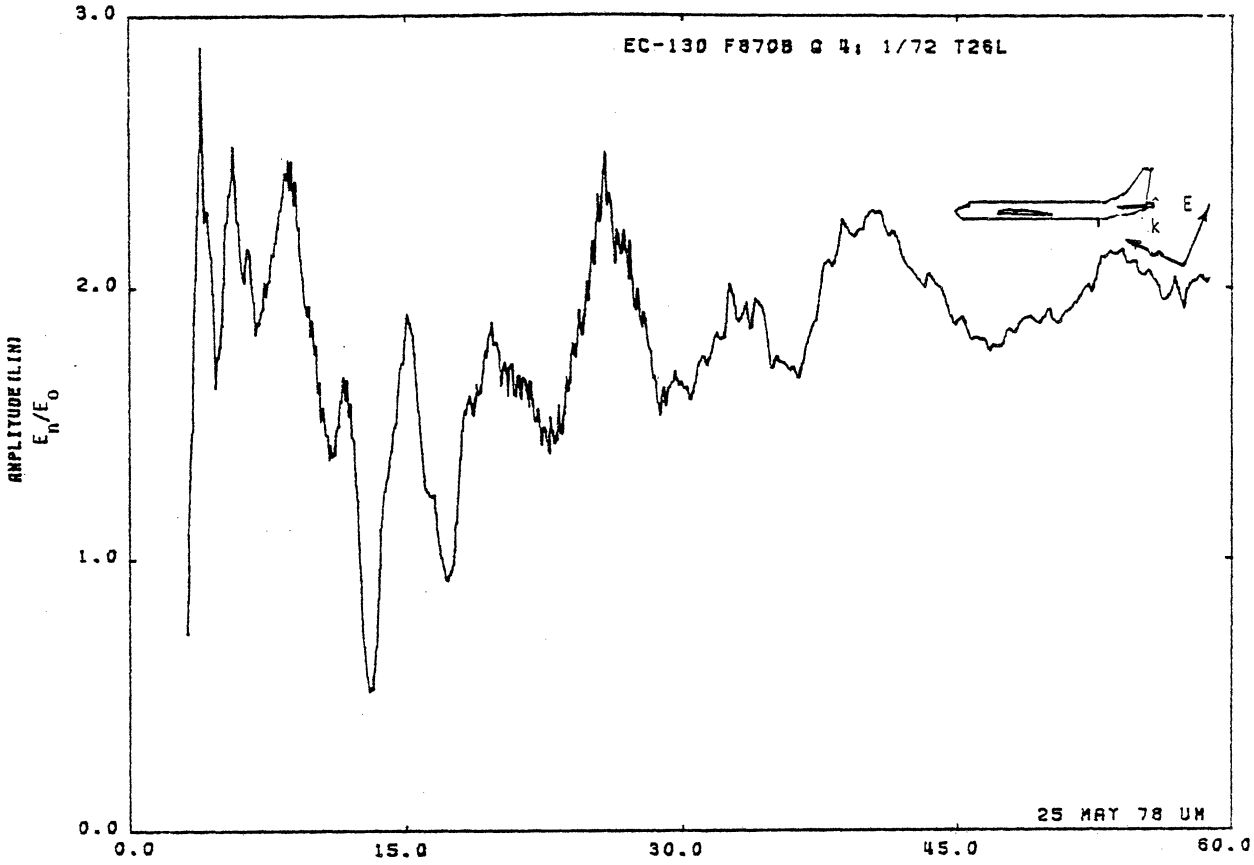

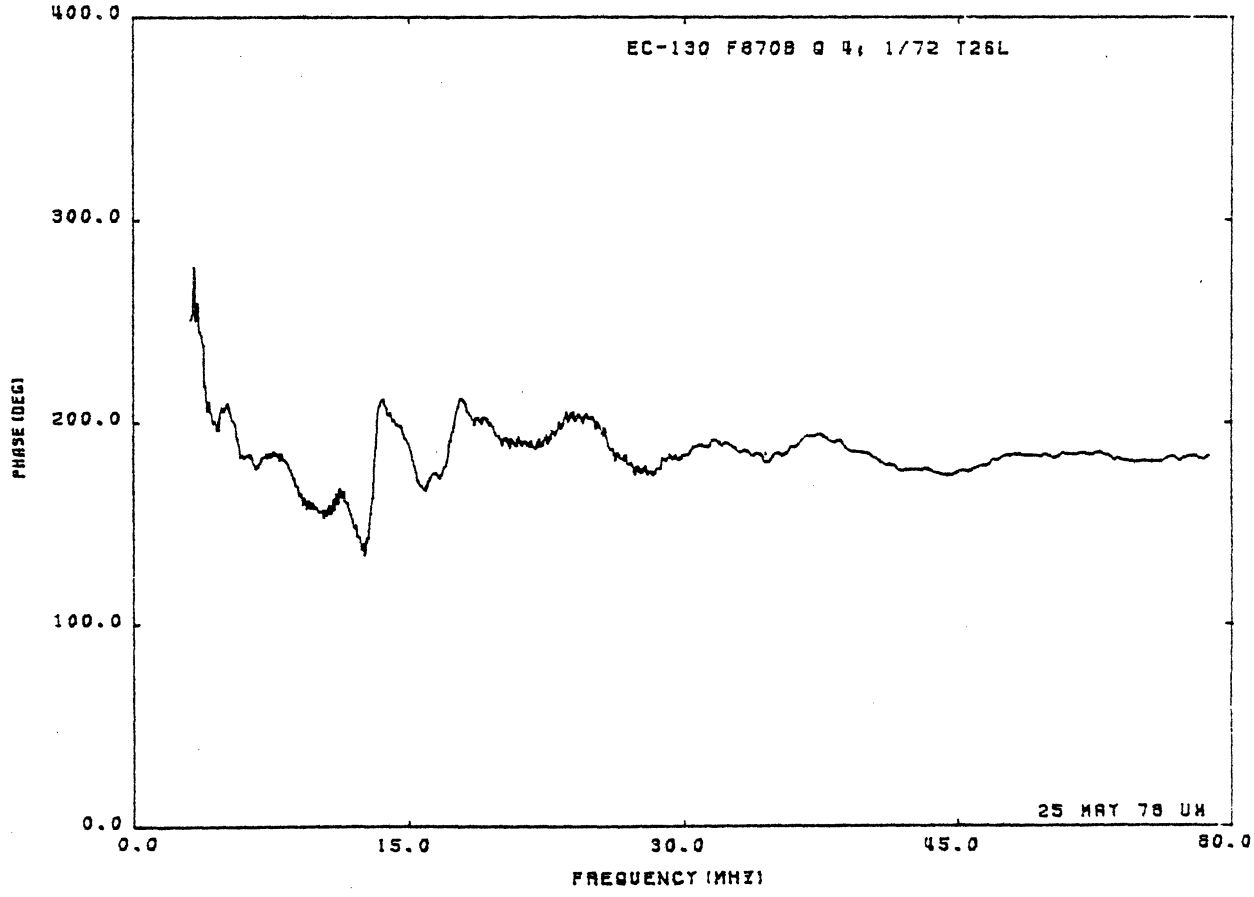

Figure 26L. Charge at STA:F870B, Excitation 4, 1/72 Model.

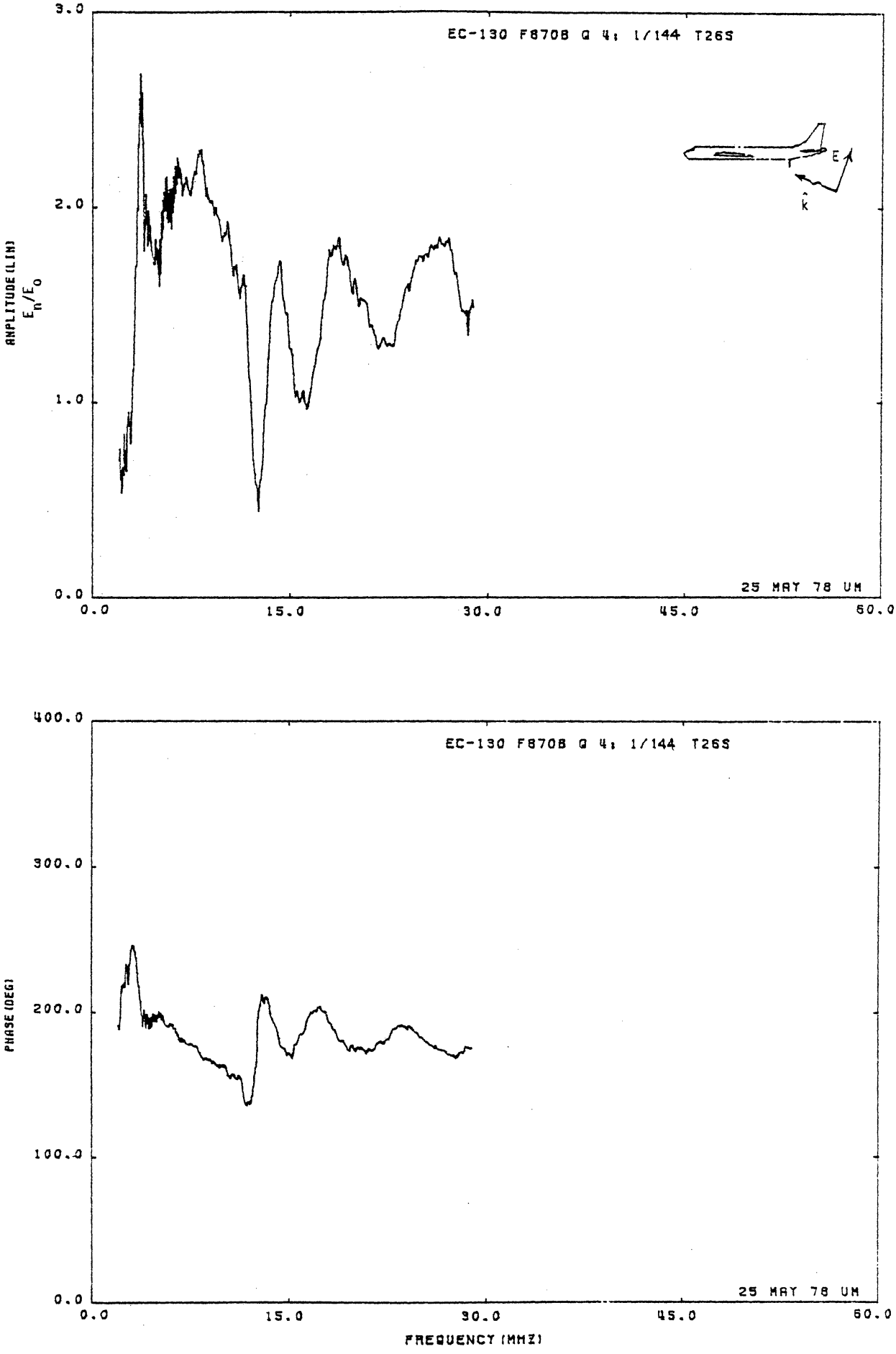

Figure 26S. Charge at STA:F870B, Excitation 4, 1/144 Model.

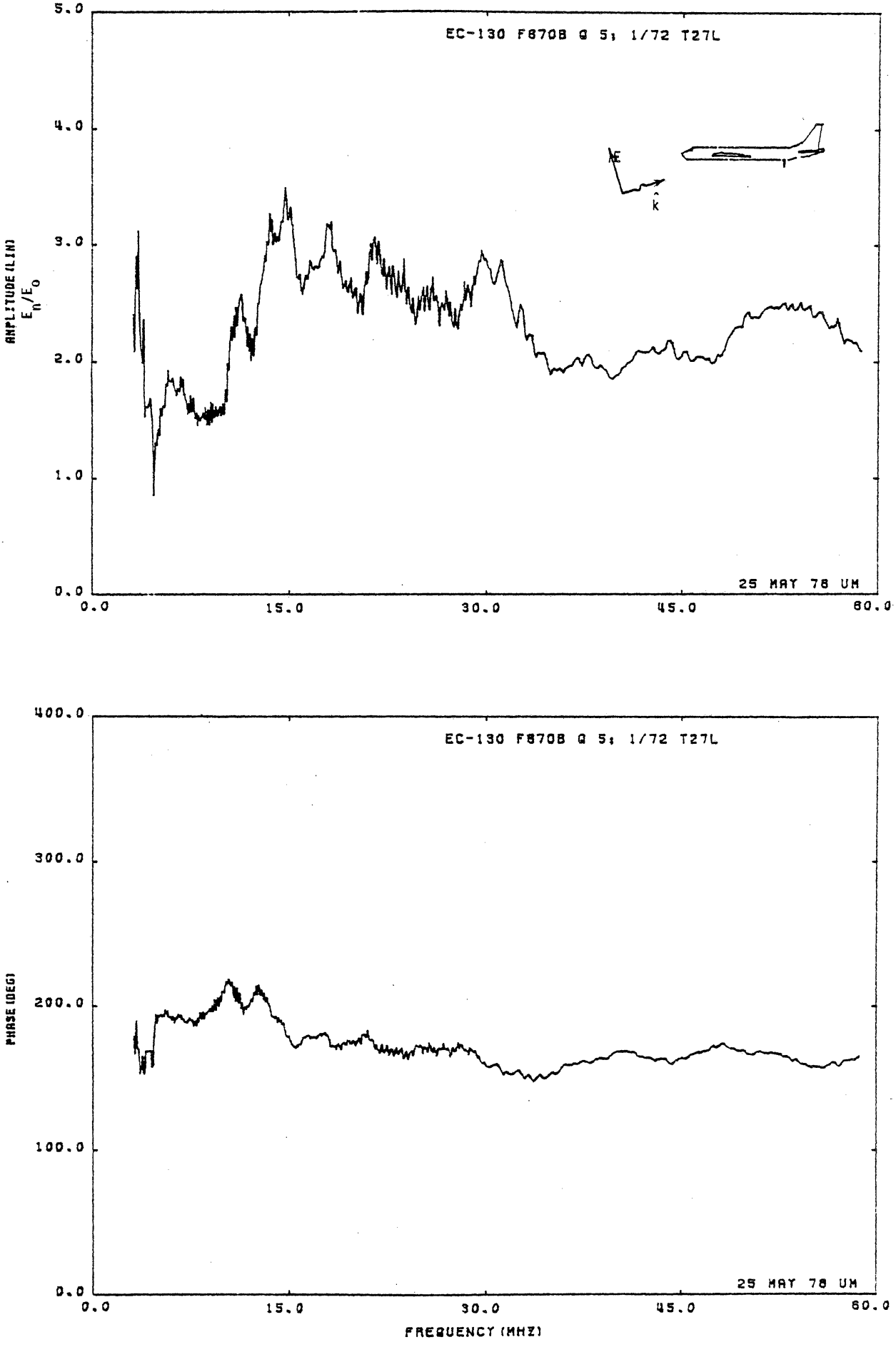

Figure 27L. Charge at STA:F870B, Excitation 5, 1/72 Model.

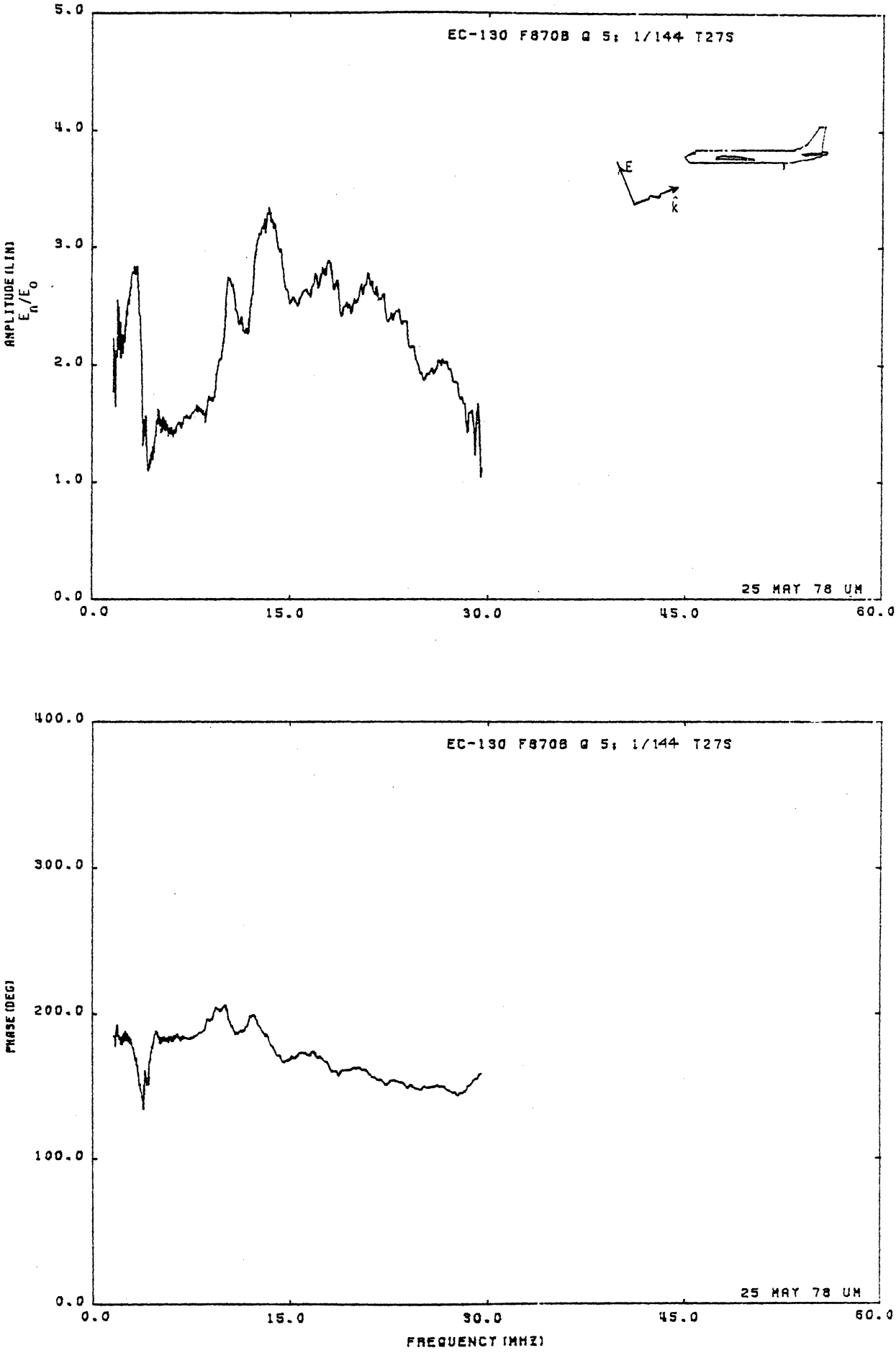

Figure 27S. Charge at STA:F345B, Excitation 5, 1/144 Model.

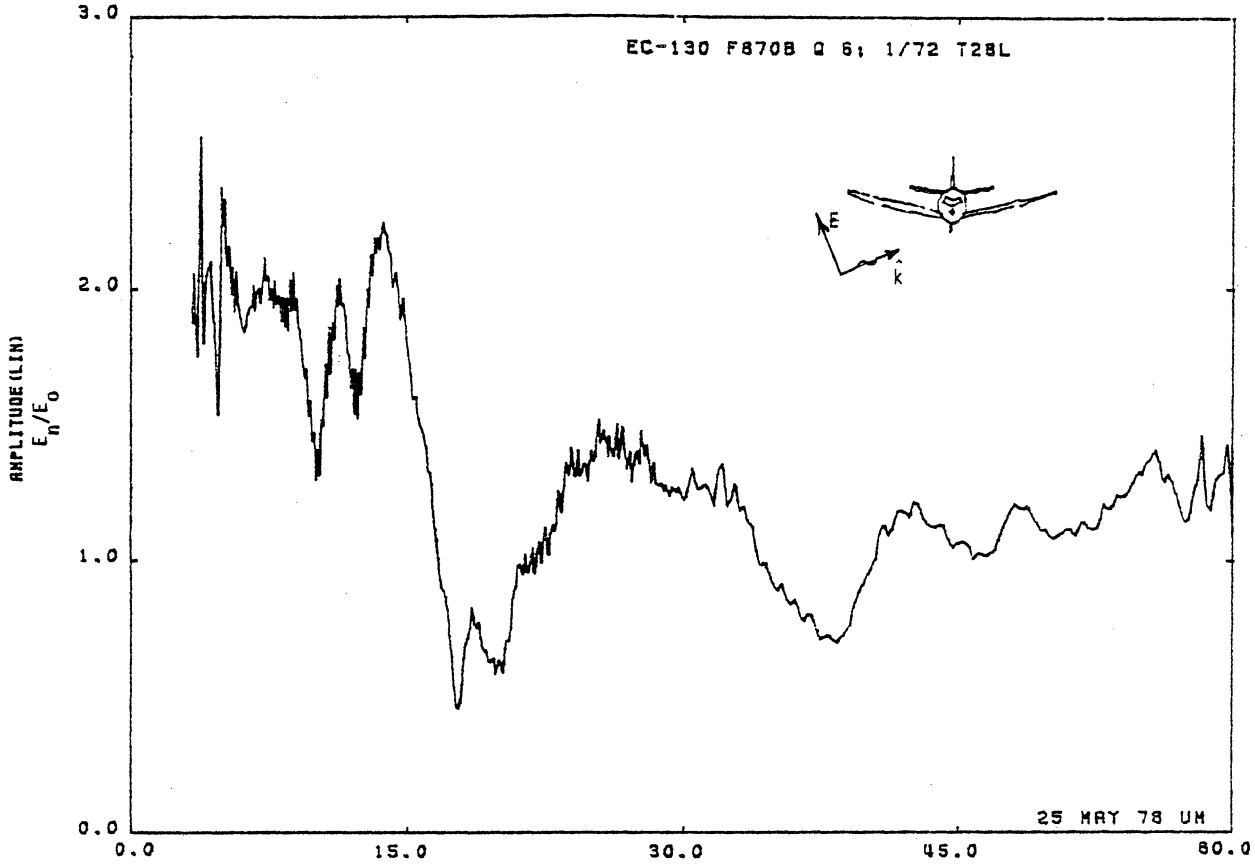

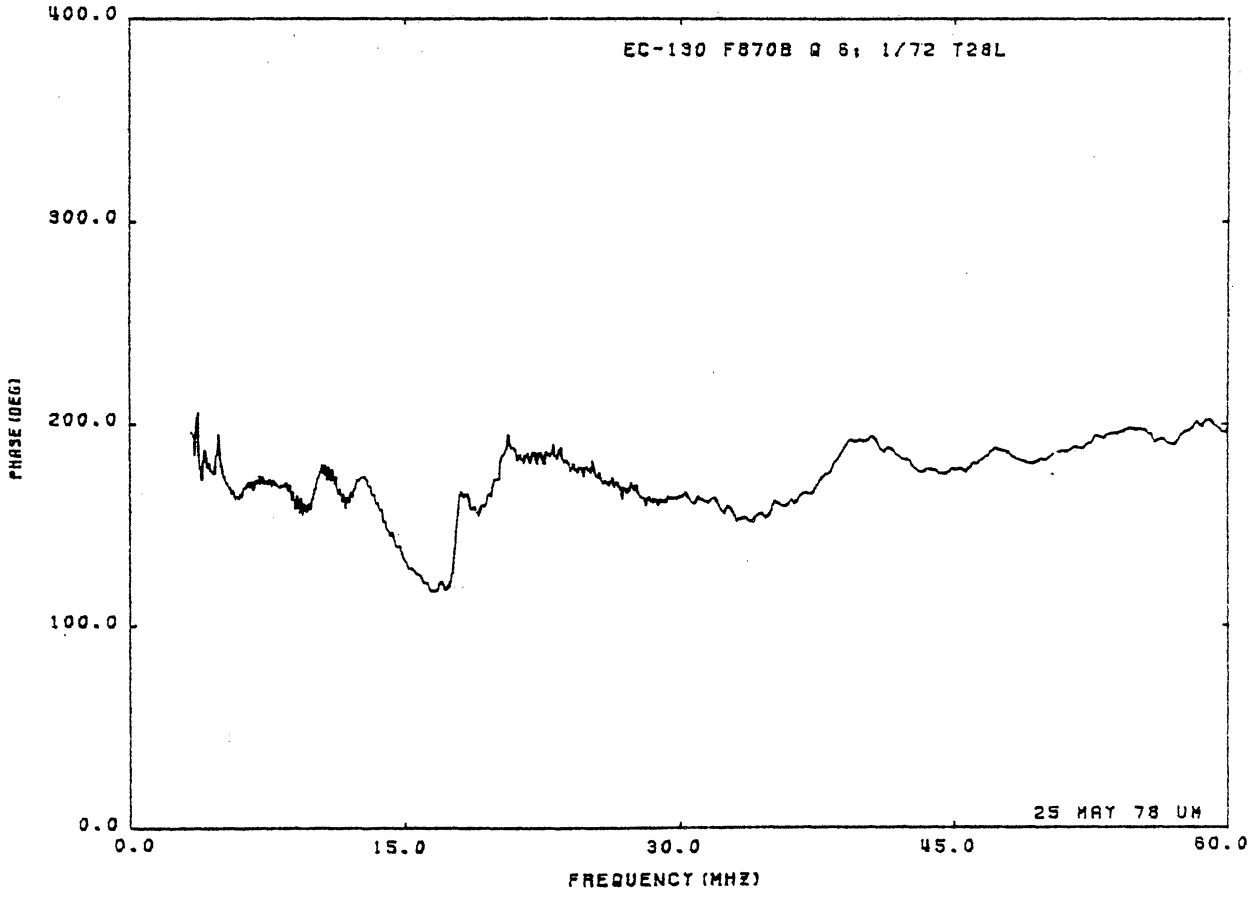

Figure 28L. Charge at STA:F870B, Excitation 6, 1/72 Model.

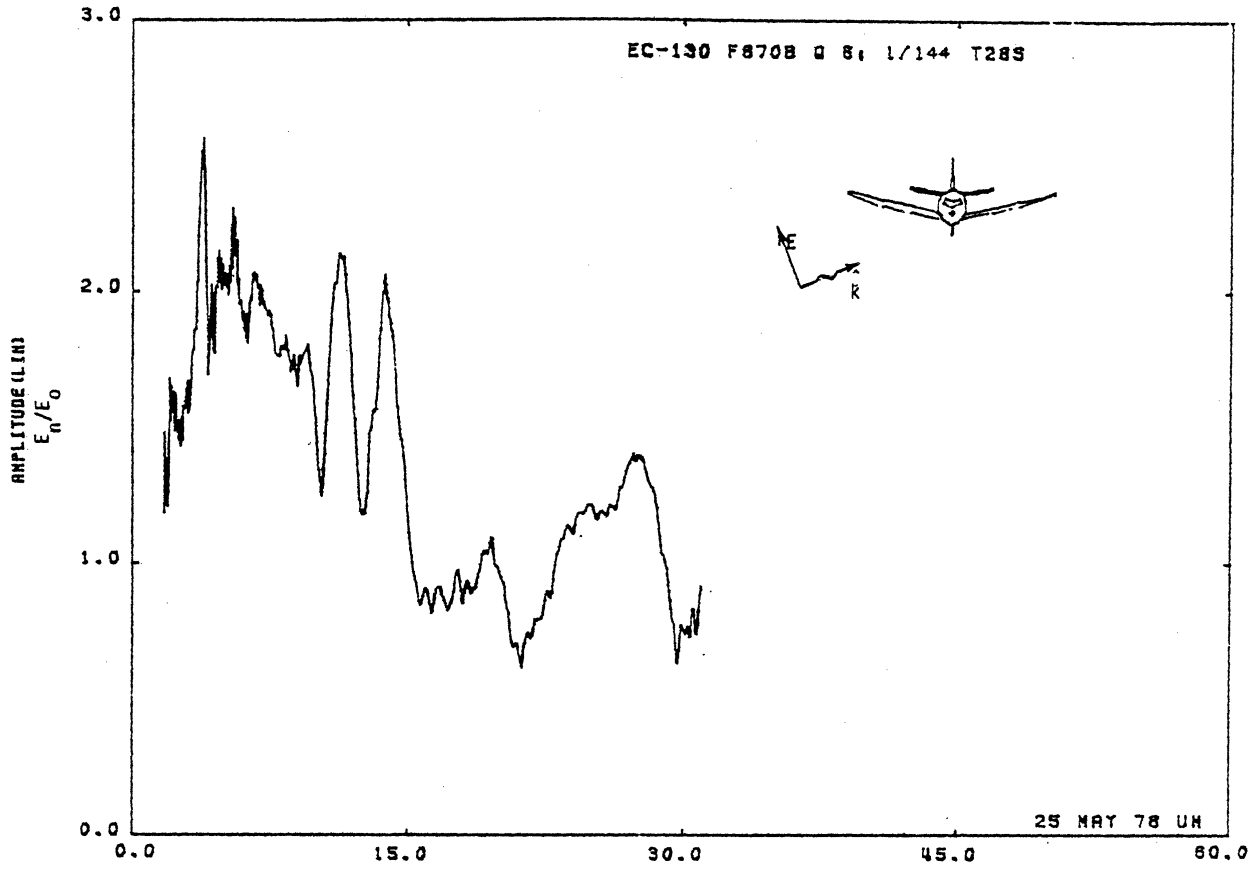

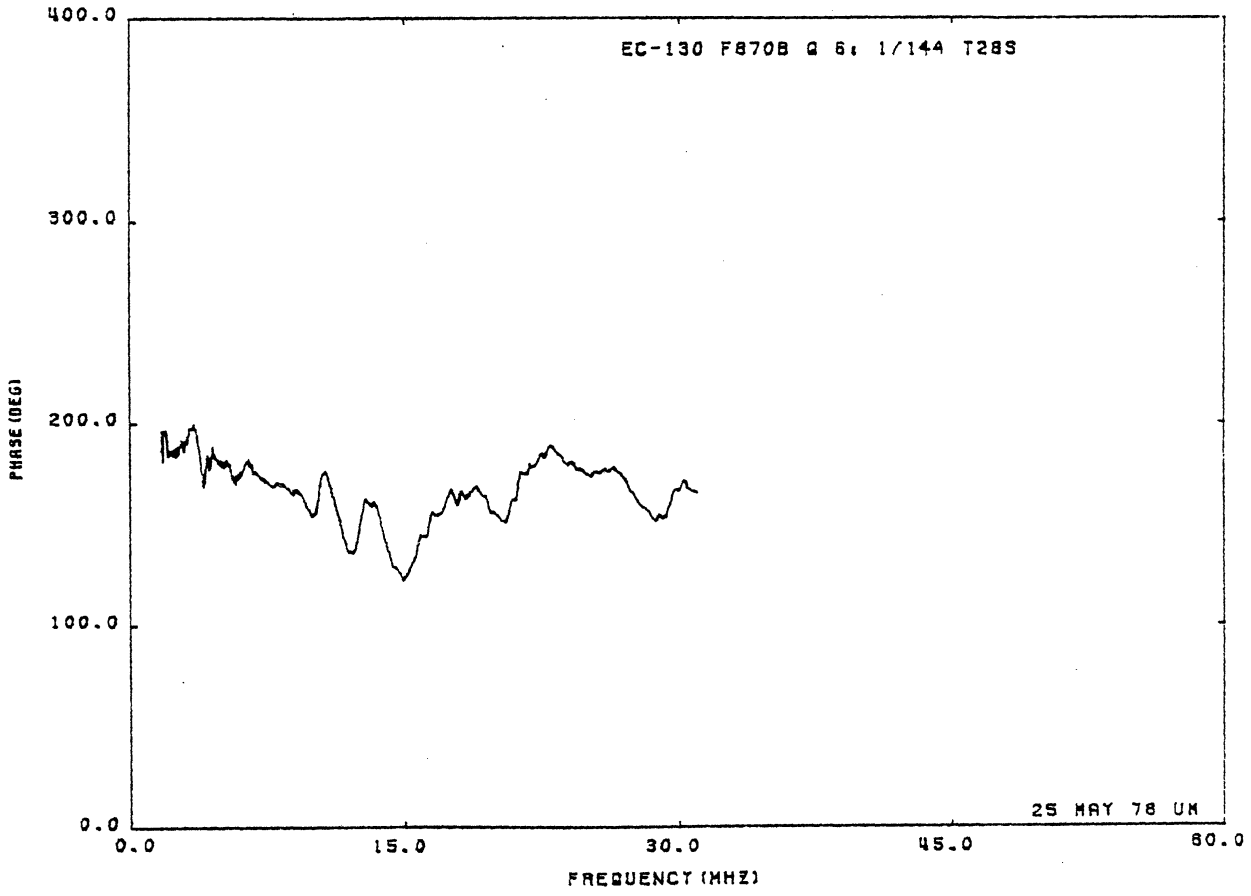

Figure 28S. Charge at STA:F870B, Excitation 6, 1/144 Model.

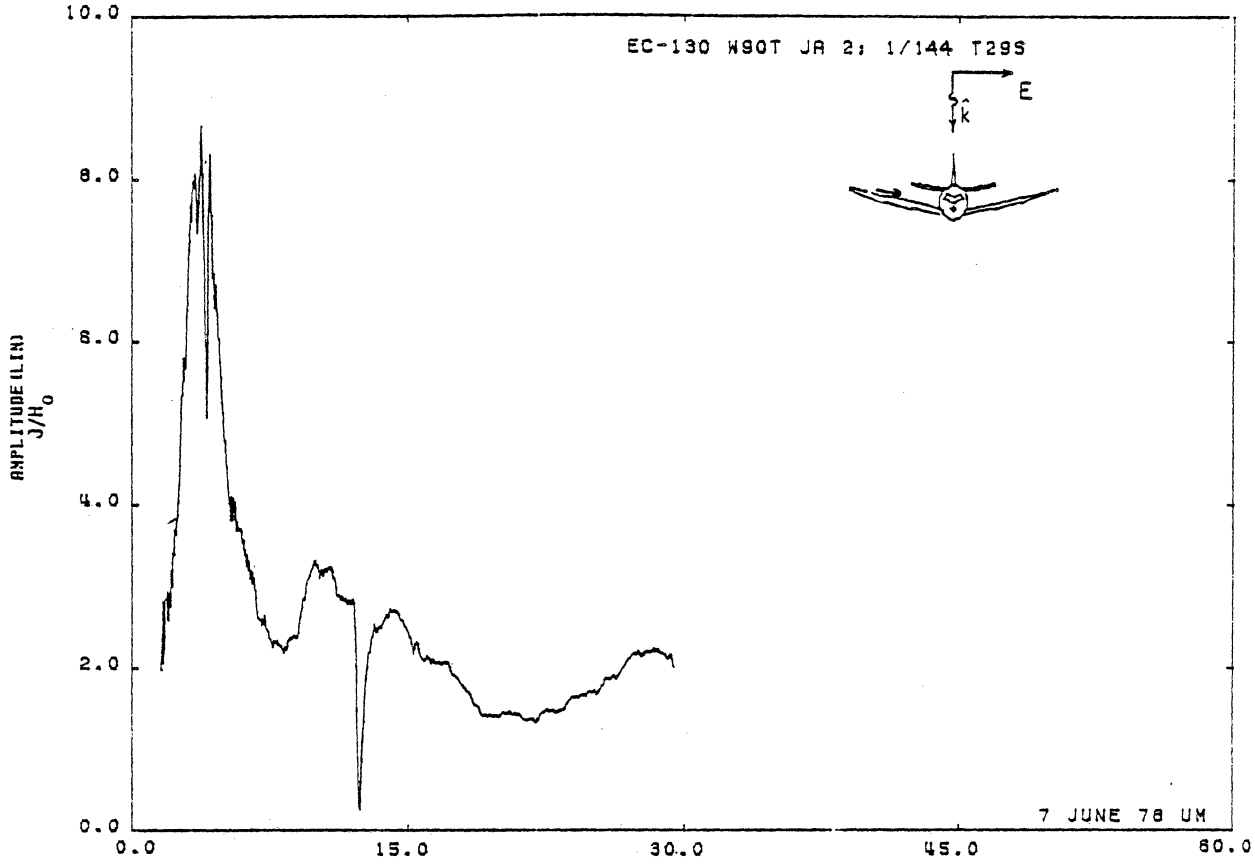

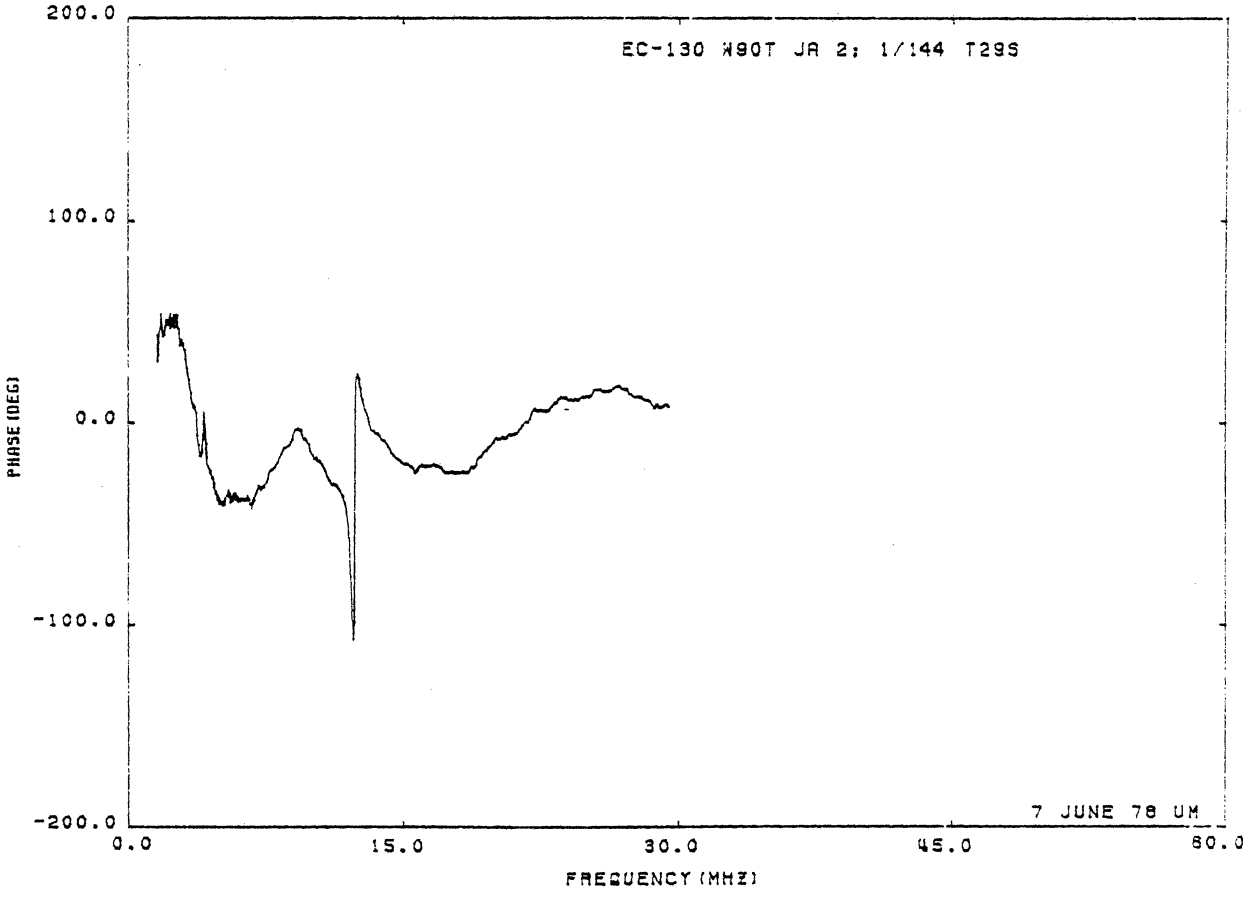

Figure 29S. Axial Current at STA:W90T, Excitation 2, 1/72 Model.

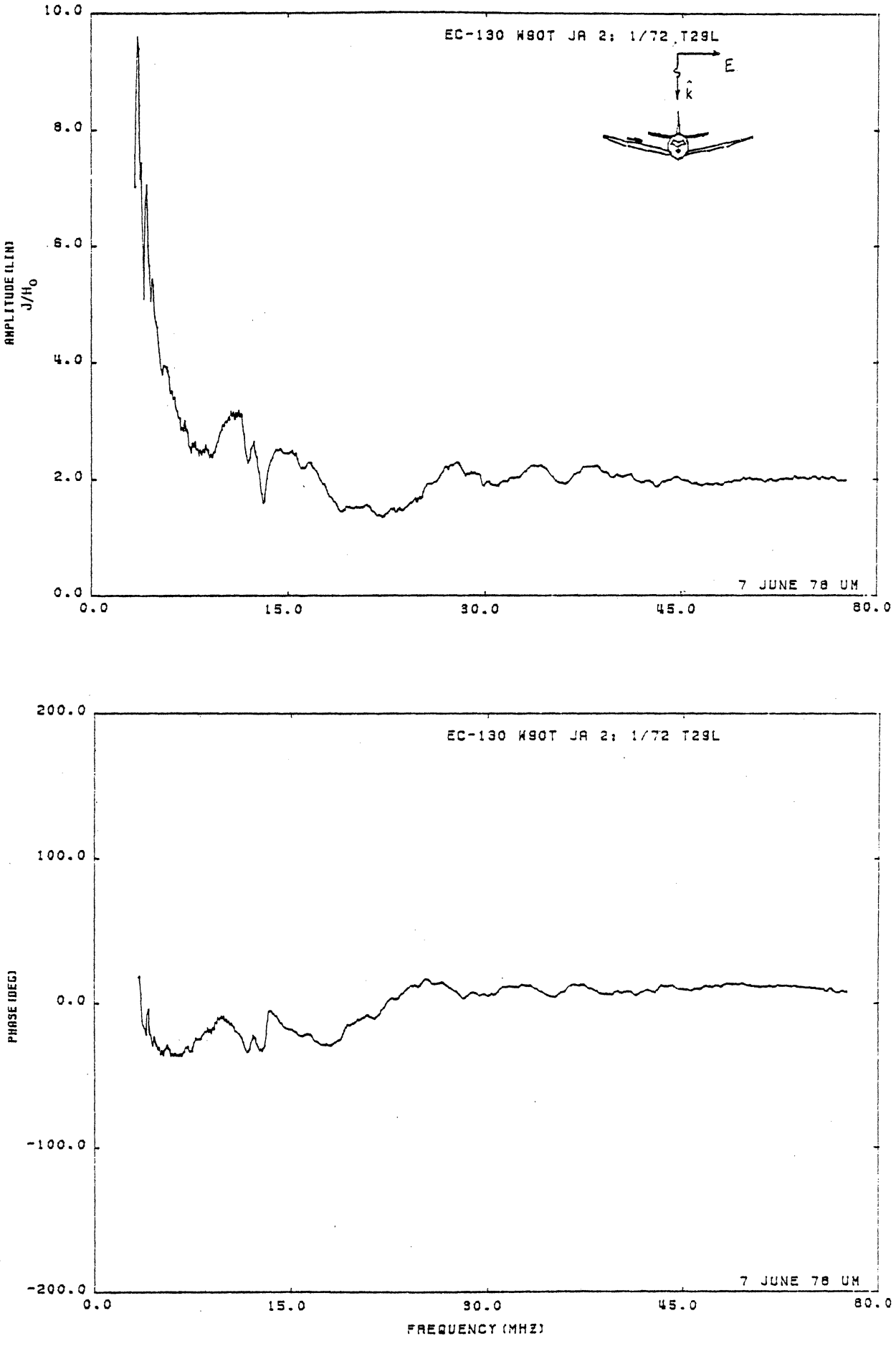

Figure 29L. Axial Current at STA:W90T, Excitation 2, 1/72 Model.

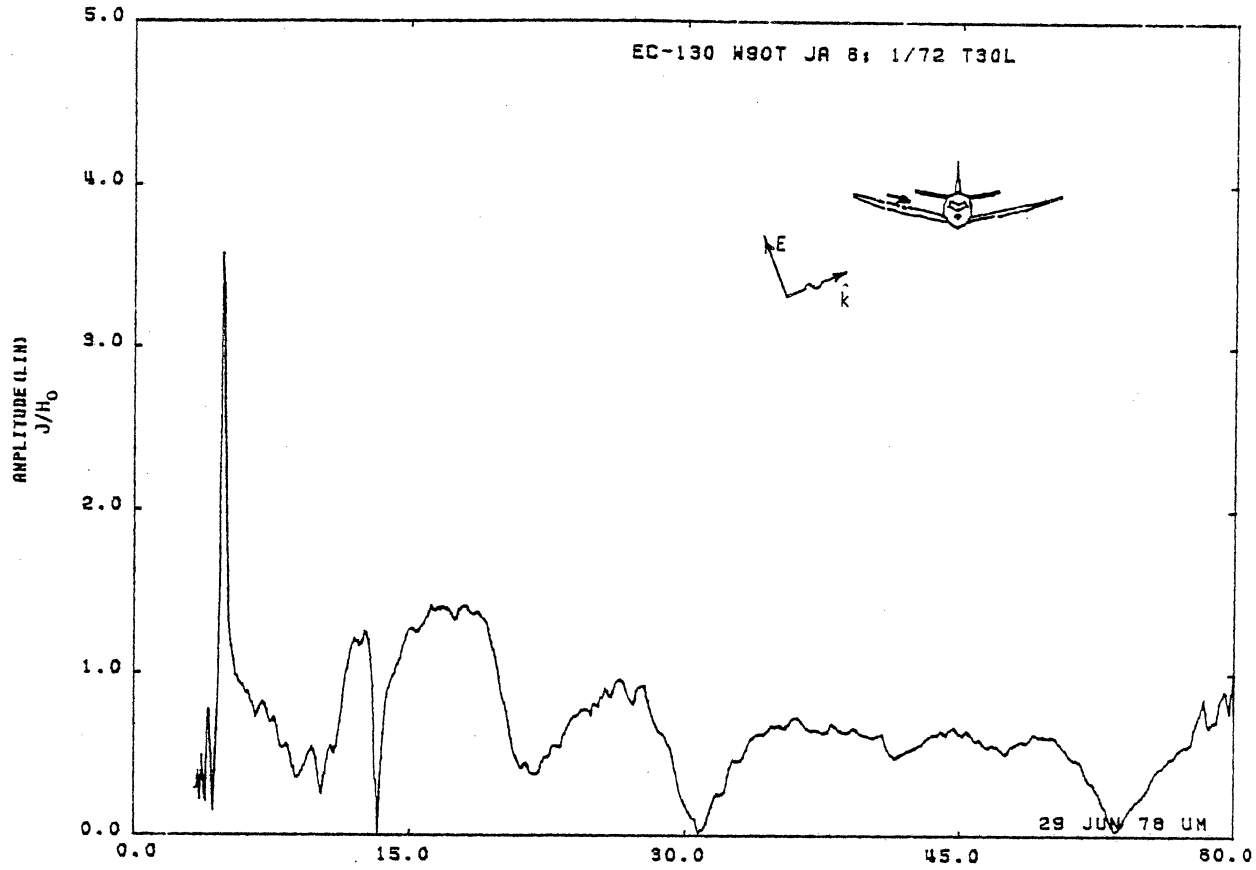

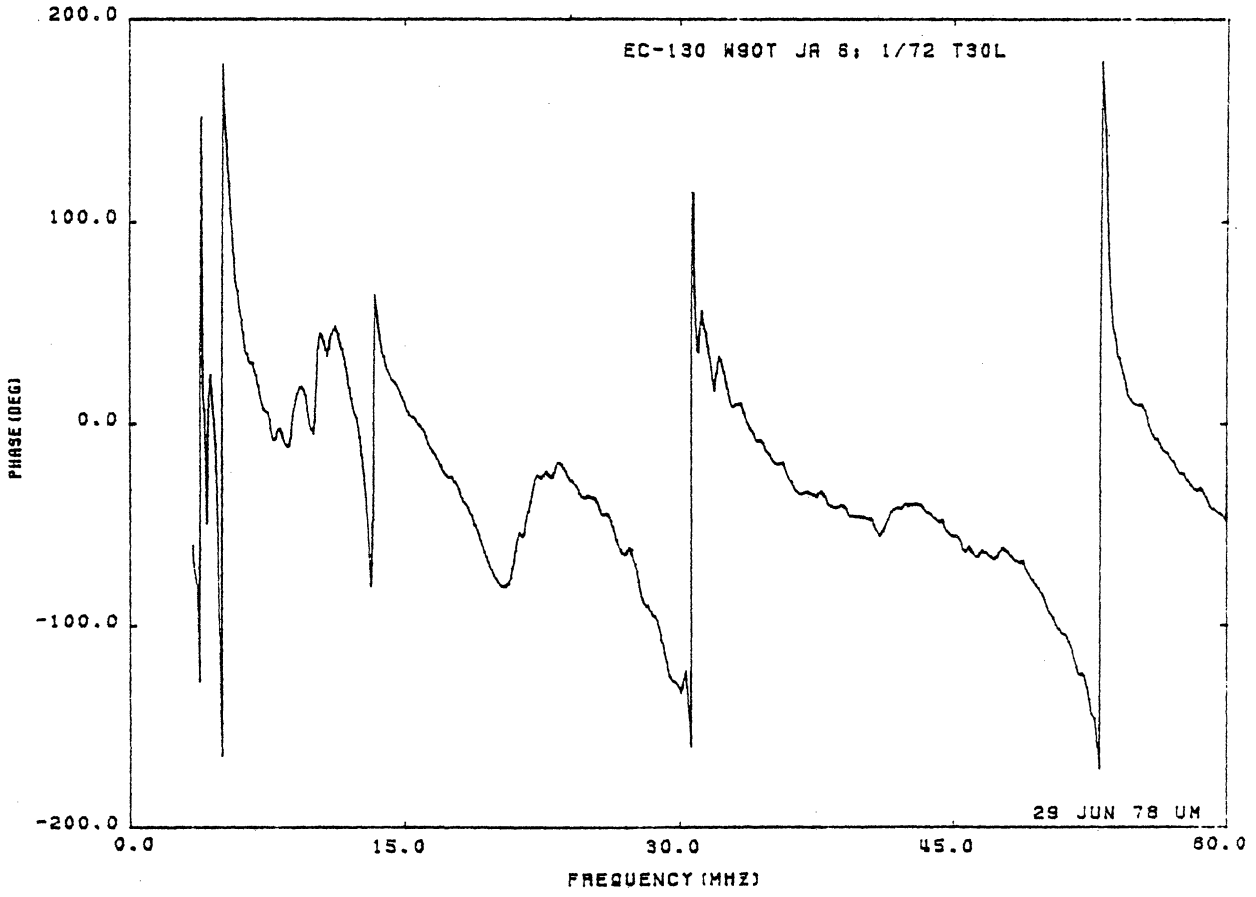

Figure 30L. Axial Current at STA:W90T, Excitation 6, 1/72 Model.

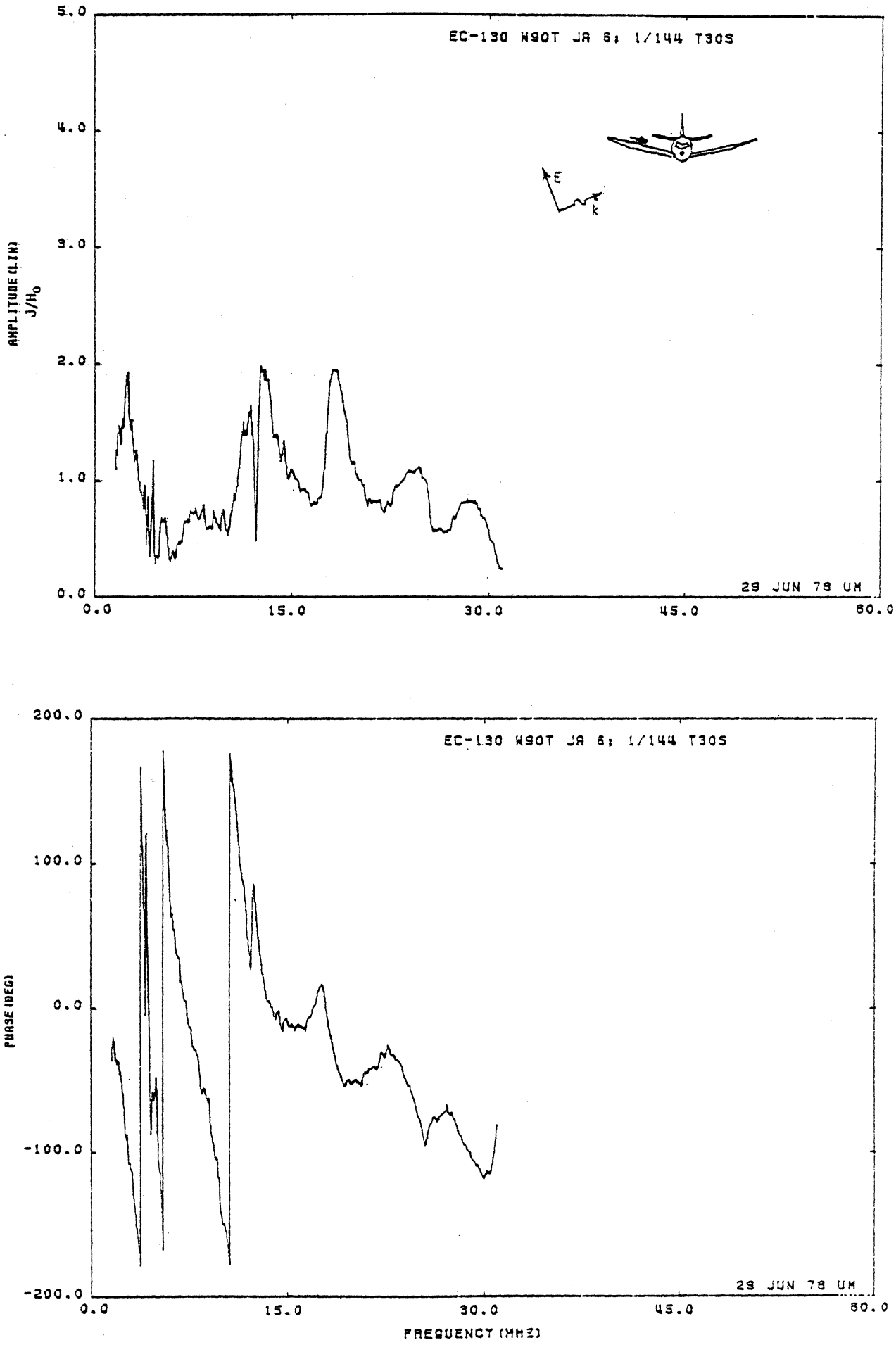

Figure 30S. Axial Current at STA:W90T, Excitation 6, 1/144 Model.

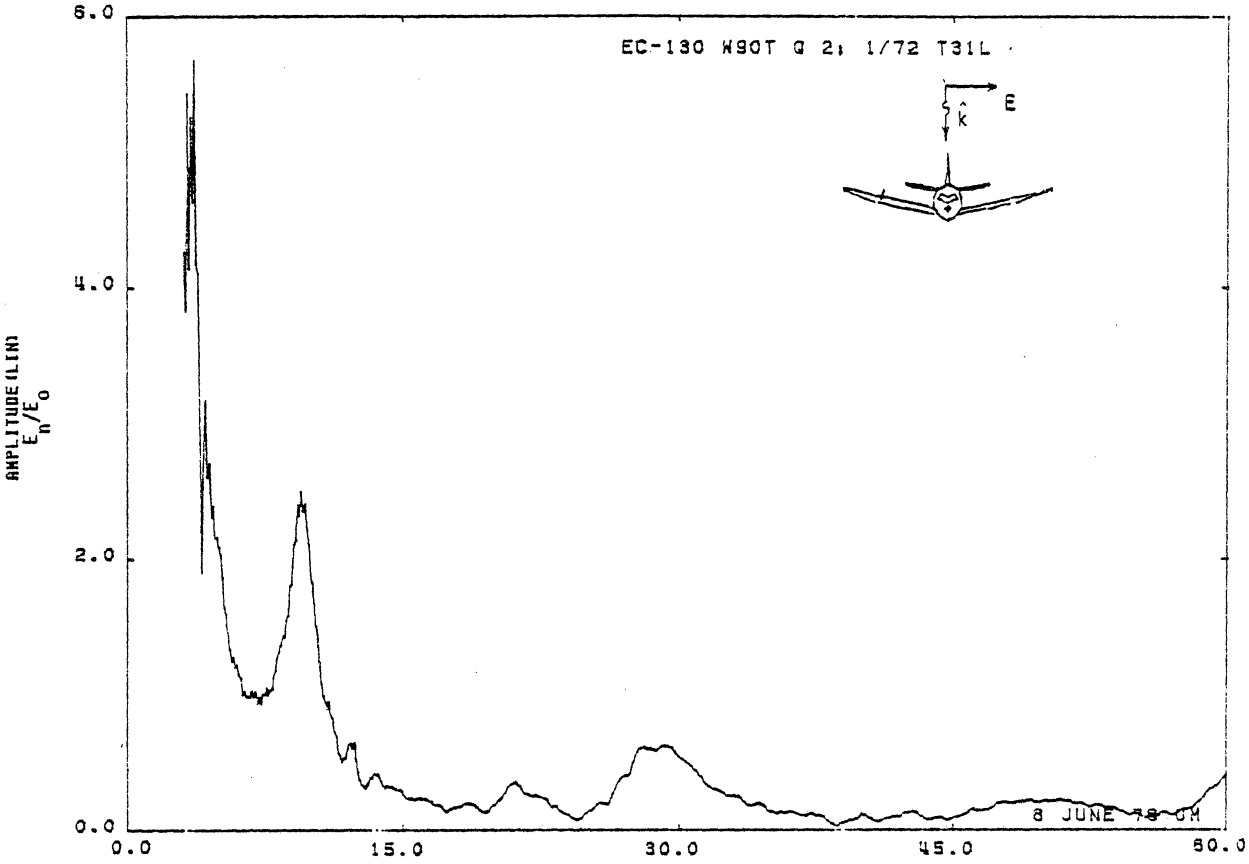

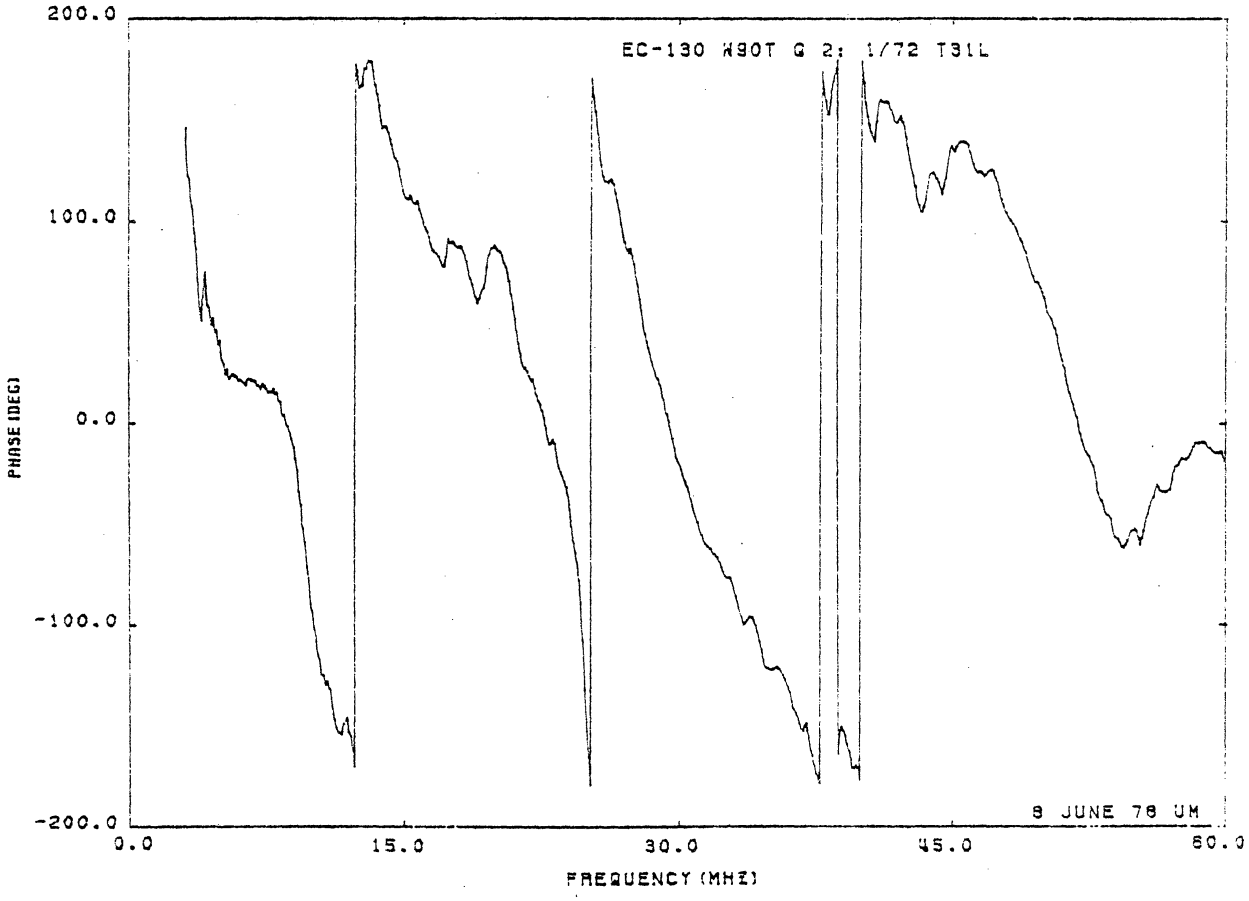

Figure 31L. Charge at STA:W90T, Excitation 2, 1/72 Model.

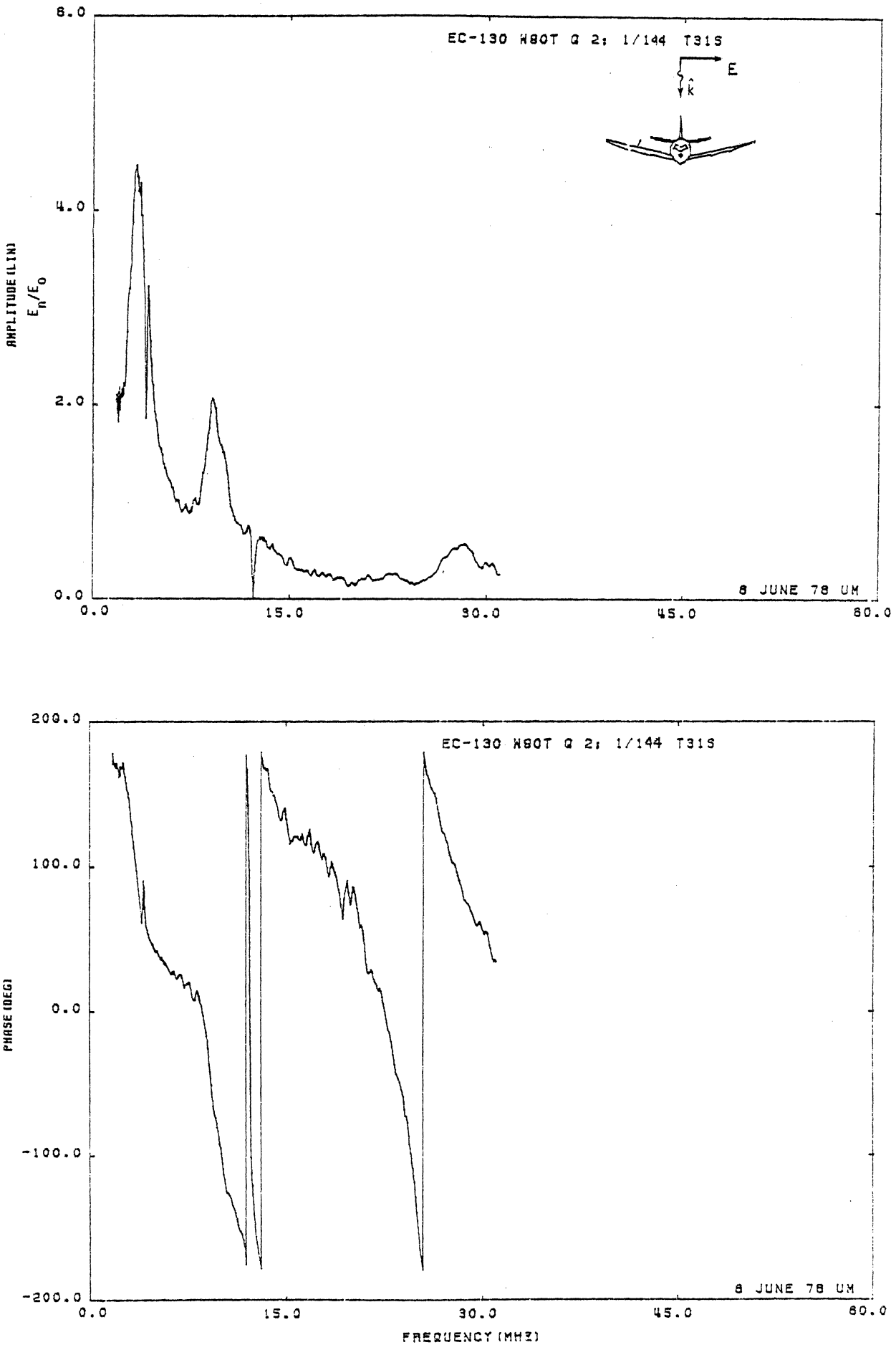

Figure 31S. Charge at STA:W90T, Excitation 2, 1/144 Model.

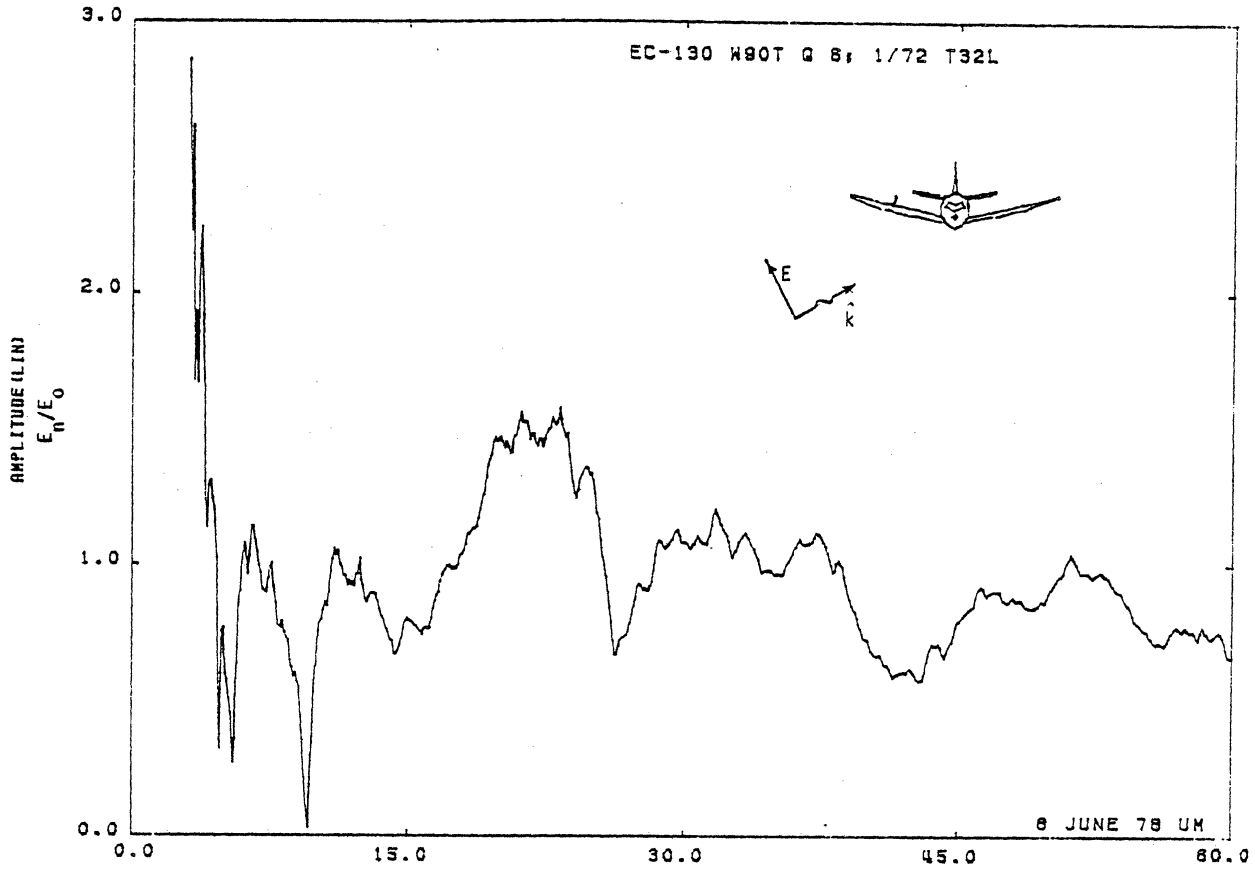

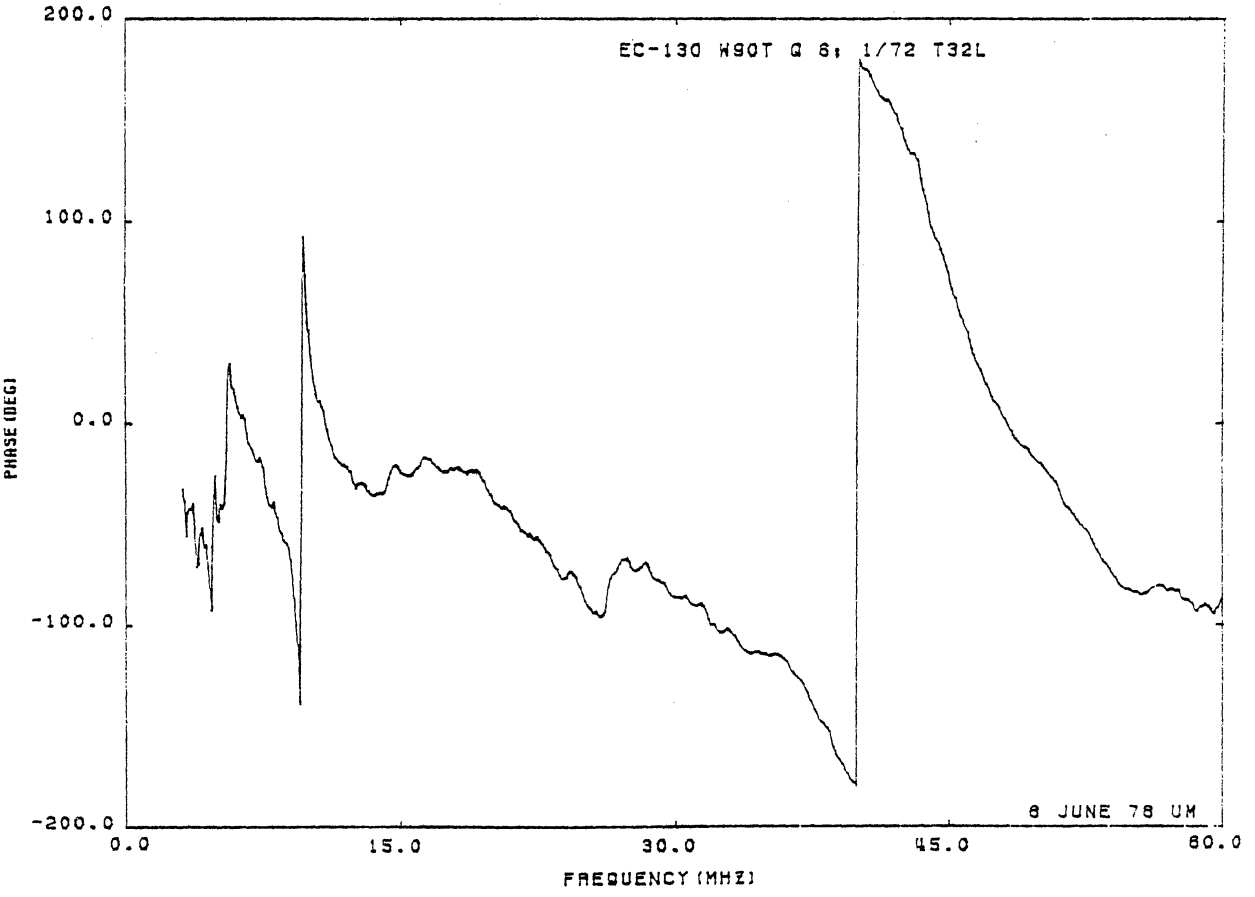

Figure 32L. Charge at STA:W90T, Excitation 6, 1/72 Model.

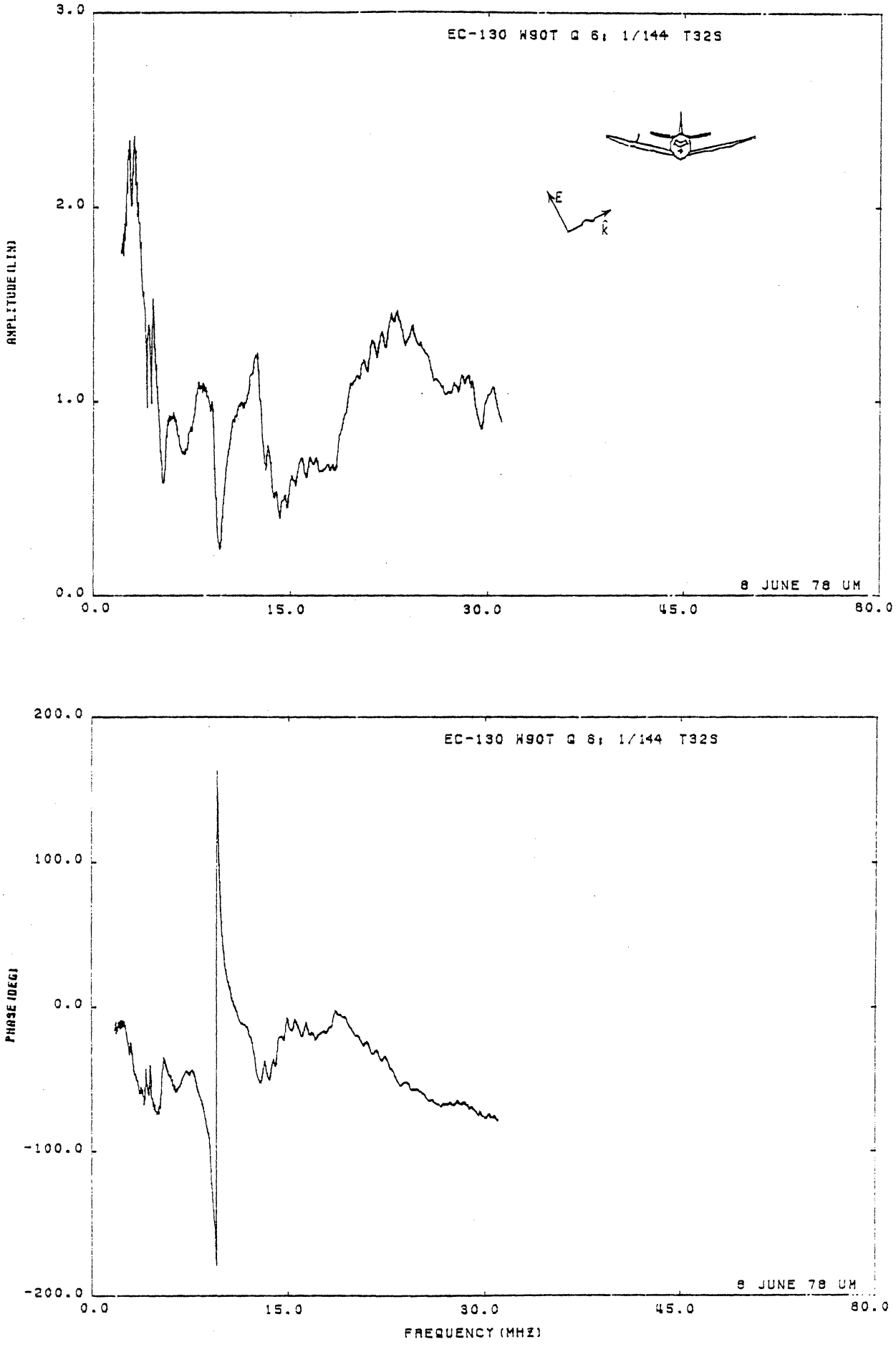

Figure 32S. Charge at STA:W90T, Excitation 6, 1/144 Model.

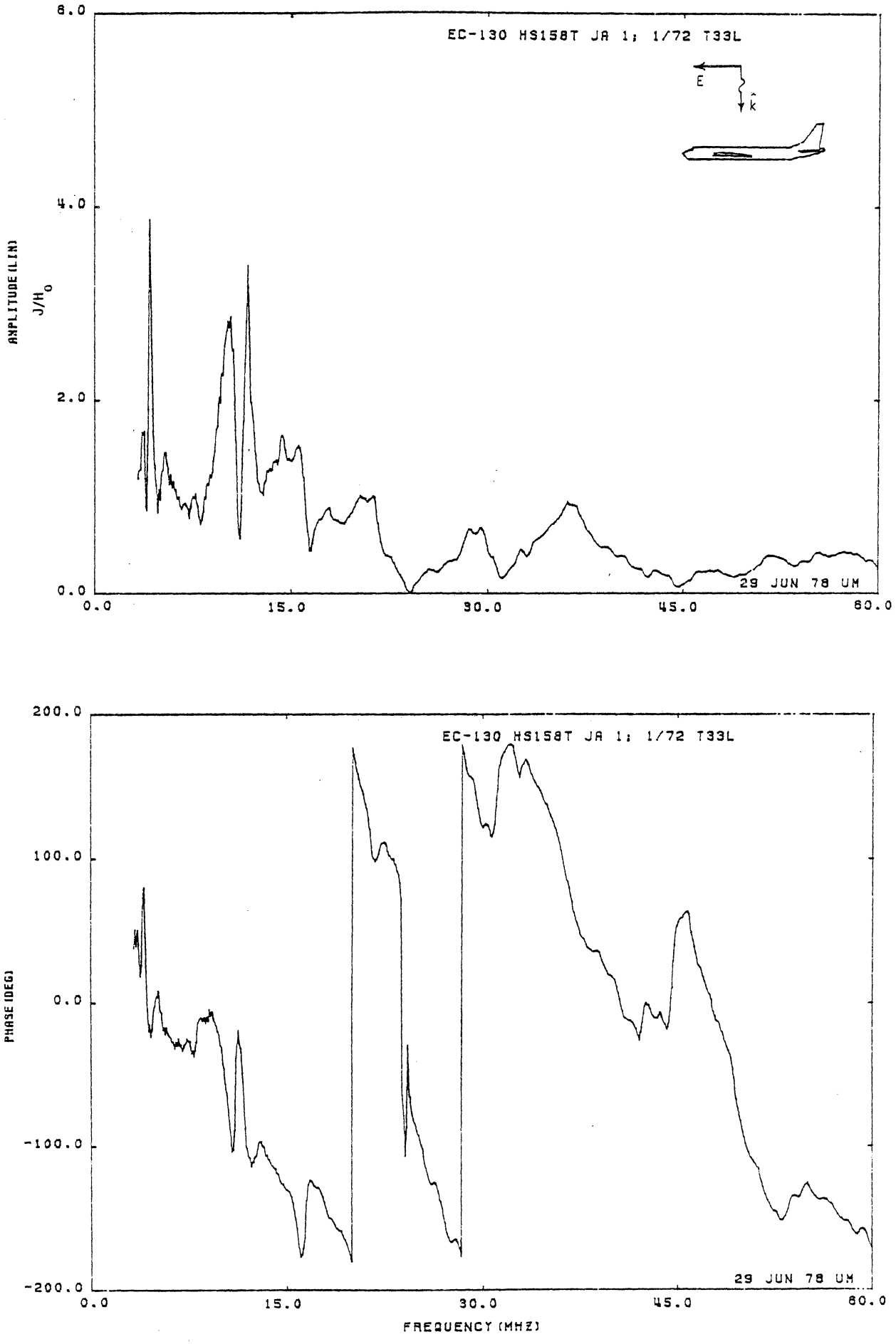

Figure 33L. Axial Current at STA:HS158T, Excitation 1, 1/72 Model.

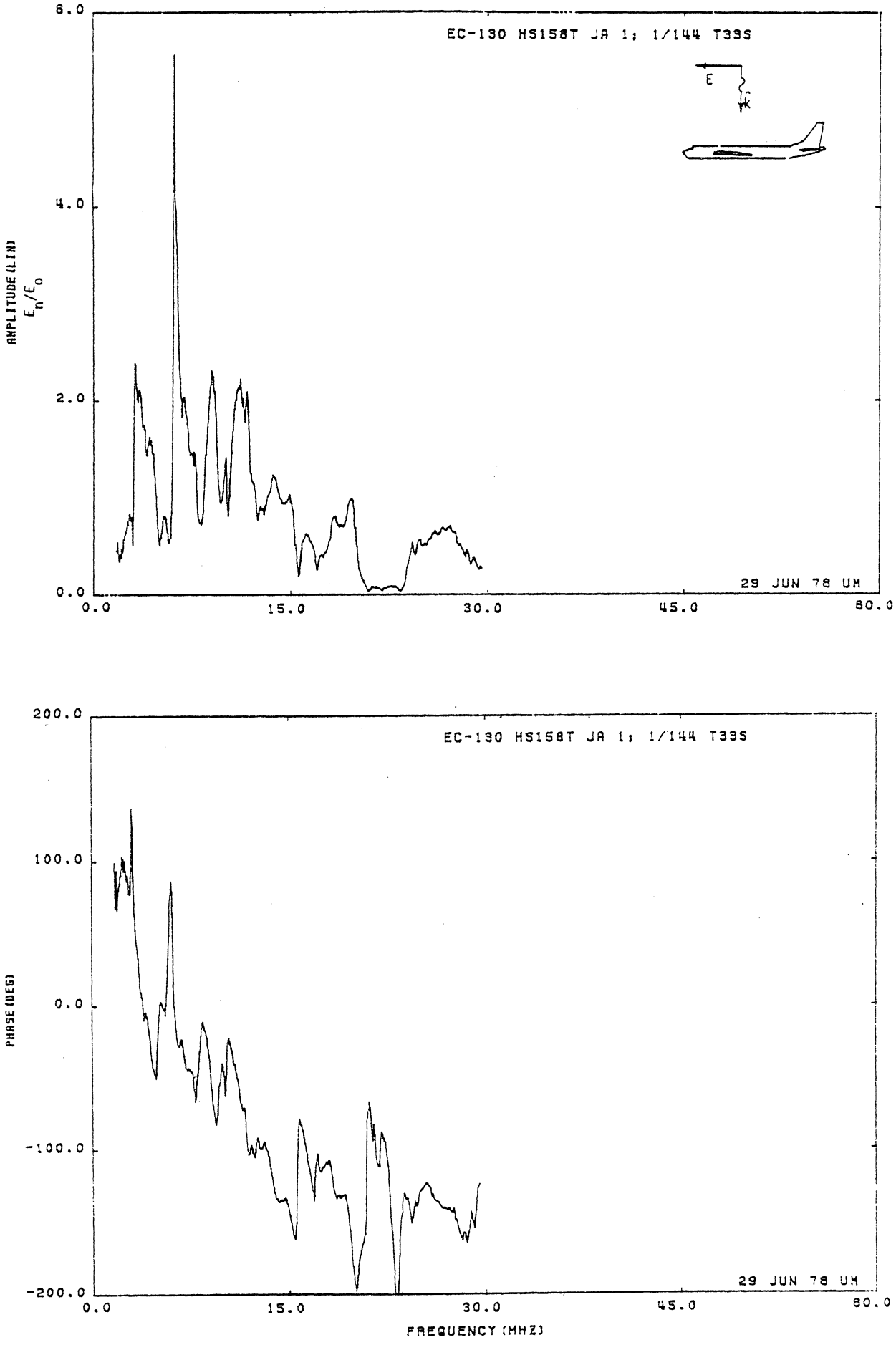

Figure 33S. Axial Current at STA:HS158T, Excitation 1, 1/144 Model.

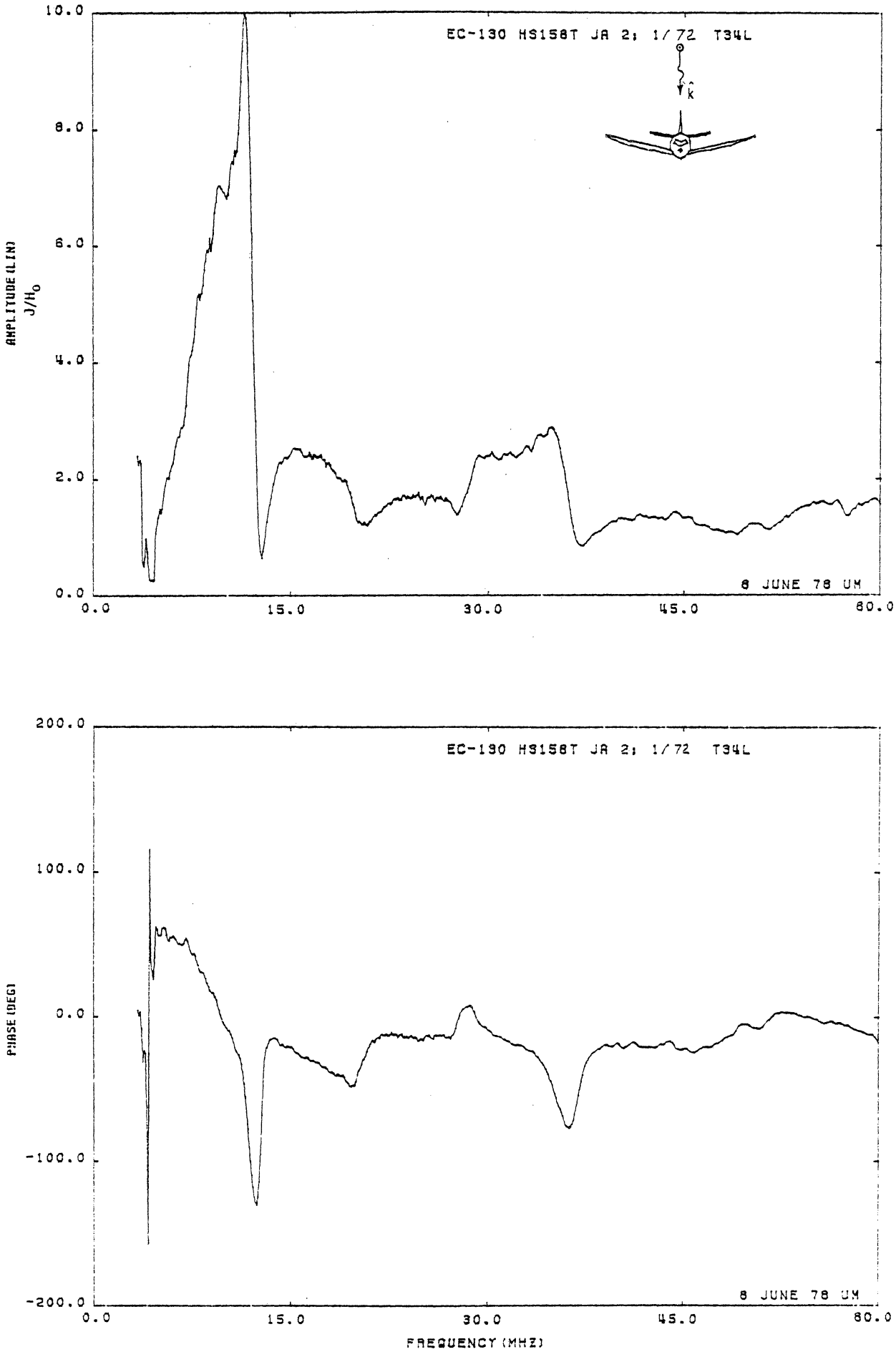

Figure 34L. Axial Current at STA:HS158T, Excitation 2, 1/72 Model.

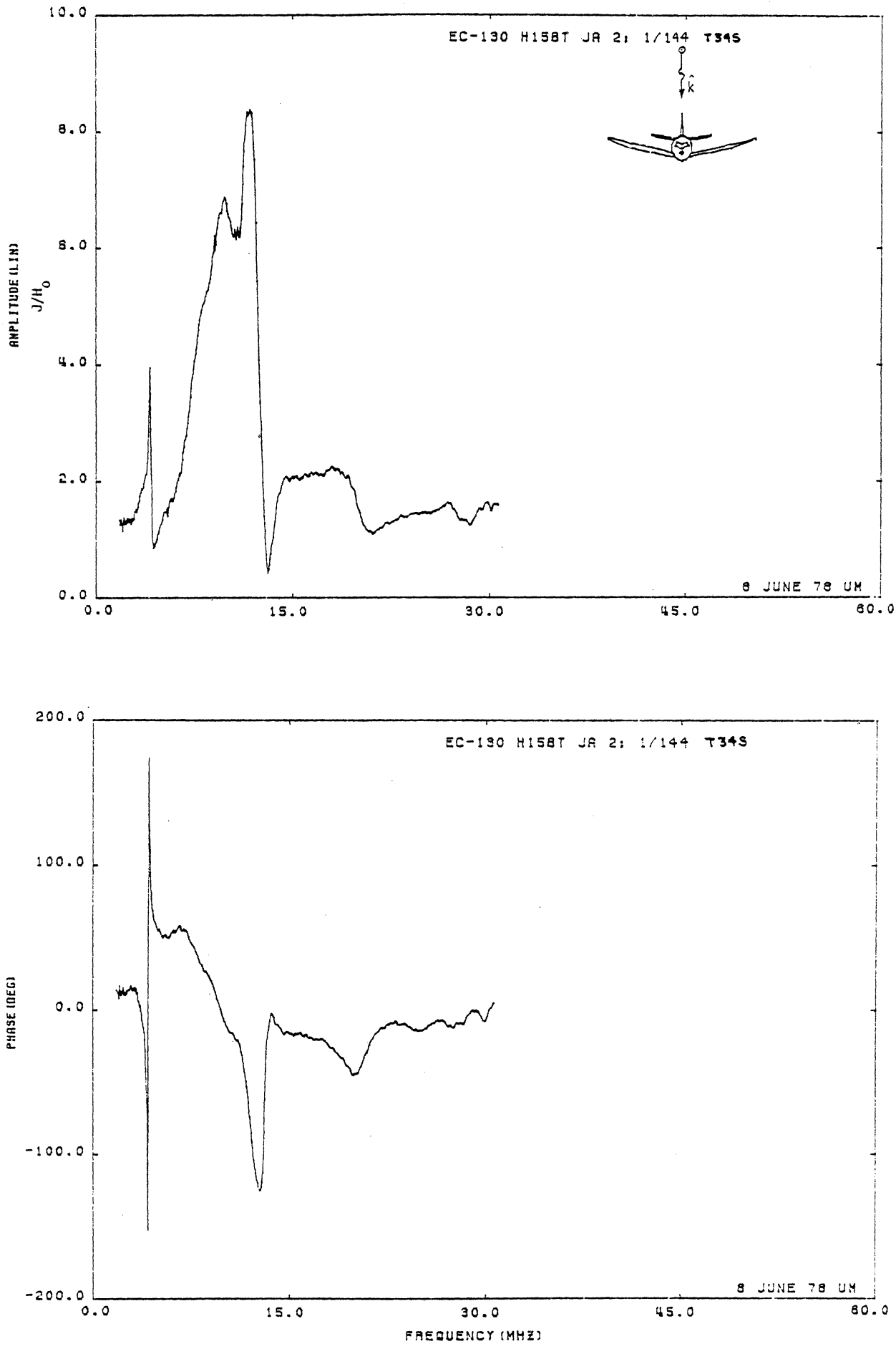

Figure 34S. Axial Current at STA:HS158T, Excitation 2, 1/144 Model.

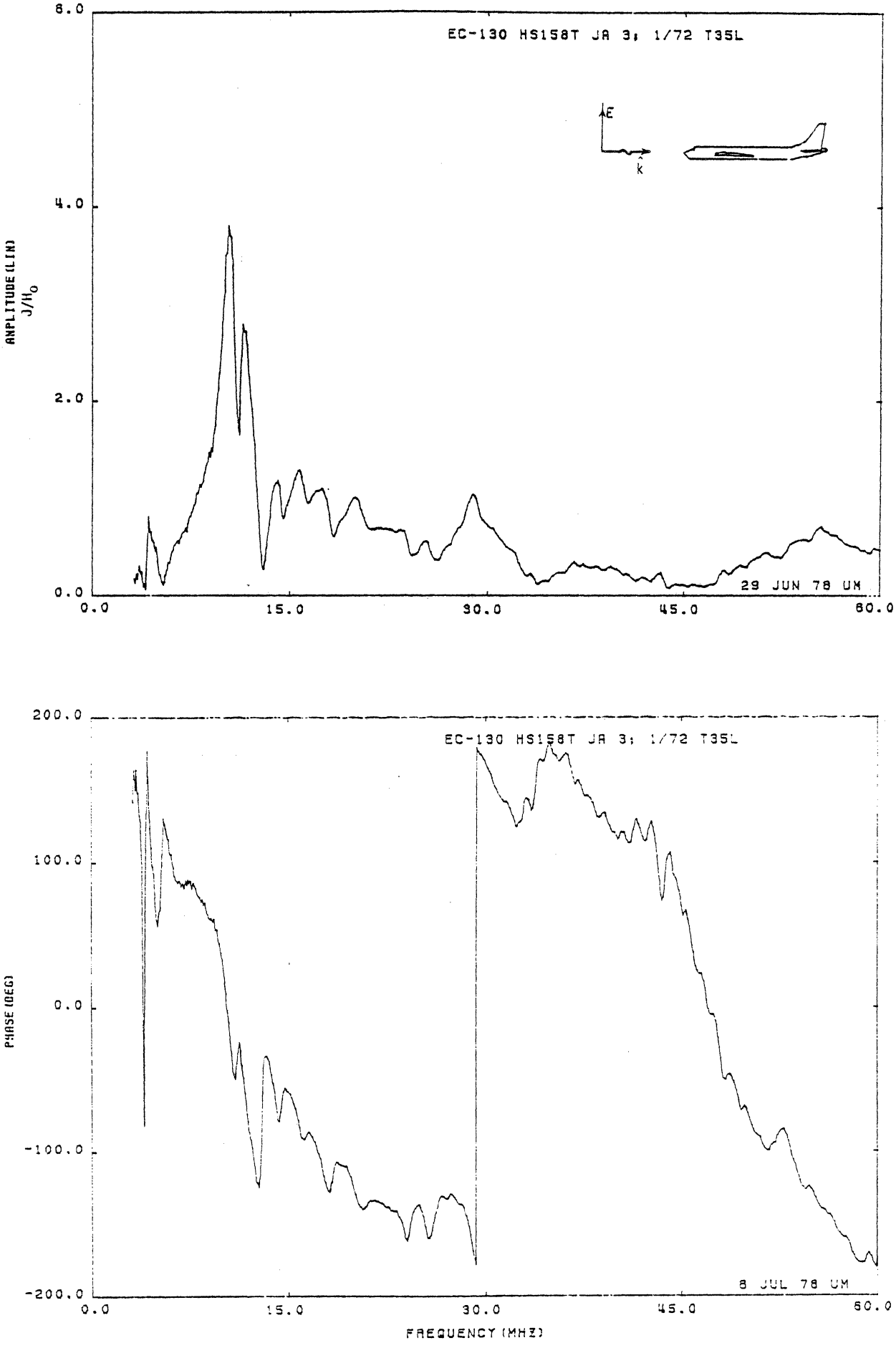

Figure 35L. Axial Current at STA:HS158T, Excitation 3, 1/72 Model.

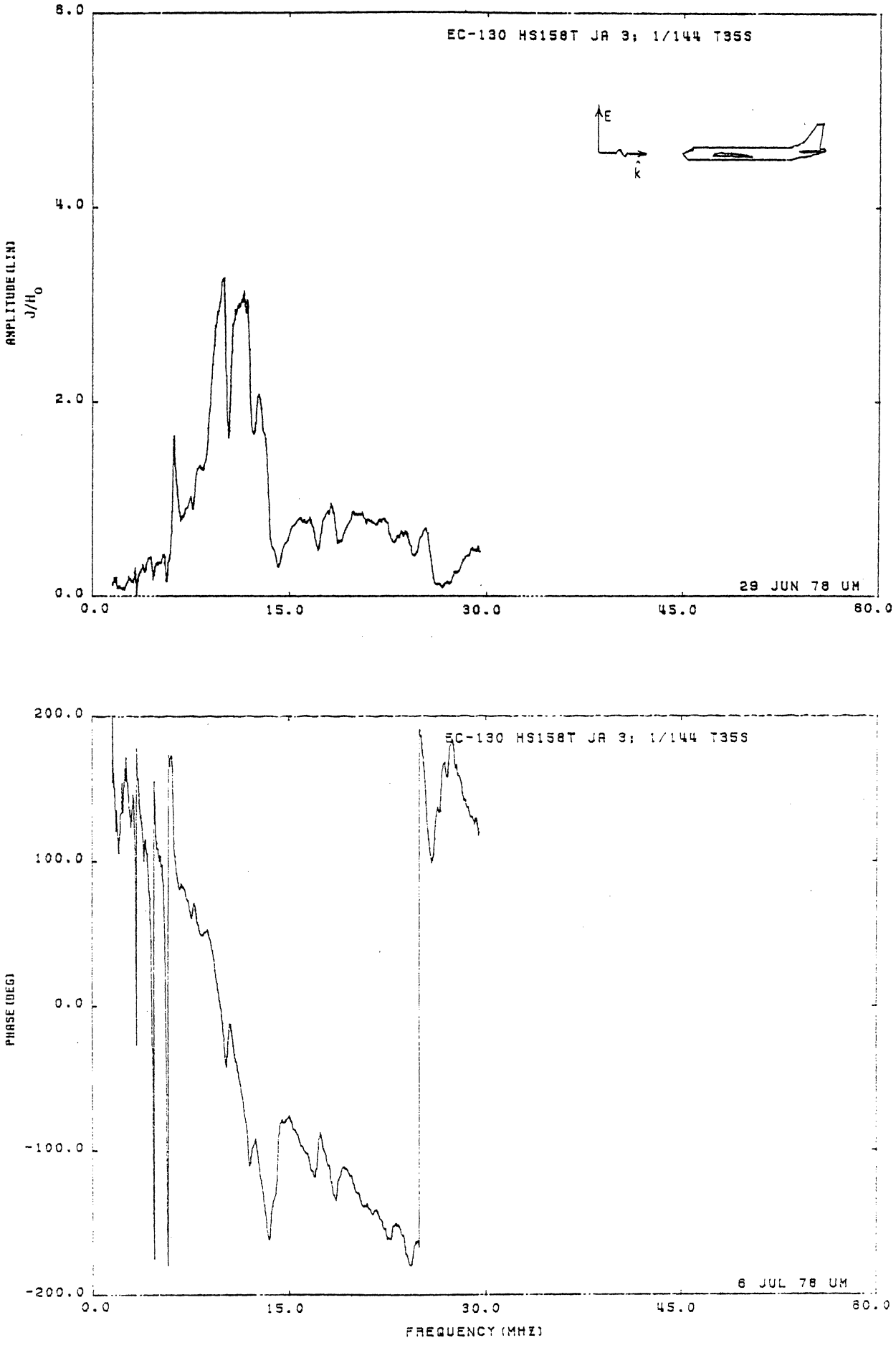

Figure 35S. Axial Current at STA:HS158T, Excitation 3, 1/144 Model.

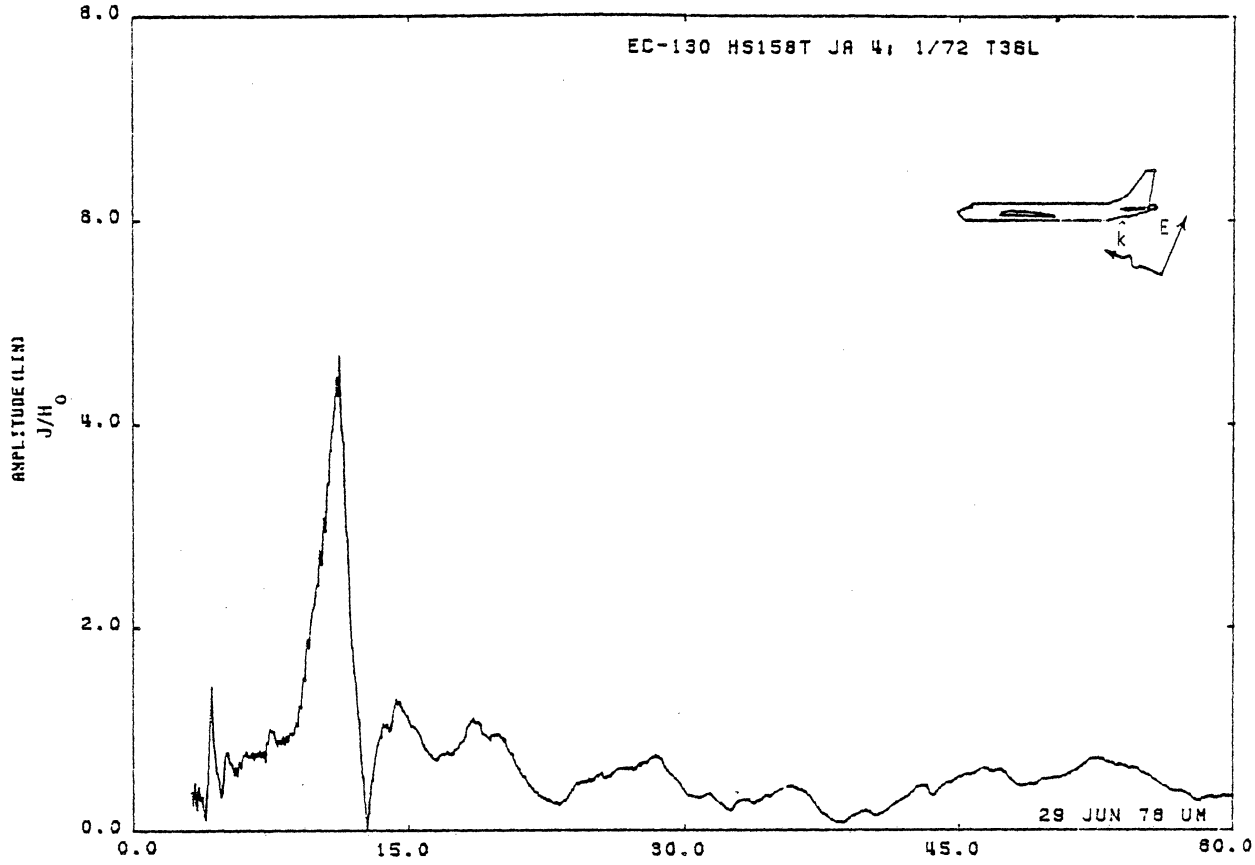

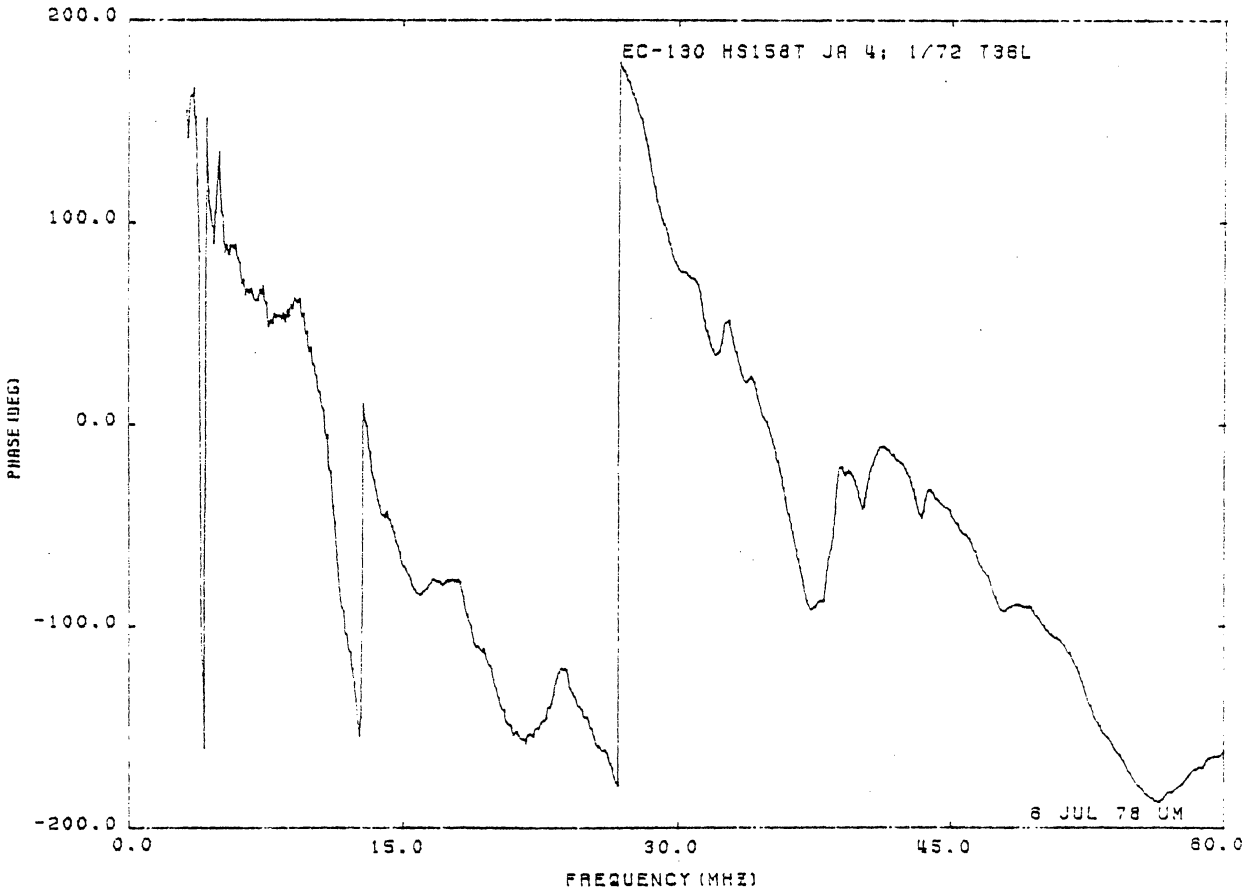

Figure 36L. Axial Current at STA:HS158T, Excitation 4, 1/72 Model.

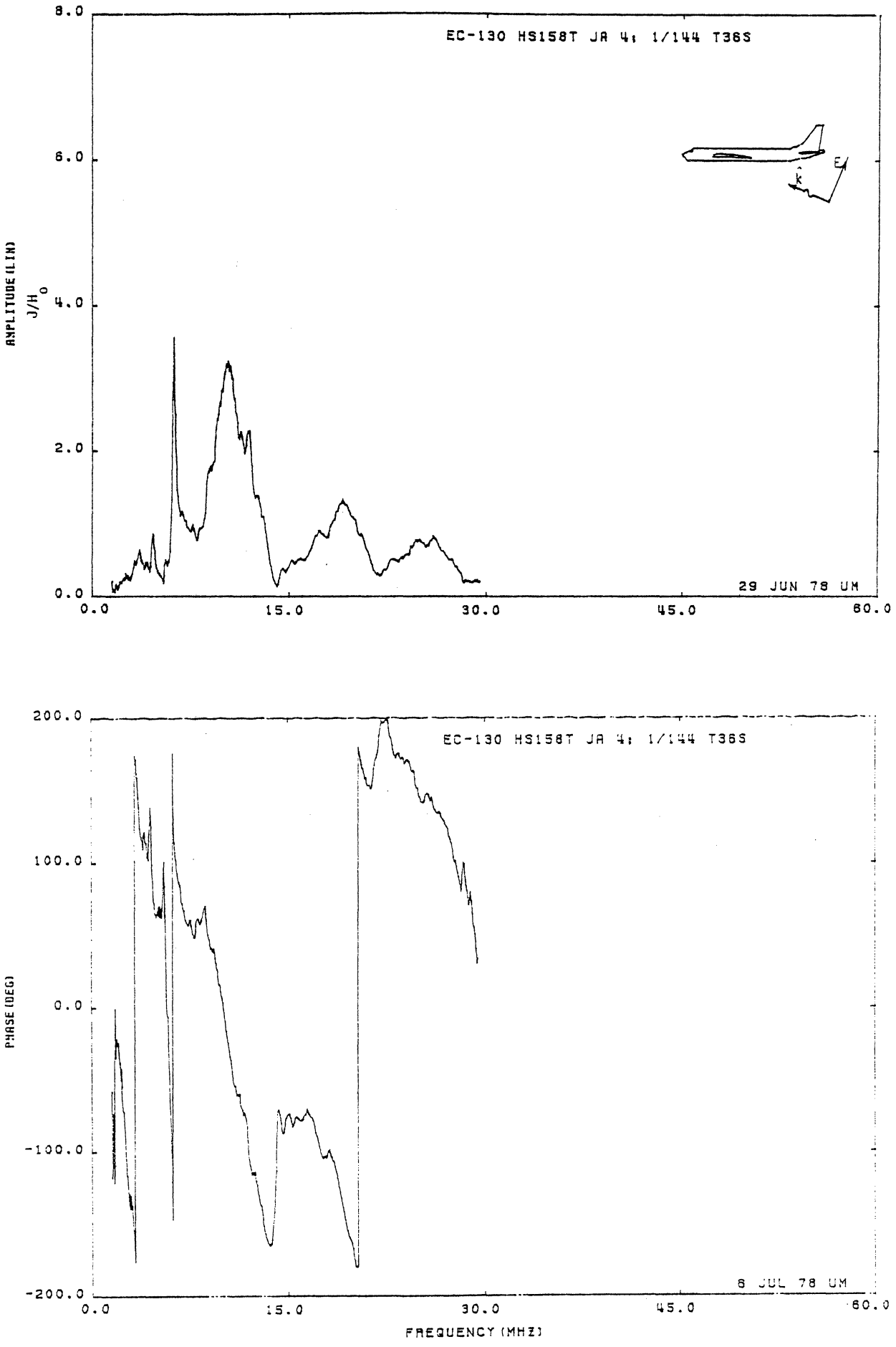

Figure 36S. Axial Current at STA:HS158T, Excitation 4, 1/144 Model.

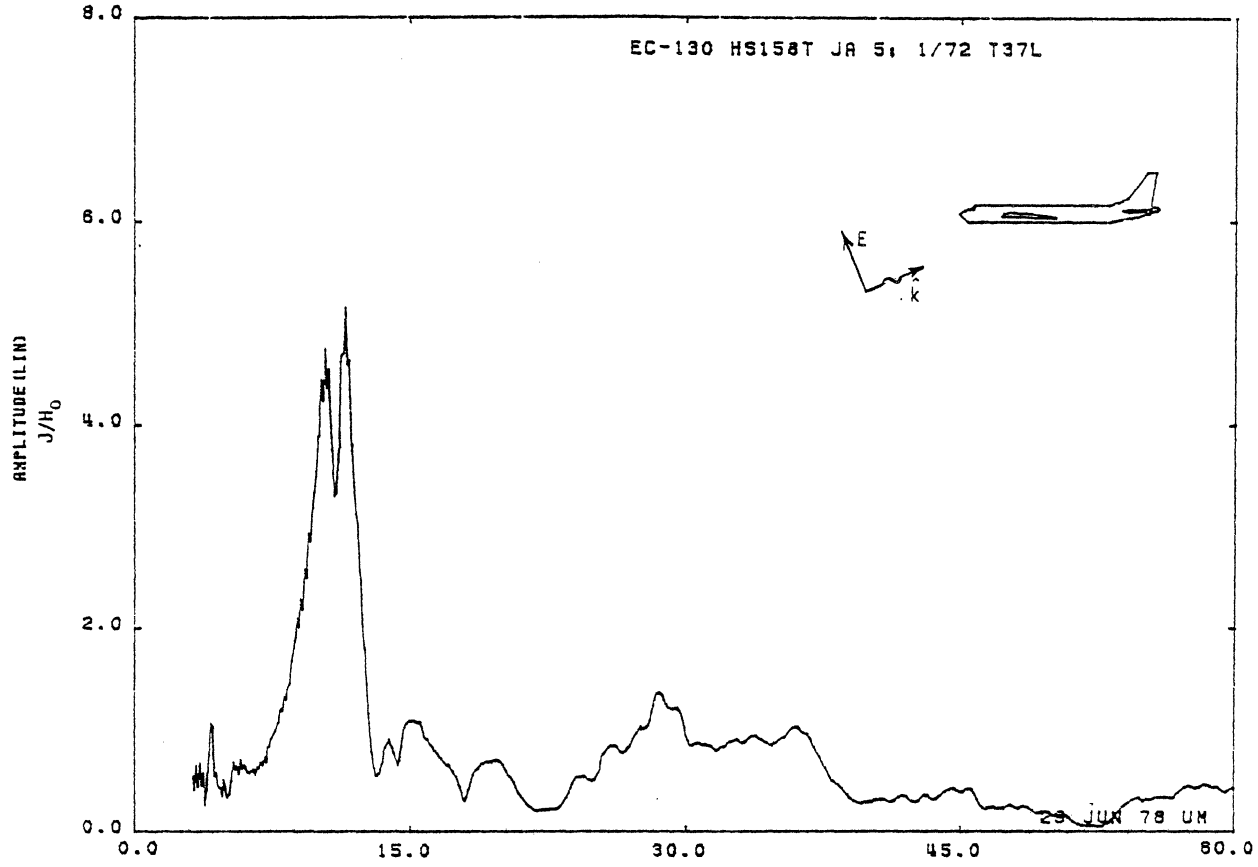

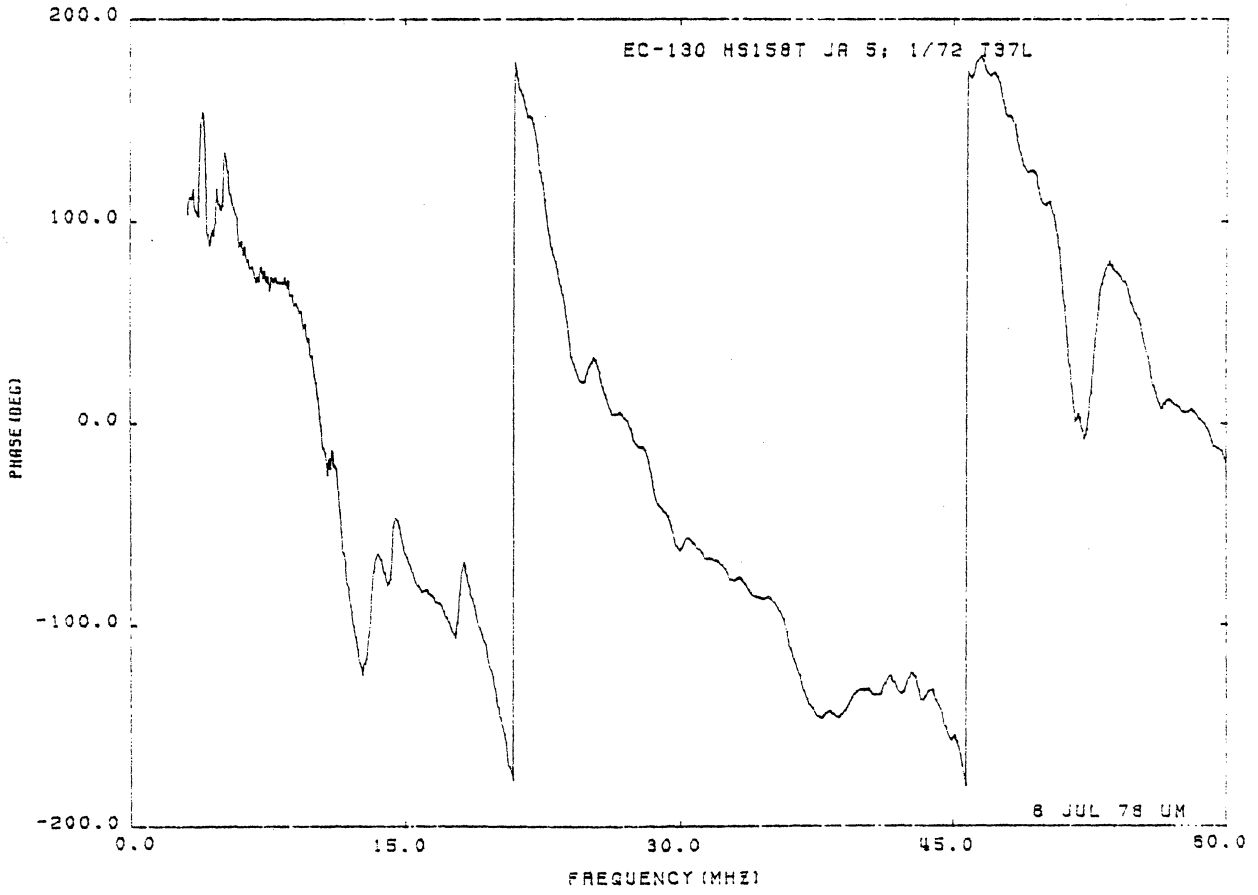

Figure 37L. Axial Current at STA:HS158T, Excitation 5, 1/72 Model.

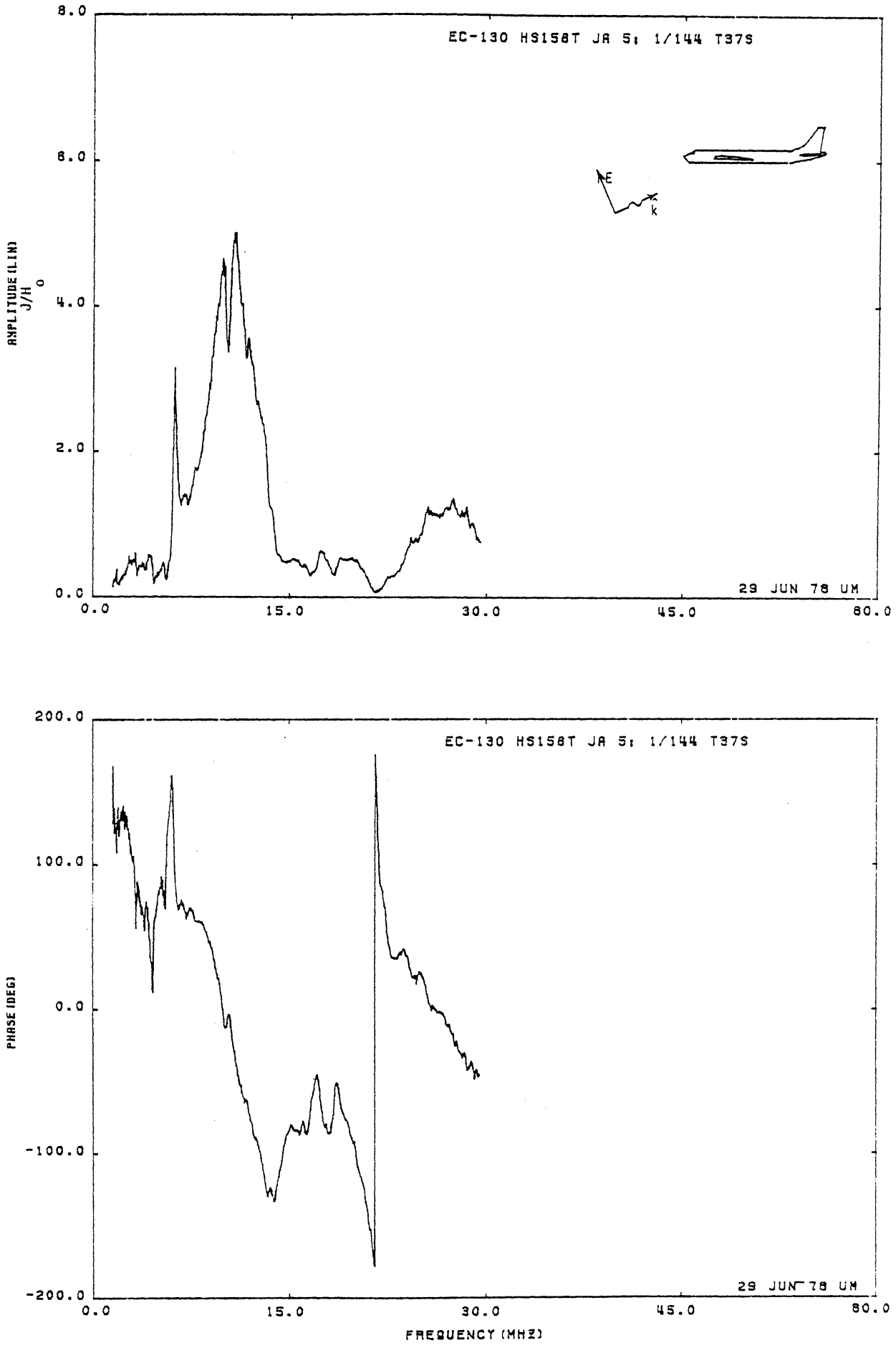

Figure 37S. Axial Current at STA:HS158T, Excitation 5, 1/144 Model.

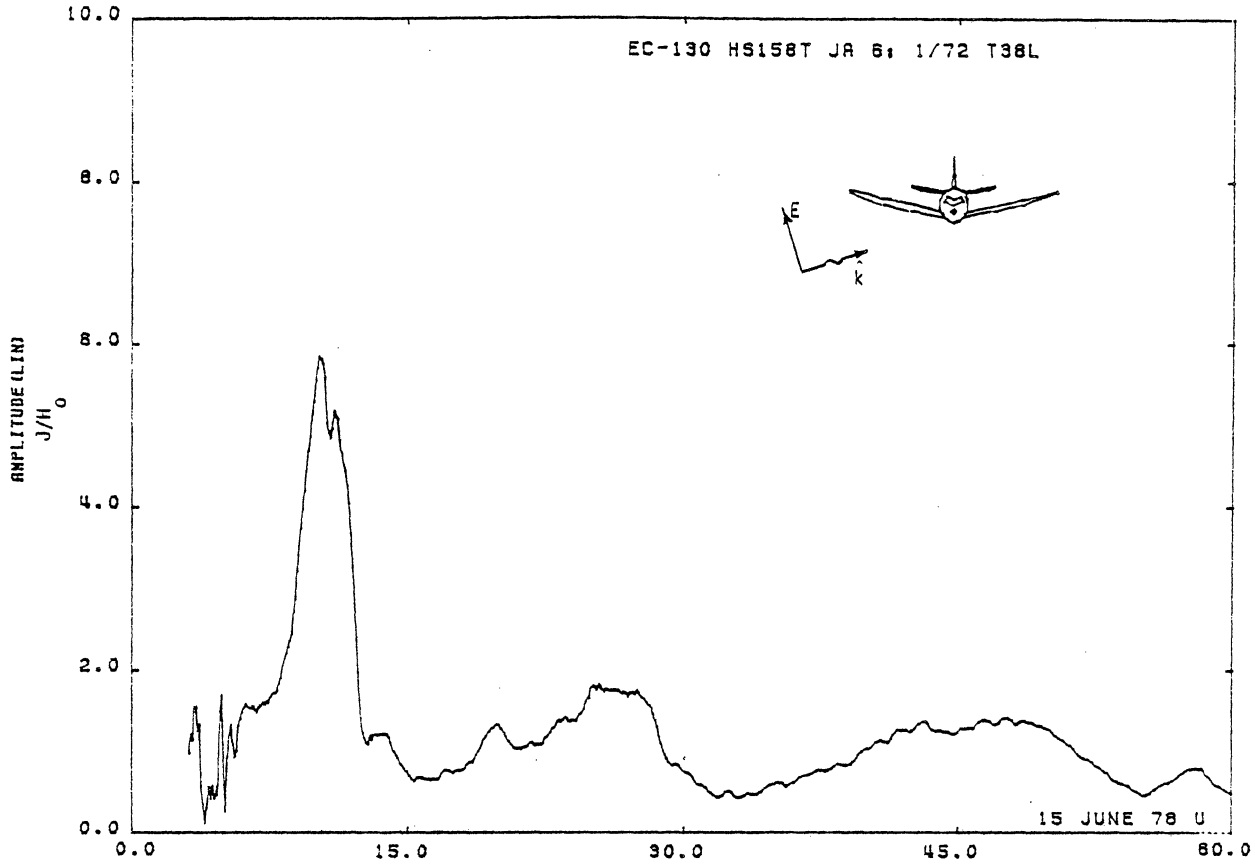

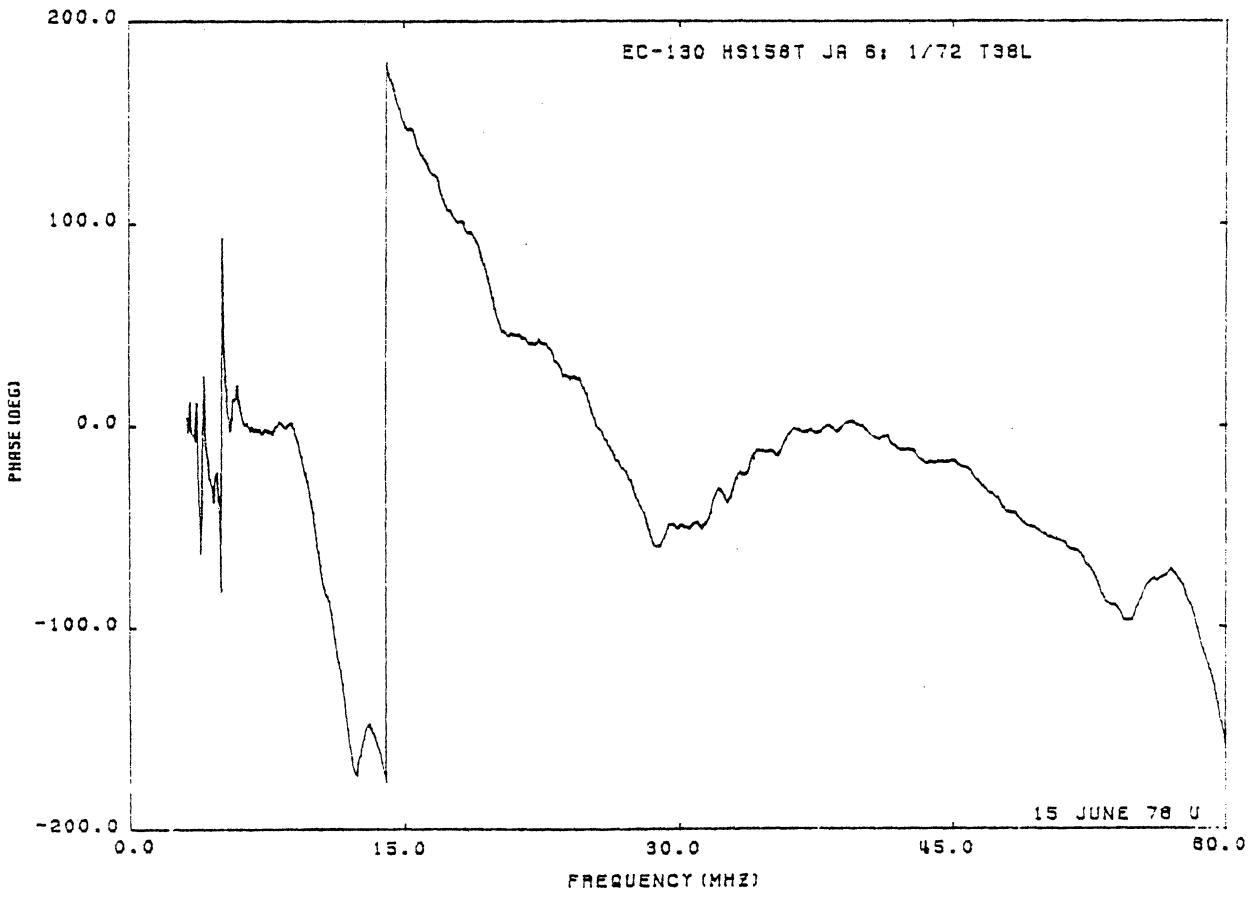

Figure 38L. Axial Current at STA:HS158T, Excitation 6, 1/72 Model.

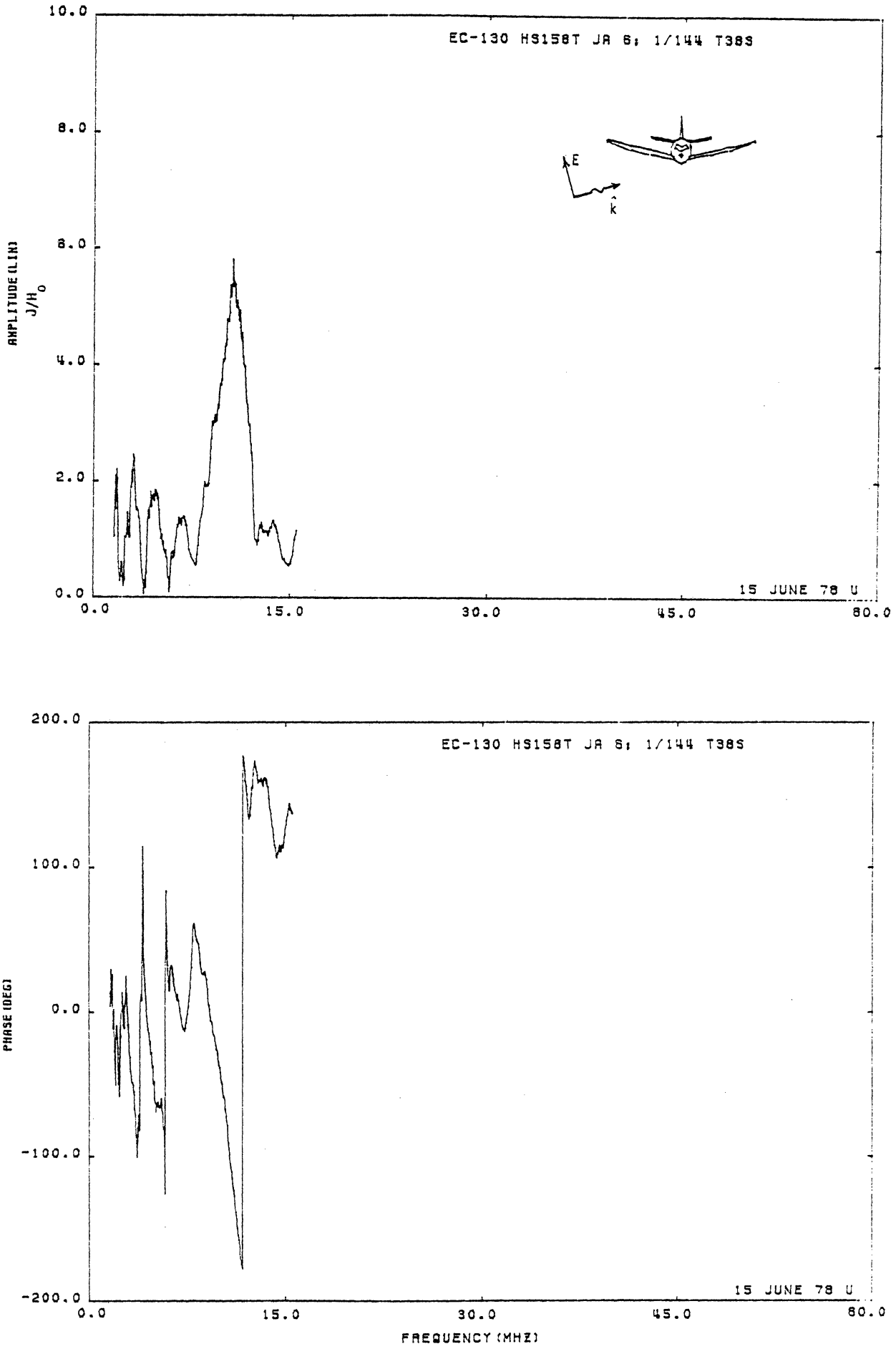

Figure 38S. Axial Current at STA:HS158T, Excitation 6, 1/144 Model.

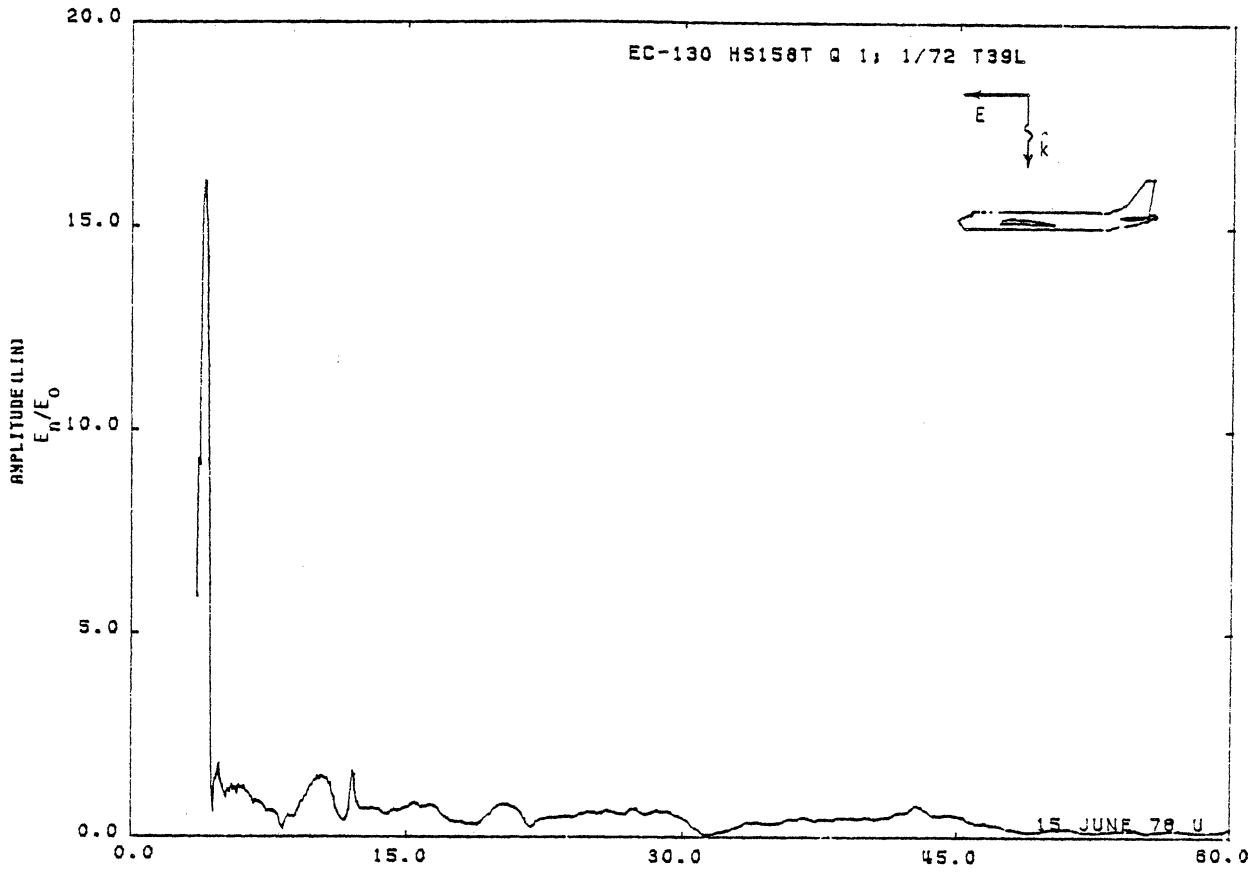

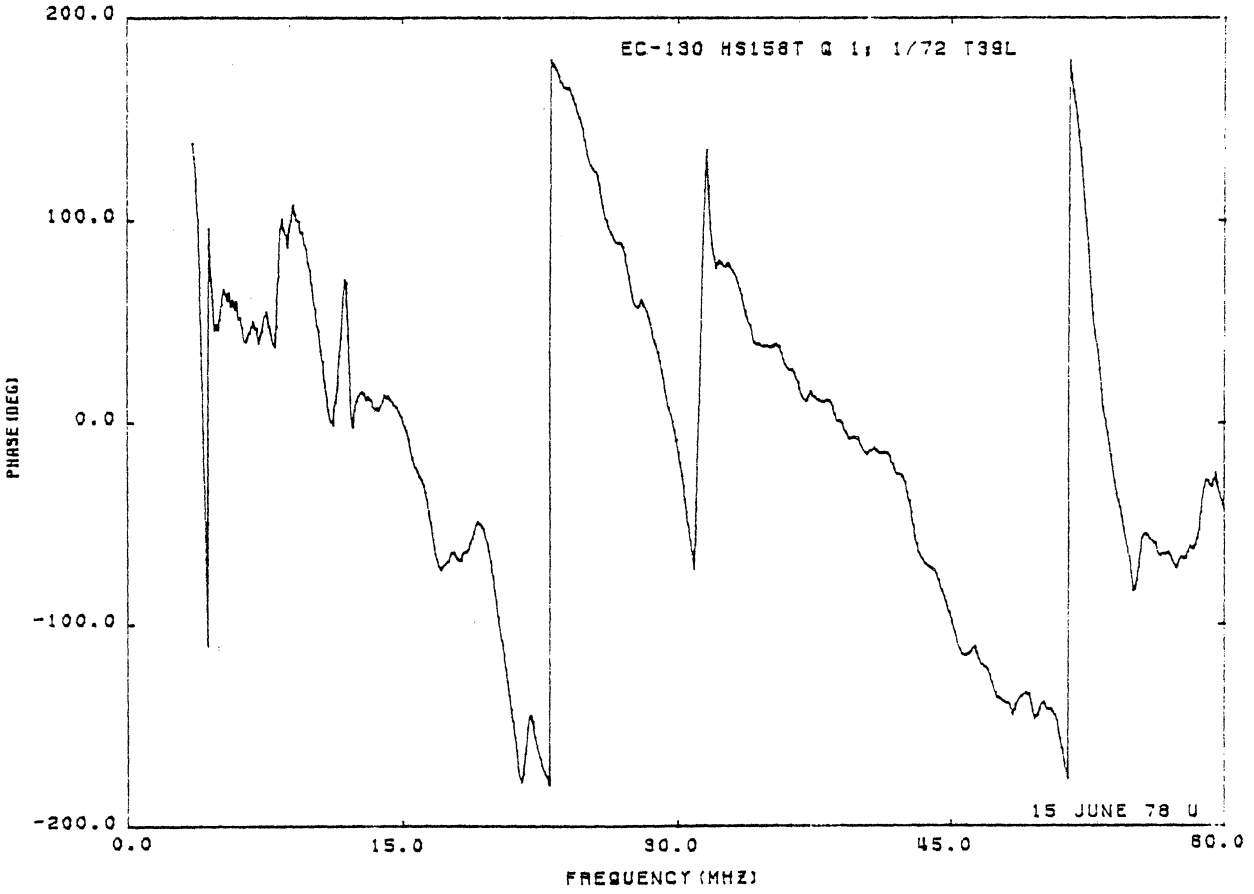

Figure 39L. Charge at STA:HS158T, Excitation 1, 1/72 Model.

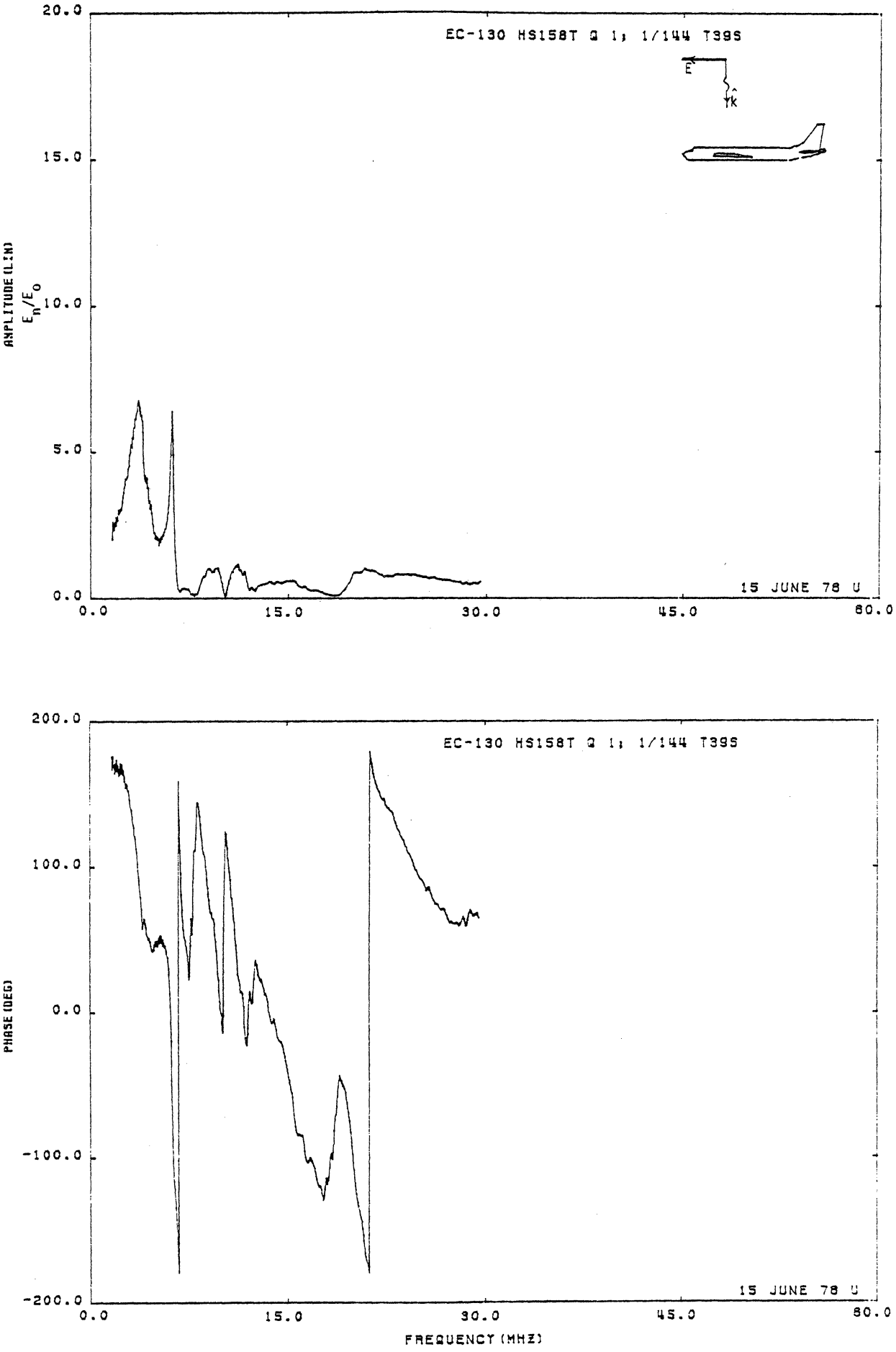

Figure 39S. Charge at STA:HS158T, Excitation 1, 1/144 Model.

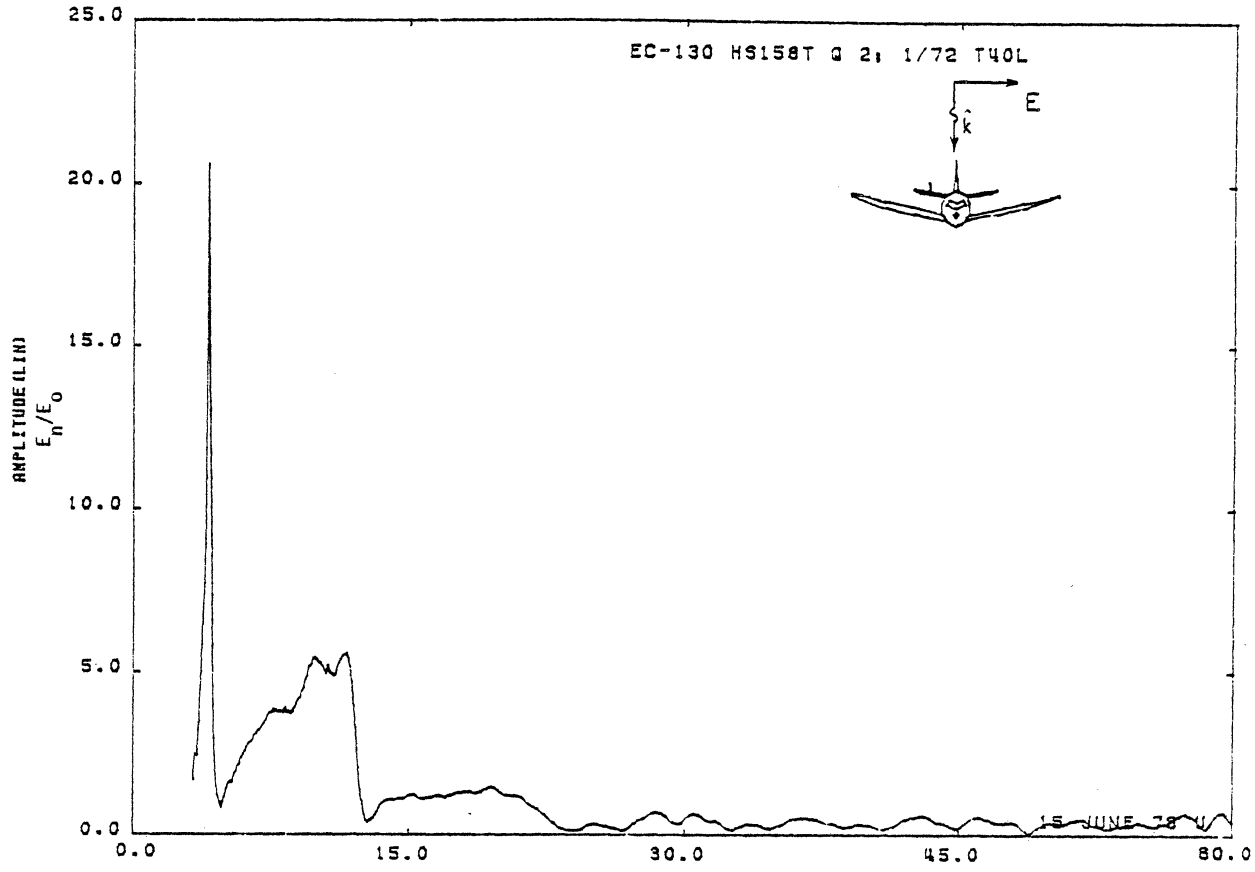

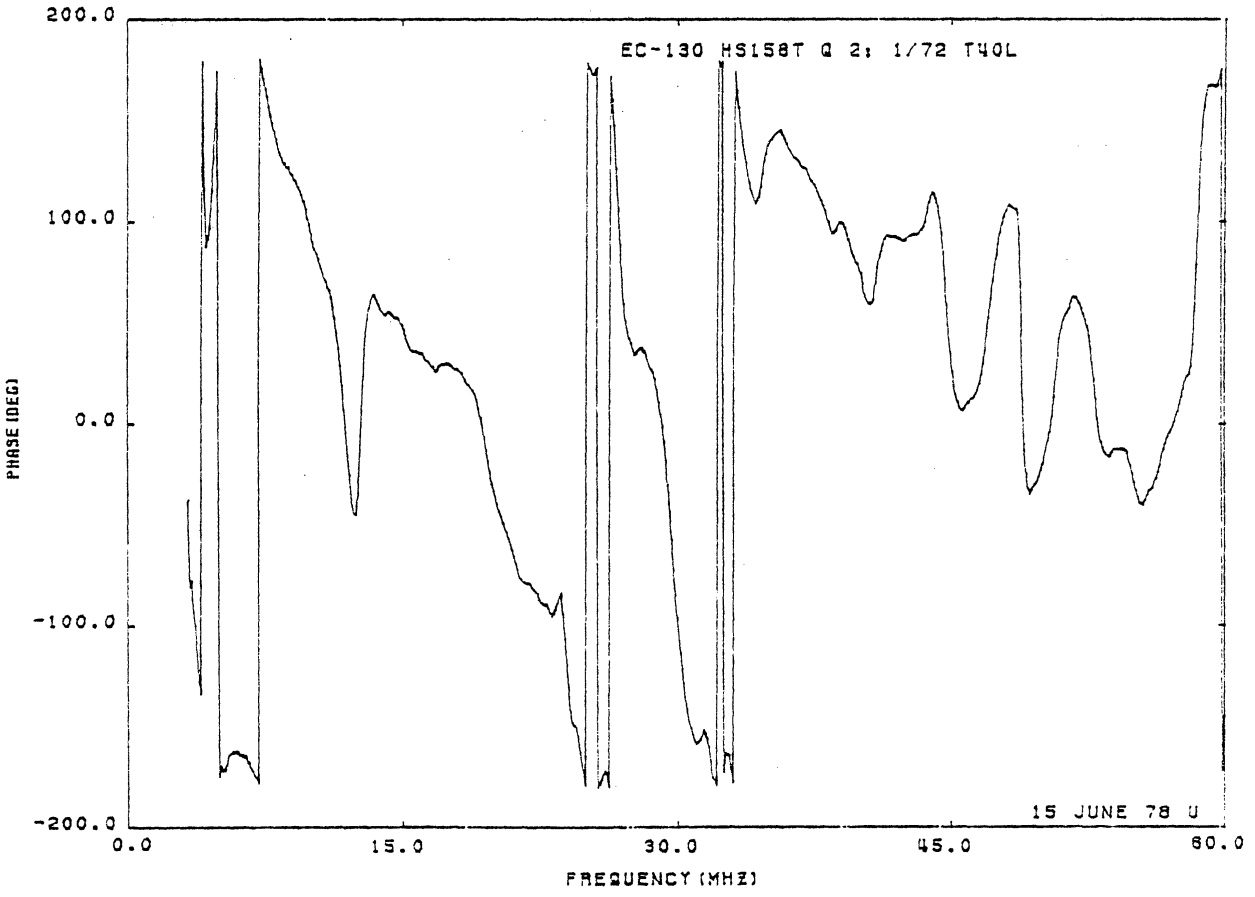

Figure 40L. Charge at STA:HS158T, Excitation 2, 1/72 Model.

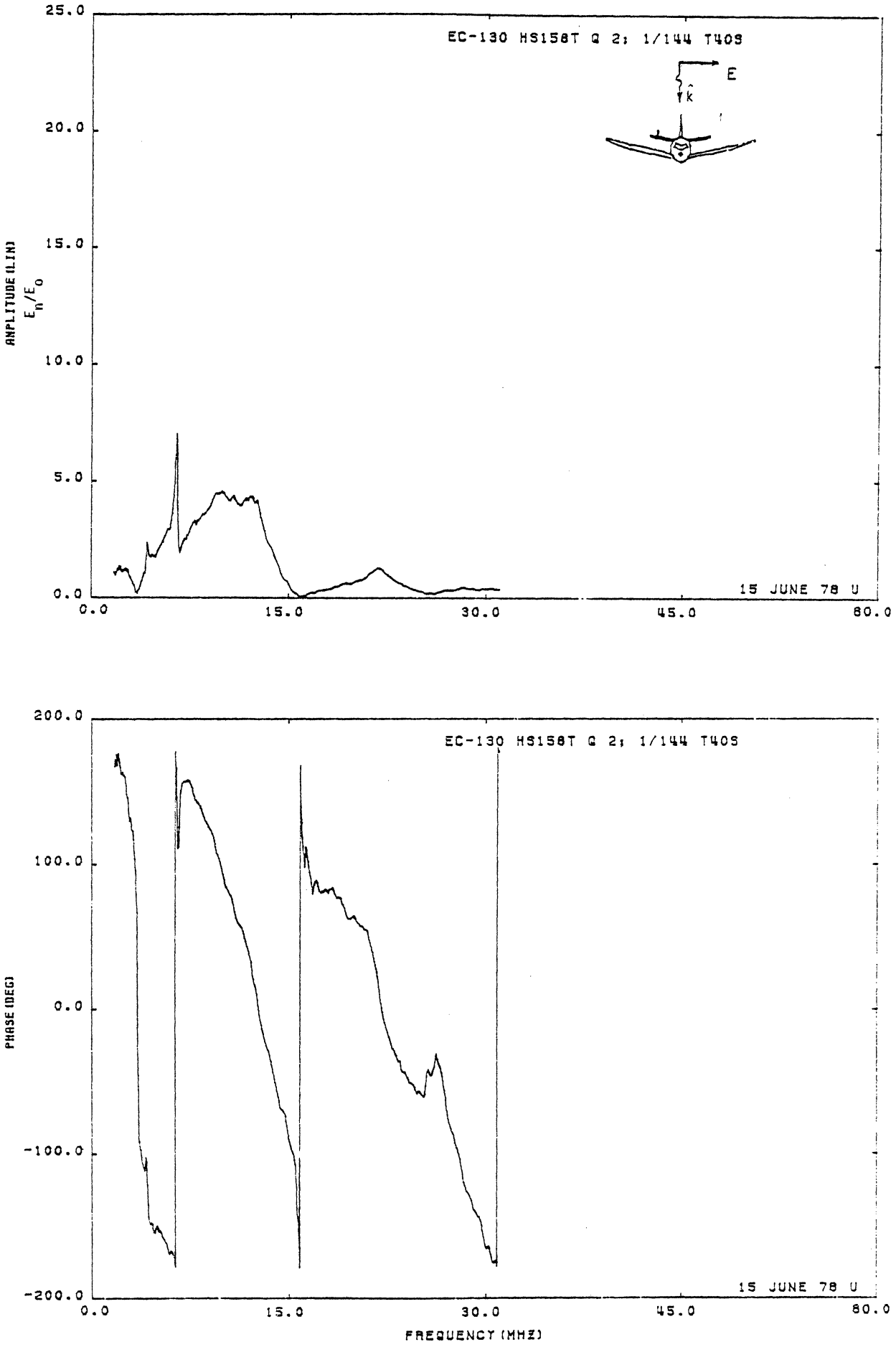

Figure 40S. Charge at STA:HS158T, Excitation 2, 1/144 Model.

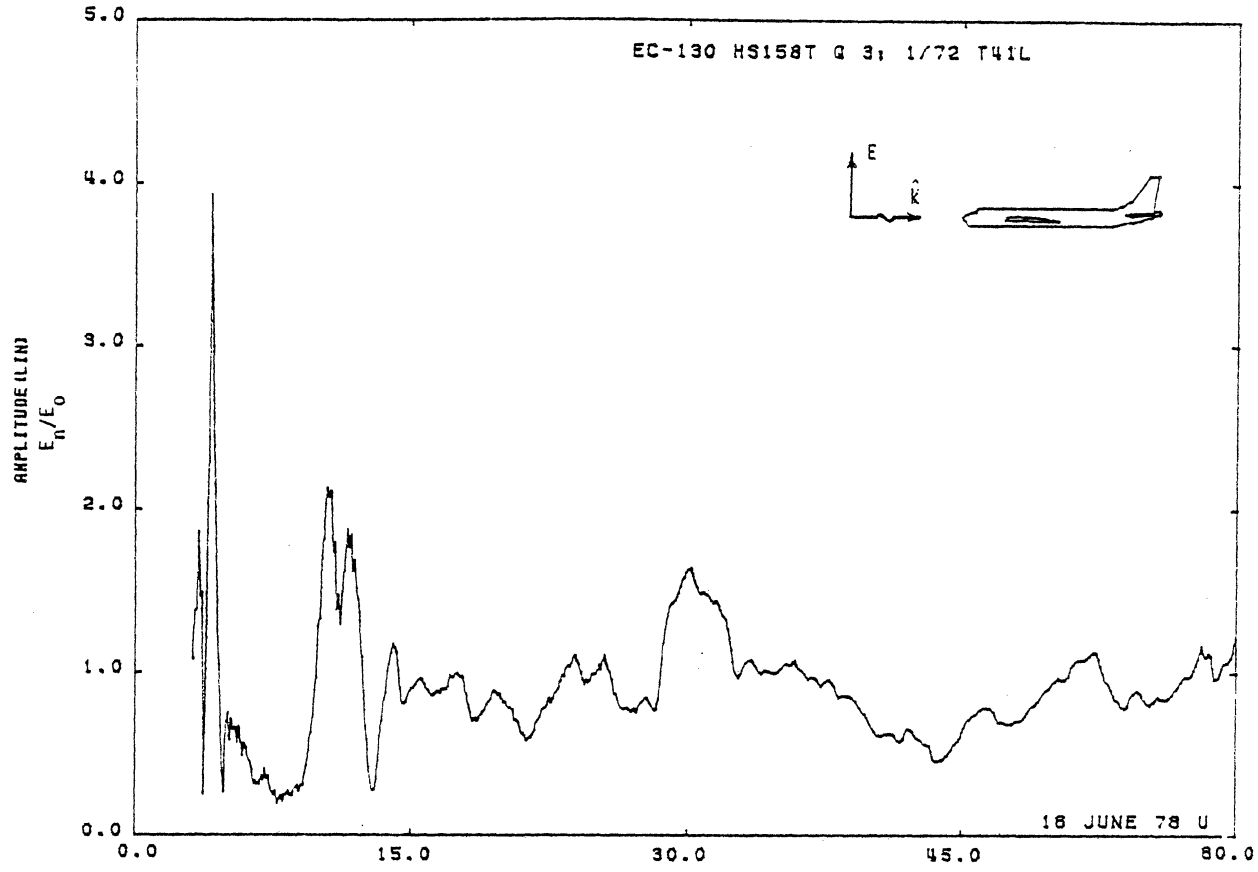

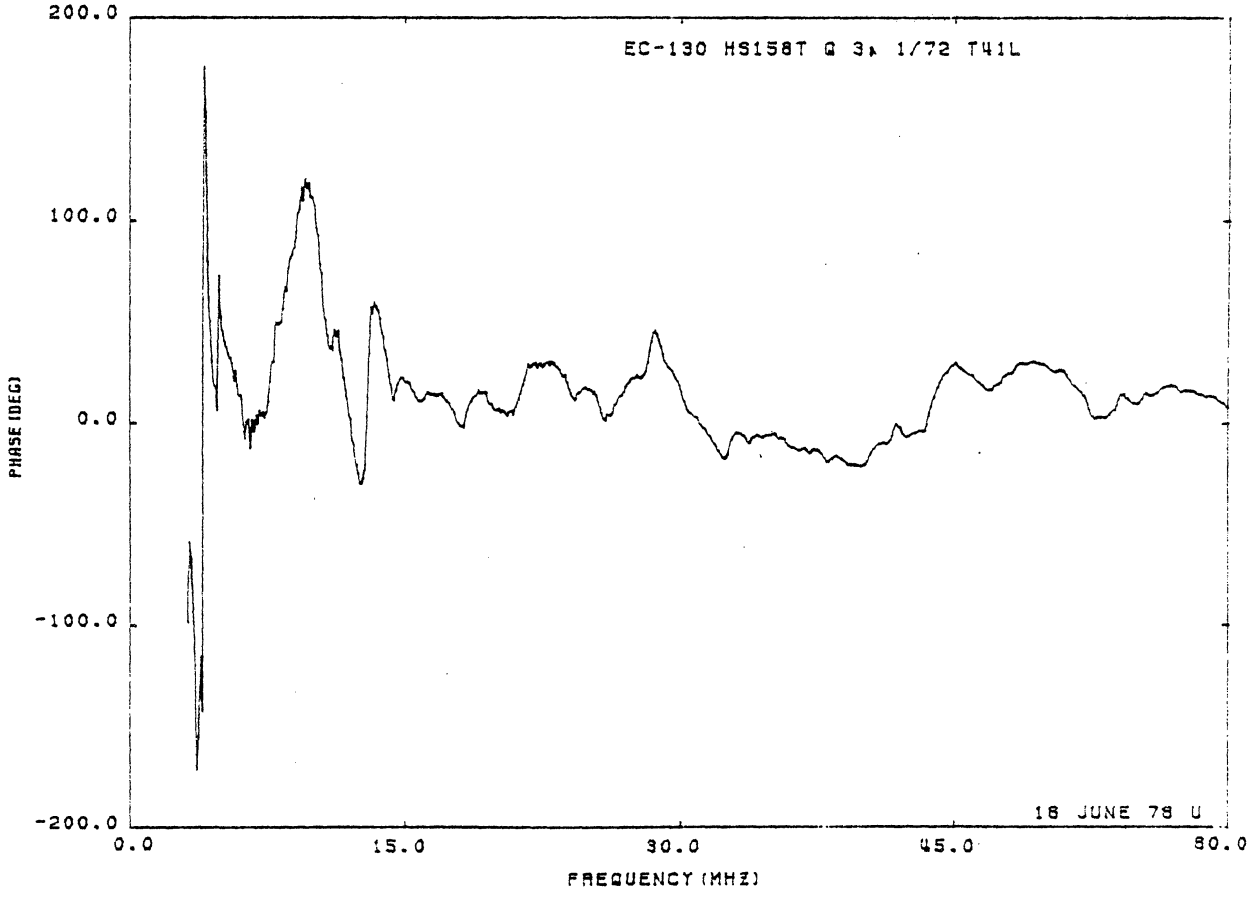

Figure 41L. Charge at STA:HS158T, Excitation 3, 1/72 Model.

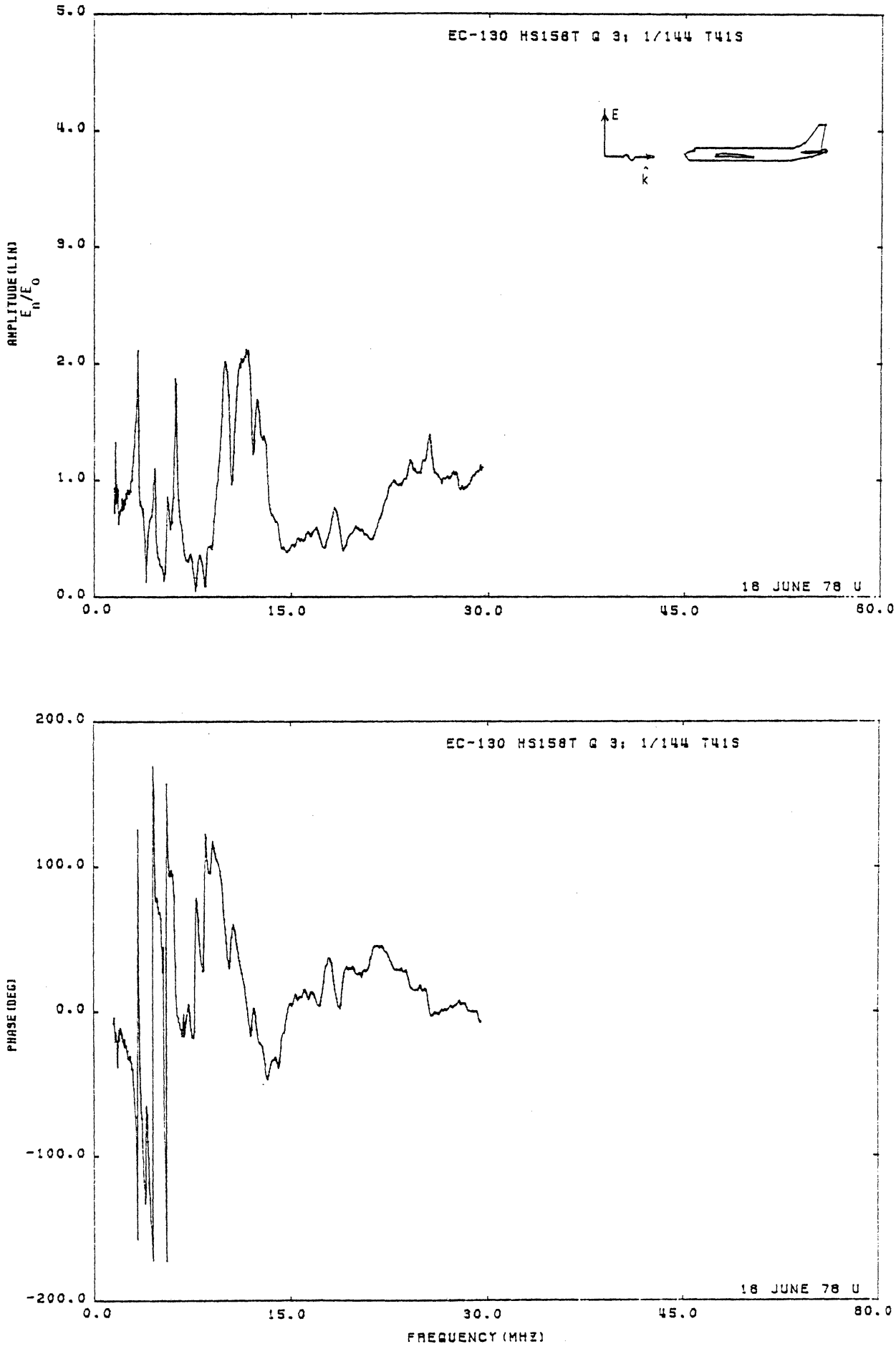

Figure 41S. Charge at STA:HS158T, Excitation 3, 1/144 Model.

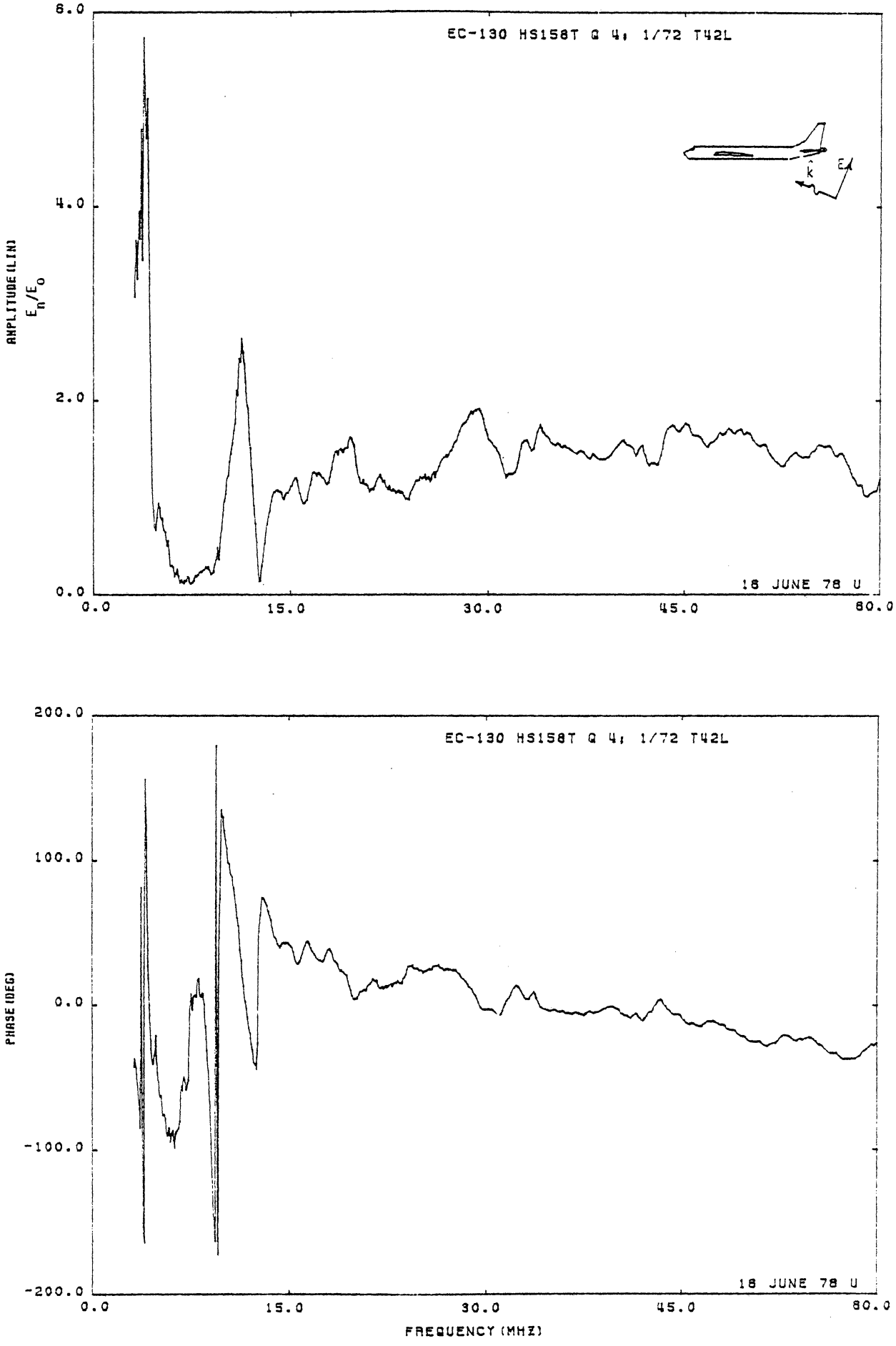

Figure 42L. Charge at STA:HS158T, Excitation 4, 1/72 Model.

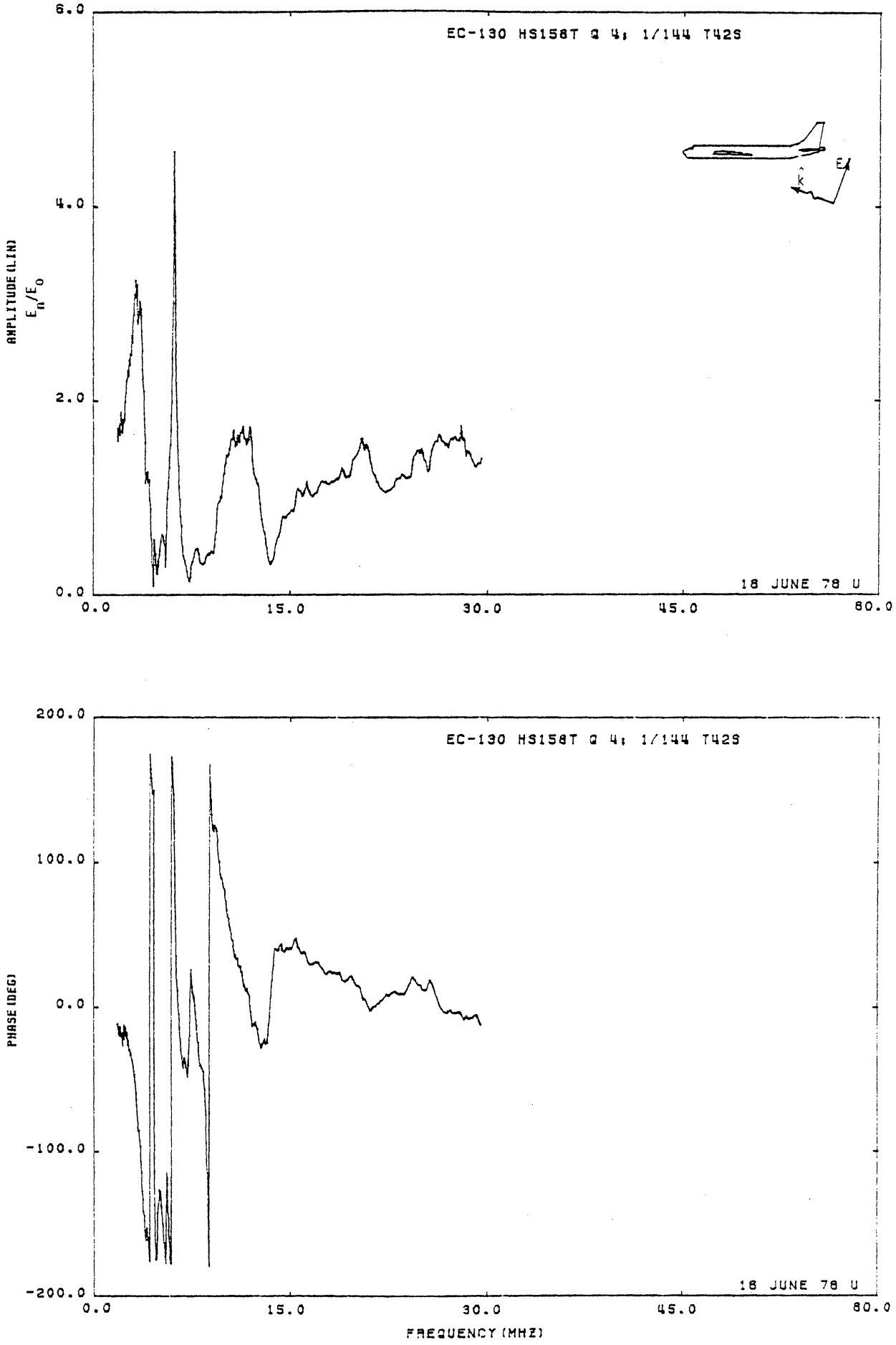

Figure 42S. Charge at STA:HS158T, Excitation 4, 1/144 Model.

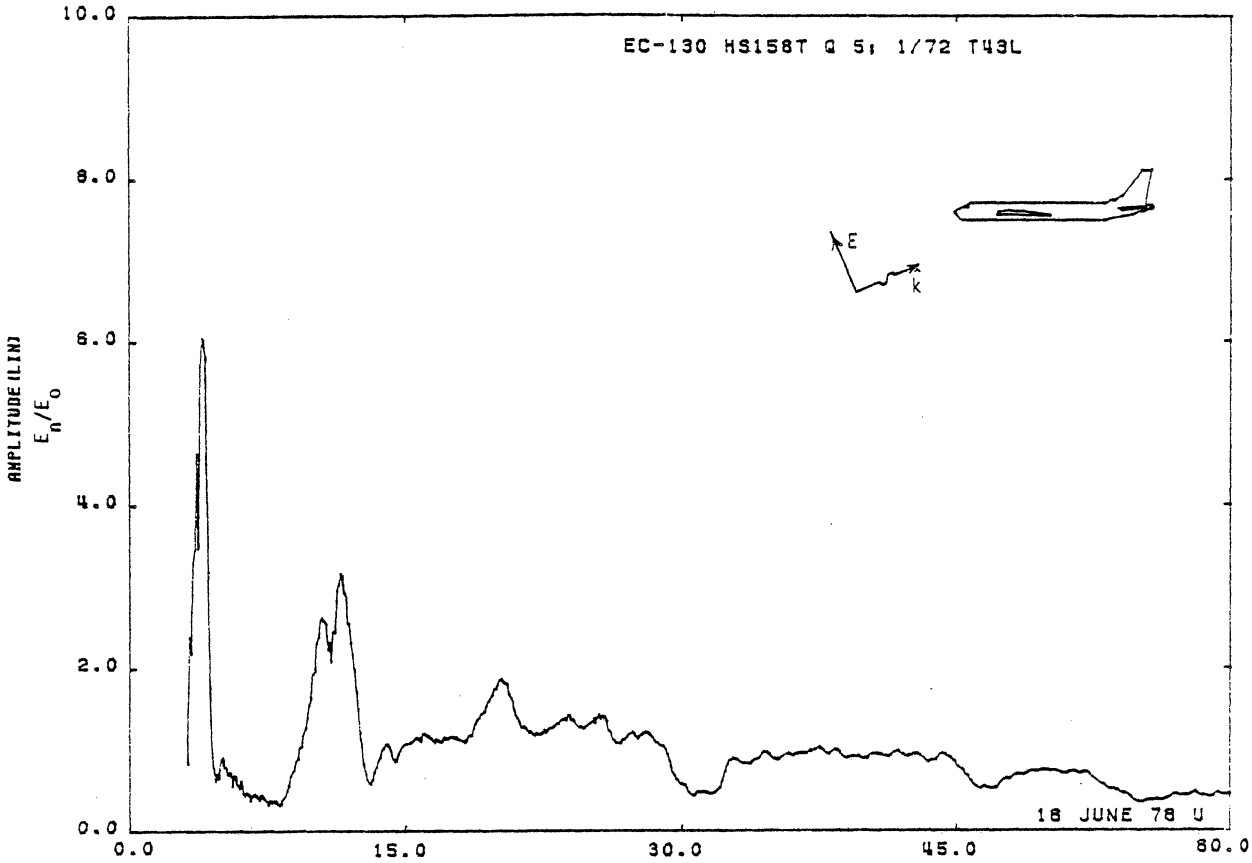

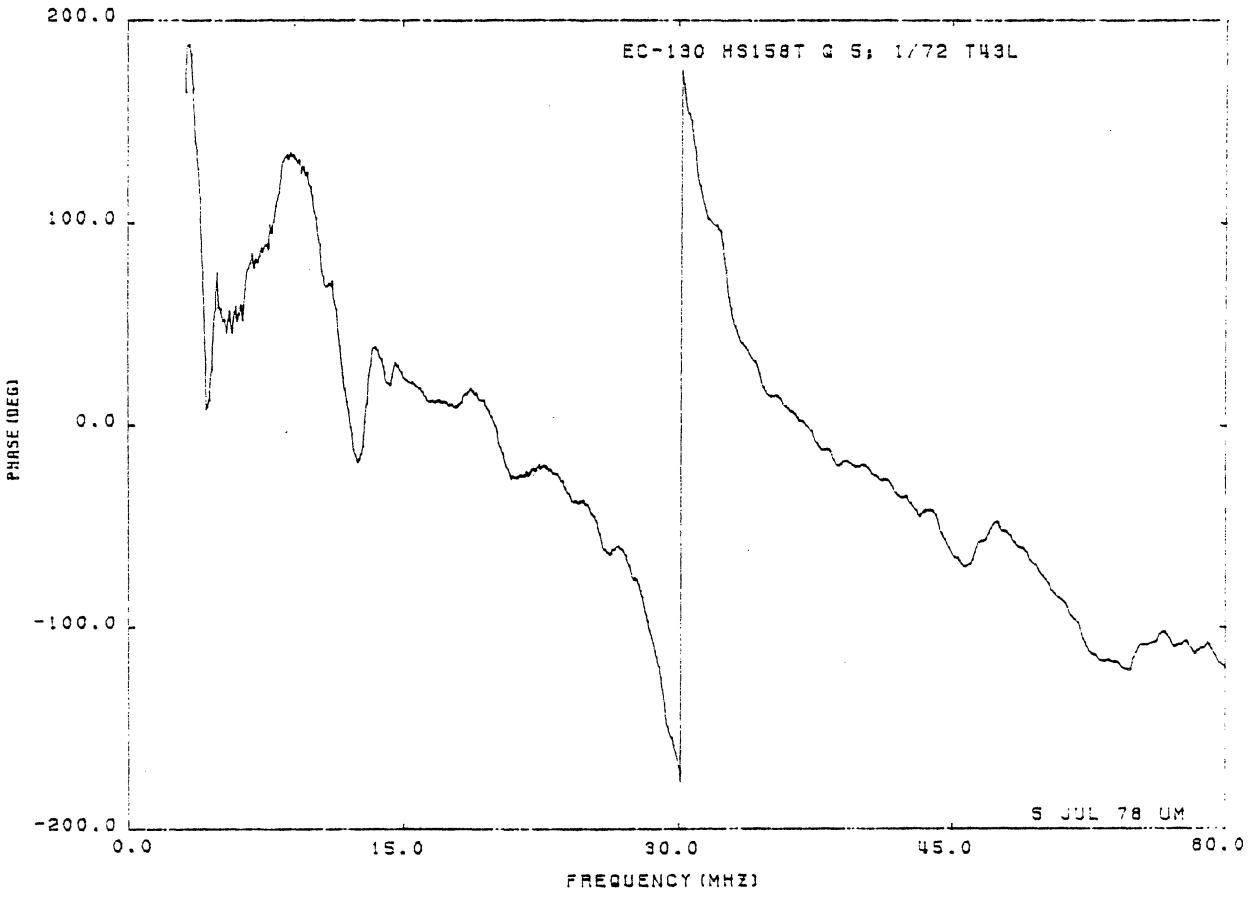

Figure 43L. Charge at STA:HS158T, Excitation 5, 1/72 Model.

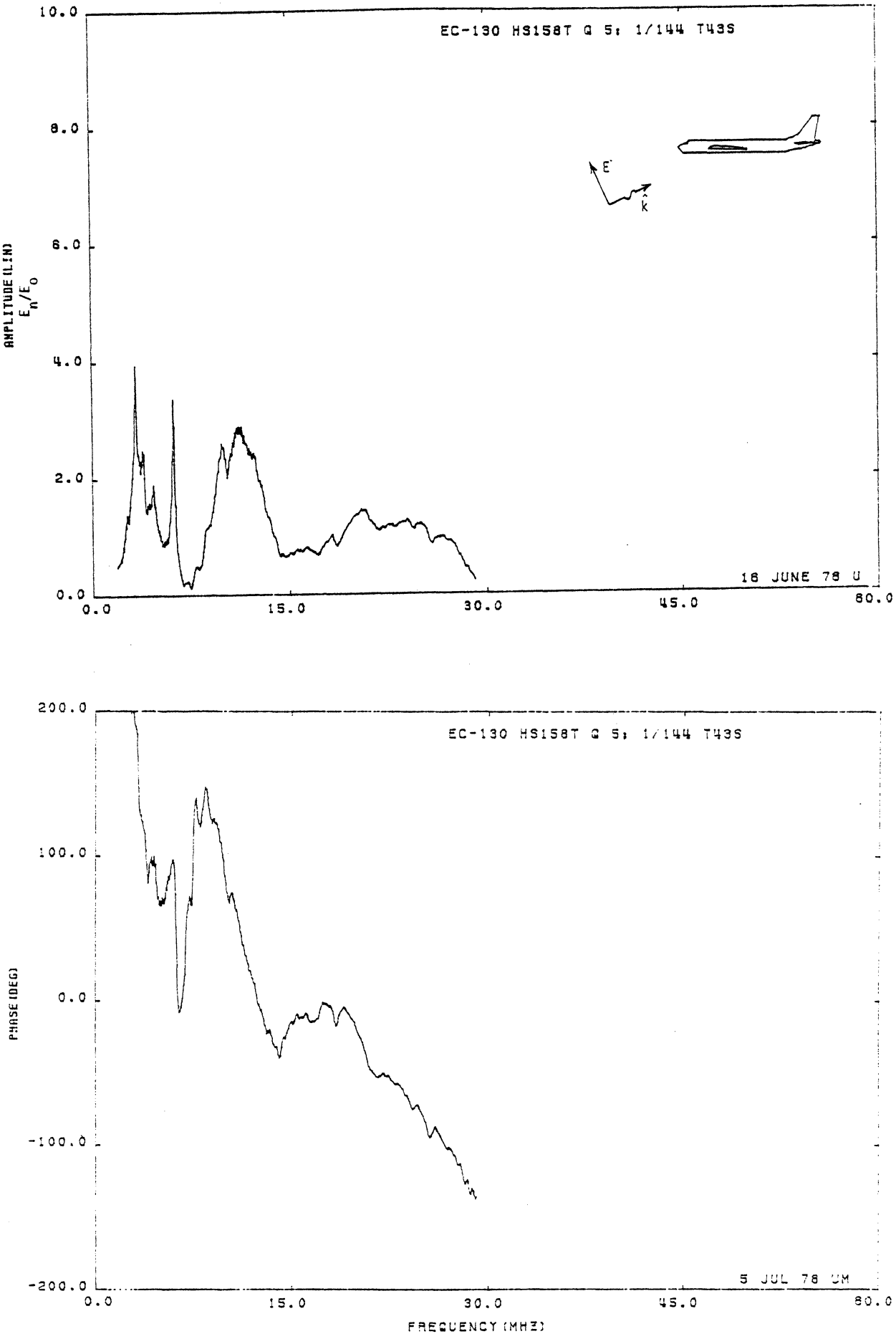

Figure 43S. Charge at STA:HS158T, Excitation 5, 1/144 Model.

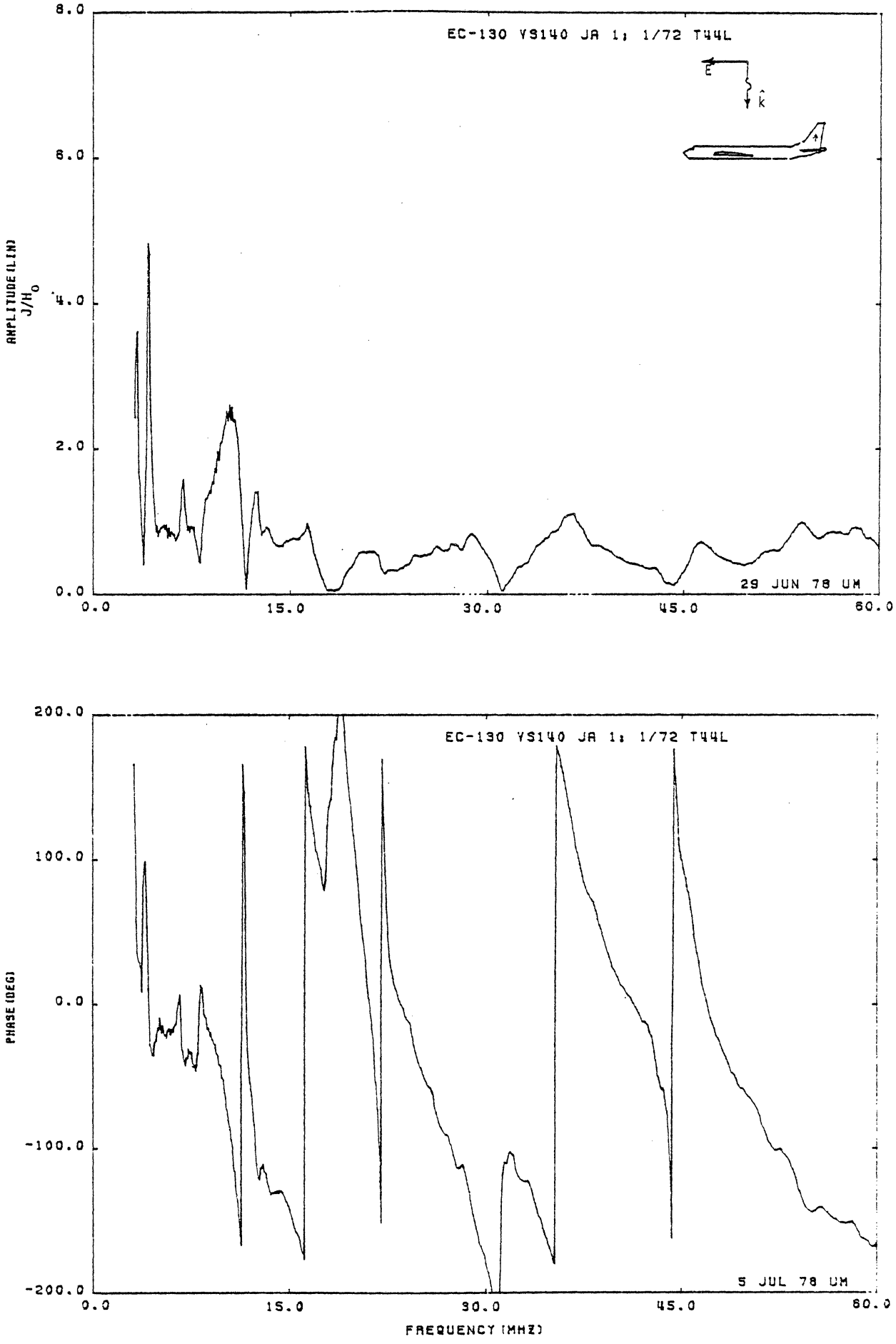

Figure 44L. Axial Current at STA:VS140, Excitation 1, 1/72 Model.

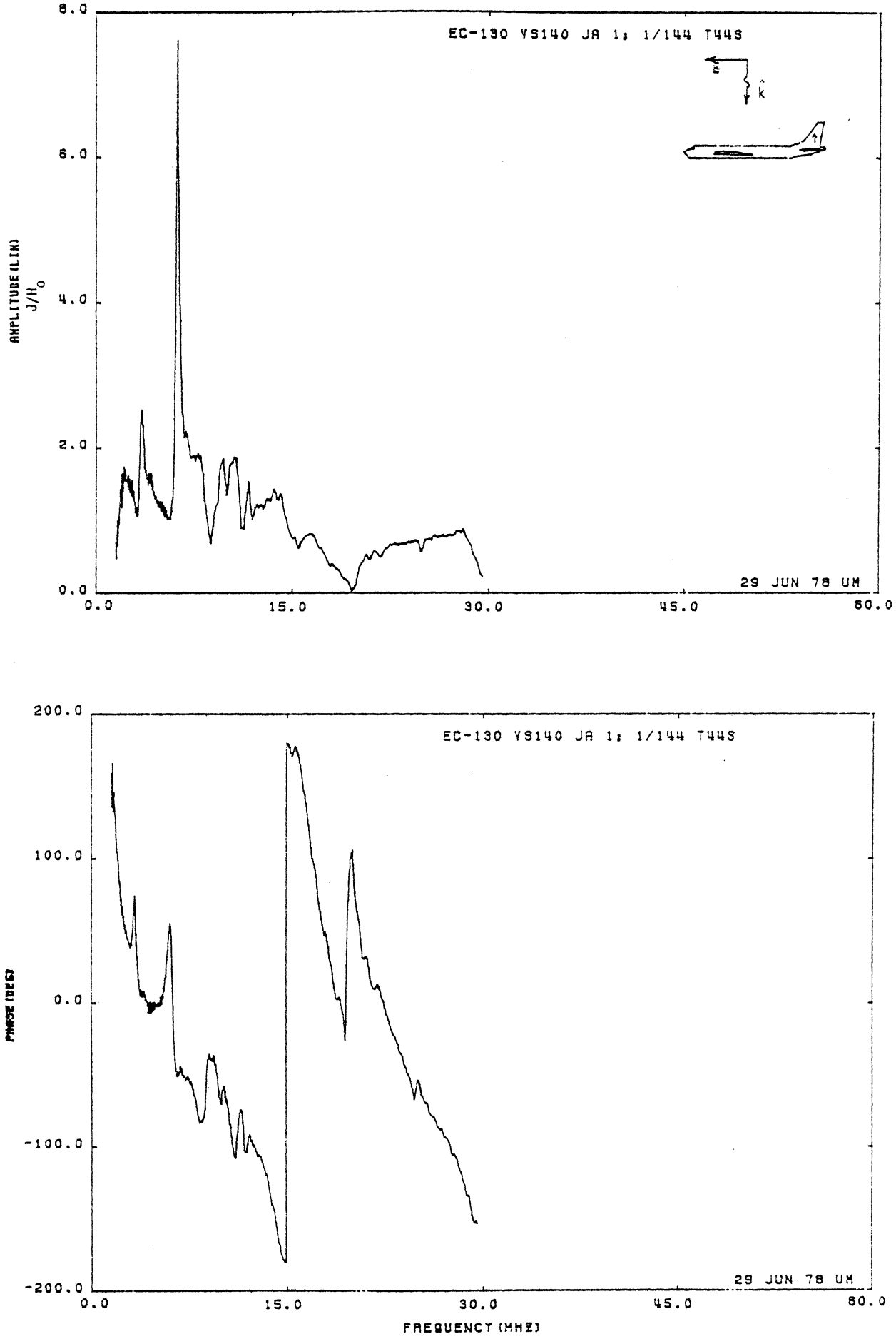

Figure 44S. Axial Current at STA:VS140, Excitation 1, 1/144 Model.

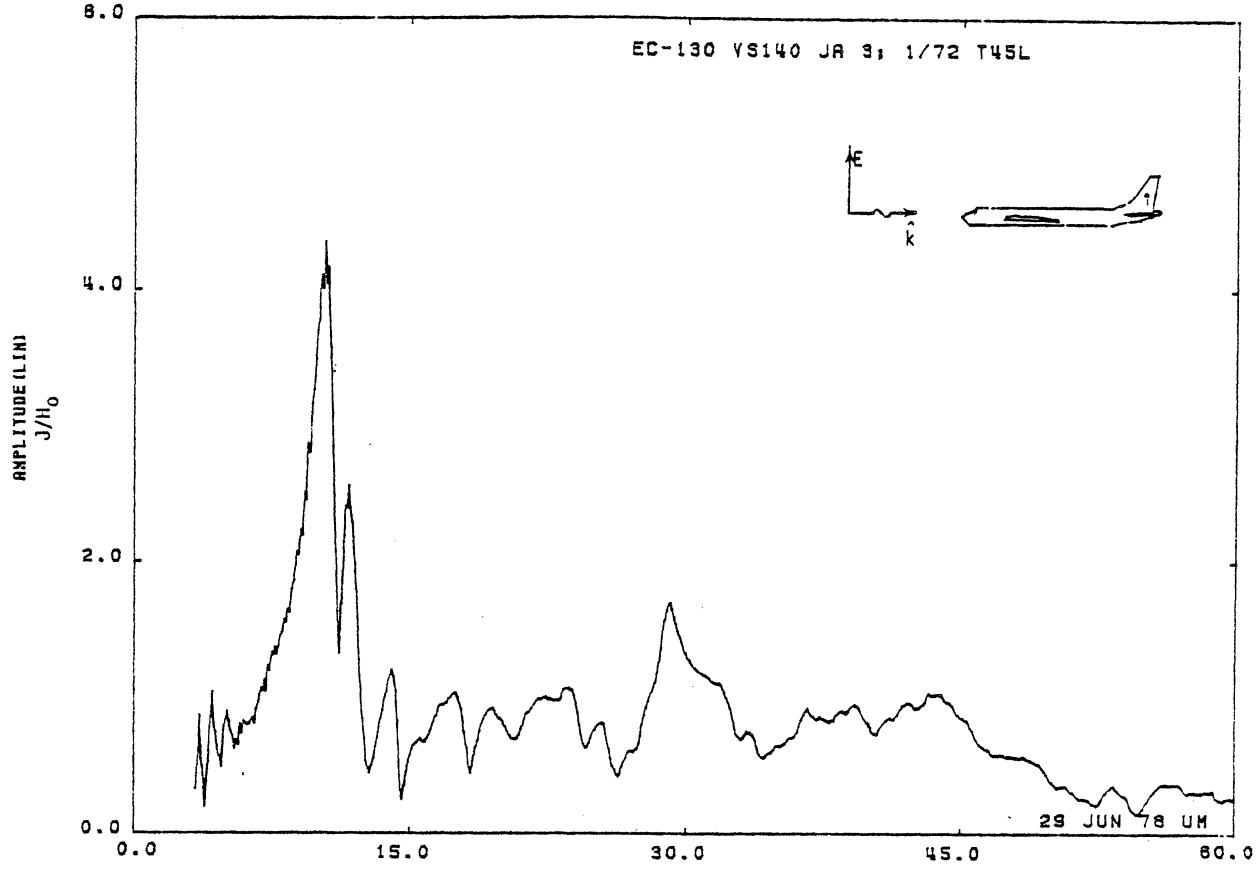

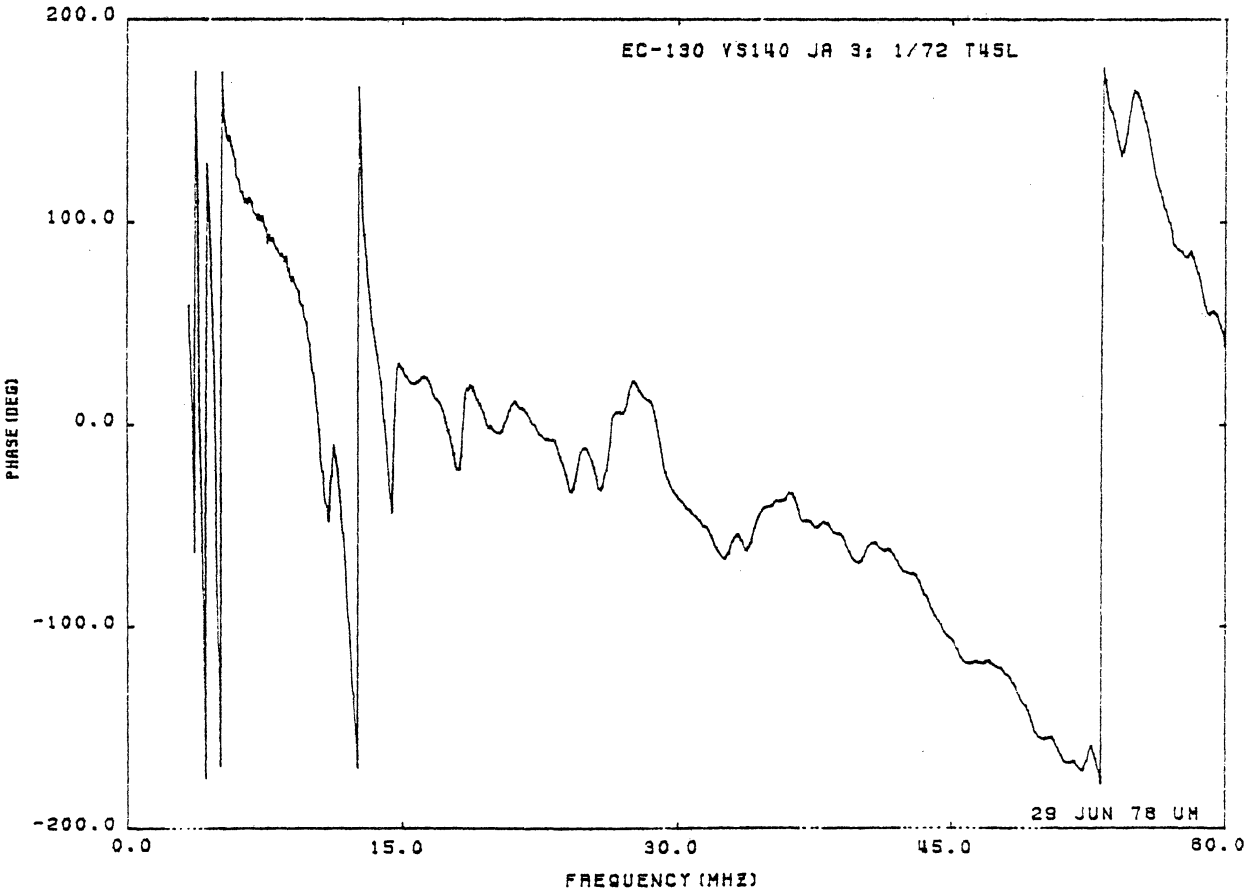

Figure 45L. Axial Current at STA:VS140, Excitation 3, 1/72 Model.

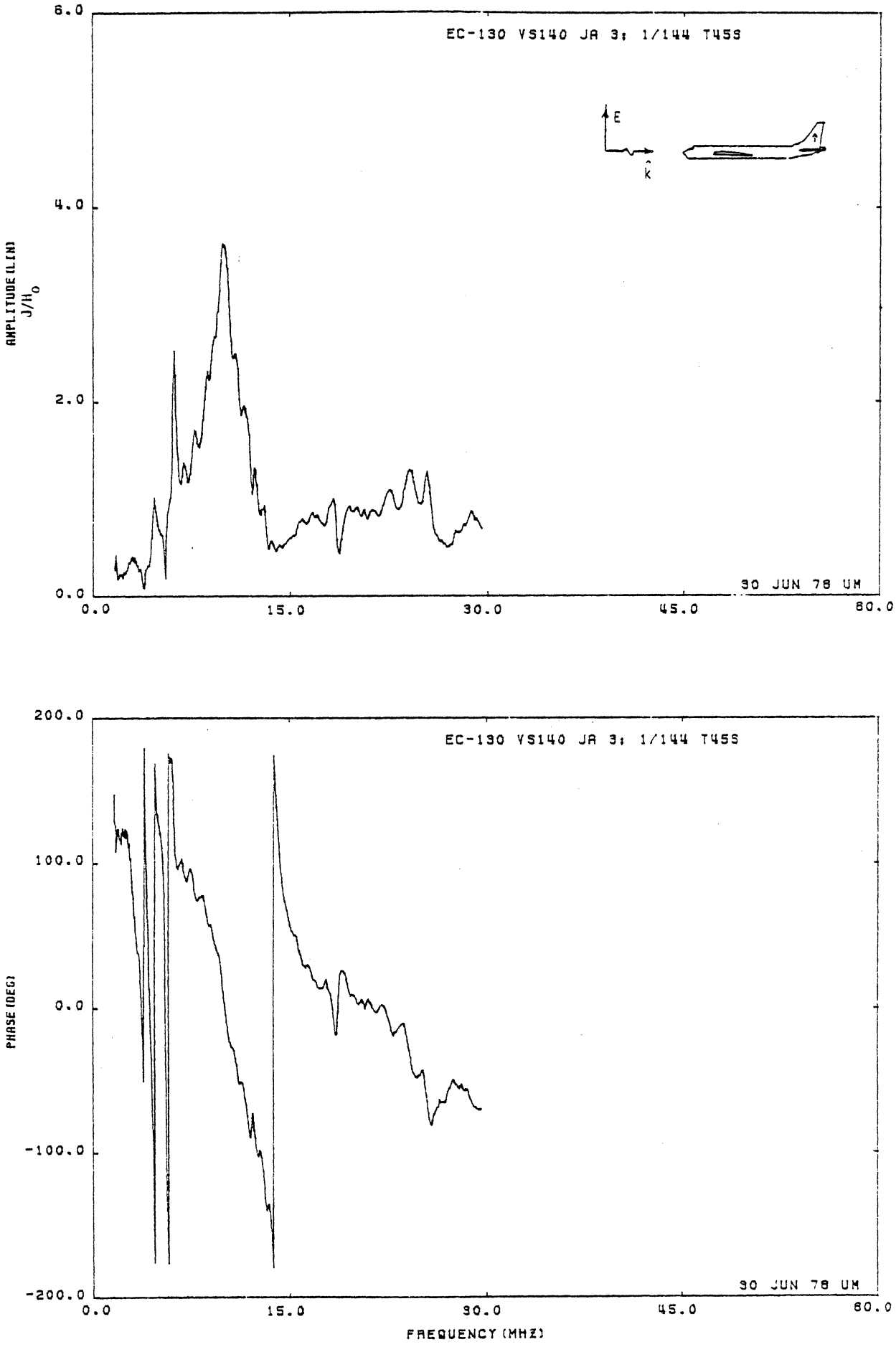

Figure 45S. Axial Current at STA:VS140, Excitation 3, 1/144 Model.

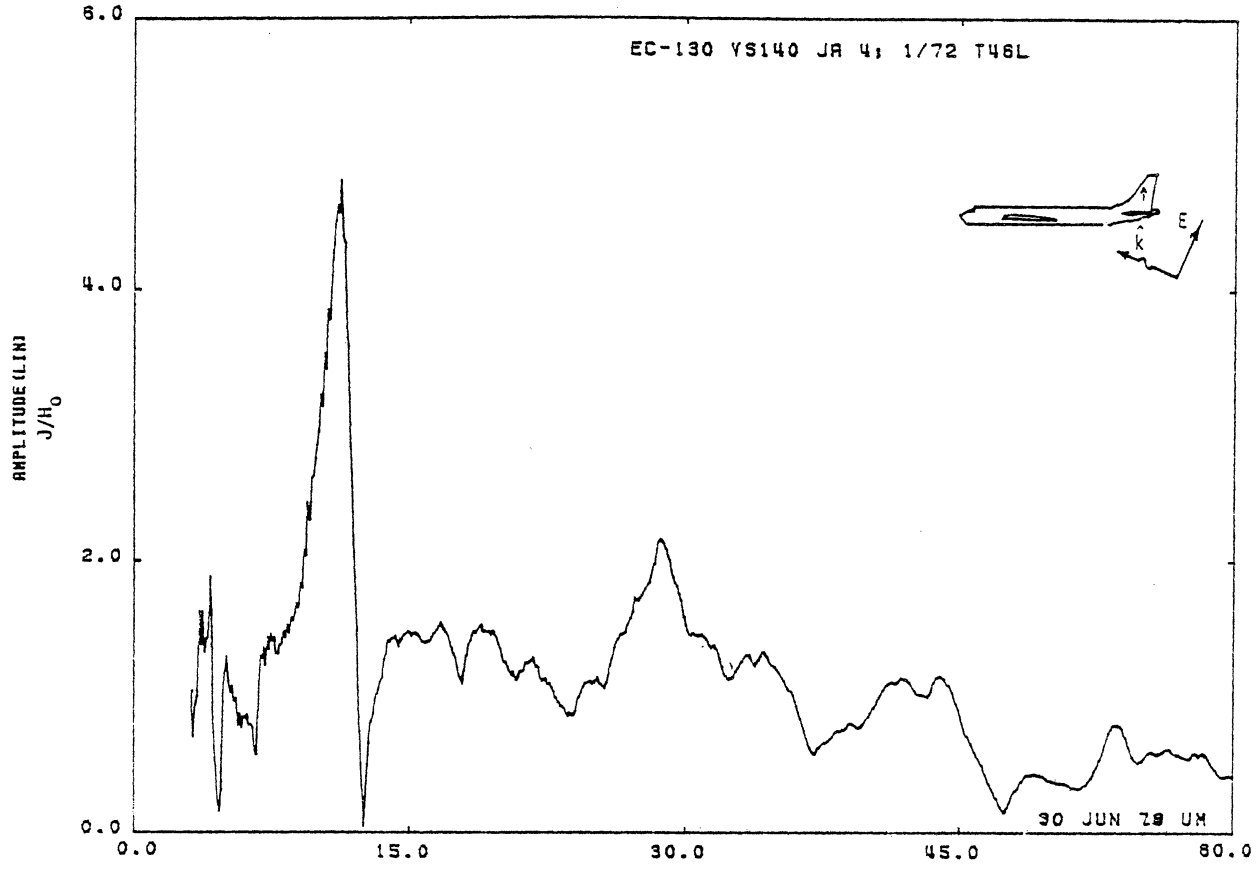

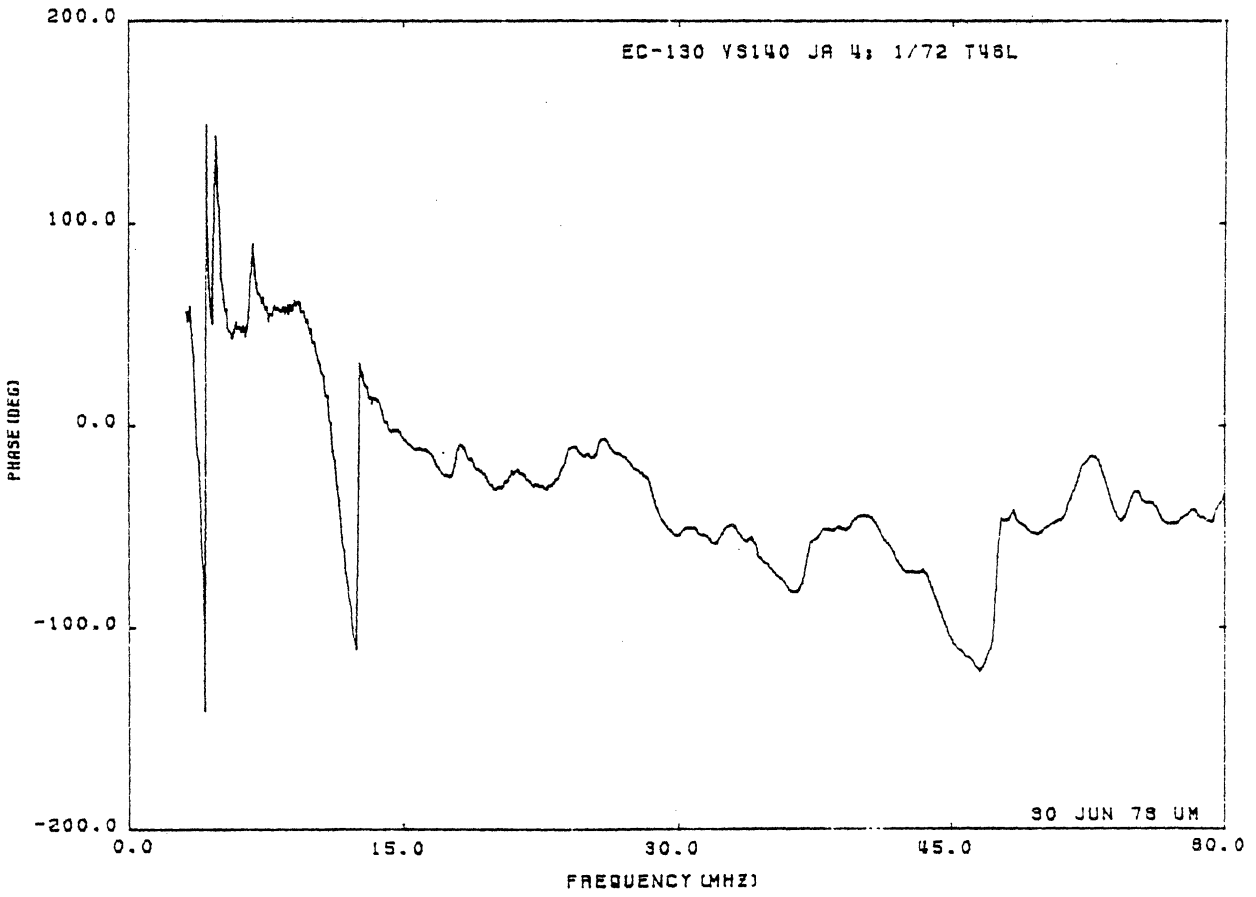

Figure 46L. Axial Current at STA:VS140, Excitation 4, 1/72 Model.

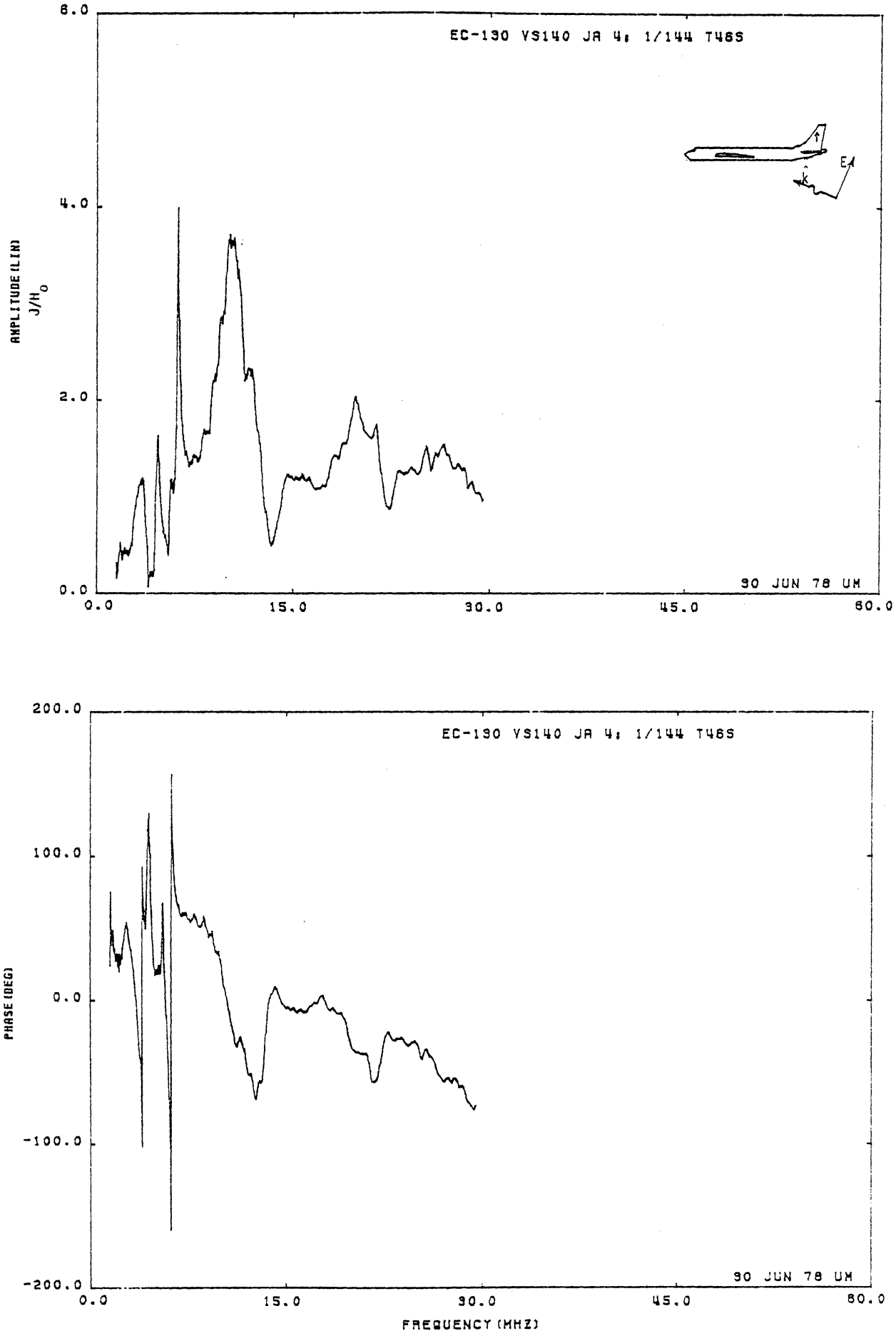

Figure 46S. Axial Current at STA:VS140, Excitation 4, 1/144 Model.

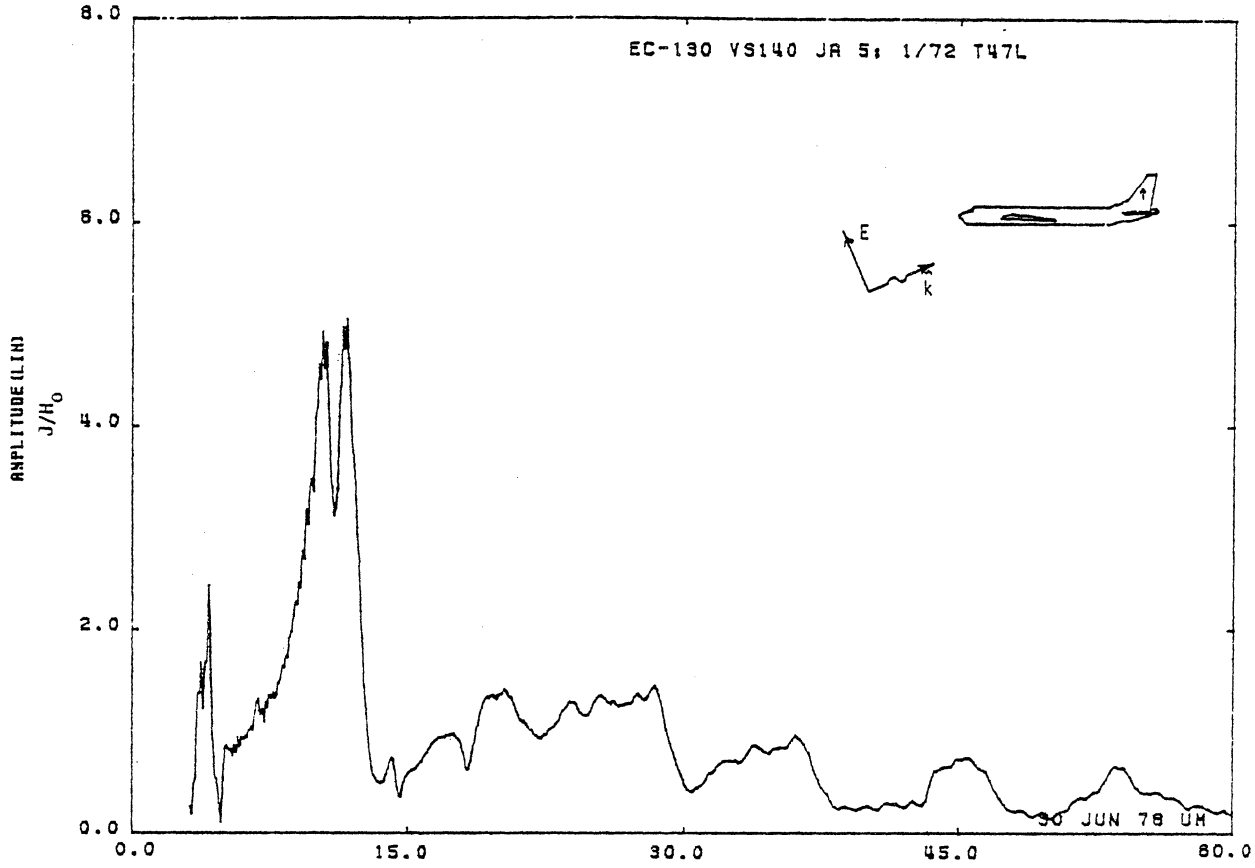

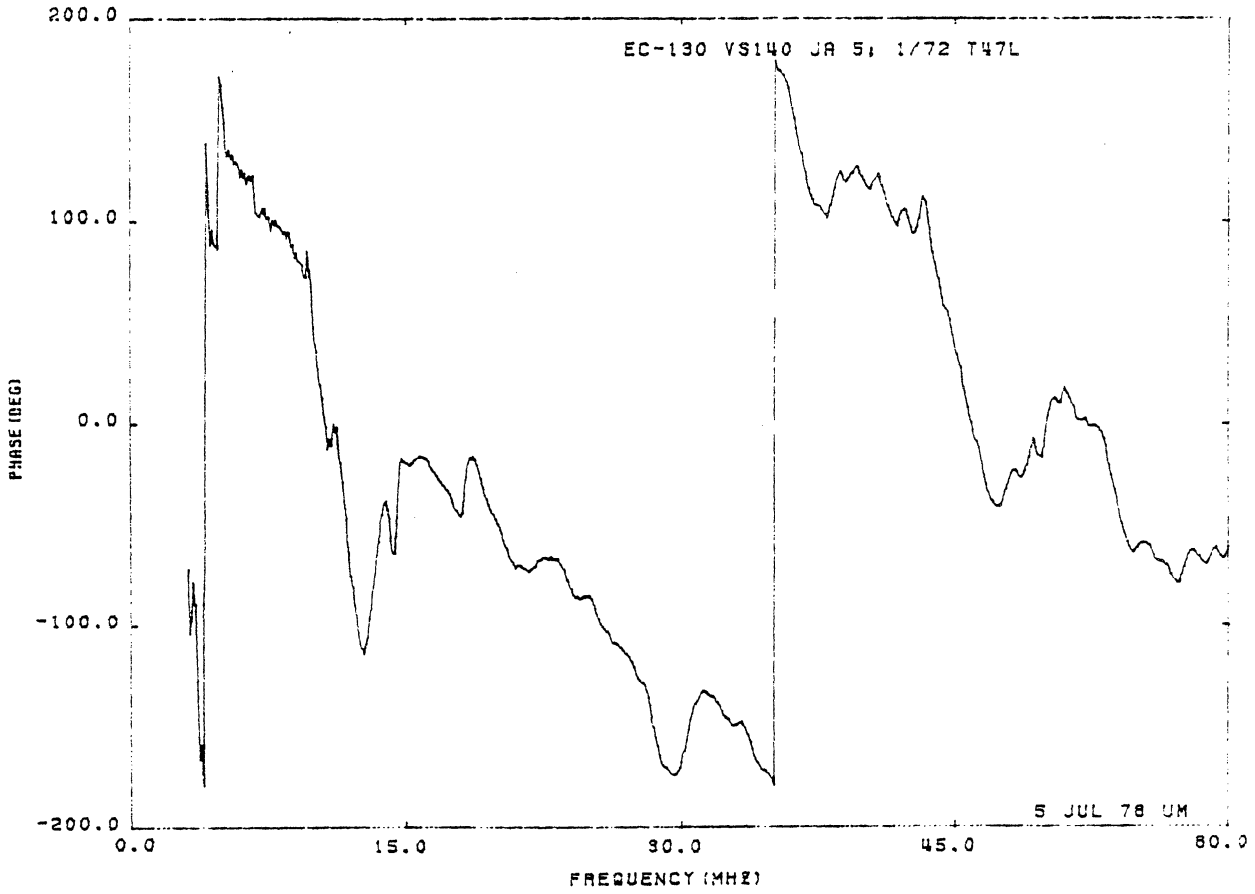

Figure 47L. Axial Current at STA:VS140, Excitation 5, 1/72 Model.

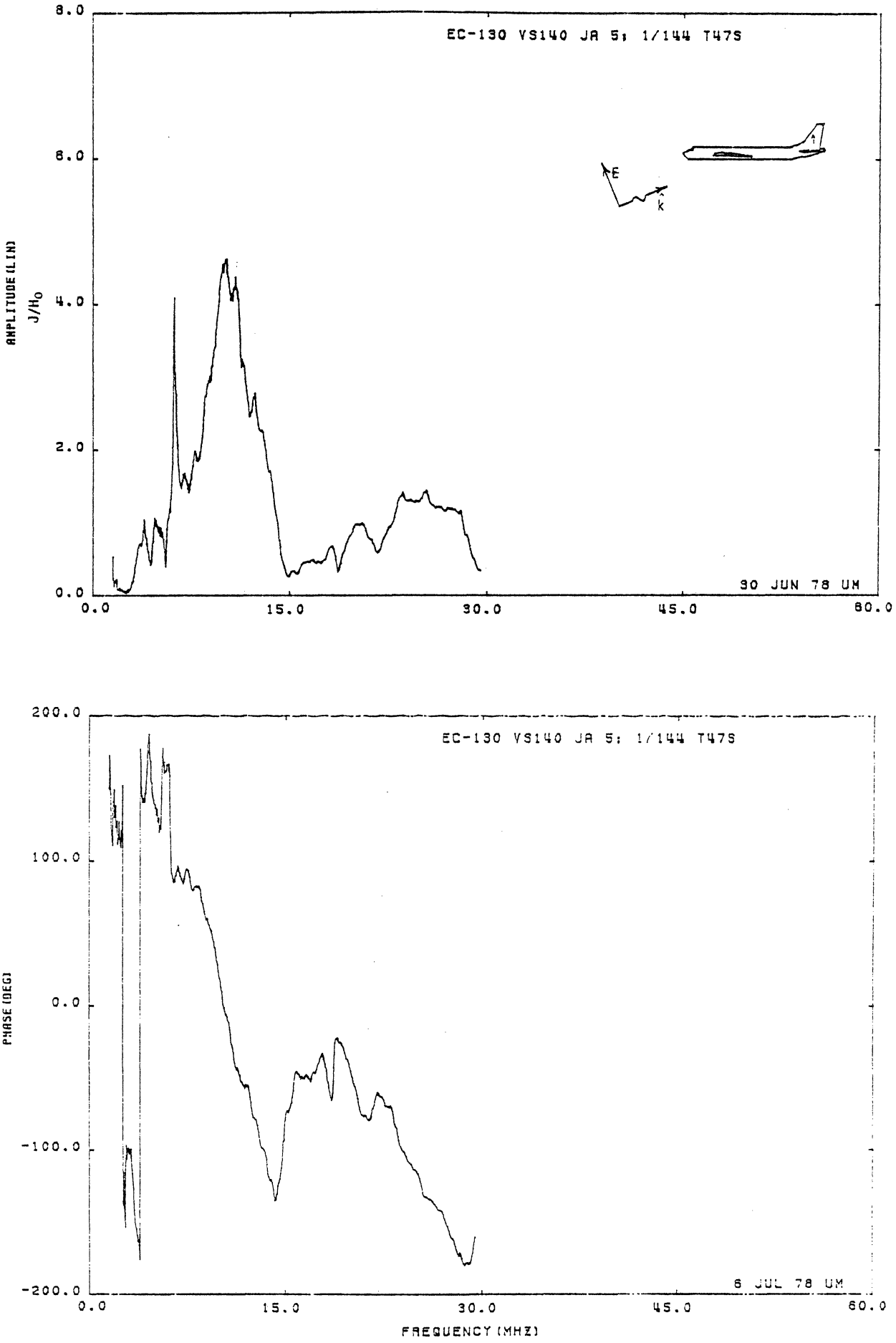

Figure 47S. Axial Current at STA:VS140, Excitation 5, 1/144 Model.

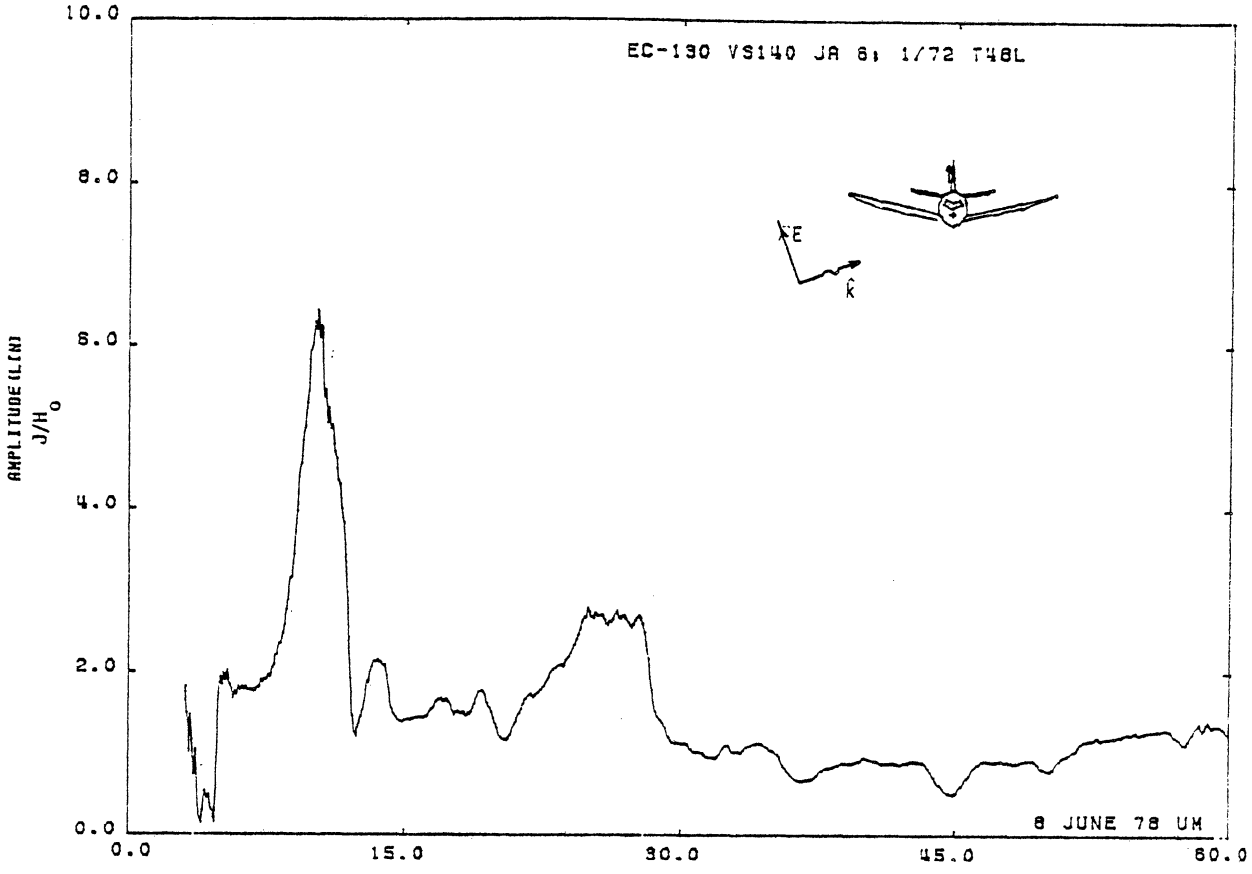

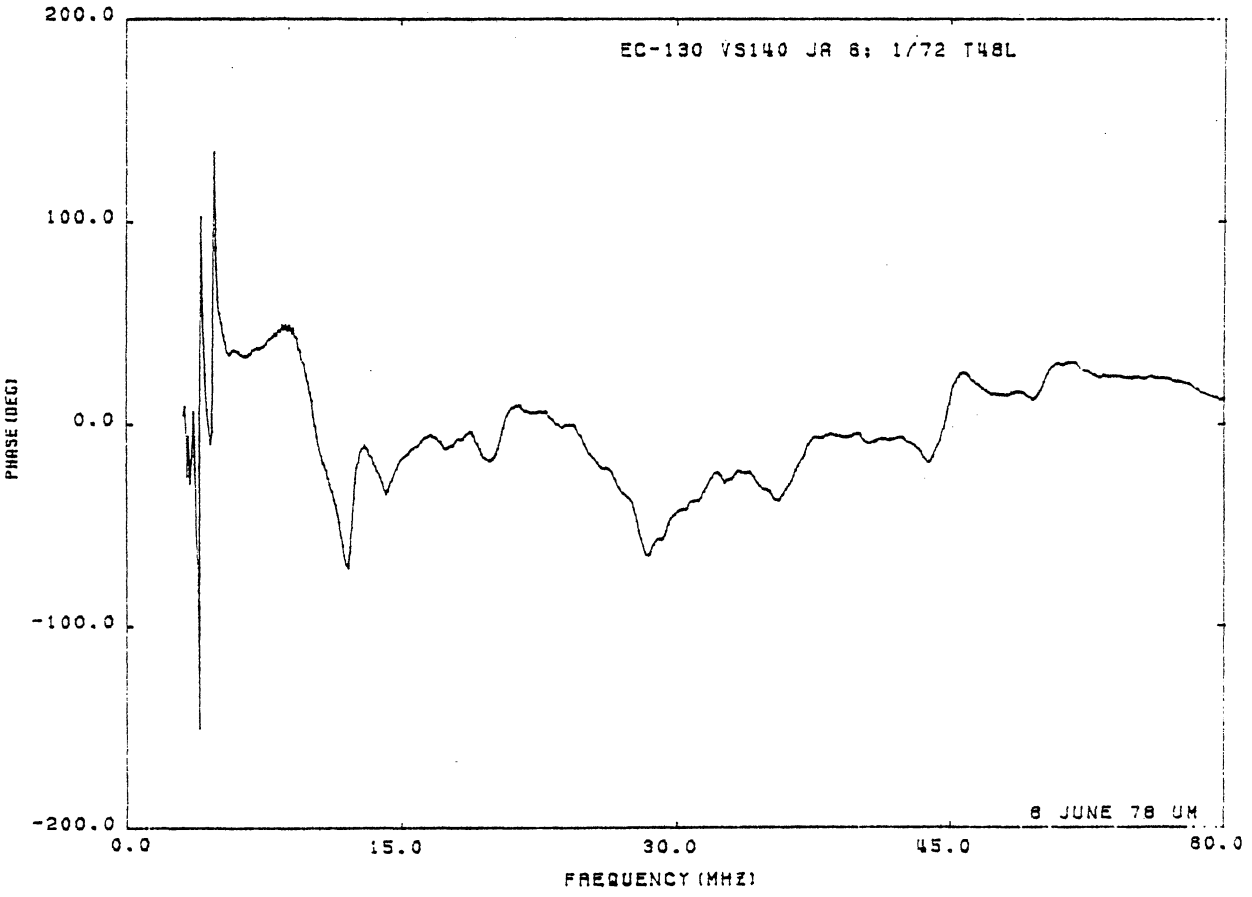

Figure 48L. Axial Current at STA:VS140, Excitation 6, 1/72 Model.

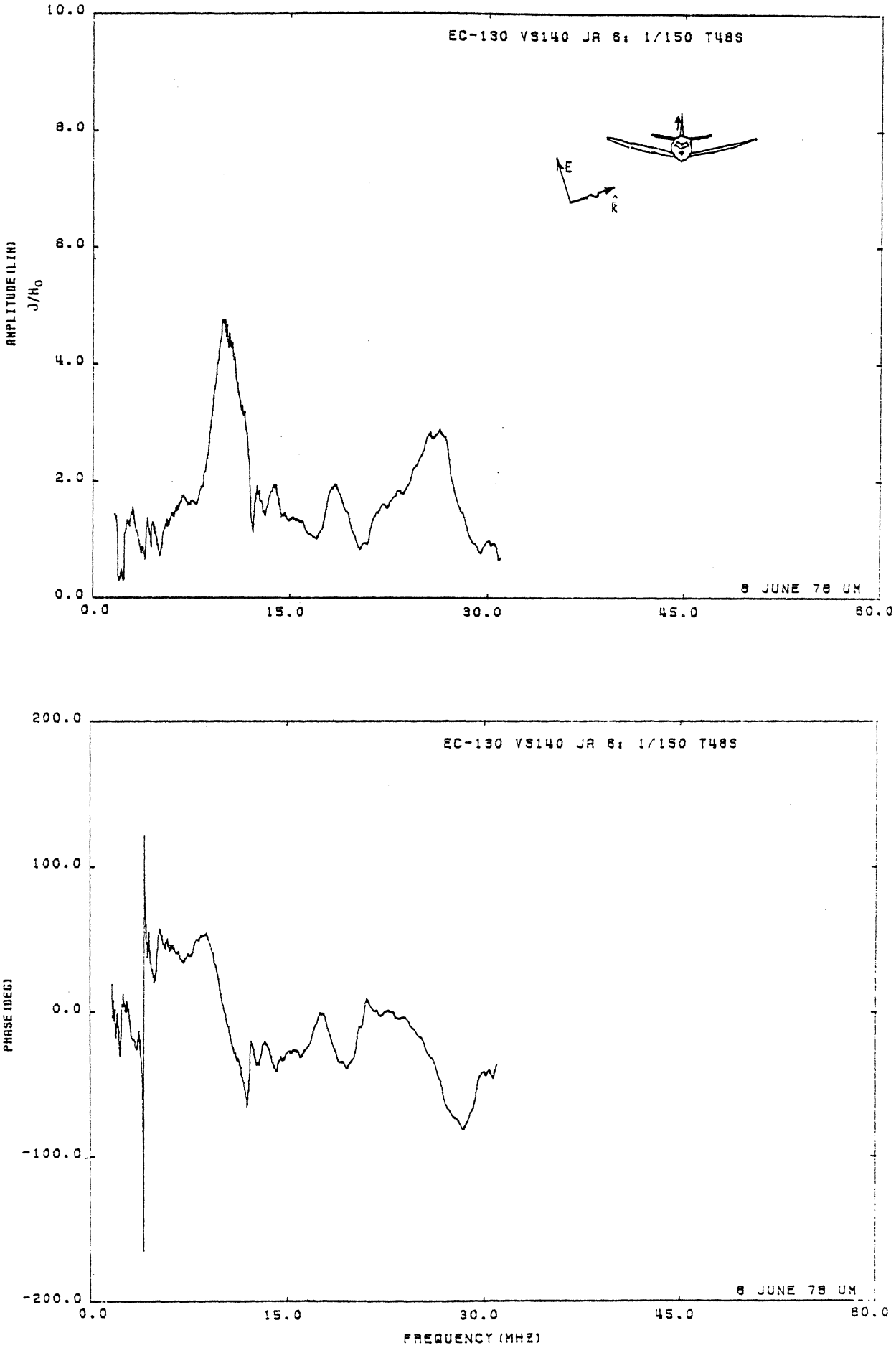

Figure 48S. Axial Current at STA:VS140, Excitation 6, 1/144 Model.

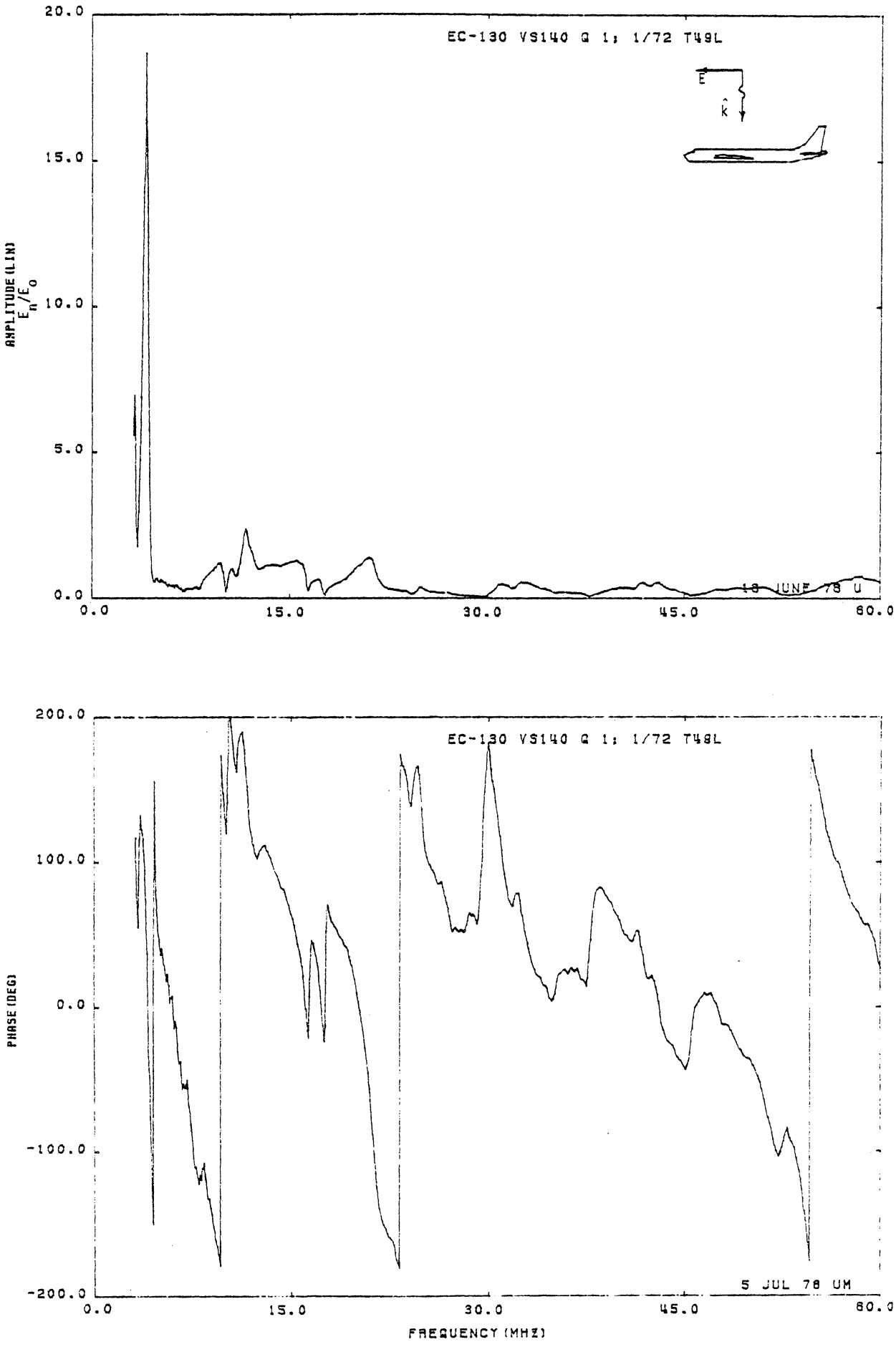

Figure 49L. Charge at STA:VS140, Excitation 1, 1/72 Model.

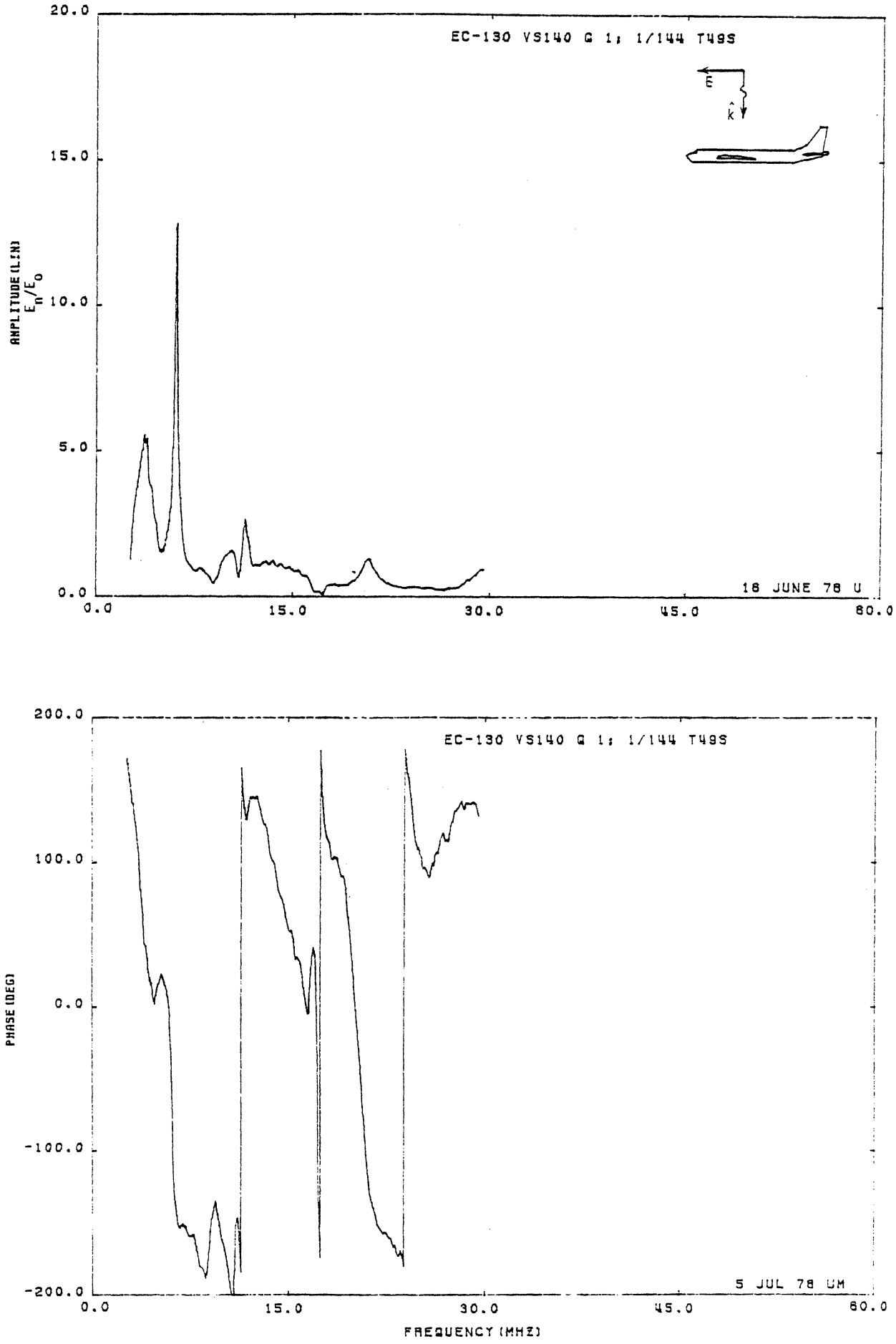

Figure 49S. Charge at STA:VS140, Excitation 1, 1/144 Model.

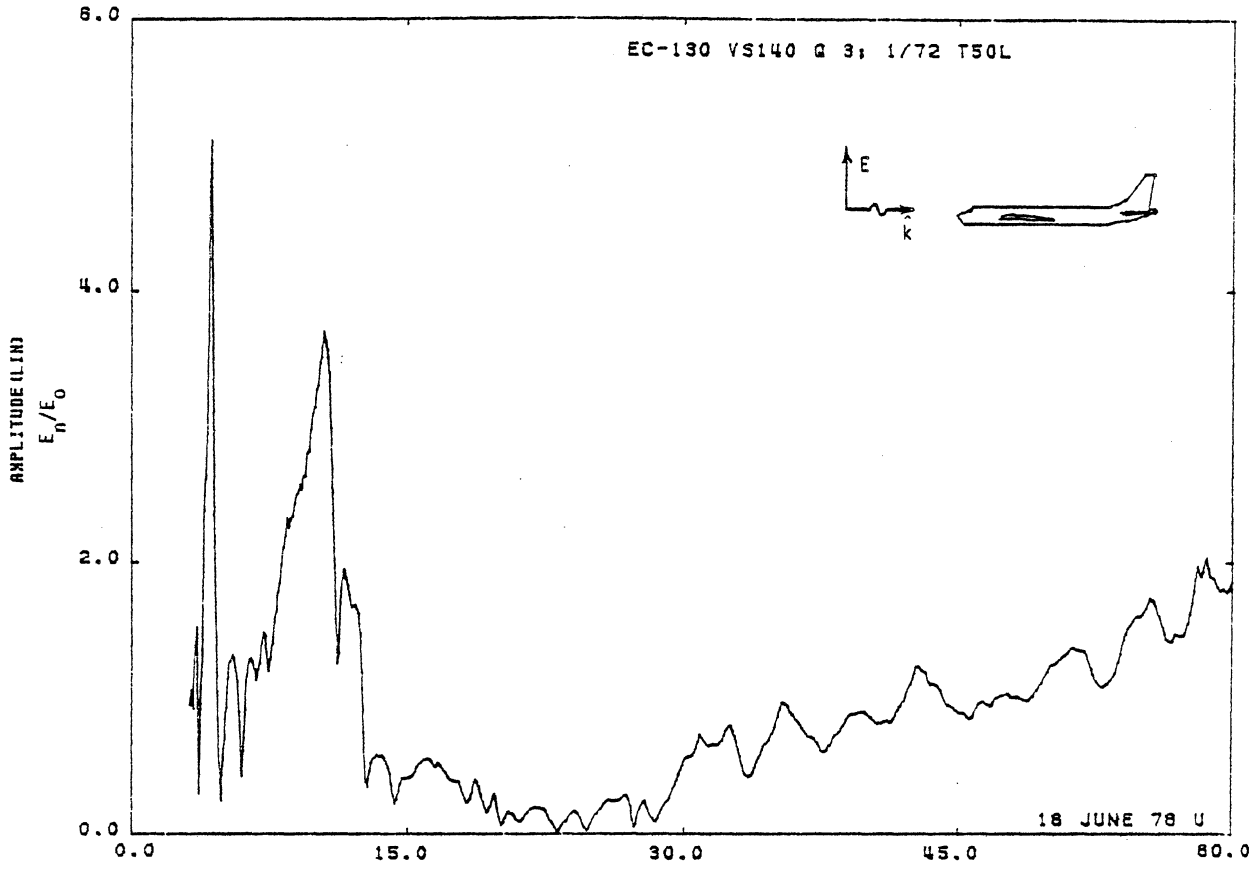

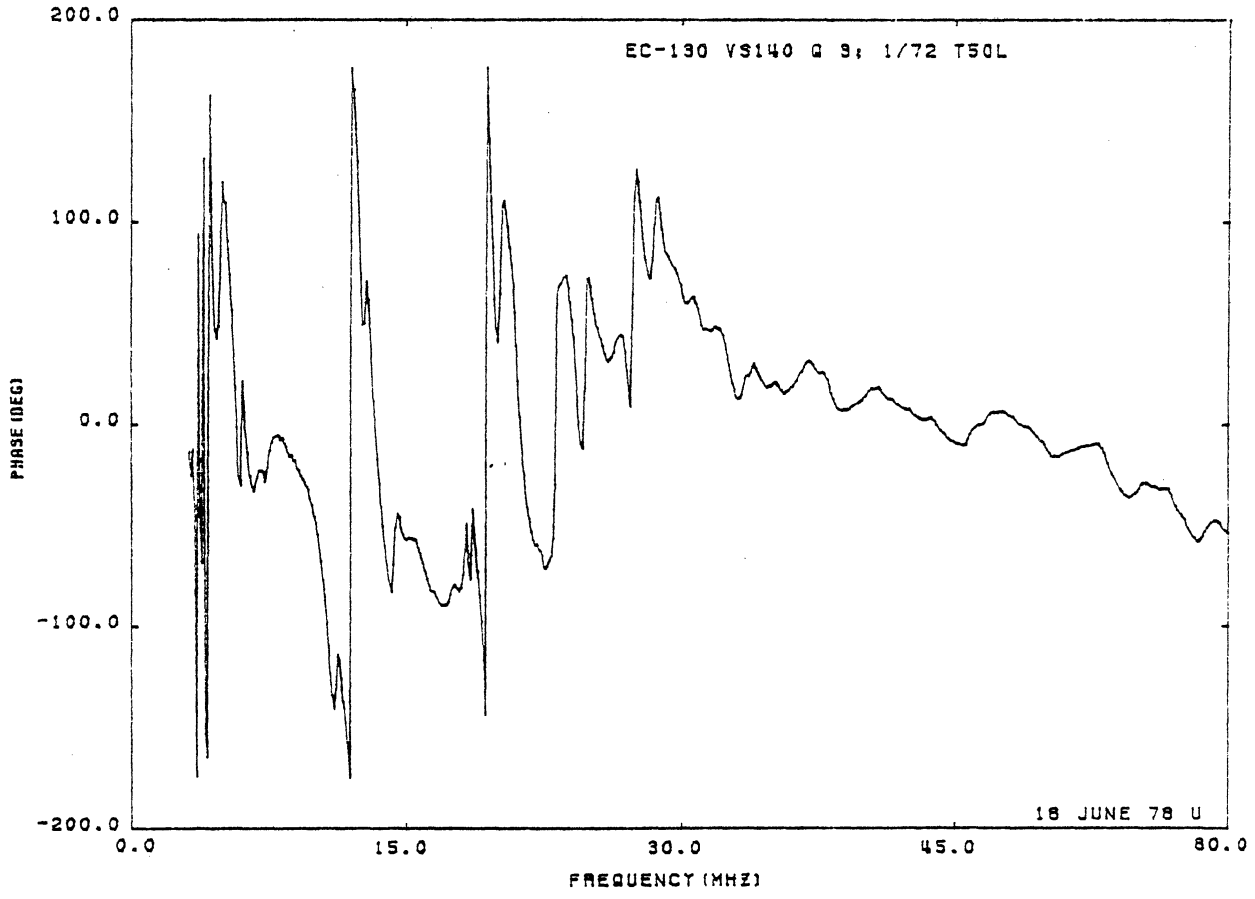

Figure 50L. Charge at STA:VS140, Excitation 3, 1/72 Model.

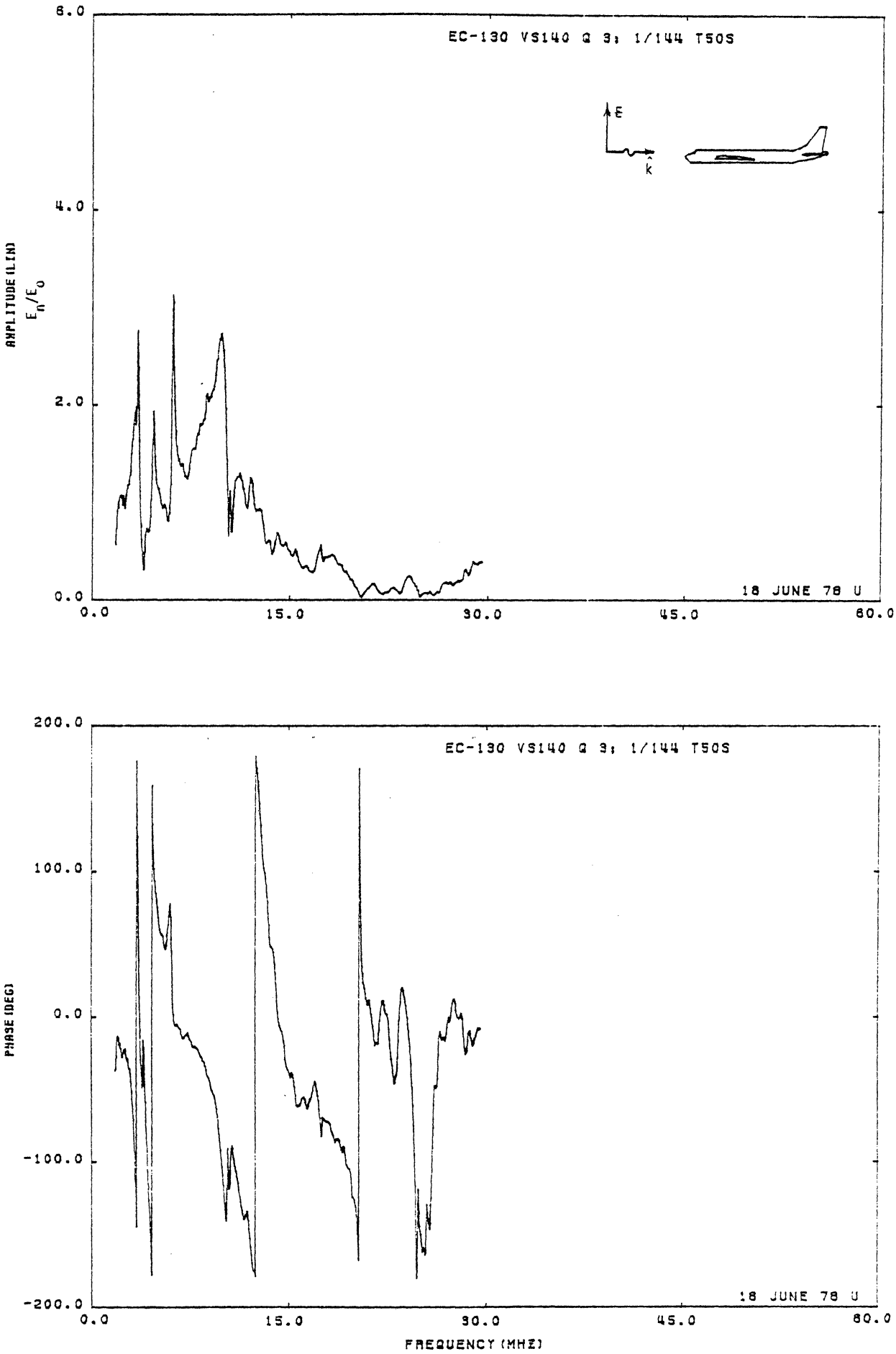

Figure 50S. Charge at STA:VS140, Excitation 3, 1/144 Model.

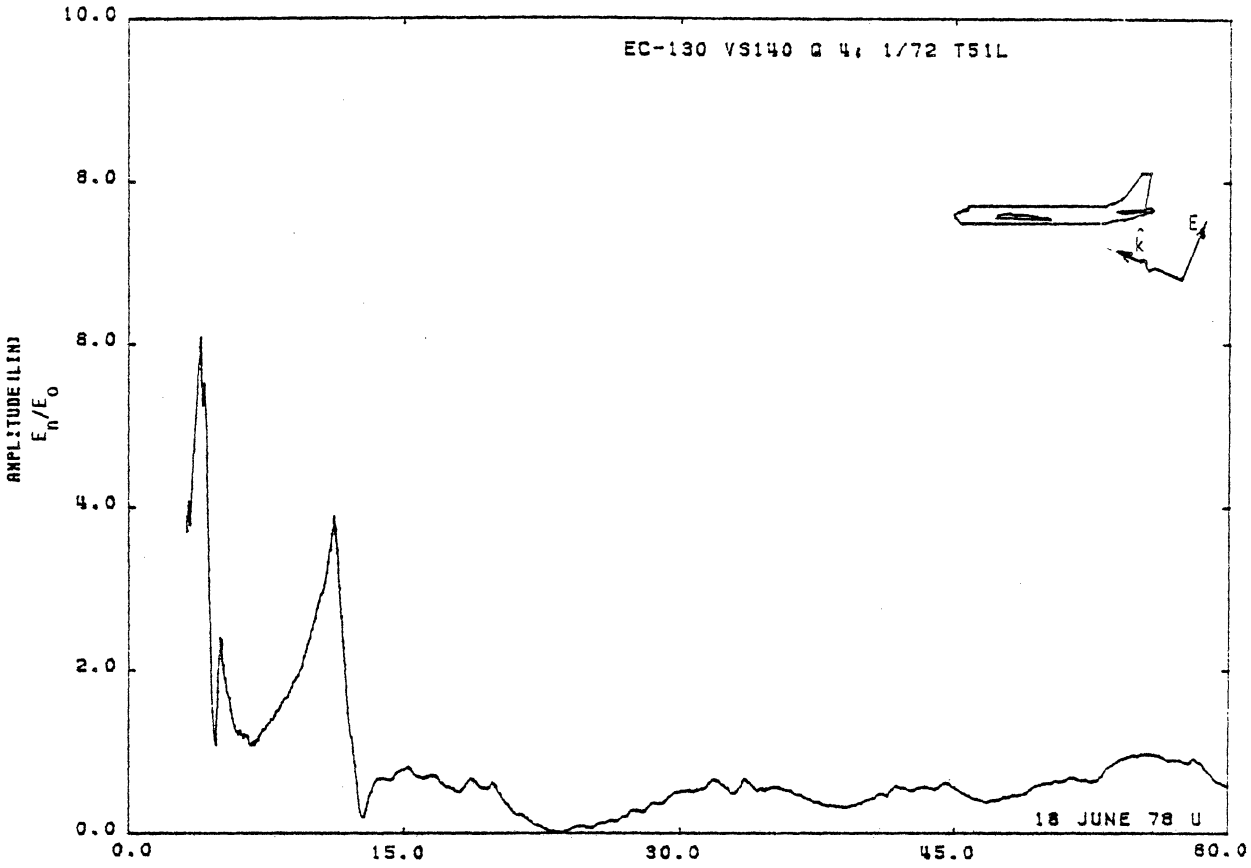

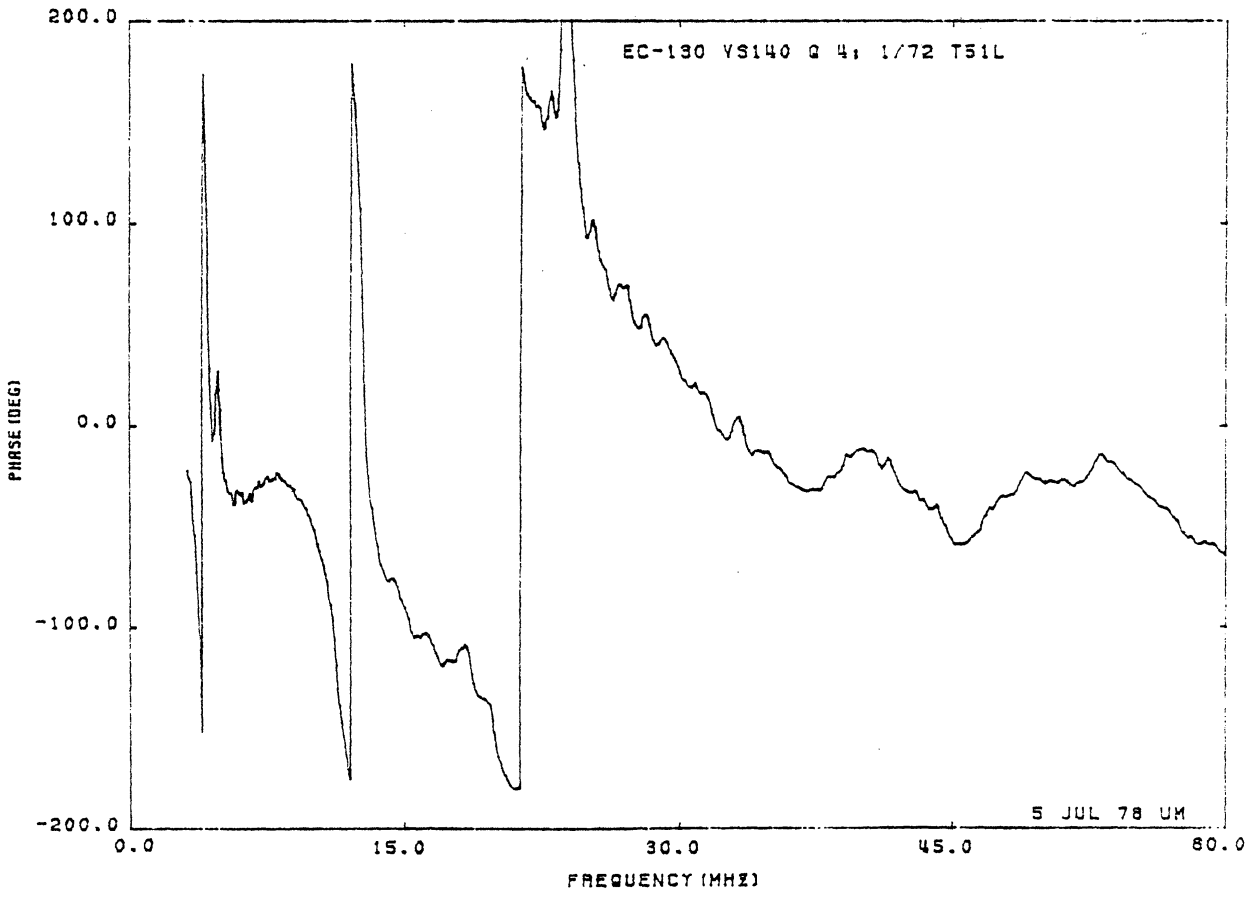

Figure 51L. Charge at STA:VS140, Excitation 4, 1/72 Model.

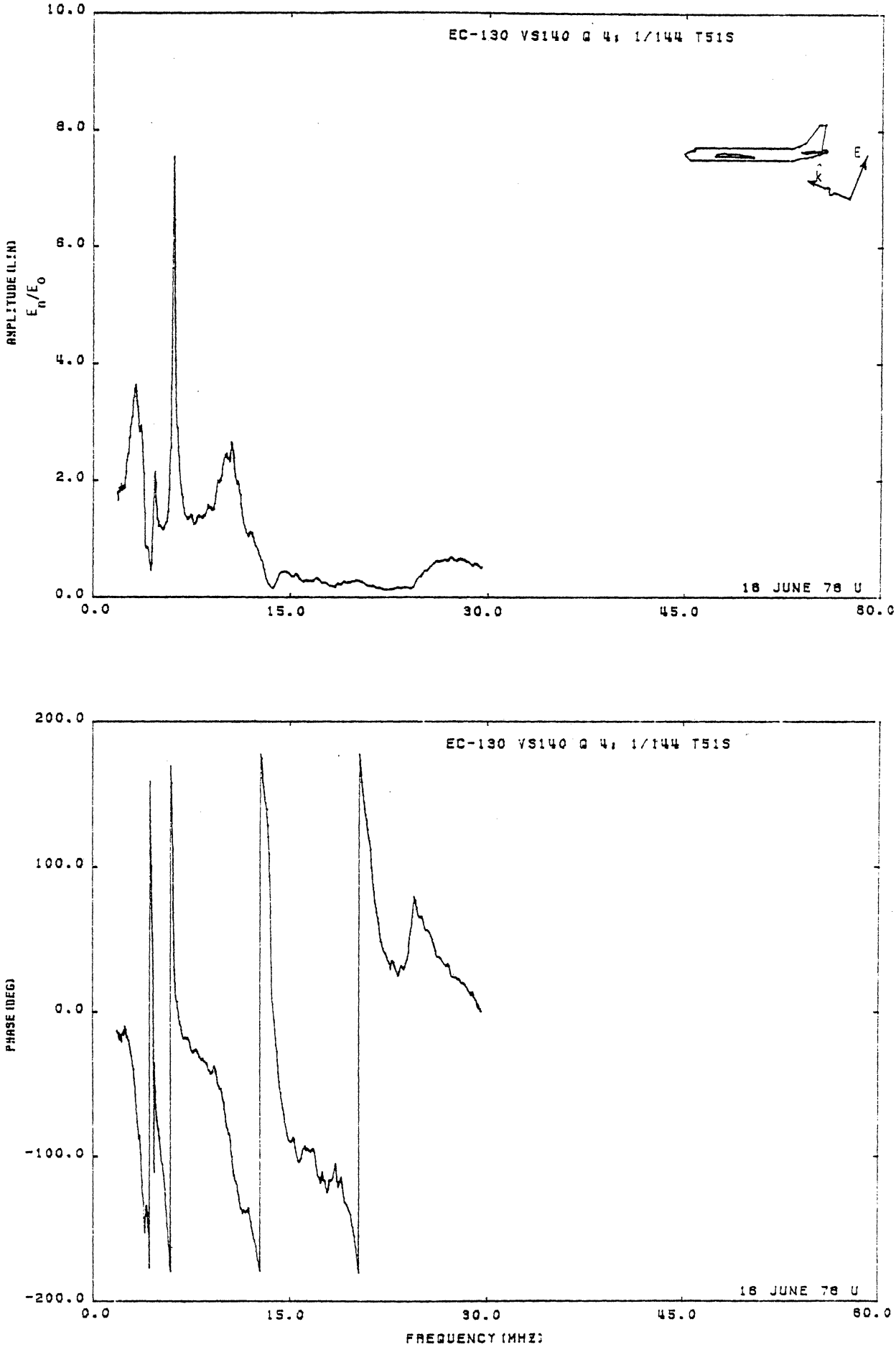

Figure 51S. Charge at STA:VS140, Excitation 4, 1/144 Model.

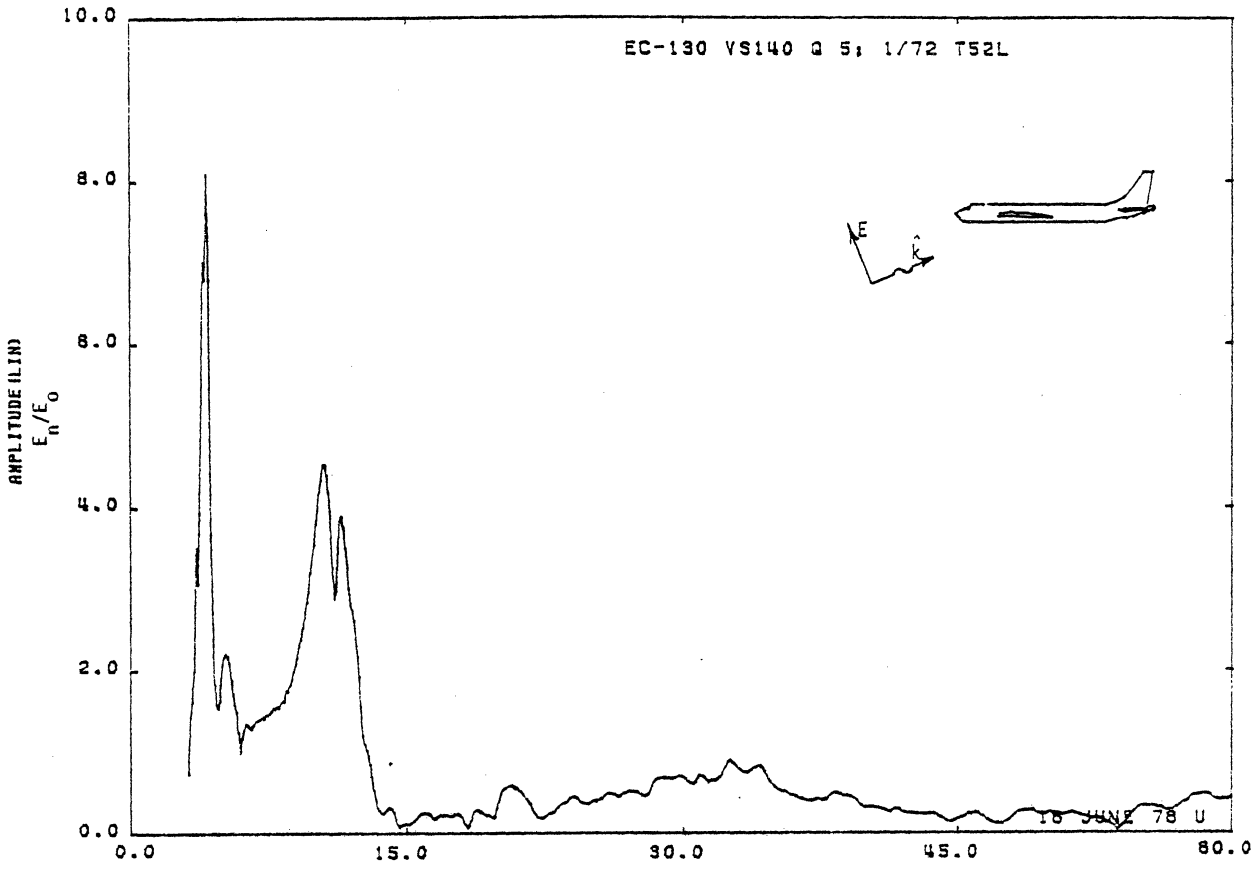

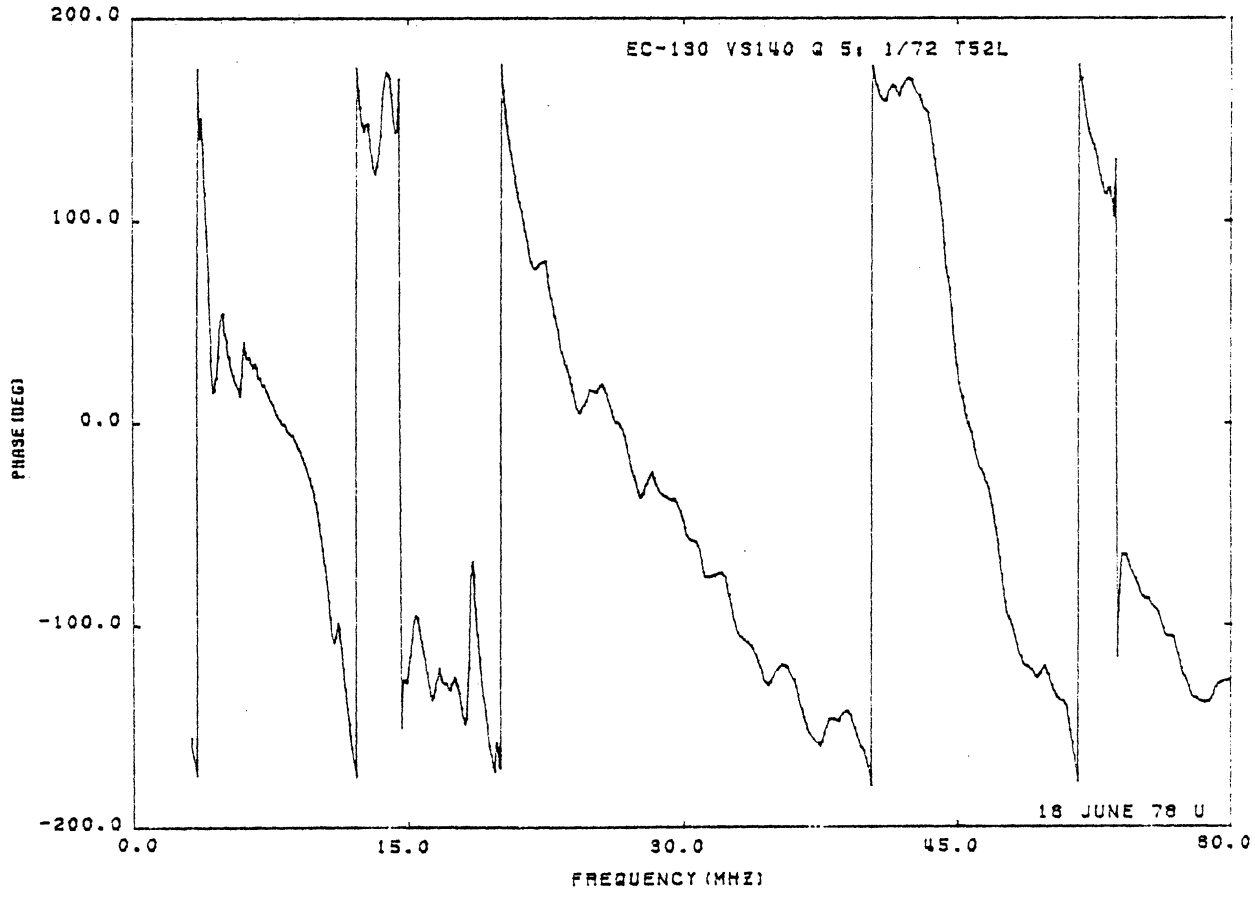

Figure 52L. Charge at STA:VS140, Excitation 5, 1/72 Model.

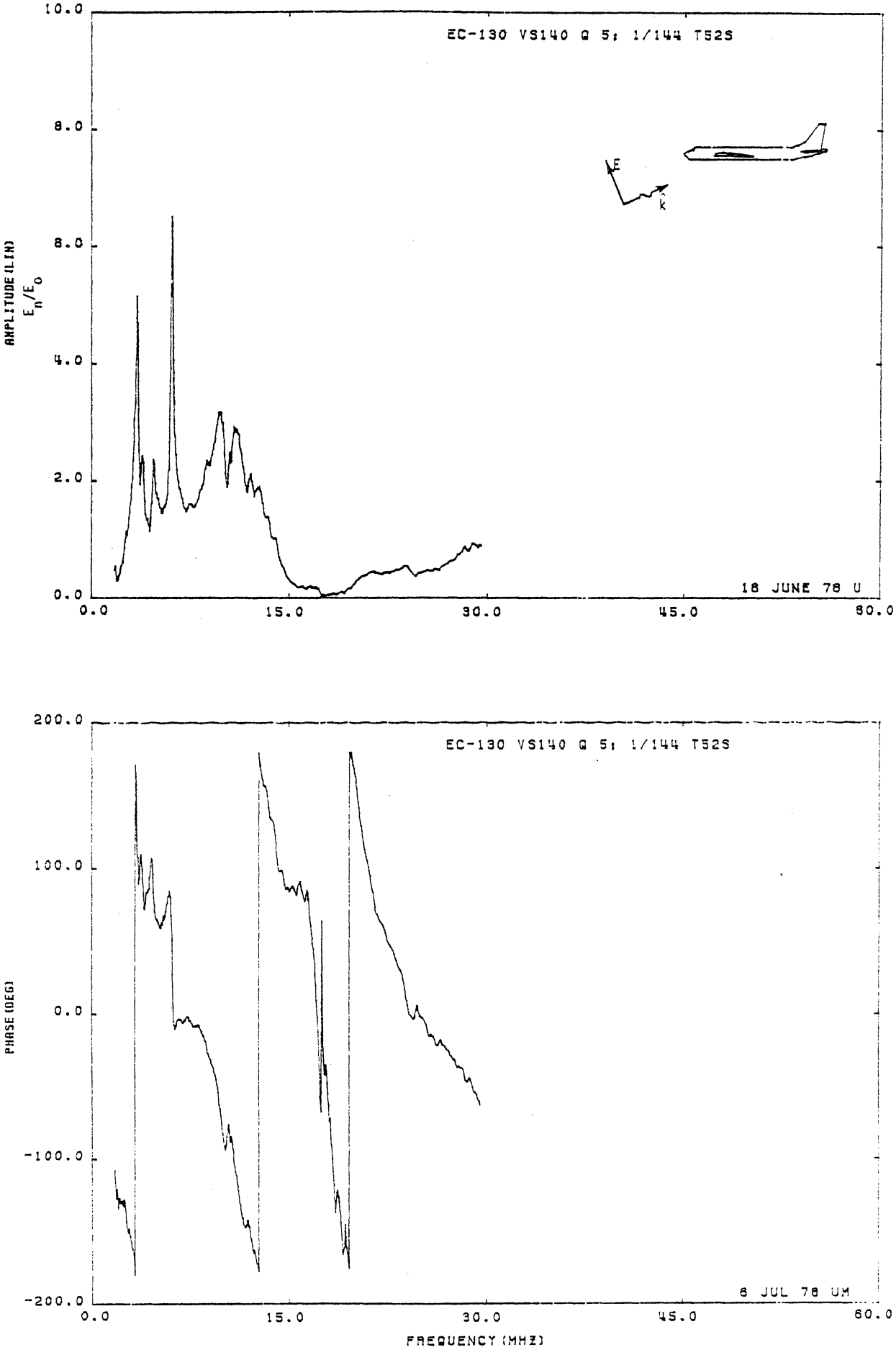

Figure 52S. Charge at STA:VS140, Excitation 5, 1/144 Model.

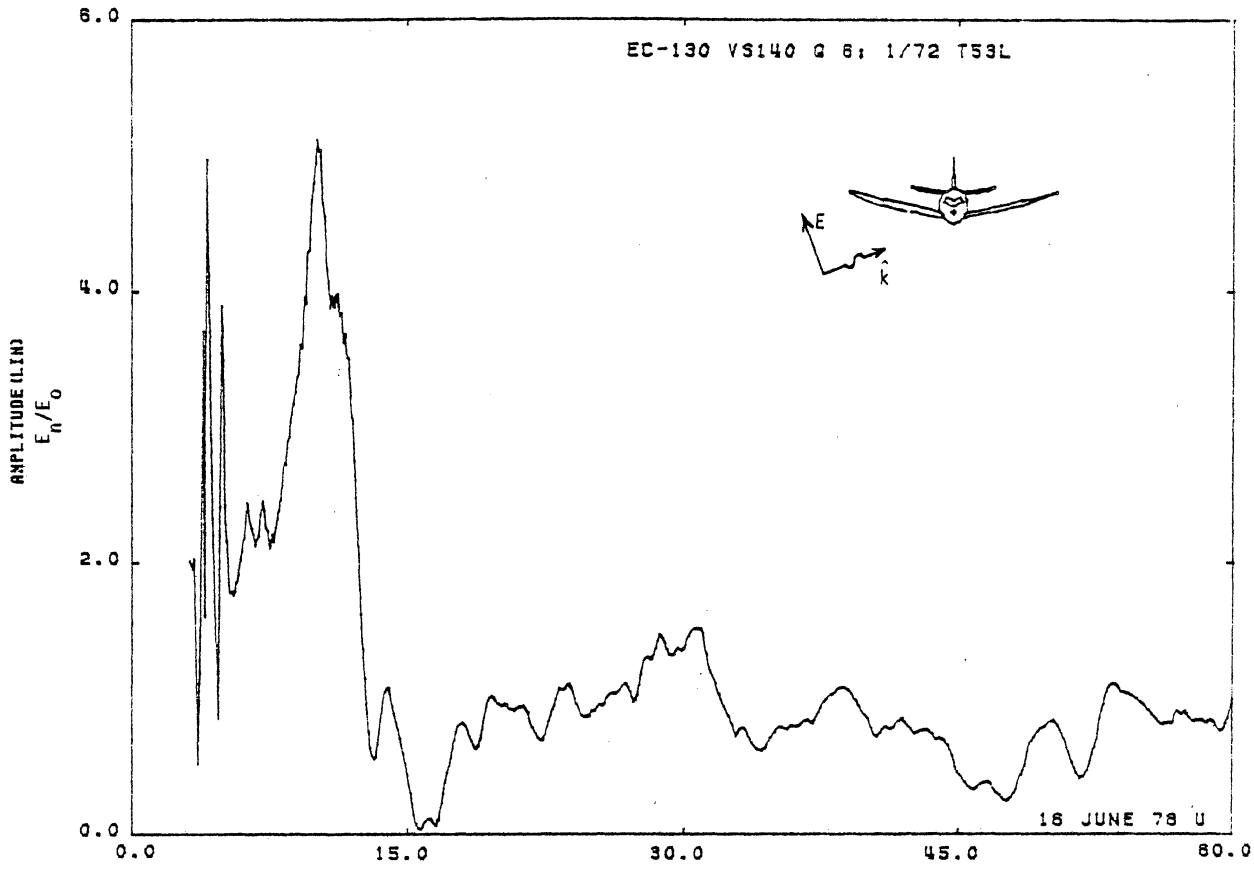

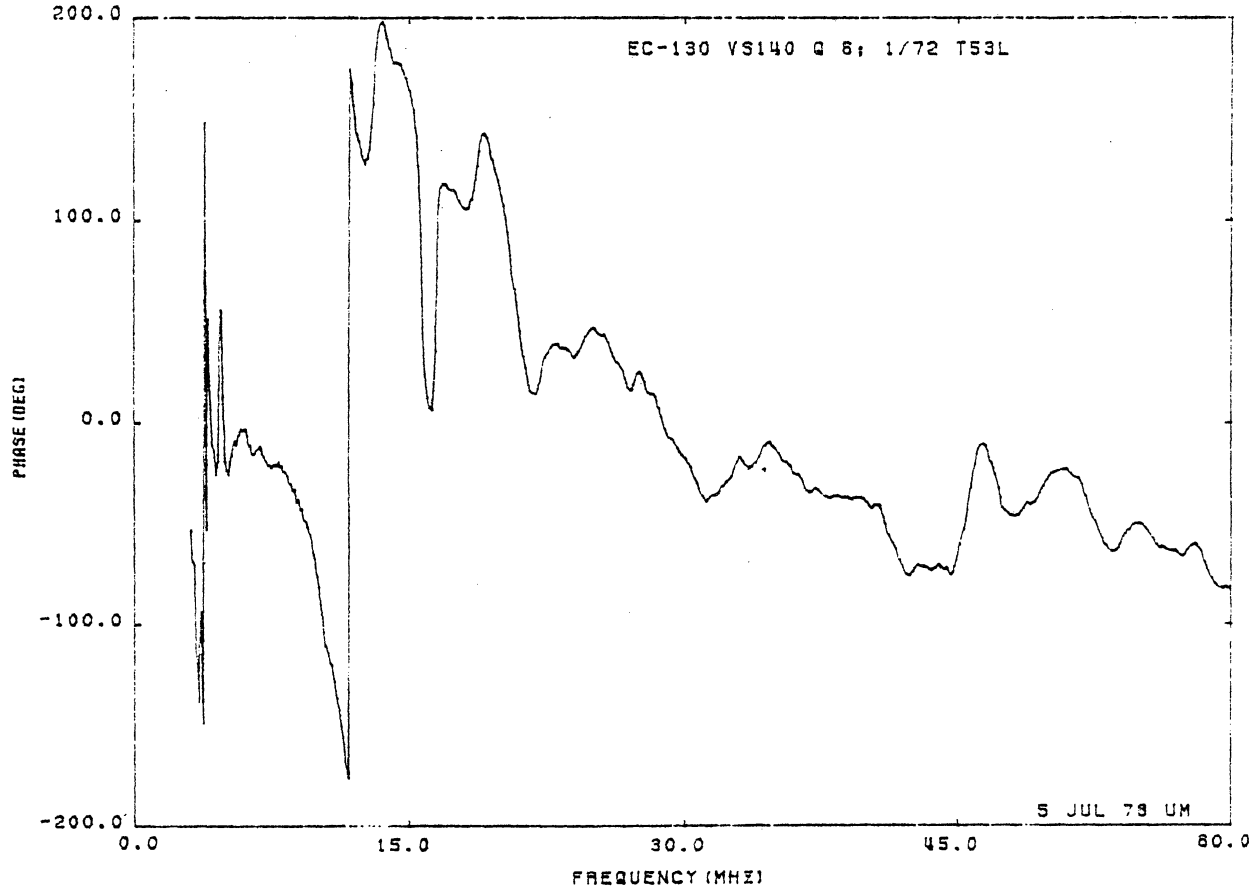

Figure 53L. Charge at STA:VS140, Excitation 6, 1/72 Model.

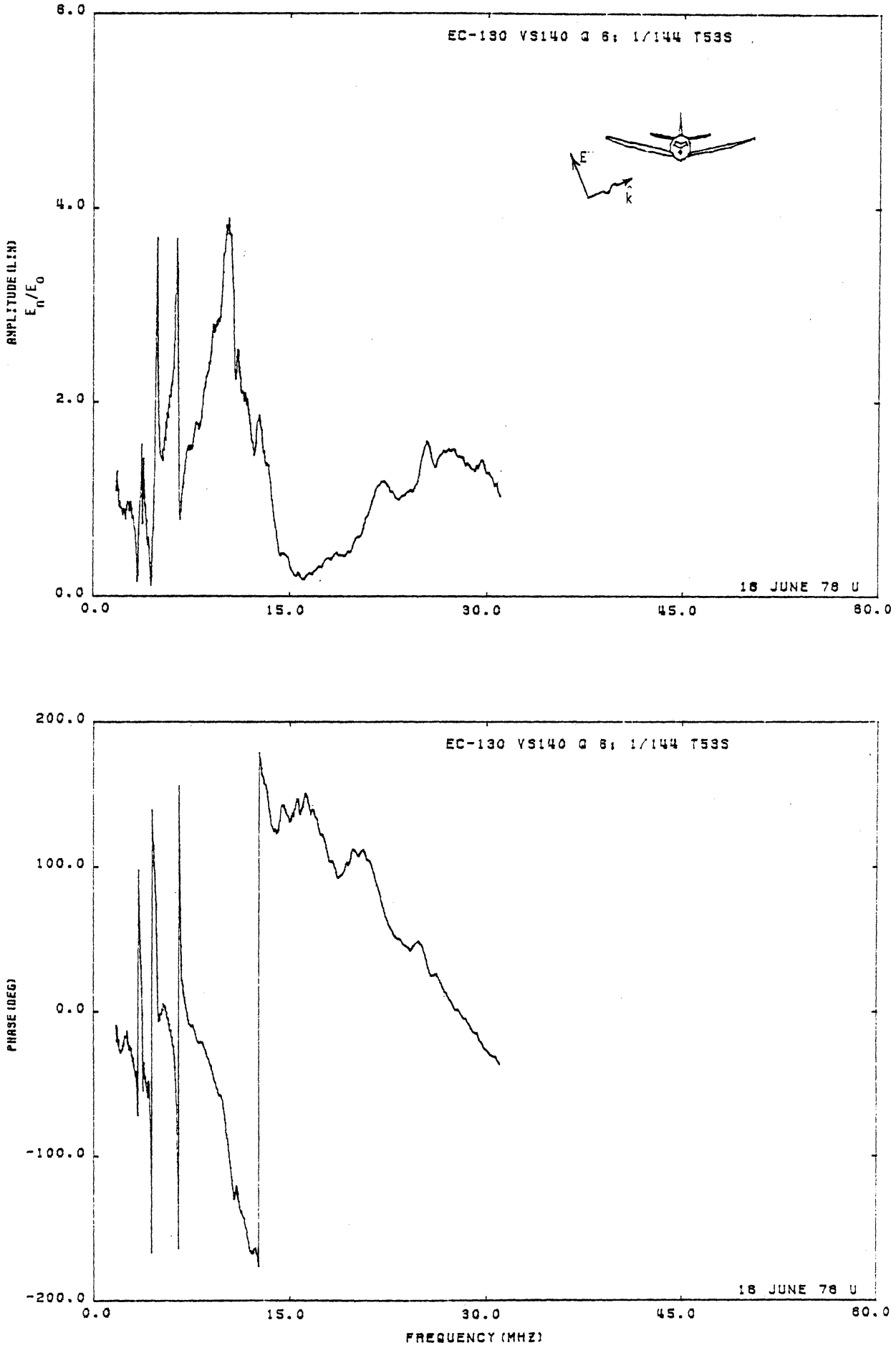

Figure 53S. Charge at STA:VS140, Excitation 6, 1/144 Model.

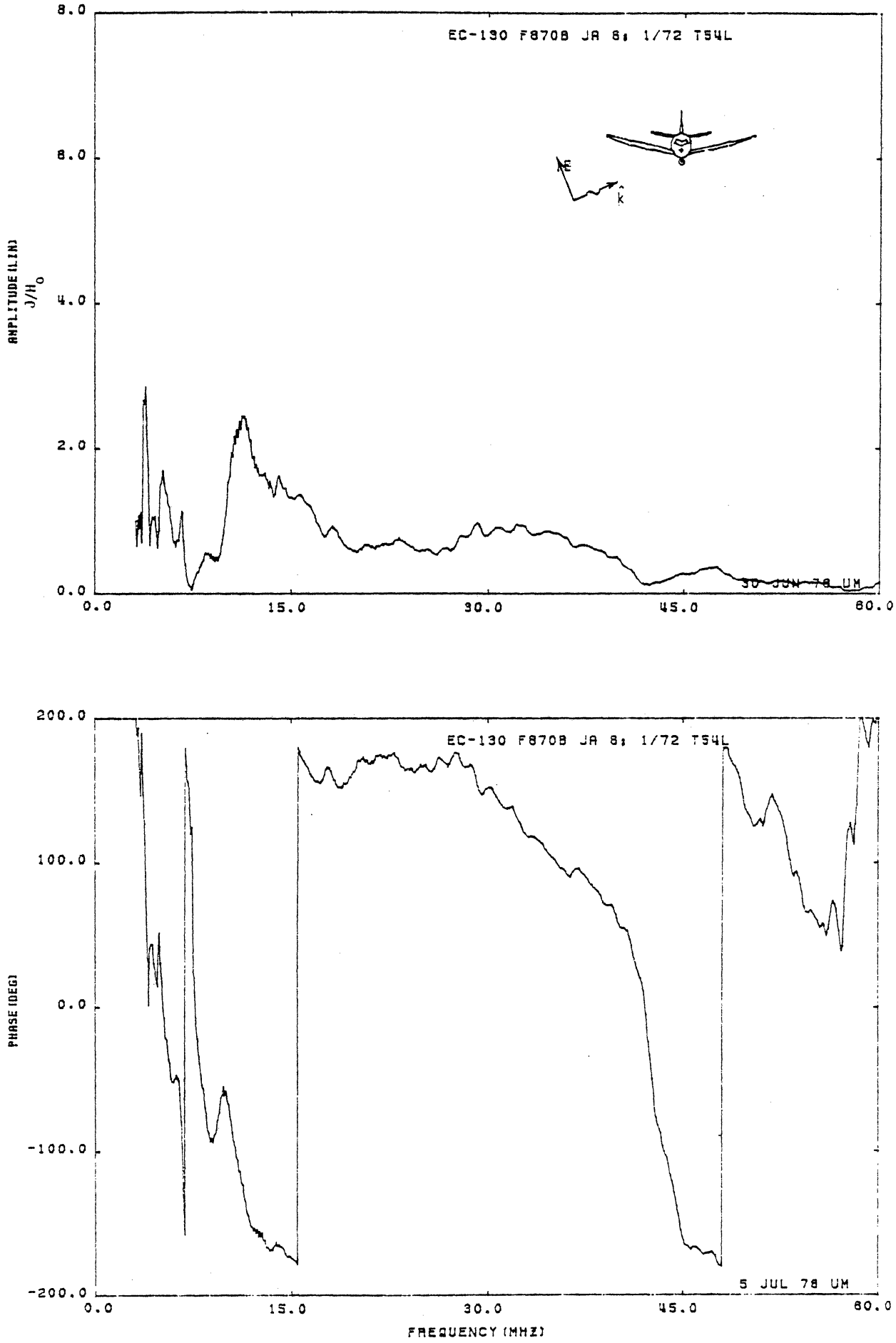

Figure 54L. Axial Current at STA:F870B, Excitation 6, 1/72 Model.

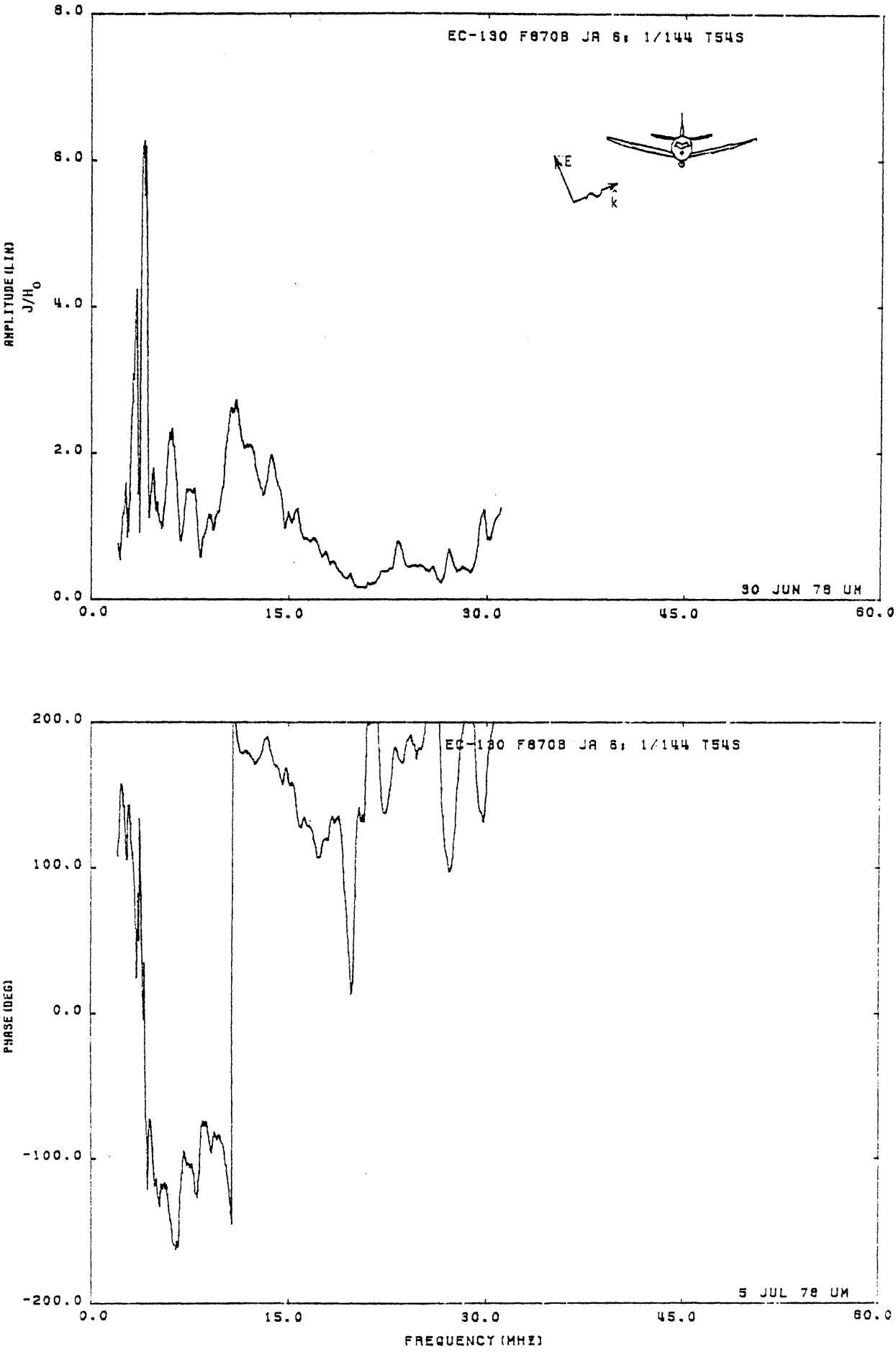

Figure 54S. Axial Current at STA:F870B, Excitation 6, 1/144 Model.

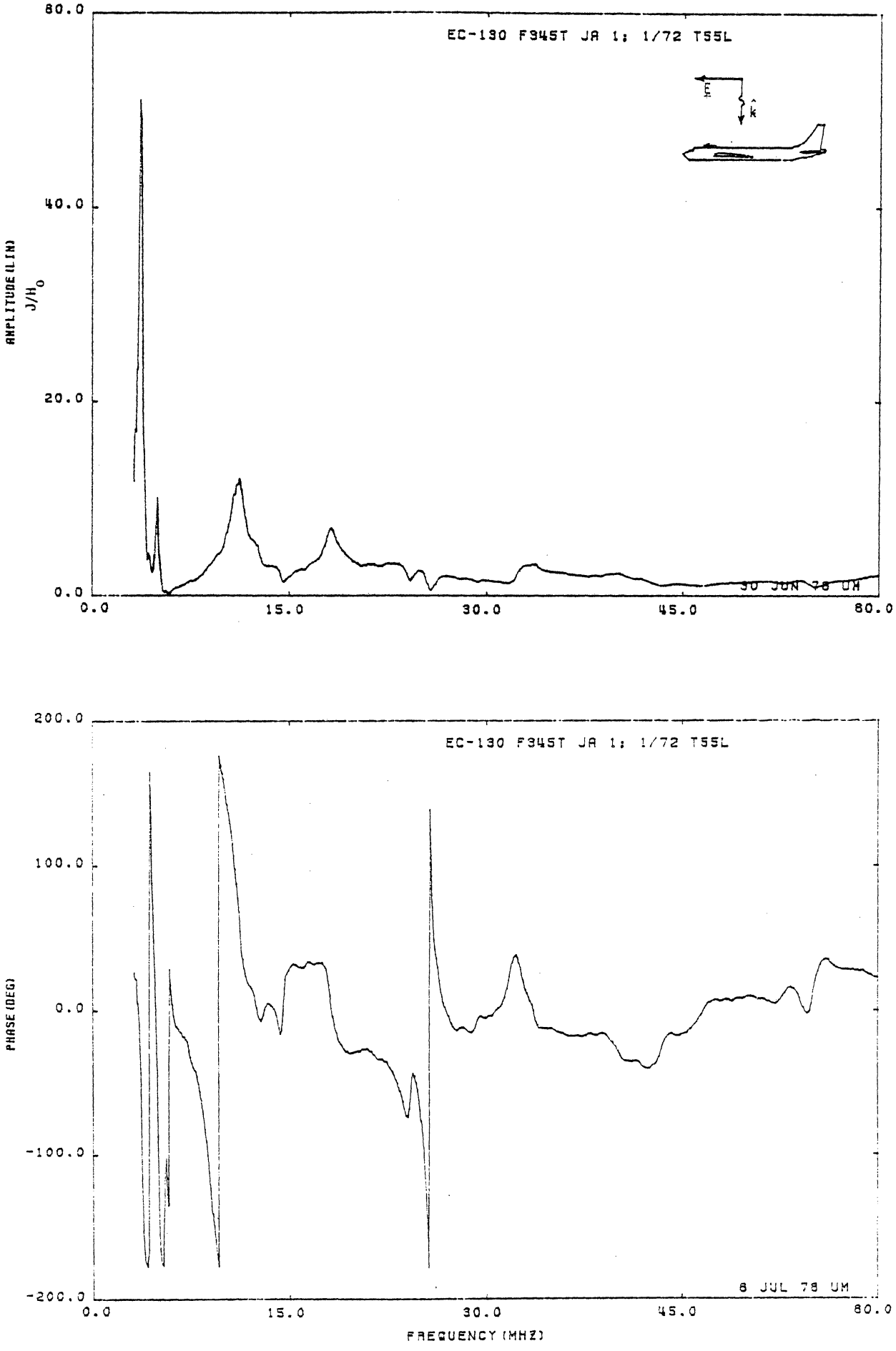

Figure 55L. Axial Current at STA:F345T, Excitation 1, 1/72 Model. (Repeated Measurement, see Table 4)

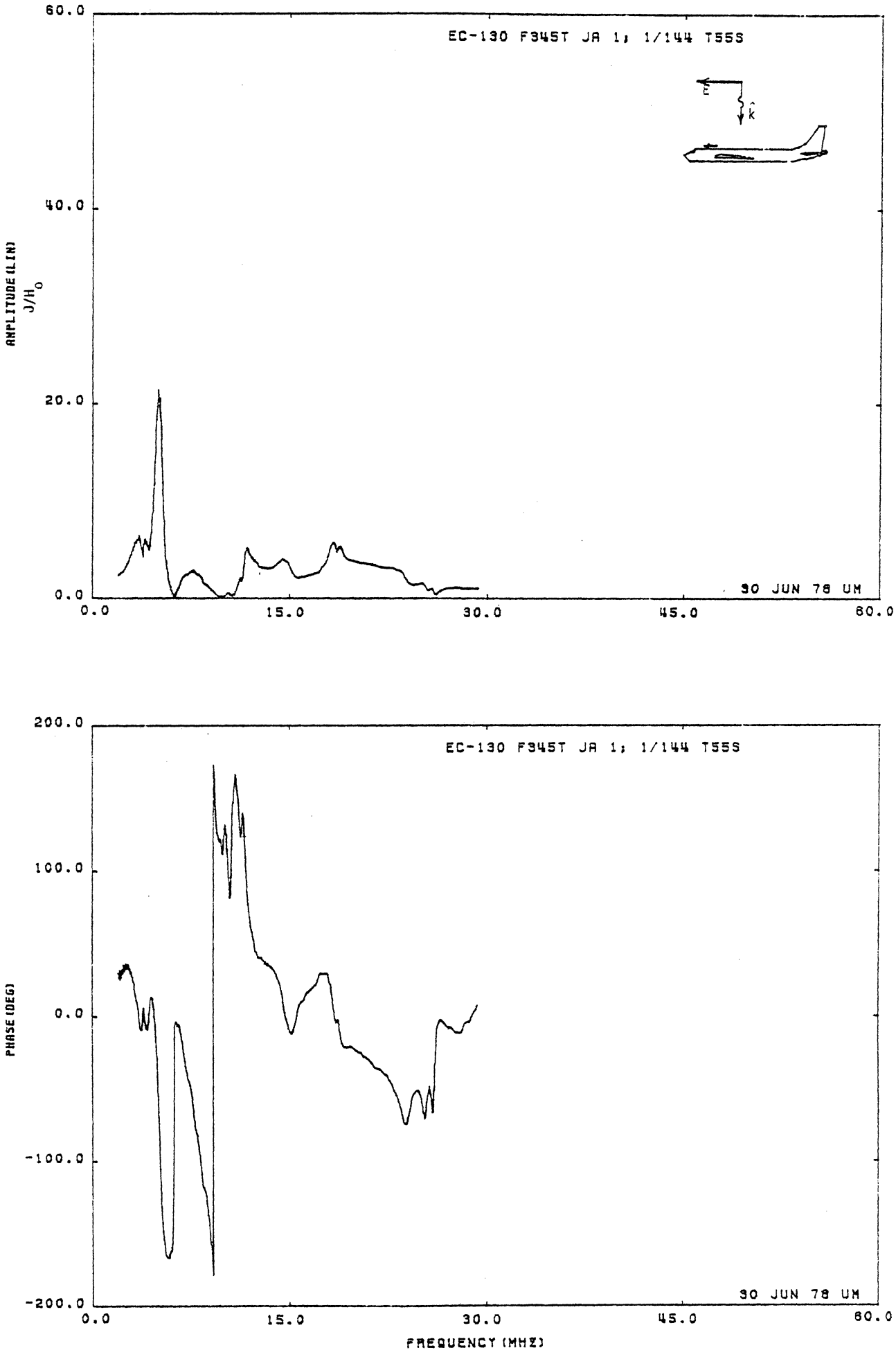

Figure 55S. Axial Current at STA:F345T, Excitation 1, 1/144 Model. (Repeated Measurement, see Table 4)

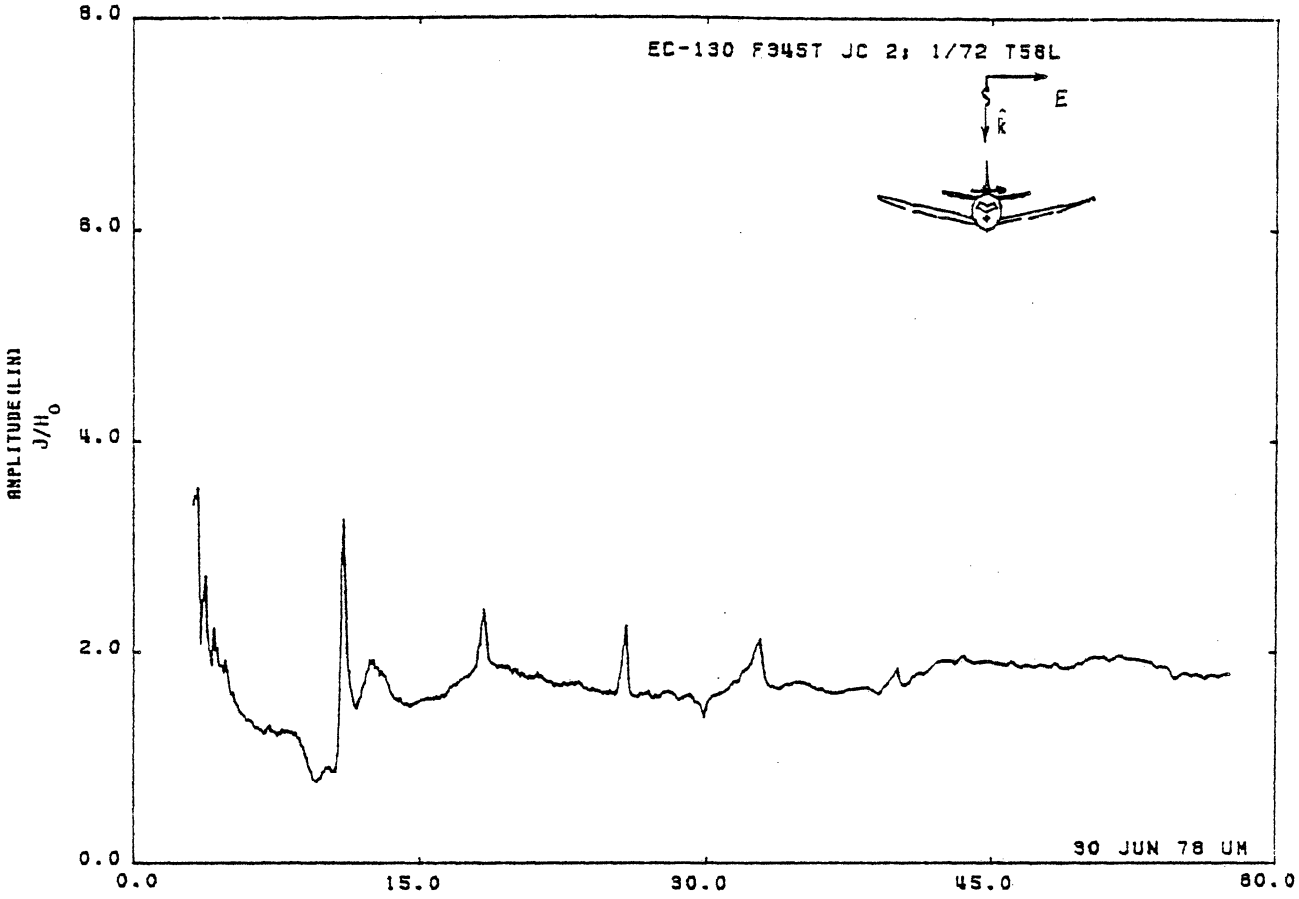

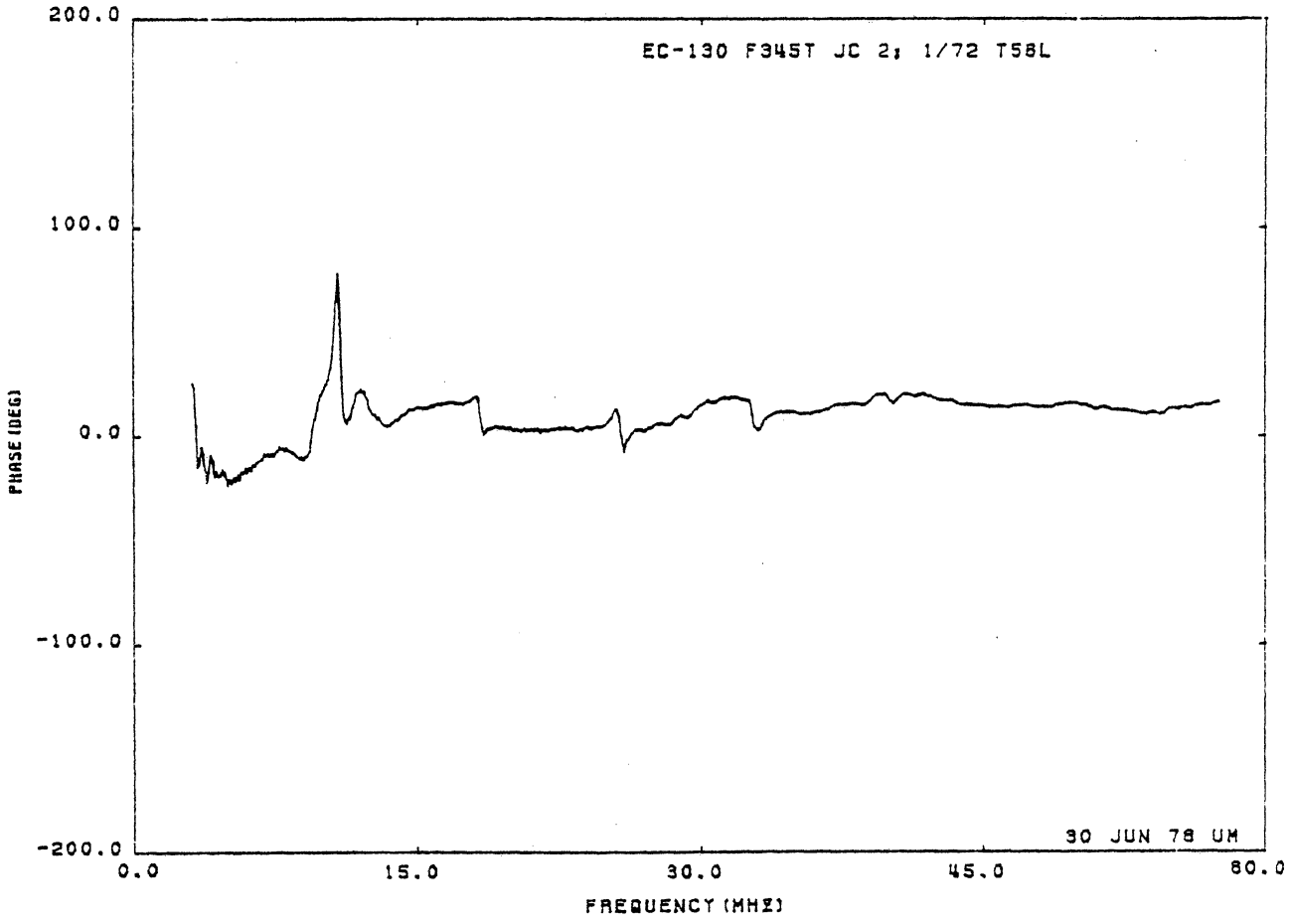

Figure 56L. Circumferential Current at STA:F345T, Excitation 2, 1/72 Model. (Repeated Measurement, see Table 4)

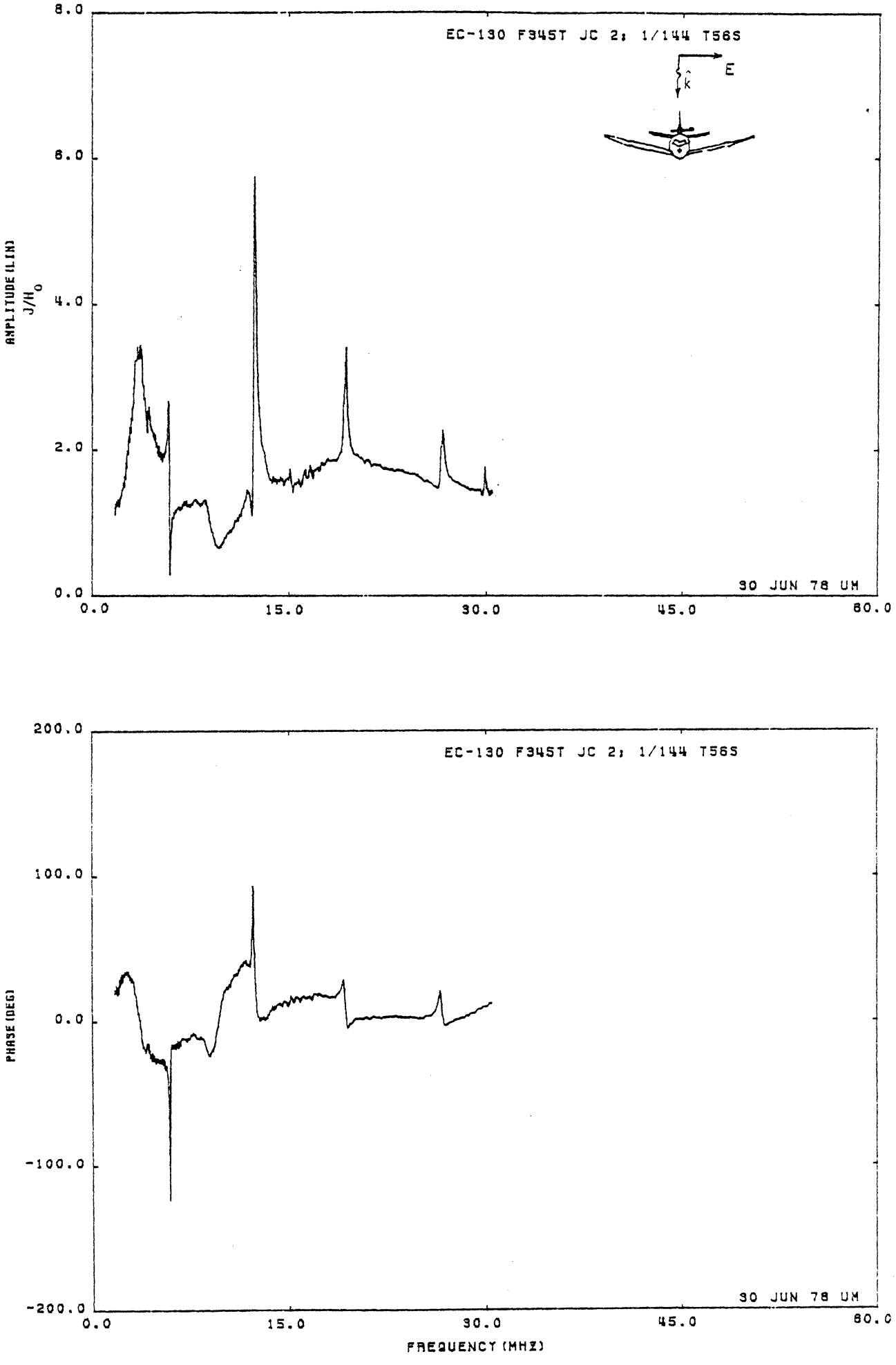

Figure 56S. Circumferential Current at STA:F345T, Excitation 2, 1/144 Model. (Repeated Measurement, see Table 4)

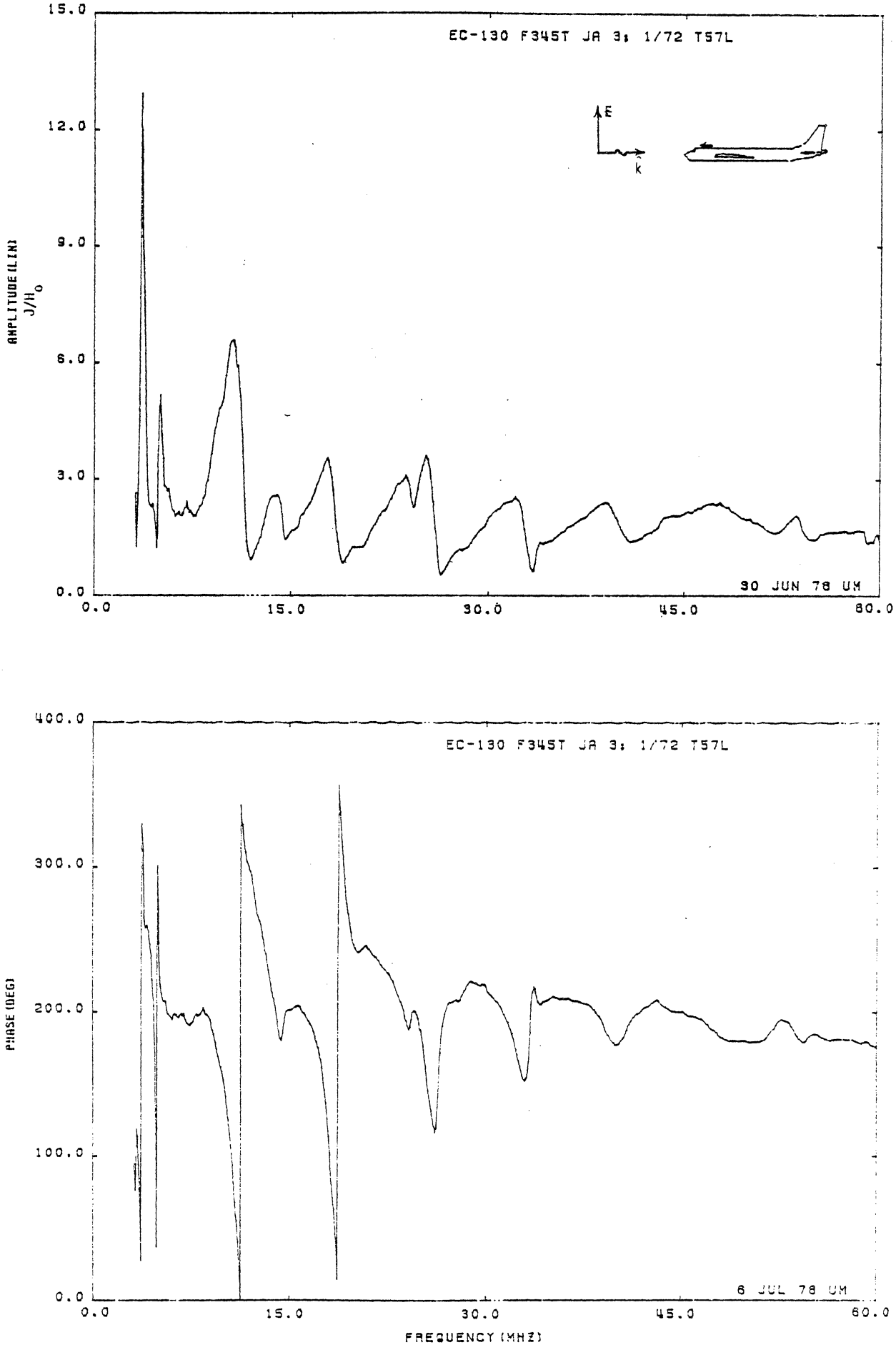

Figure 57L. Axial Current at STA:F345T, Excitation 3, 1/72 Model.
(Repeated Measurement, see Table 4)

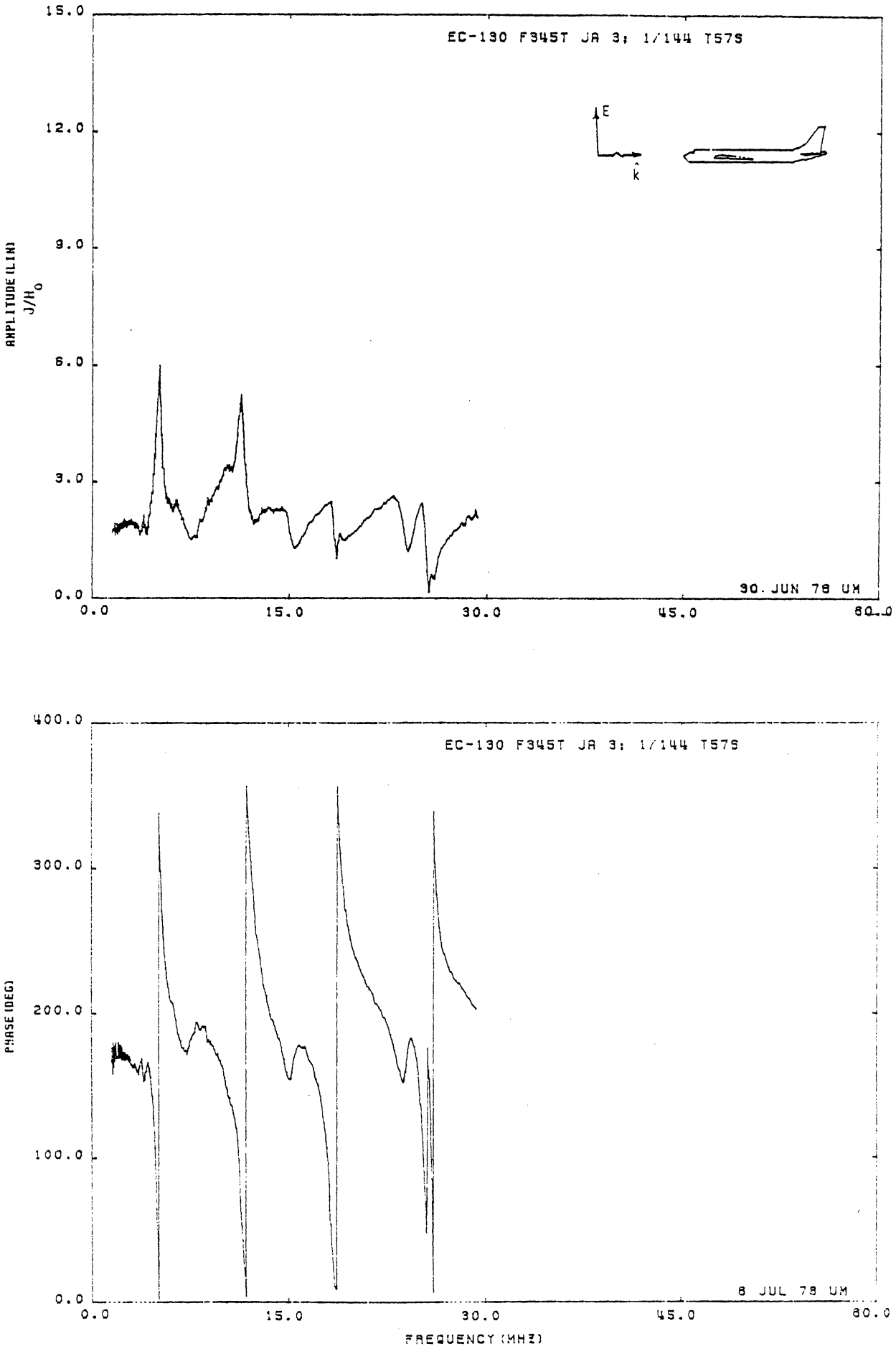

Figure 57S. Axial Current at STA:F345T, Excitation 3, 1/72 Model. (Repeated Measurement, see Table 4)

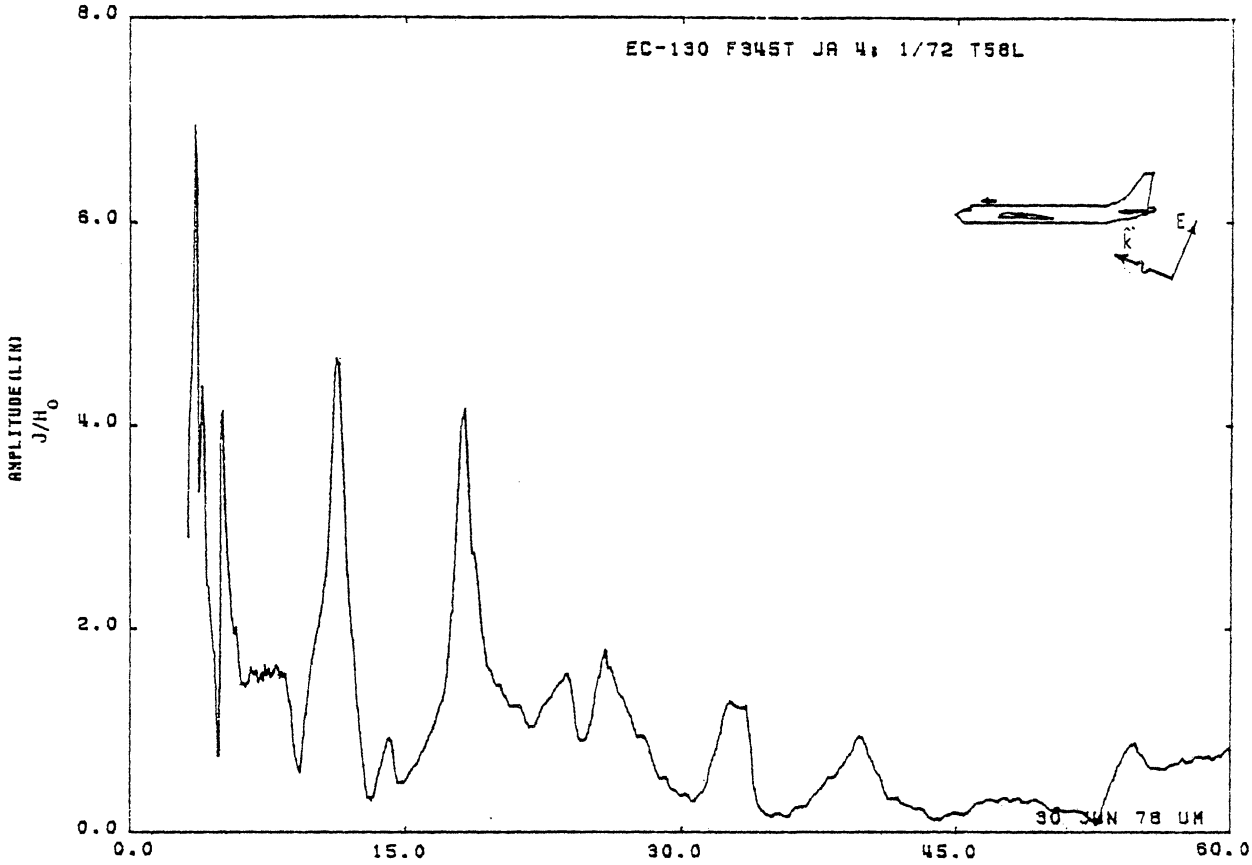

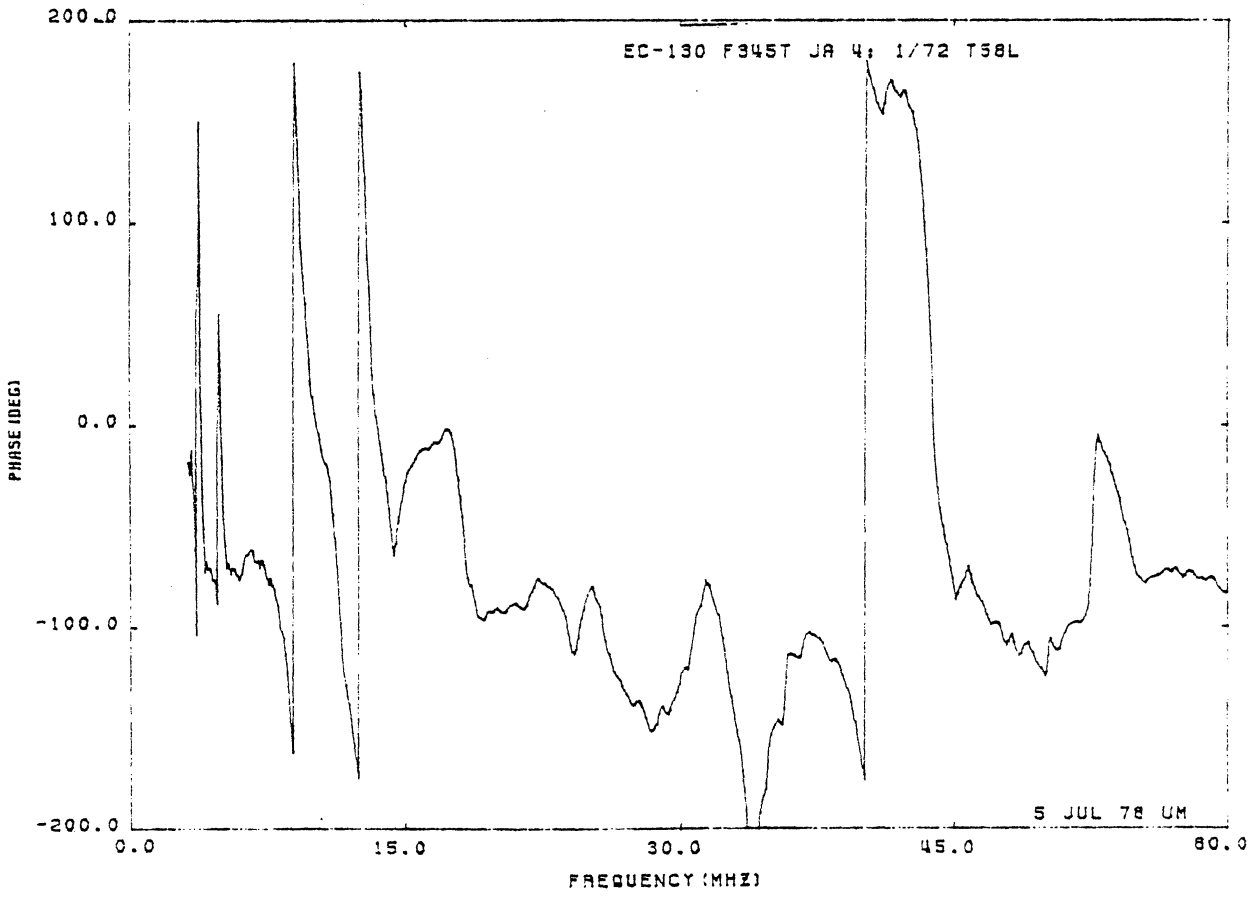

Figure 58L. Axial Current at STA:F345T, Excitation 4, 1/72 Model.
(Repeated Measurement, see Table 4)

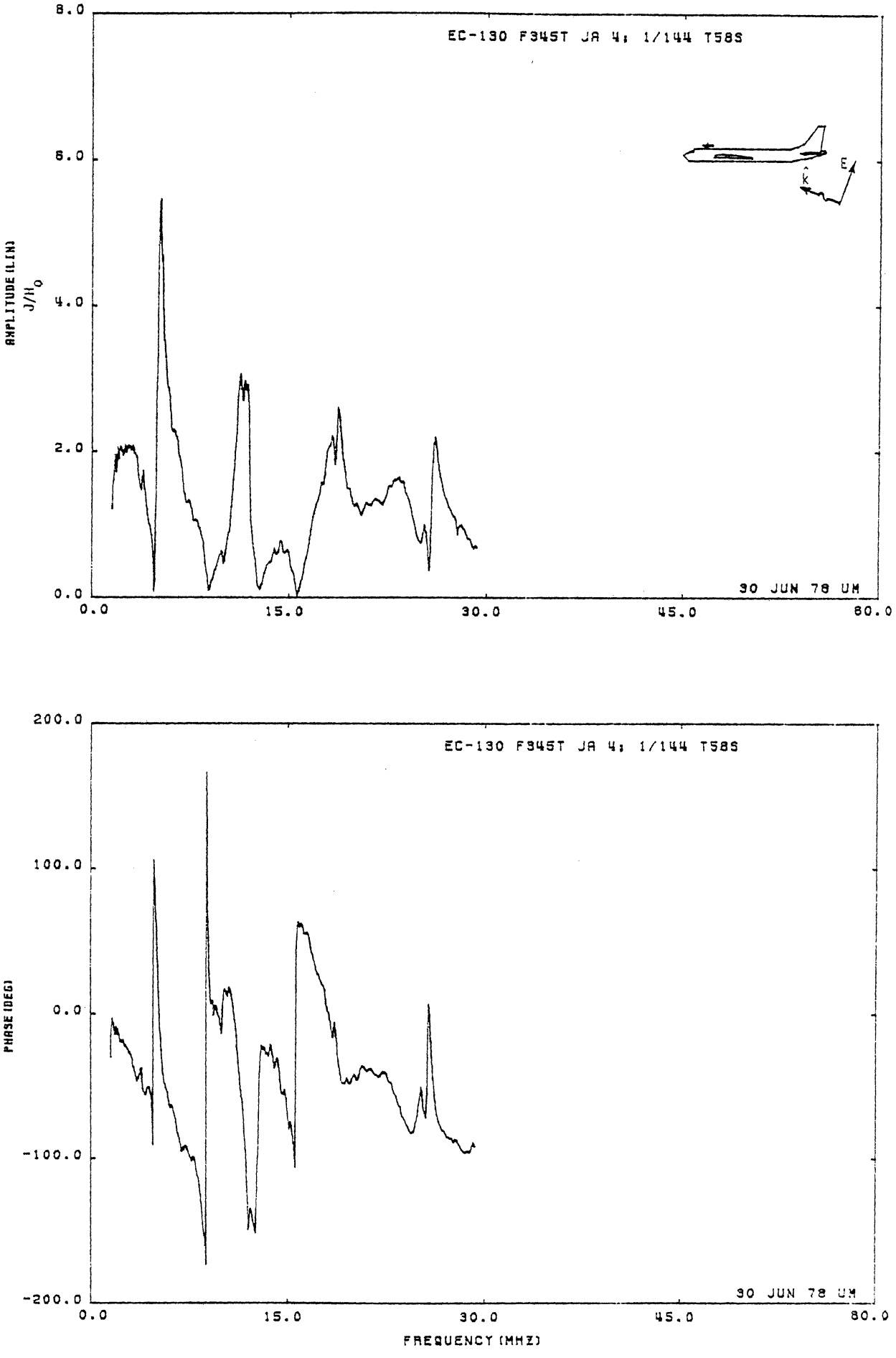

Figure 58S. Axial Current at STA:F345T, Excitation 4, 1/144 Model.
(Repeated Measurement, see Table 4)

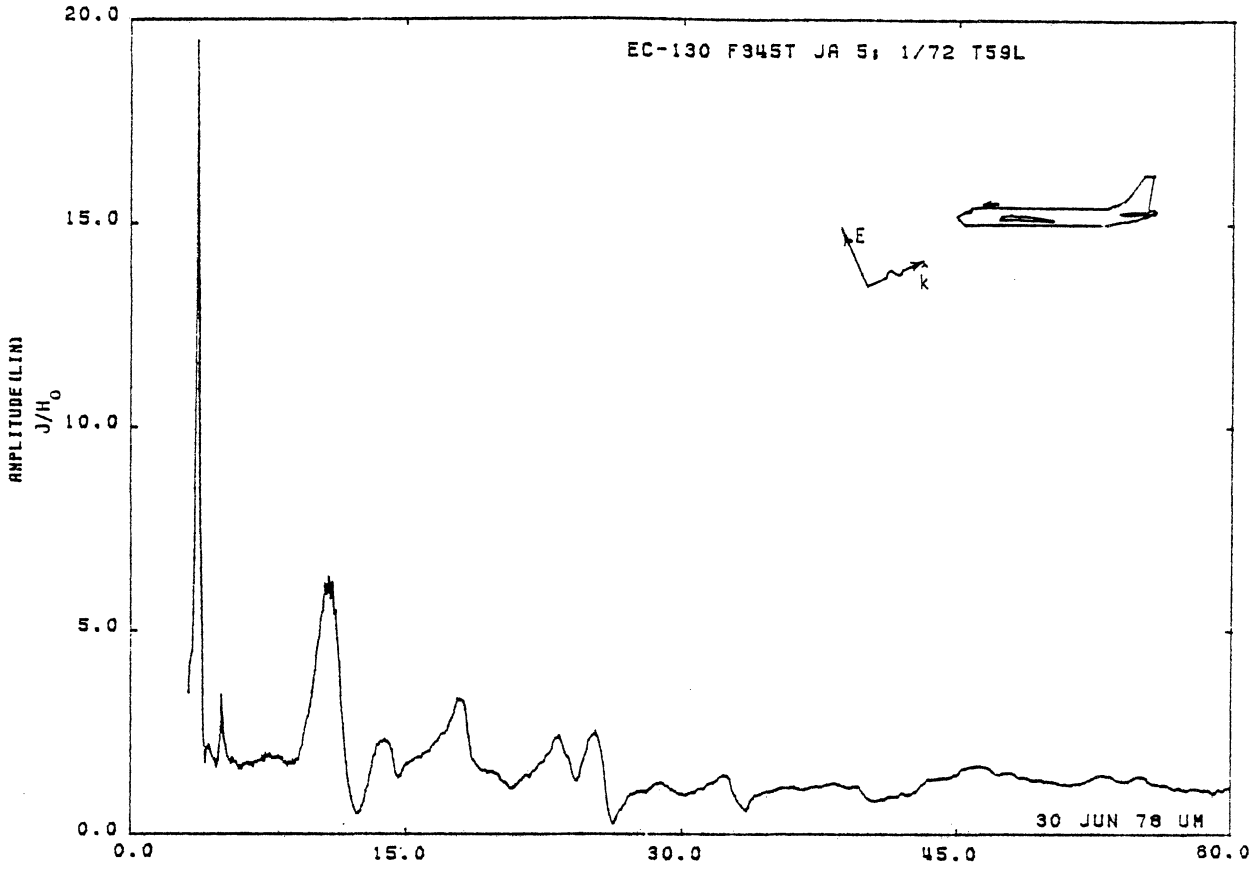

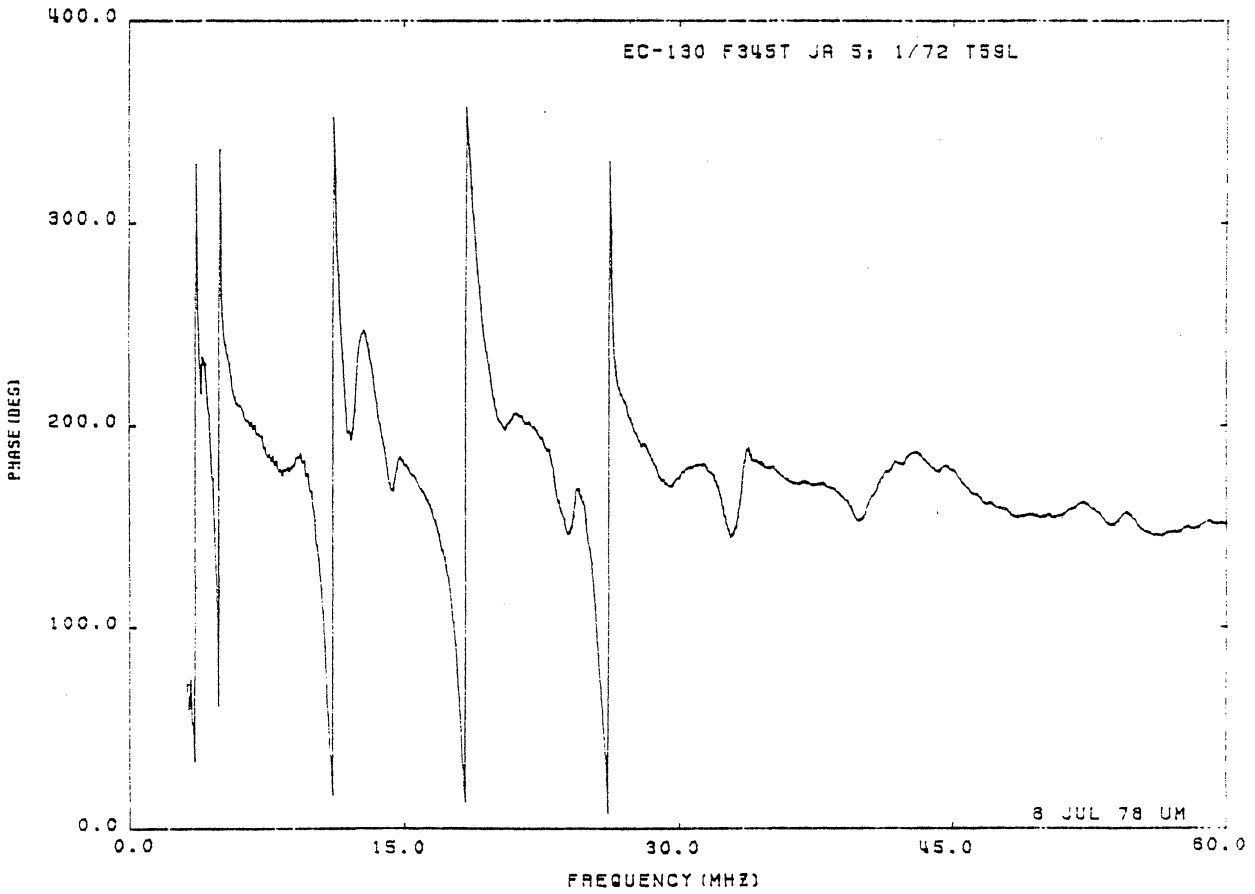

Figure 59L. Axial Current at STA:F345T, Excitation 5, 1/72 Model.
(Repeated Measurement, see Table 4)

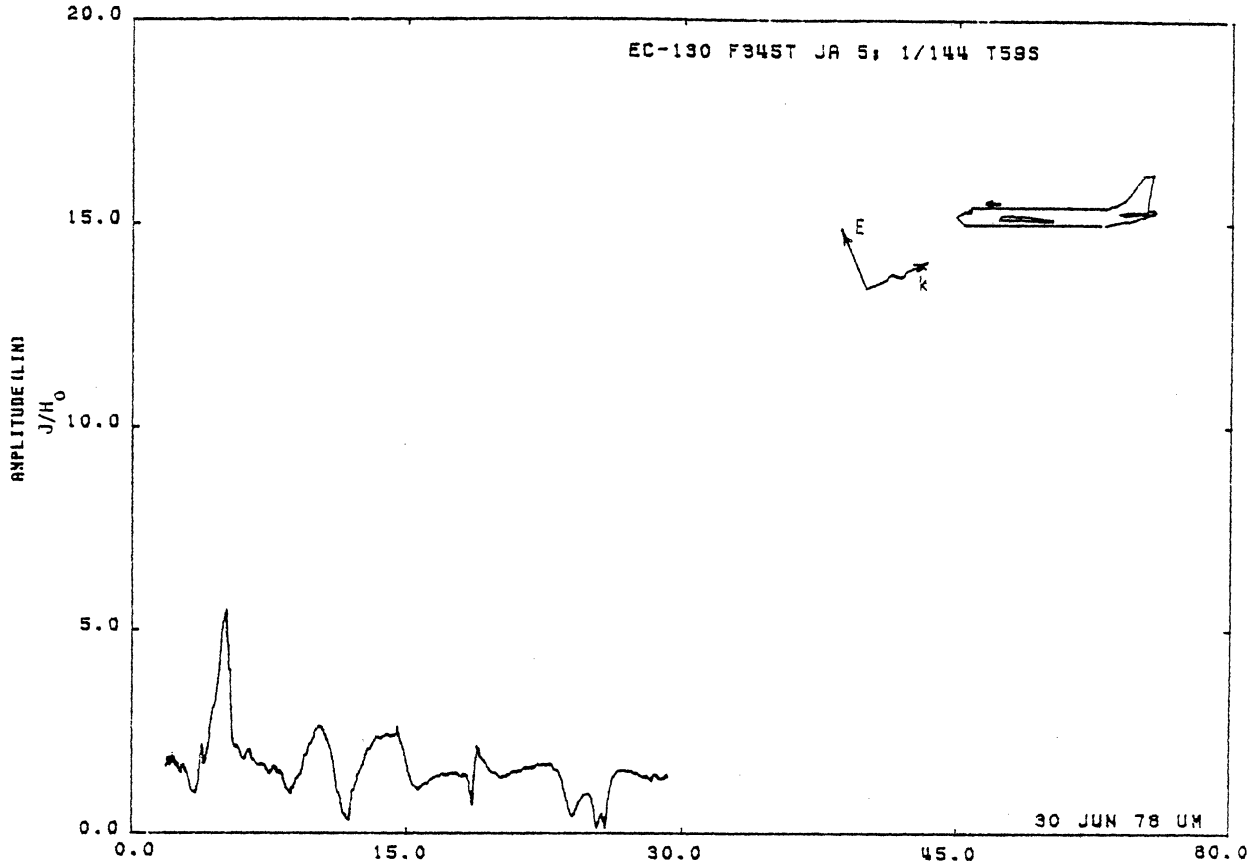

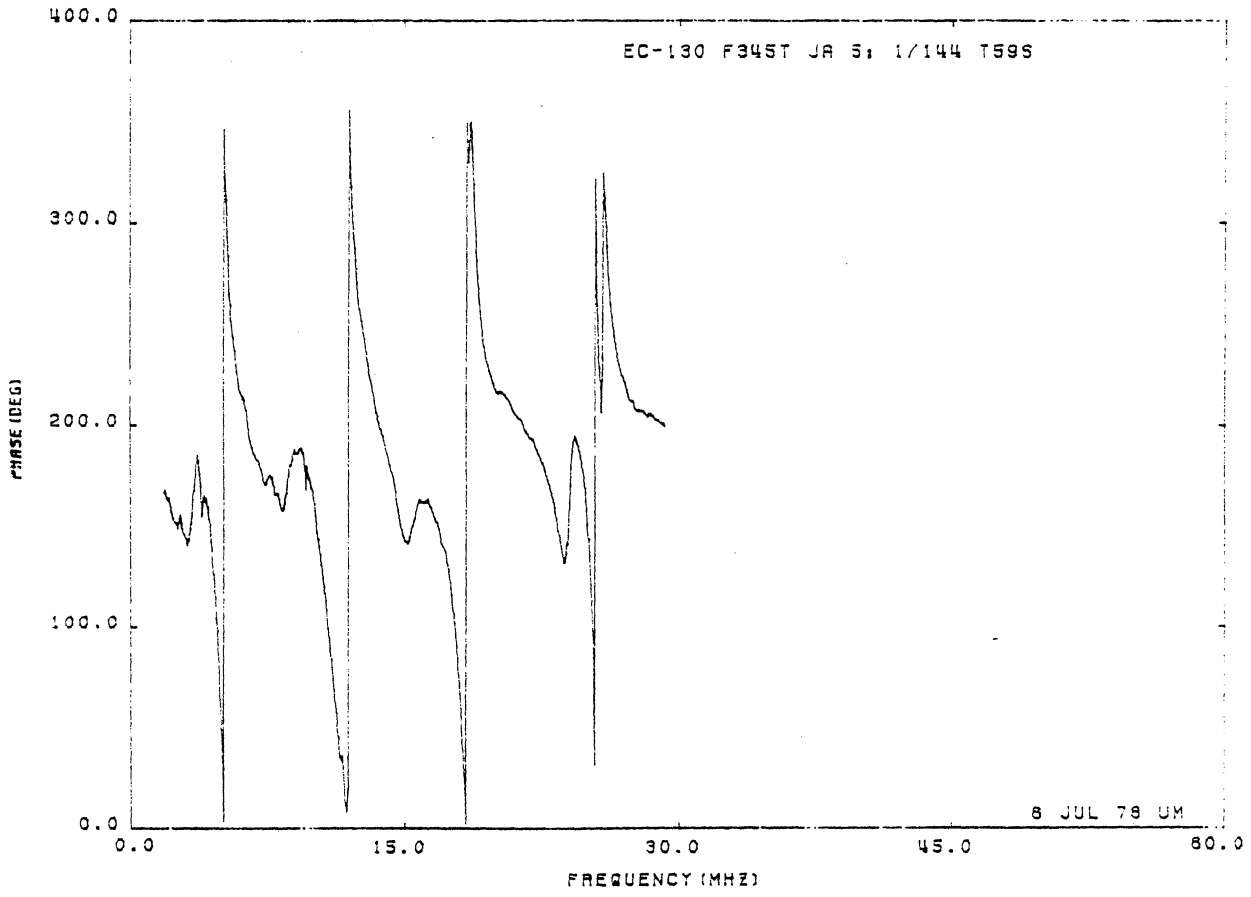

Figure 59S. Axial Current at STA:F345T, Excitation 5, 1/144 Model. (Repeated Measurement, see Table 4)

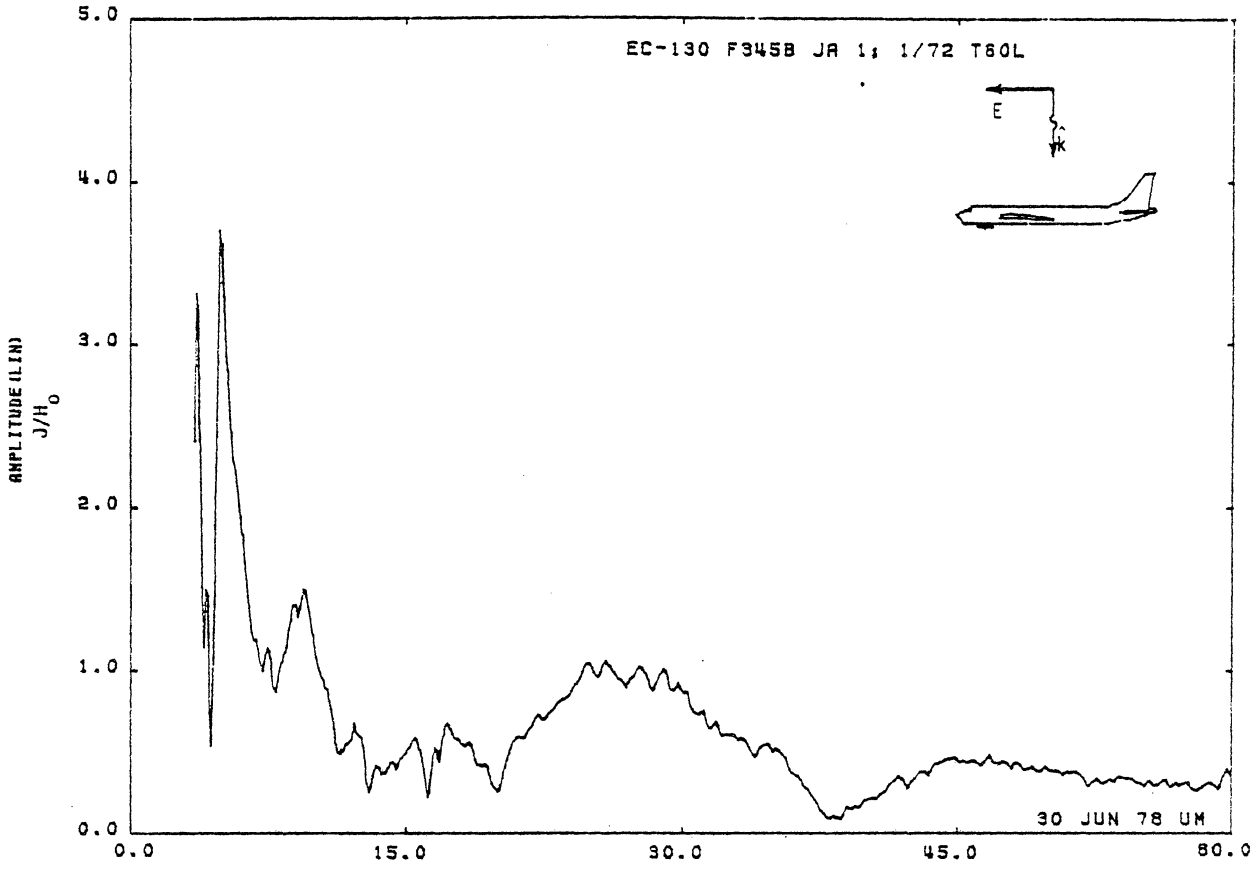

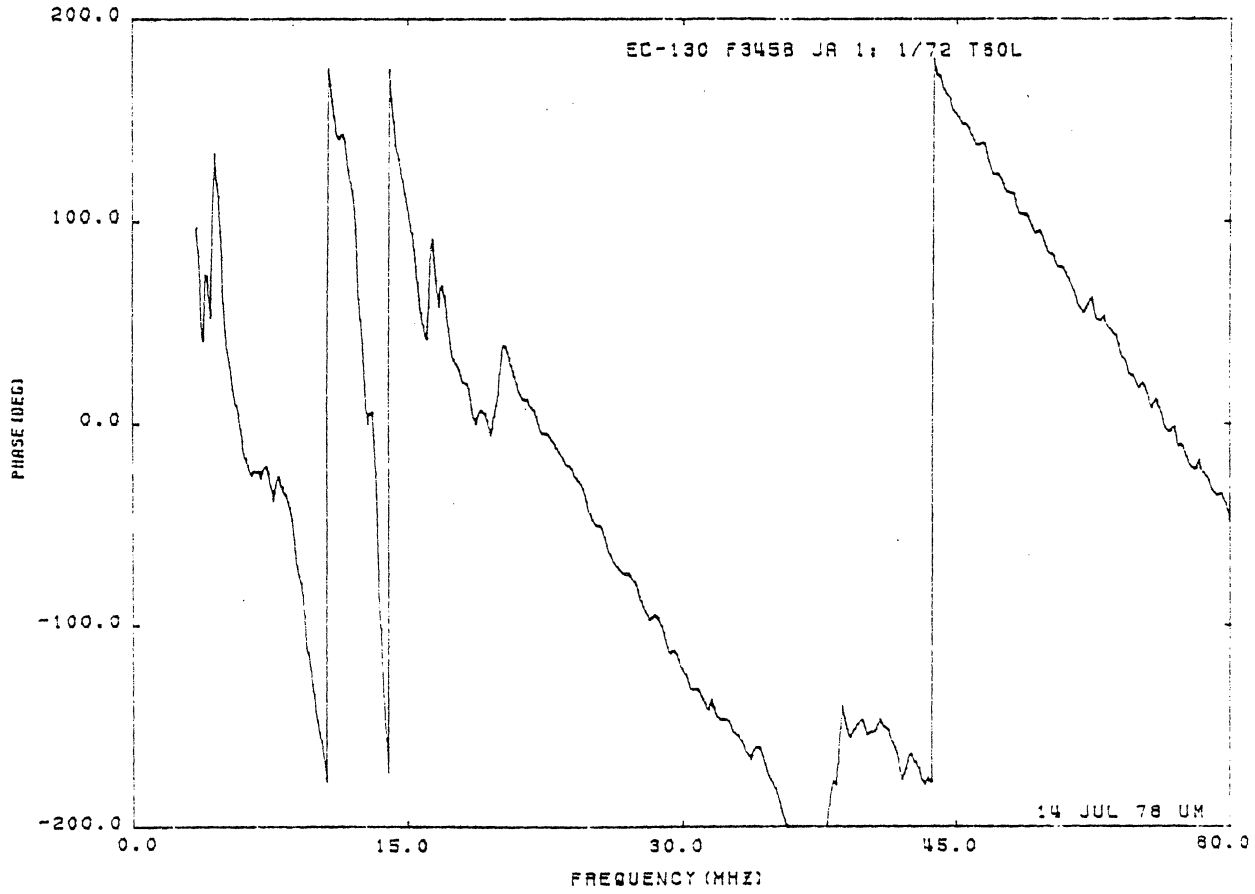

Figure 60L. Axial Current at STA:F345B, Excitation 1, 1/72 Model.
(Repeated Measurement, see Table 4)

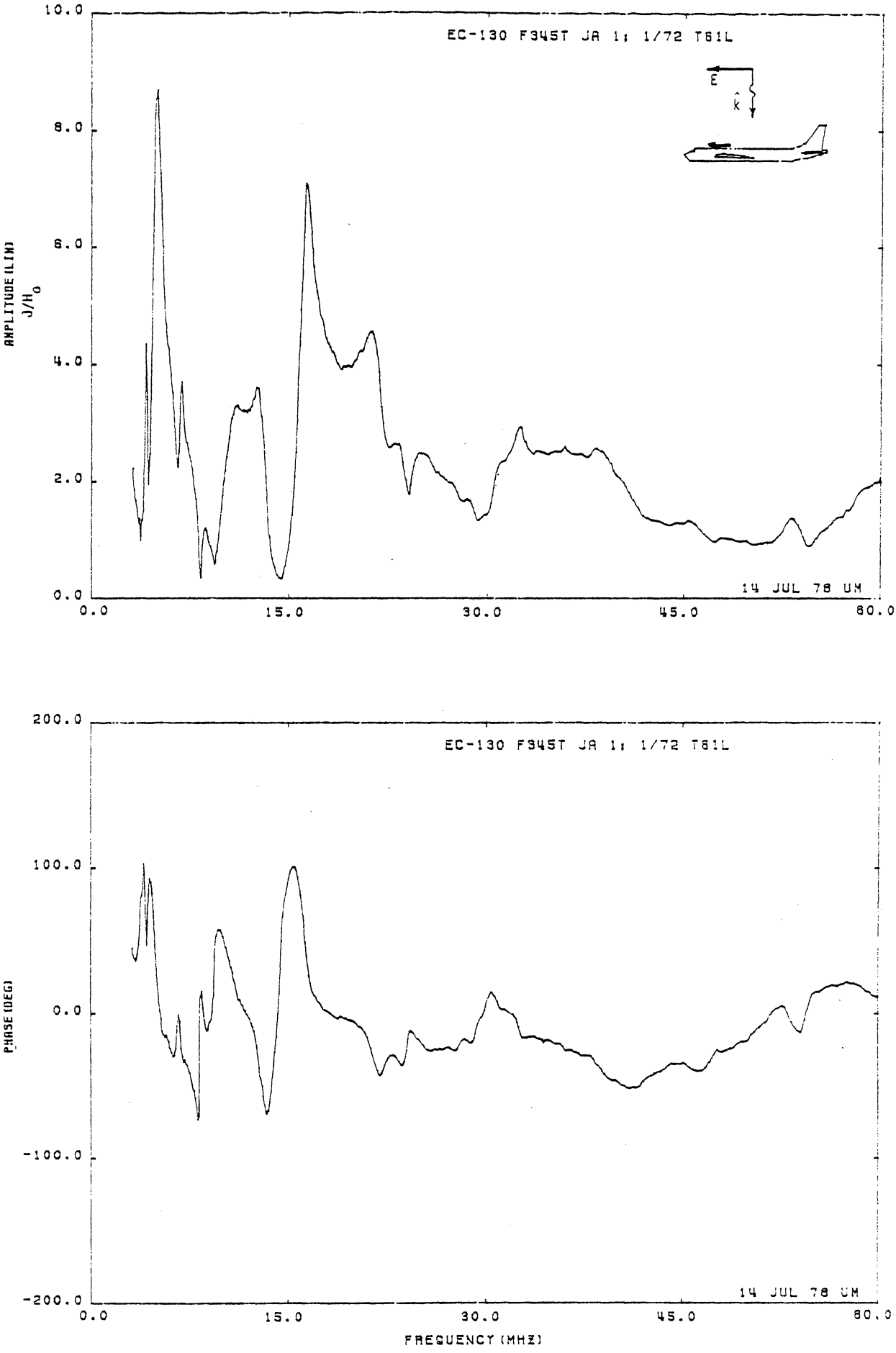

Figure 61L. Axial Current at STA:F345T, Excitation 1, 1/72 Model. (Repeated Measurement, see Table 4)

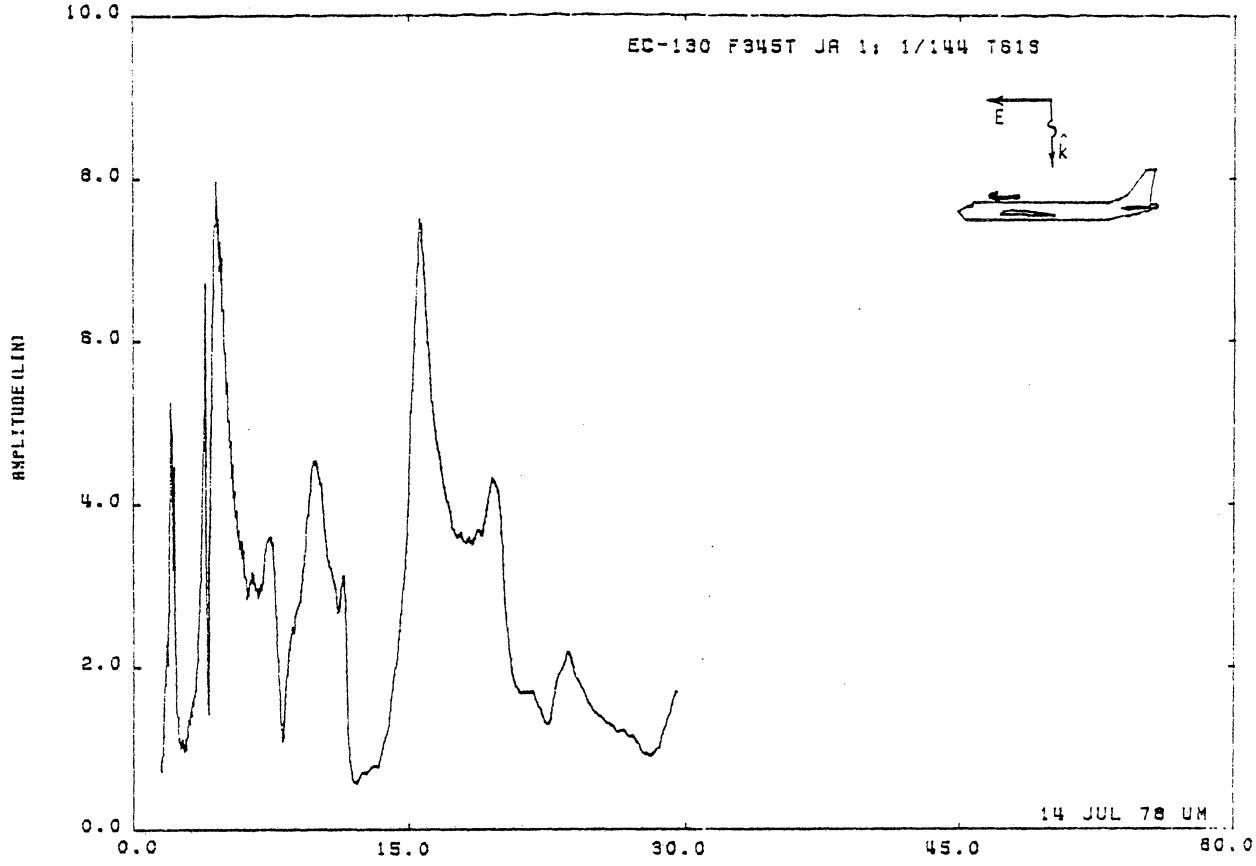

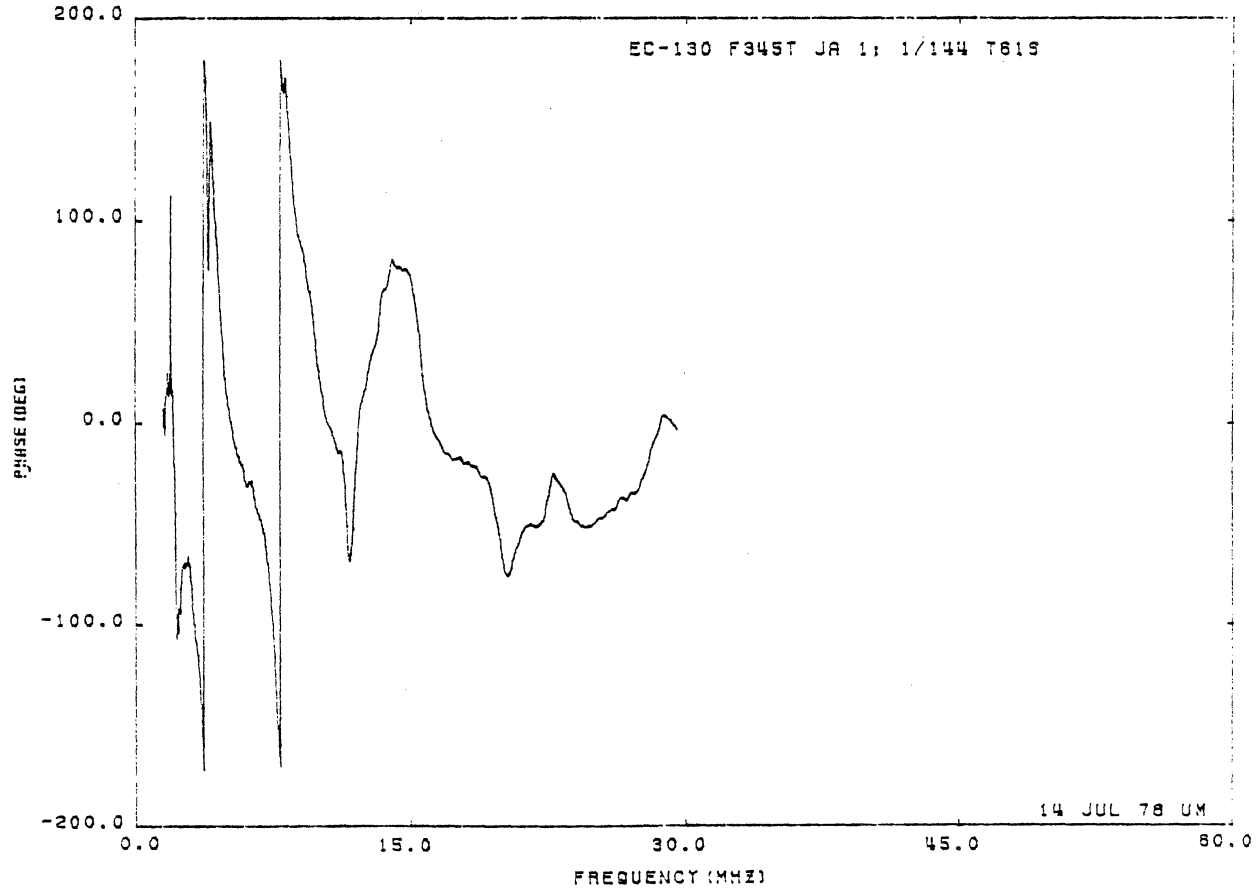

Figure 61S. Axial Current at STA:F345B, Excitation 1, 1/144 Model. (Repeated Measurement, see Table 4)

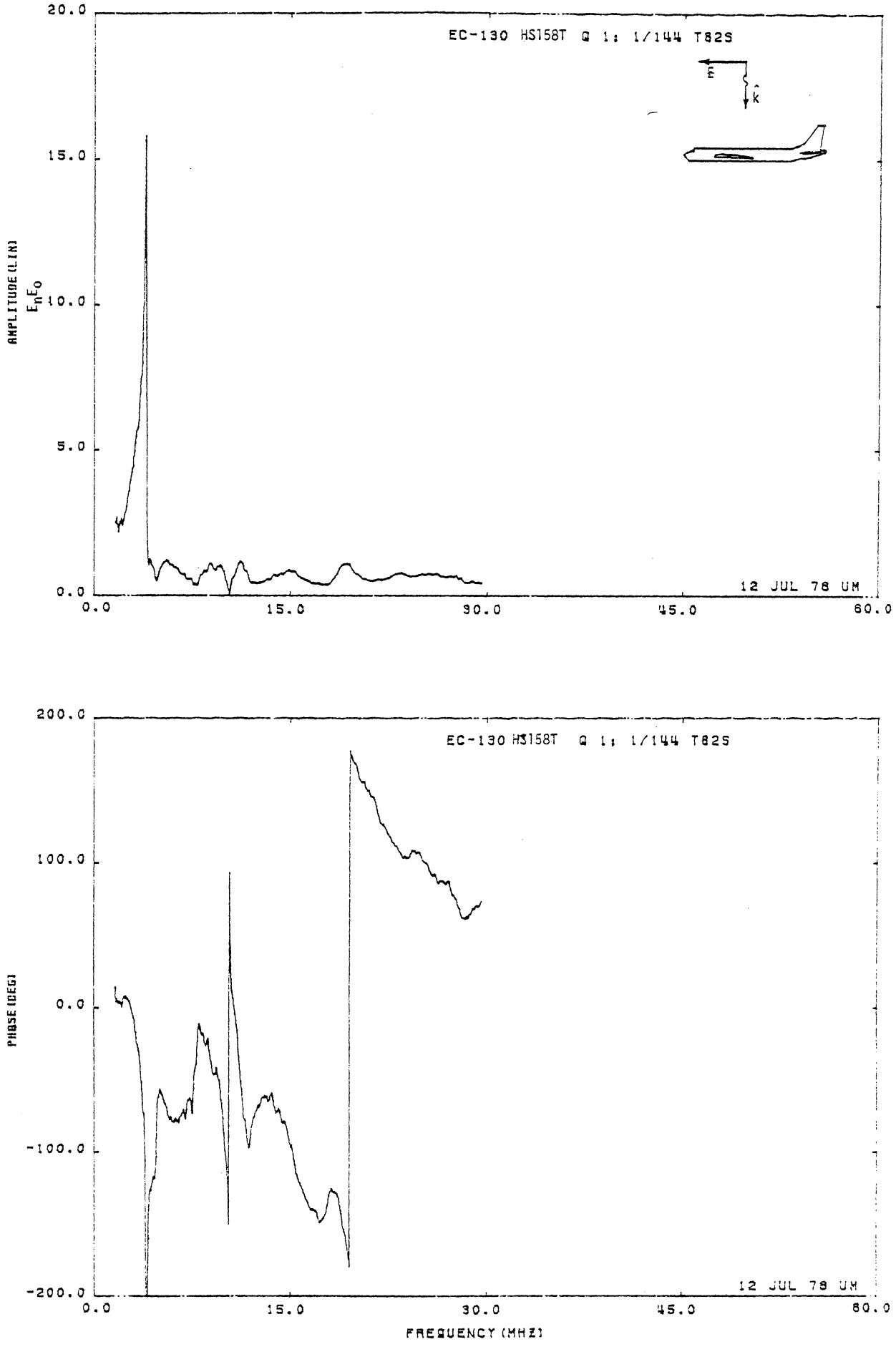

Figure 62S. Charge at STA:HS158T, Excitation 1, 1/144 Model.
(Repeated Measurement, see Table 4)

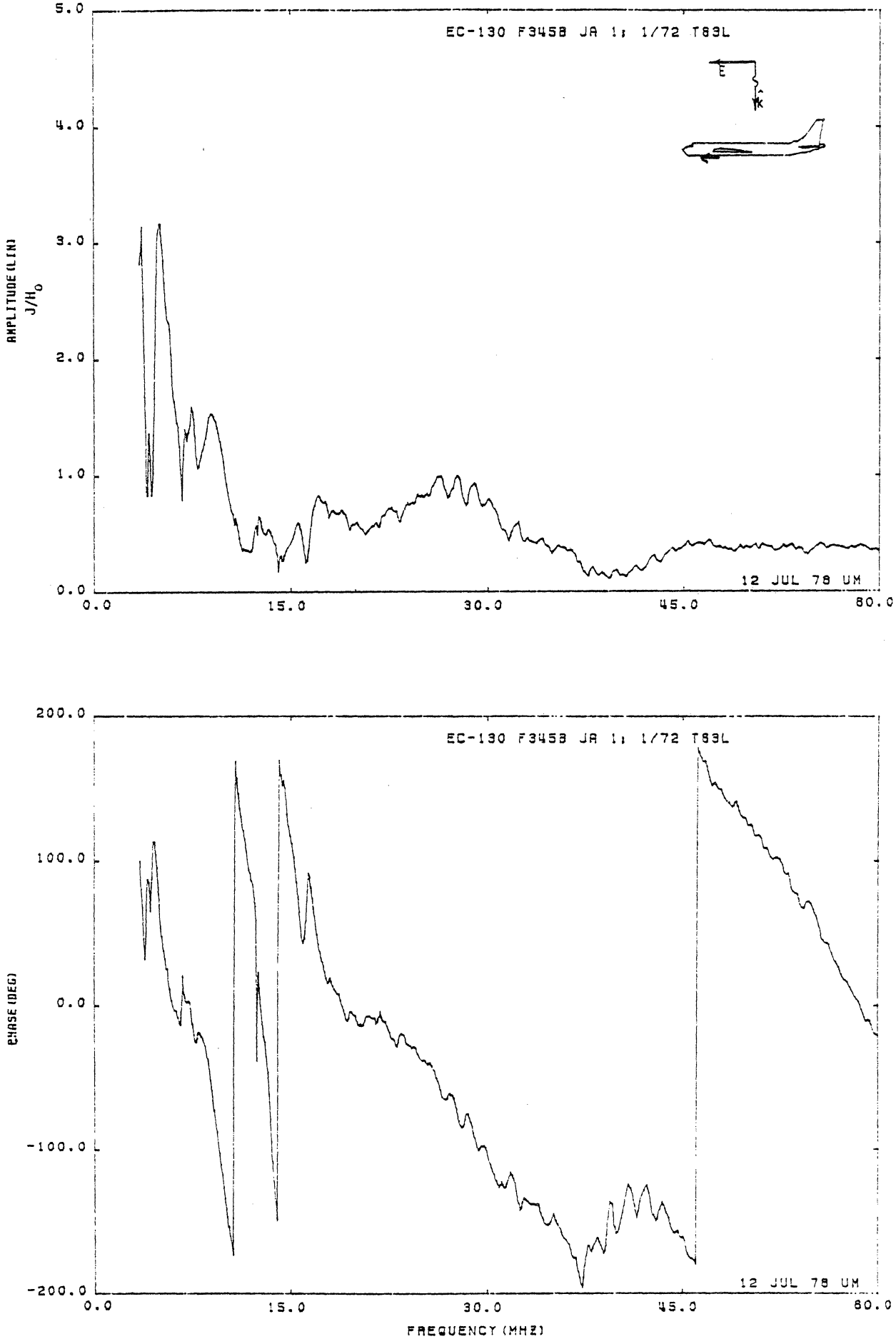

Figure 63L. Axial Current at STA:F345B, Excitation 1, 1/72 Model.
(Repeated Measurement, see Table 4)

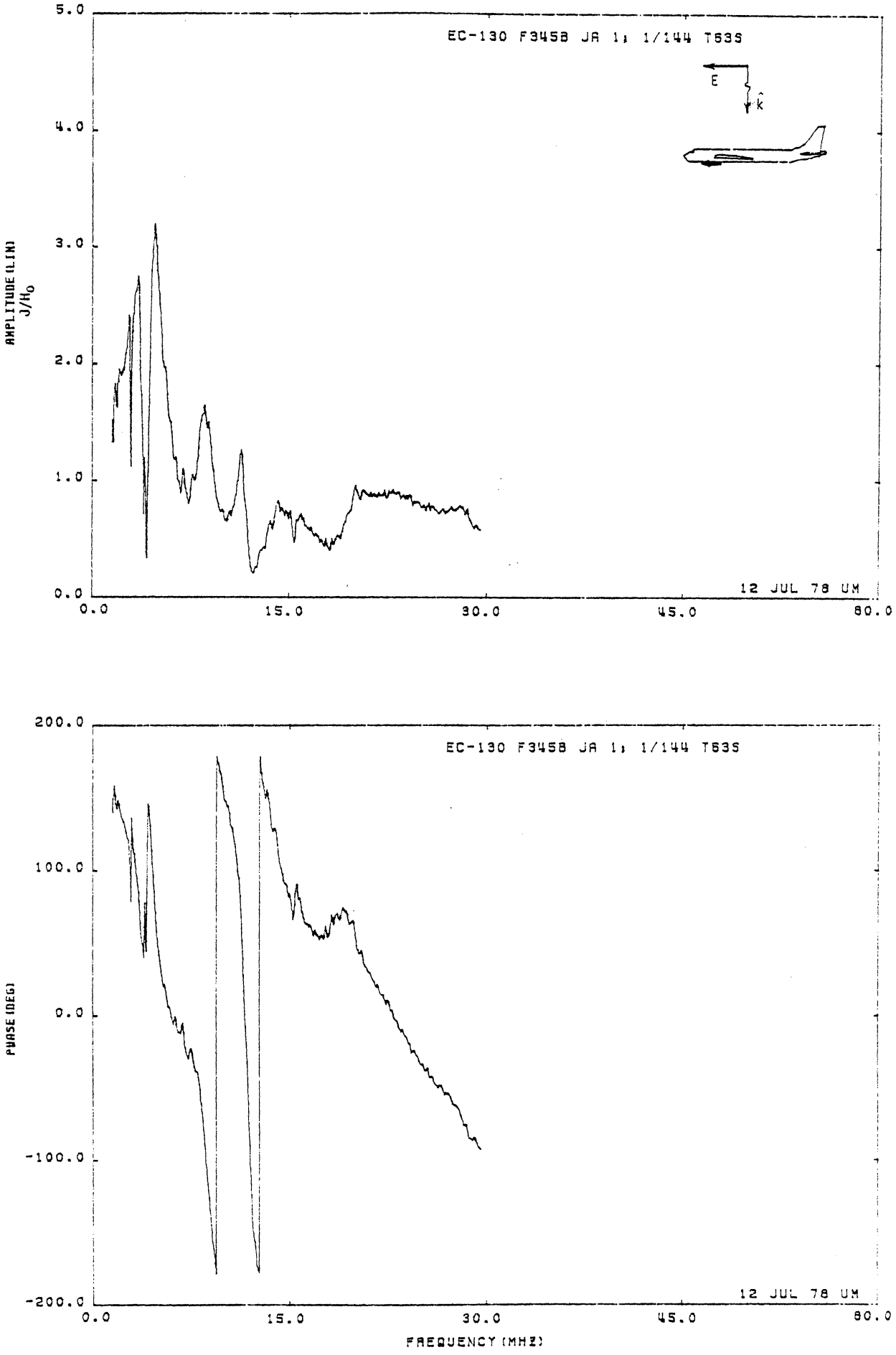

Figure 63S. Axial Current at STA:F345B, Excitation 1, 1/144 Model.
(Repeated Measurement, see Table 4)

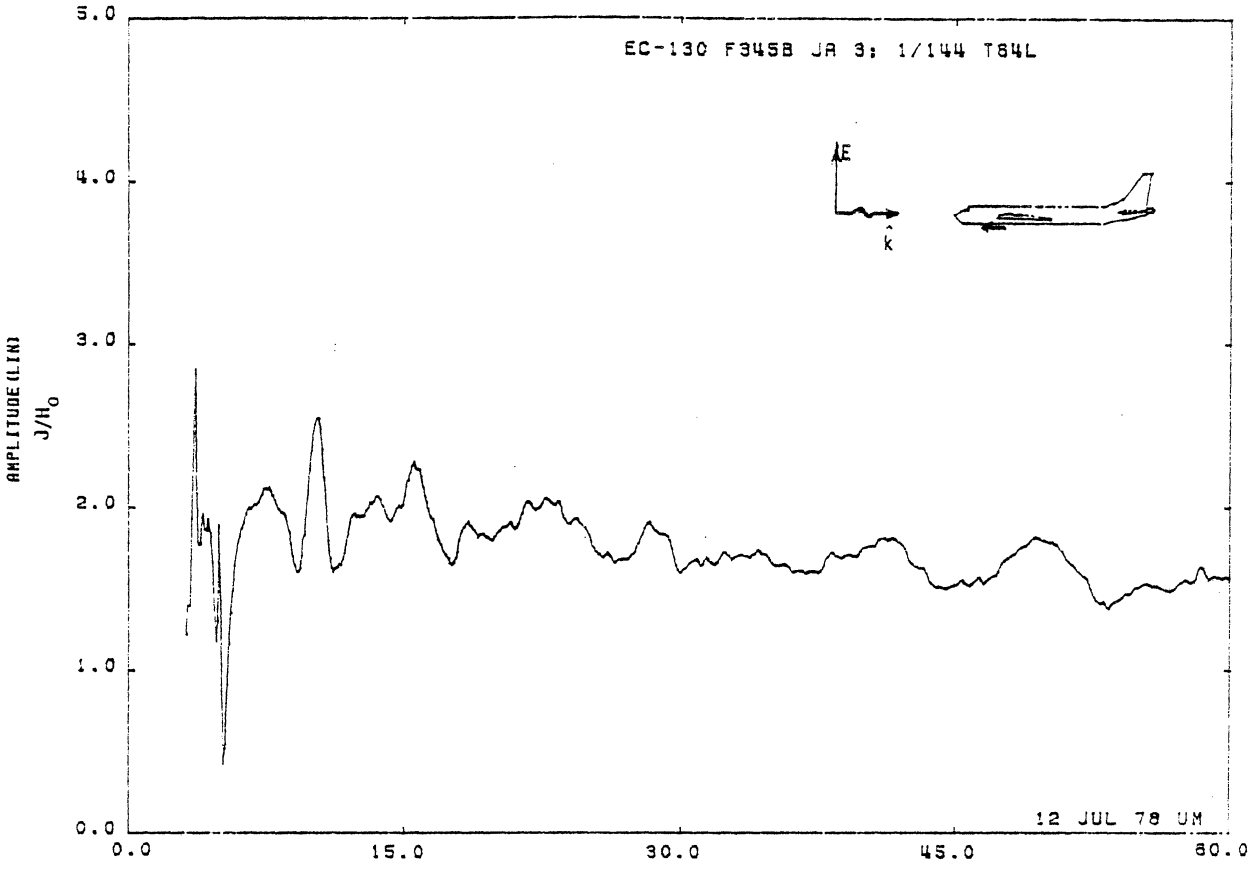

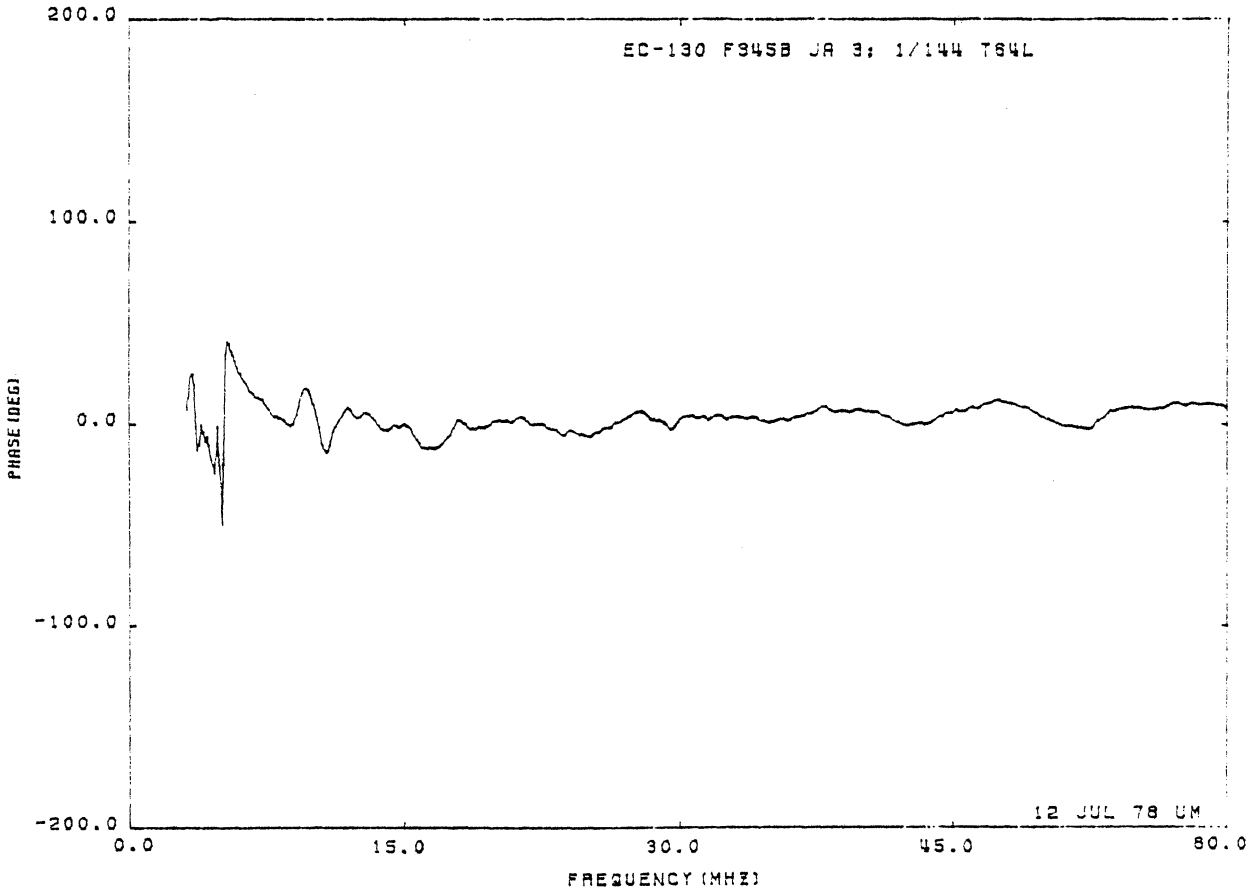

Figure 64L. Axial Current at STA:F345B, Excitation 3, 1/72 Model.
(Repeated Measurement, see Table 4)

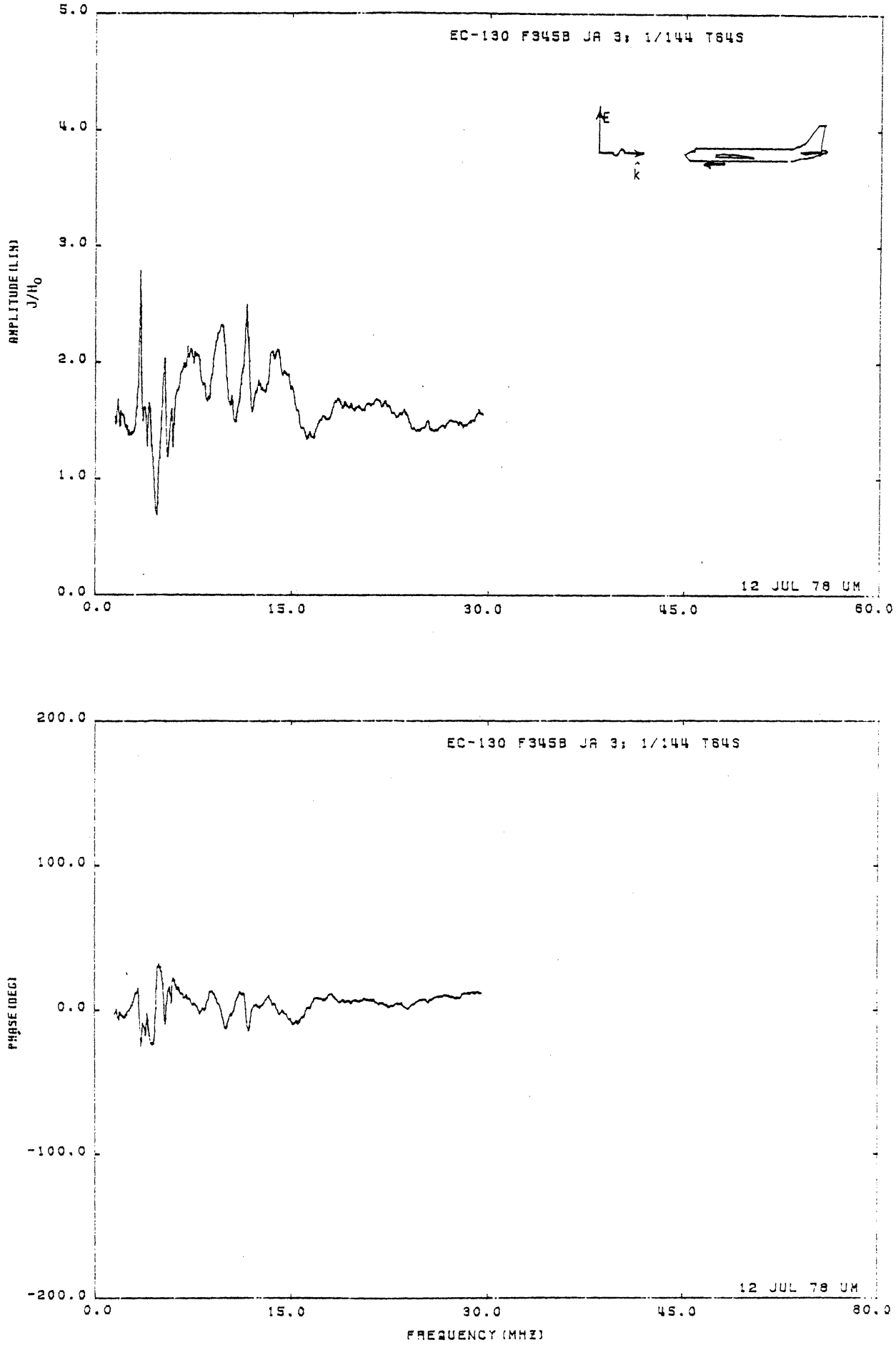

Figure 64S. Axial Current at STA:F345B, Excitation 3, 1/144 Model. (Repeated Measurement, see Table 4)

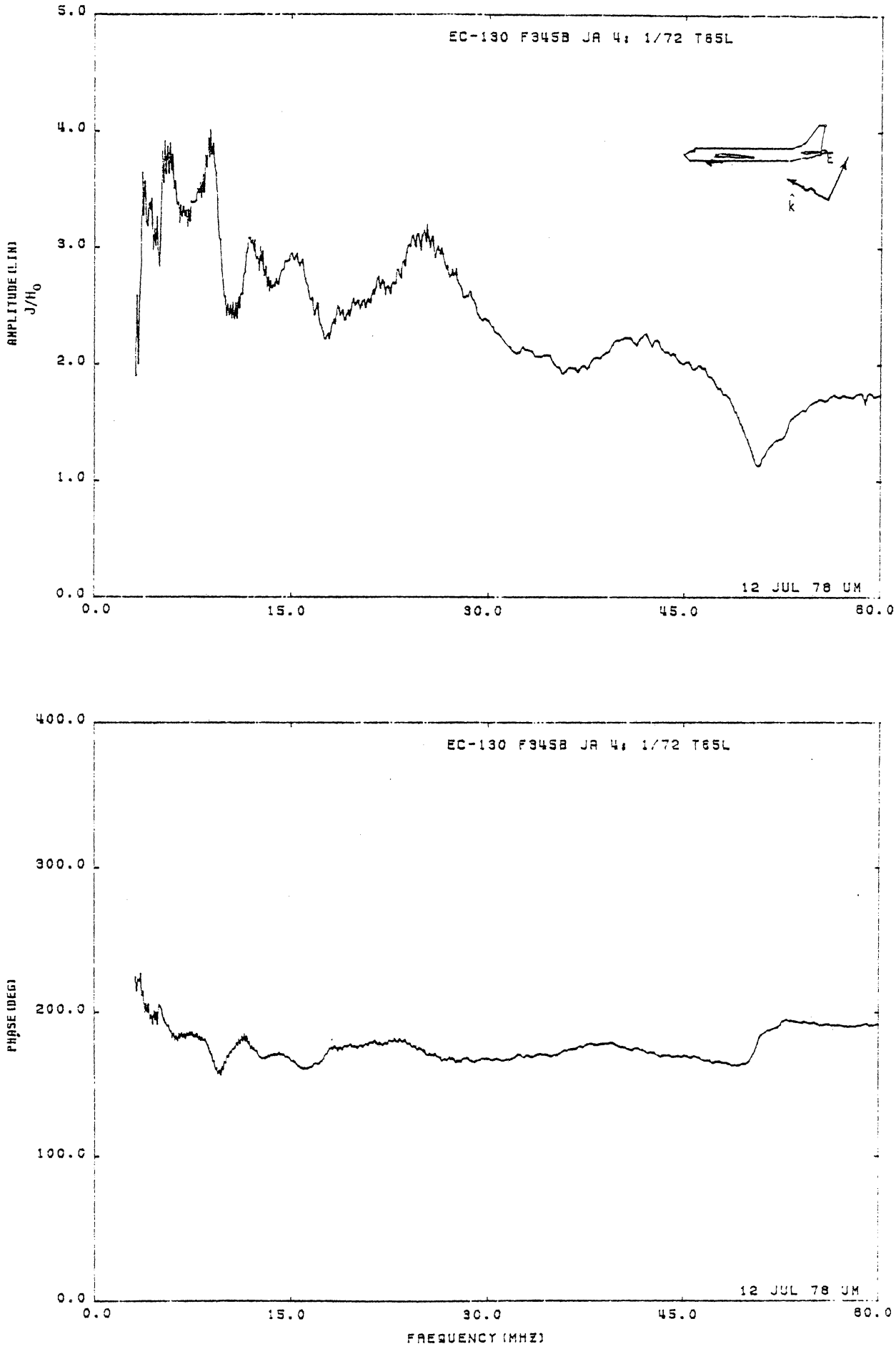

Figure 65L. Axial Current at STA:F345B, Excitation 4, 1/72 Model. (Repeated Measurement, see Table 4)

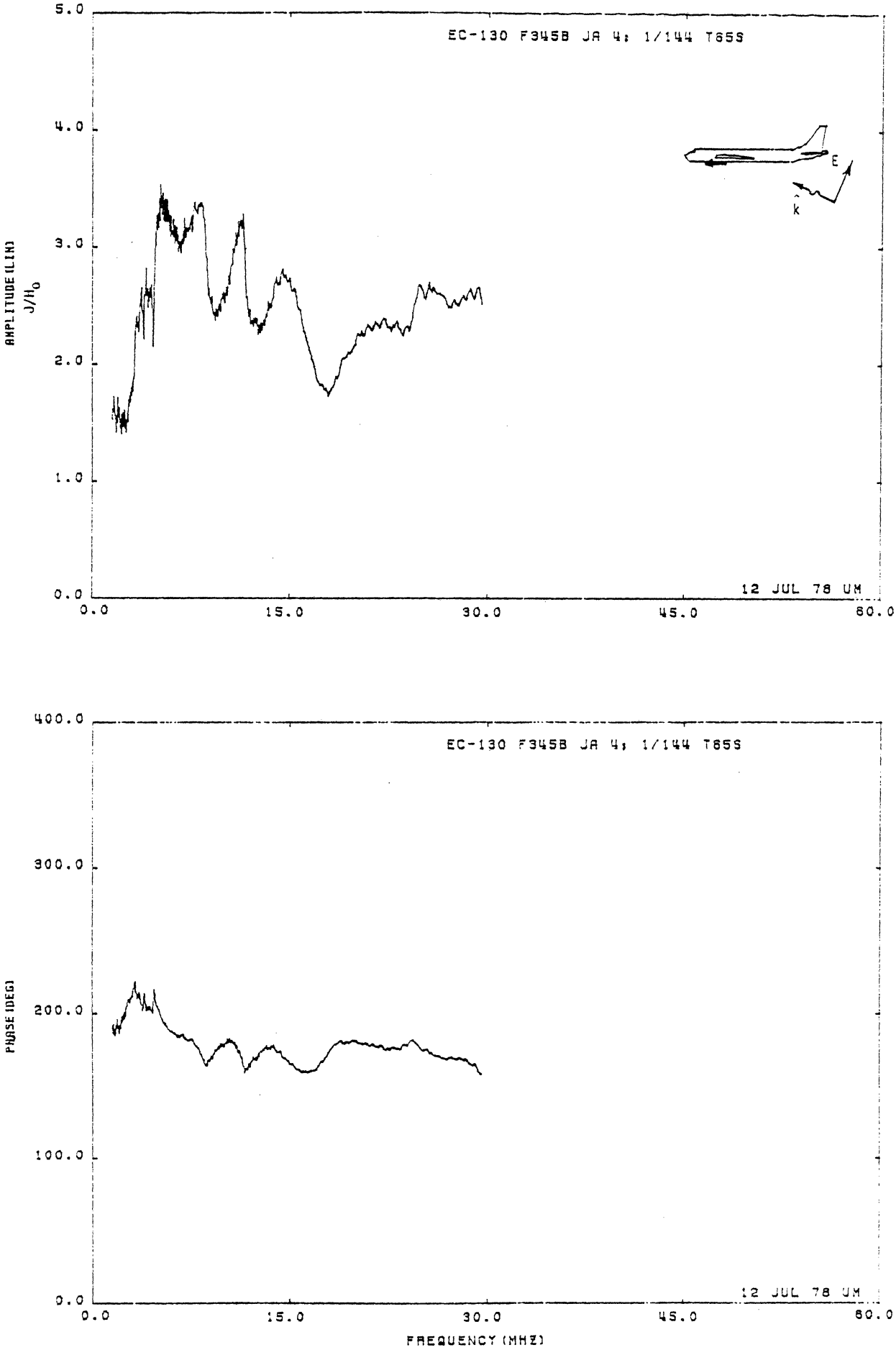

Figure 65S. Axial Current at STA:F345B, Excitation 4, 1/72 Model. (Repeated Measurement, see Table 4)

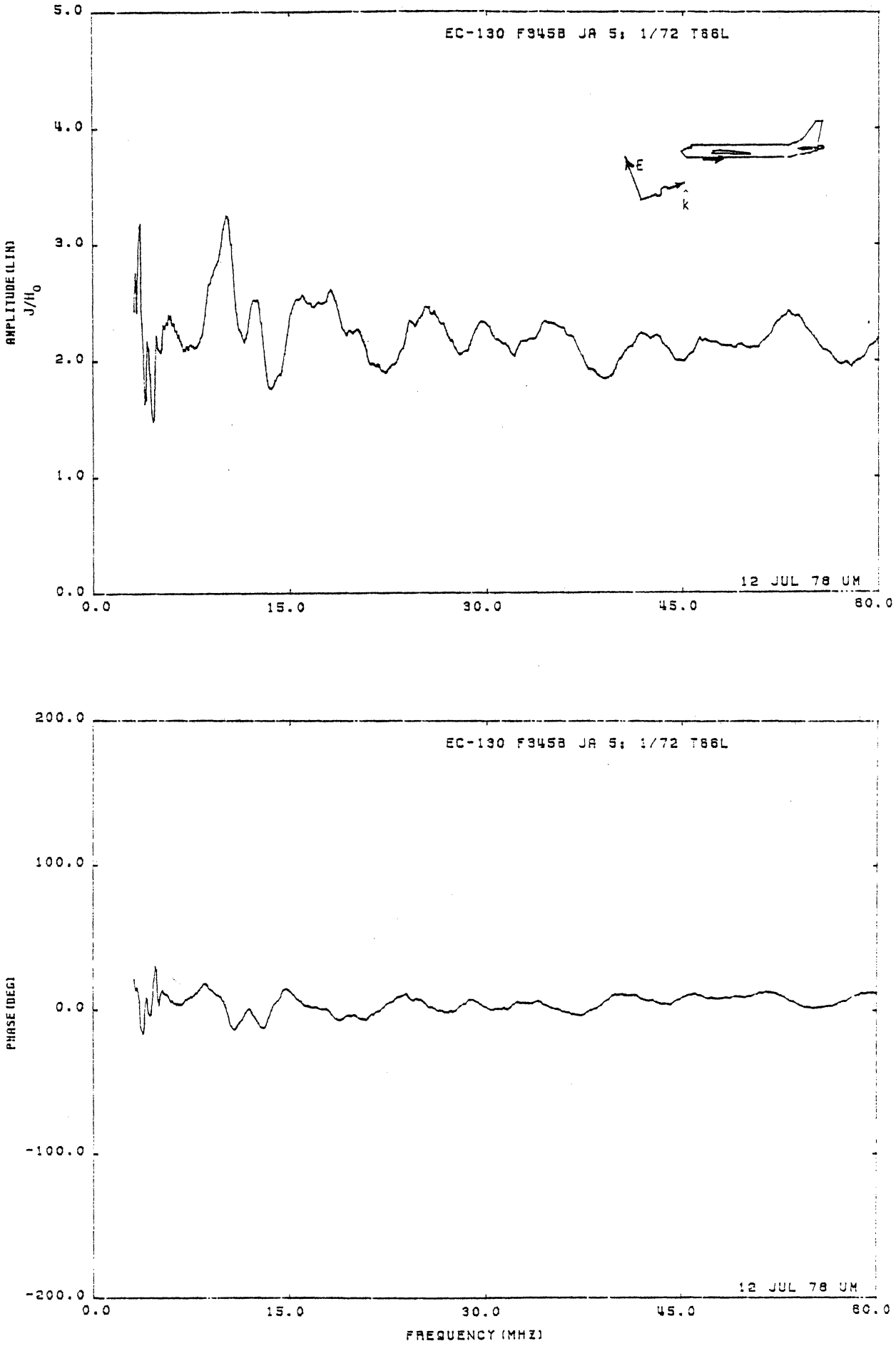

Figure 66L. Axial Current at STA:F345B, Excitation 5, 1/72 Model.
(Repeated Measurement, see Table 4)

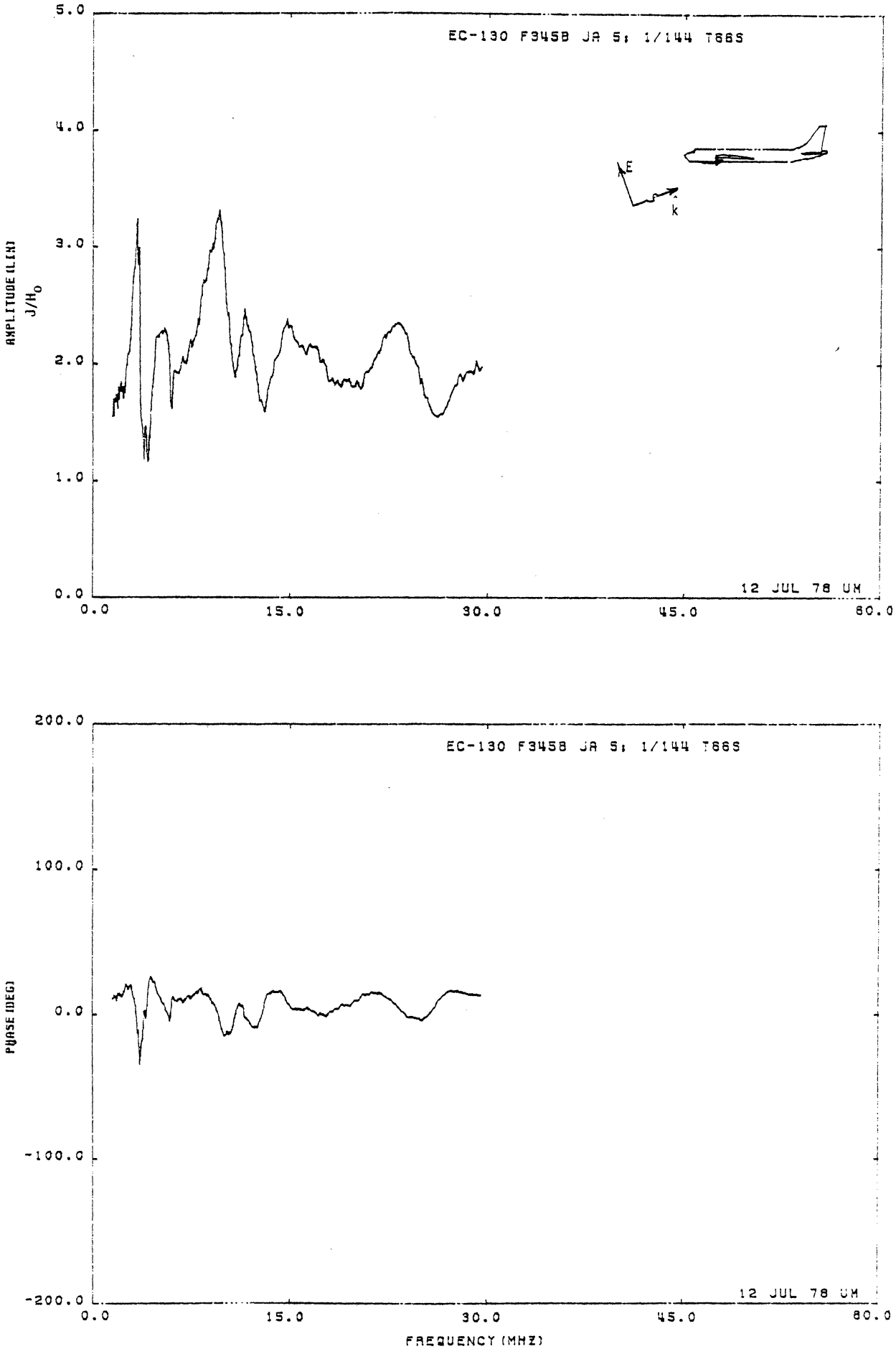

Figure 66S. Axial Current at STA:F345B, Excitation 5, 1/144 Model. (Repeated Measurement, see Table 4)